



## THÈSE

**Pour obtenir le diplôme de doctorat**

**Spécialité PHYSIOLOGIE ET BIOLOGIE DES ORGANISMES - POPULATIONS -  
INTERACTIONS**

**Préparée au sein de l'Université de Caen Normandie**

**Impacts de l'ostréiculture à mésoéchelle sur le microphytobenthos et ses performances photosynthétiques, la macrofaune benthique et rôle de l'érosion estuarienne dans les mortalités de naissains d'huîtres *Crassostrea gigas* liées à OsHV-1 μ Var**

**Présentée et soutenue par  
Charles VANHUYSEN**

**Thèse soutenue publiquement le 16/12/2019  
devant le jury composé de**

Mme ISABELLE ARZUL	Chargé de recherche, IFREMER - LA TREMBLADE	Rapporteur du jury
M. LAURENT BARILLE	Professeur des universités, Université de Nantes	Rapporteur du jury
M. PASCAL CLAQUIN	Professeur des universités, Université Caen Normandie	Président du jury
Mme CHRISTINE DUPUY	Professeur, Université de La Rochelle	Membre du jury

**Thèse dirigée par FRANCIS ORVAIN, Biologie des organismes et écosystèmes aquatiques (Caen)**



UNIVERSITÉ  
CAEN  
NORMANDIE



NBISE  
Normande de Biologie Intégrative,  
Santé, Environnement







Ce travail de recherche a été réalisé au sein de l'Ecole Doctorale Normande de Biologie Integrative, Santé et Environnement (ED nBISE) dans le laboratoire Biologie des Organismes et Ecosystèmes Aquatiques (FRE BOREA) de l'Université de Caen-Normandie.



Normande de Biologie Intégrative,  
Santé, Environnement



Cette thèse a été financée par le Ministère de l'enseignement supérieur de la Recherche et de l'Innovation.





# Table des matières

<b>Remerciements .....</b>	<b>VI</b>
<b>Liste des abréviations.....</b>	<b>XI</b>
<b>Chapitre 1 : Introduction générale .....</b>	<b>1</b>
1. L'aquaculture .....	3
2. Environnement ostréicole estuarien .....	4
2.1. Les zones estuariennes .....	4
2.2. Dynamique environnementale des zones estuariennes .....	4
2.3. Le viriobenthos .....	12
2.4. Le microphytobenthos .....	6
2.5. La macrofaune benthique.....	13
2.6. L'huître creuse <i>Crassostrea gigas</i> (Thunberg, 1793) .....	13
3. Impact des techniques ostréicoles sur l'environnement à l'échelle de la table .....	17
3.1. Influences physiques .....	17
3.2. Influences biogéochimiques.....	19
3.3. Structuration de l'habitat à mésoéchelle .....	20
4. Dynamique environnementale viriobenthique, tables à huîtres et épisodes de mortalités liés à OsHV-1 μVar.....	22
4.1. Rôle des EPS sur la survie virale .....	23
4.2. Rôle de la lumière sur la survie virale .....	24
4.3. Interactions avec la macrofaune.....	24
4.4. Rôle de l'habitat table à huître sur le viriobenthos .....	26
5. Etudes antérieures en baie des Veys .....	27
5.1. Résultats préliminaires.....	28
6. Objectifs .....	31
6.1. Expérimentations réalisées lors de ce projet de thèse .....	31
6.2. Site d'étude .....	34

<b>Chapitre 2 : Drivers of the epipelagic microphytobenthic photobiology and growth in oyster farm .....</b>	<b>40</b>
1. Introduction .....	43
2. Material & Method.....	47
2.1. Study site and sampling design .....	47
2.2. Abiotic parameters .....	48
2.3. Biotic parameters .....	48
3. Results .....	52
3.1. ANCOVA Analysis .....	52
3.2. Microphytobenthic variables .....	54
3.3. Multivariate analysis .....	57
4. Discussion .....	60
Impact of oyster tables on the benthic habitat.....	60
Response of photobiological variables to habitat characteristics.....	62
Summer thermoinhibition versus photoinhibition for MPB .....	65
5. Conclusion.....	67
Acknowledgements .....	68
<b>Chapitre 3 : Benthic macrofaunal changes in oyster parks during an OsHV-1 μVar oyster spat mortality outbreak .....</b>	<b>72</b>
1. Introduction .....	75
2. Material & method .....	77
2.1. Study site.....	77
2.2. Experimental design.....	78
2.3. Macrofaunal sampling .....	78
2.4. OsHV-1 sampling .....	79
2.5. Data analysis .....	79
3. Results .....	81
3.1. Abundance, diversity and specific richness .....	81

3.2.	Frequency rank chart.....	82
3.3.	Ecological indicators.....	83
3.4.	Multivariate analysis.....	84
3.5.	Oyster mortality episode .....	87
4.	Discussion .....	89
	Macrofaunal community structure of soft sediments in oyster park of Baie des veys.....	89
	Evolution of benthic indexes.....	91
	Multivariate analysis .....	93
	OsHV-1 $\mu$ Var DNA detection in macrozoobenthos .....	95
5.	Conclusion.....	96
	Acknowledgements .....	97

**Chapitre 4 : Environmental dynamics of the Ostreid herpes virus (OsHV-1  $\mu$ Var) in oyster spats and microphytobenthic biofilms during an *in situ* mortality outbreak .... 102**

1.	Introduction .....	105
2.	Material & method .....	108
2.1.	Study site.....	108
2.2.	Experimental design.....	109
2.3.	Oyster spat survival.....	110
2.4.	OsHV-1 $\mu$ Var and bacterial sampling in oysters .....	110
2.5.	OsHV-1 $\mu$ Var extraction and bacterial sampling in the biofilm.....	110
2.6.	Statistical analyses .....	111
3.	Results .....	112
3.1.	Oyster mortality episode .....	112
3.2.	OsHV-1 $\mu$ Var in oysters .....	112
3.3.	OsHV-1 $\mu$ Var in the sediment .....	114
3.4.	OsHV-1 $\mu$ Var in the biofilm.....	115
4.	Discussion .....	115

Spat mortality and risk factors .....	115
Role of microphytobenthic biofilmin the transmission of OsHV-1 μVar.....	118
5. Conclusion.....	120
Acknowledgments.....	121
<b>Chapitre 5 : <i>In situ</i> resuspension of benthic sediments and biofilm components during an OsHV-1 μVar <i>Crassostrea gigas</i> oyster spat mortality episode.....</b>	<b>126</b>
1. Introduction .....	129
2. Material & method .....	132
3. Results.....	137
4. Discussion .....	146
5. Conclusion .....	150
Ackowlegments .....	150
<b>Chapitre 6 : Synthèse générale, discussion et conclusion .....</b>	<b>154</b>
Caractérisation de l'environnement benthique ostréicole à l'échelle de la table à huître: conséquences sur le microphytobenthos, la macrofaune et l'érodabilité du sédiment.....	156
Dynamique environnementale de OsHV-1 μvar et conséquences des mortalités de naissains d'huîtres.....	161
Conclusion générale .....	165
<b>Annexes .....</b>	<b>168</b>
<b>Références bibliographiques .....</b>	<b>183</b>
<b>Liste des figures .....</b>	<b>213</b>
<b>Liste tableaux.....</b>	<b>217</b>

v

# Remerciements

Je tiens à remercier en premier lieu Francis Orvain pour avoir été mon directeur de thèse. Merci pour ton expérience, tes conseils et ta bonne humeur à toute épreuve. Merci aussi pour les discussions musicales. Je me souviens des campagnes de terrain à l'été 2017, une belle expérience. Merci de m'avoir fait confiance pour ce projet.

Je remercie également M. Laurent Barillé et Mme Isabelle Arzul pour avoir accepté d'être rapporteur et rapportrice de cette thèse. Merci également aux autres membres du jury, Christine Dupuy et Pascal Claquin pour avoir accepté d'évaluer ce travail de thèse de doctorat.

Je remercie également les membres de mon Comité de Suivi Individuel : Muriel Bardor, Christine Dupuy, Aurore Sauvey et Hélène Montanié pour qui j'ai une pensée toute particulière. Merci pour votre investissement et vos remarques constructives au long de ces 3 années de thèse.

Je tiens à remercier Clarisse Mallet pour m'avoir accueilli au pied des volcans à Clermont-Ferrand le temps d'une semaine. Merci Clarisse pour ton aide, ton implication sans faille malgré les innombrables conditions de PCR testées, pour ton encadrement scientifique et ta gentillesse.

Merci également à Christophe Lelong qui aura toujours été présent quand cela était nécessaire. Merci pour ta sympathie et tes conseils. Merci également à Fabrice Pernet pour les discussions et l'aide ponctuelle que tu as pu me procurer.

Je tiens tout particulièrement à remercier Julien Normand pour son aide sur les statistiques notamment. Grâce à toi j'aurais pris plaisir à réutiliser R-Studio et réussi à réunir R et plaisir dans une même phrase. Merci également pour les précieux conseils et les discussions que nous avons pu avoir.

Un très grand merci à Mélanie Lepoittevin qui du début à la fin aura été là pour m'aider lors des manips en laboratoire et sur le terrain. Merci de m'avoir accompagné, pour les discussions et les coups de main même hors du travail.

Un très grand merci à André-Gilles Taillepied et à toute son équipe (mention spéciale à Eric) pour nous avoir si gentiment hébergés dans son local à Grandcamp-Maisy pour notre campagne de terrain en 2017.

Merci à Pascal Sourdaine puis Céline Zatylny-Gaudin pour avoir été successivement directeur et directrice du laboratoire BOREA

Merci à tout le personnel du laboratoire pour leur aide et leur gentillesse quotidienne notamment Catherine, Myriam, Fabienne, Sandra et Christophe Roger pour tous les coups de main à droite à gauche, sa gentillesse son humour et sa détermination infatigable.

Un grand merci à toutes les personnes ayant participer à la campagne de terrain de 2017 en Baie des Veys : Francis, Mélanie, Christiane, Christophe R, Marie-Pierre, Béatrice, Fabrice, Christophe L. Je me souviens de ces longues journées de terrain à l'été 2017 mais des trop courtes soirées.

Je tiens à remercier les étudiants ayant contribué à ce travail de thèse : Kevin, Guillaume et Lauriane lors de leur projet tuteuré et Tom, Gaylord, Gaétan et Nathan lors de leurs stages. Merci également aux autres étudiants que j'ai pu côtoyer au laboratoire notamment Mathias (pensée spéciale pour Beauregard), Florian, Anna et Alex. Merci à Guillaume Meynard pour son aide sur la partie érodémétrie

Merci à Anne-Sophie Martinez pour les discussions que nous avons pu avoir et sa gentillesse quotidienne. Je me souviens également de la joie de vivre de Bertrand Le Roy et surtout de ses tomates ! Merci aussi à Christiane pour son aide, son soutien et les discussions que nous avons pu avoir.

A mes partenaires de navigation Alexis, Baptiste H., Laura, Aurore R., Aurore S., Lorane, Julie, Louis, Quentin, Baptiste V., Kouka, un grand merci pour tout. Que serait notre bureau sans toutes nos chères plantes... Je ne détaillerai pas ici toutes nos aventures. Simplement, merci.  
*What is dead may never die.*

Aussi, quel bonheur de vivre dans notre si belle Normandie !

A mes amis Chloé, Iris, Clairette, Aurélien, Guigui, Elise, Justin et votre petit Anakin. Merci pour tout, merci d'être vous. A Anakin, bienvenue dans ce monde et que la force soit avec toi. En tous cas je le serais toujours. Une pensée également pour les anciens, les Nantais et les Rochelais.

A mes parents et ma sœur, merci pour votre soutien inconditionnel. A Winston, woof !

A Johana, les mots ne pourraient exprimer tout ce nous avons vécu durant ces 3 années...



*A mon grand-père Albert, parti quelques semaines avant le rendu de ce manuscrit,  
à ma grand-mère Francine.*

X

# Liste des abréviations

Chl *a* : chlorophylle a

Ek: Light saturation coefficient

EPS : Substances Polymeriques Extracellulaires

ETRmax: maximum electron transport rates

MPB : Microphytobenthos

MWH: Maximum water height

OM : Organic matter

OMF : Organic matter fraction

Pemax: Maximum productivity

Pmax: Maximum production

PY : Photosynthetic yield

SLI : Surface light intensity

SPM : Matière en suspension particulaire

SST : Surface sediment temperature



# **Chapitre 1 : Introduction générale**



## 1. L'aquaculture

Depuis des millénaires, l'Homme a tenté de mettre au point des techniques d'élevage d'organismes aquatiques. De façon empirique, les prémisses de l'aquaculture seraient apparues en Chine il y a 4000 ans puis par la suite en Egypte et en Assyrie (Nash, 2010) pour devenir aujourd'hui un secteur d'activité à part entière. Cette activité désigne la production d'organismes aquatiques en eau douce, saumâtre ou marine dans des conditions contrôlées ou semi-contrôlées par l'homme, qu'il s'agisse d'animaux (poissons, crustacés, mollusques...) ou de végétaux (algues). Cette activité serait apparue en France il y a environ 1000 ans (Figure 1) avec la pisciculture qui fut principalement réalisée par les moines (Nash, 2010).



Figure 1 © RMN-Grand Palais / Martine Beck-Coppola - Louis-Joseph Yperman, *La pêche au vivier*, peinture murale du Palais des Papes, Avignon, France, 1910 (œuvre originale : 1343-1344)

Au cours des siècles cette activité s'est diversifiée pour devenir le secteur alimentaire ayant présenté le taux de croissance le plus élevé au monde (7,8 %) lors des trois dernières décennies (contre 4,6 % pour l'aviculture, 2,2 % pour la porciculture et 1,0 % pour l'élevage bovin). Ainsi cette activité pourrait être un moyen de réduire la pauvreté des pays en voie de développement et d'en augmenter la sécurité alimentaire (Béné et al., 2016). De plus, cette industrie pourrait représenter une alternative durable à la surpêche des ressources marines (Troell et al., 2014) profondément menacées par la pêche et les conséquences des activités anthropiques telles que les apports fluviaux liés à la gestion des bassins versants et la régulation des intrants agricoles et/ou industriels, le changement climatique, l'acidification des océans, la pollution terrigène (*e.g.* déchets plastiques, rejets physico-chimiques...) et l'introduction d'espèces invasives. Ainsi, l'étude des environnements aquacoles apparaît cruciale afin de pérenniser cette activité et améliorer sa gestion notamment face aux épisodes de mortalités massives en lien avec la qualité de l'eau et la prolifération de pathogènes.

## 2. Environnement ostréicole estuaire

### 2.1. Les zones estuariennes

Fort de leur important potentiel productif, les zones estuariennes constituent le lieu privilégié pour l'implantation d'une activité d'exploitation (eg. conchyliculture). En effet, les écosystèmes estuariens constituent un type d'environnement particulier par leur diversité d'influences car ils sont à l'interface entre le continent, un fleuve, la mer et l'atmosphère. Cette particularité place les zones estuariennes parmi les biotopes les plus productifs au monde (Whittaker and Likens, 1975) avec des pics de biomasse phytoplanctonique pouvant dépasser  $100 \mu\text{g chlorophylle a (Chl }a\text{).L}^{-1}$  (Cloern et al., 2014). Un facteur supplémentaire jouant en faveur du fort potentiel productif des estuaires est la quantité renouvelable de nutriments apportée par le fleuve tout comme le temps de résidence des mases d'eau marines (Grangeré et al., 2009). Les apports de nutriments sont sujets à variations mais restent néanmoins importants et dépendent des caractéristiques du fleuve (débit, longueur, barrages...) et de son bassin versant (surface, pente...). Le lieu de déversement des apports terrigènes drainés le long du bassin versant vers le milieu marin s'effectuent à l'exutoire du fleuve (Dagg et al., 2004). Ces apports terrigènes sont majoritairement composés de sédiments, de nutriments nécessaires à la croissance des organismes autotrophes et de matière organique particulaire ou dissoute (Hedges et al., 1997) mais aussi de polluants divers (micros plastiques, métaux lourds) liés aux activités humaines. En effet, selon le Programme des Nations Unies pour l'Environnement la pollution marine serait à plus de 80 % d'origine terrigène et anthropique. Ces apports terrigènes auront donc une importance capitale dans la dynamique biogéochimique et biologique des zones estuariennes. La présence de vases dans des zones calmes le long du fleuve en amont ou bien à son embouchure peut former des étendues de vasières, susceptibles d'être érodées en cas de phénomènes de crues intenses. Ce phénomène d'érosion peut entraîner des pics de turbidité intenses et la formation de bouchons vaseux très dynamiques (Guillaud, 1983).

### 2.2. Dynamique environnementale des zones estuariennes

Lors du flot, la marée montante exerce une force d'érosion croissante à la surface du sédiment. Cet écoulement entraînera une suspension de particules benthiques augmentant ainsi la turbidité de la colonne d'eau. Selon l'intensité de la contrainte de cisaillement (force érosive) causée par la marée et la cohésion du sédiment, les sédiments cohésifs peuvent être mis en suspension en générant des taux de turbidité élevés (Murray, 1977; Joensuu et al., 2018; Le Hir et al., 2007). Ce phénomène de remise en suspension du sédiment dépend également de la taille des particules

sédimentaires (granulométrie) et du degré de consolidation des sédiments cohésifs (vases). Pour les mélanges sablo-vaseux le seuil critique, c'est-à-dire la contrainte de cisaillement nécessaire à la mise en resuspension des particules de sédiment, augmente avec la proportion de particules sédimentaires fines dans l'échantillon de sédiment (Murray, 1977). Ainsi, un sédiment sableux est plus facilement mis en suspension qu'un sédiment vaseux en raison de la forte cohésion des particules fines, mais ce transport édimentaire se fait d'abord par charriage (en restant au fond) puis par saltation en cas de frottement très élevé. Une fois dans la colonne d'eau, les particules les plus grossières seront les premières à sédimenter vers le benthos avec des vitesses de chute très élevées. Pour les sédiment fins (diamètre < 63µm), la quantité de particules en suspension (Suspended particular matter : SPM) constitue la turbidité. Lorsque cette turbidité est importante, cela peut limiter la pénétration de la lumière et ainsi réduire l'épaisseur de la zone photique (Cloern et al., 2014; Wofsy, 1983). La vitesse de chute des particules dépend également des concentrations en turbidité et des processus de flocculation.

Dans les écosystèmes côtiers, la couche euphotique (espace où le phytoplancton est capable de réaliser la photosynthèse) est susceptible de se retrouver réduite en épaisseur à cause d'une forte turbidité et cette atténuation de la lumière défavorise le développement du phytoplancton (Cloern, 1987). En effet, dans certains cas, une forte turbidité peut inhiber le bloom phytoplanctonique printanier (May et al., 2003). Les activités humaines peuvent également réguler la turbidité et ainsi impacter le fonctionnement des zones estuariennes à grande échelle. A titre d'exemple, depuis 1975 les concentrations de SPM et la turbidité dans le nord de la baie de San Francisco ont diminué de 50 % (Cloern et al., 2014). Cet appauvrissement en SPM a été observé après des décennies de modifications (*e.g.* canalisations, barrages) des affluents de la baie de San Francisco. La dynamique sédimentaire est donc un phénomène clé pour le fonctionnement d'un écosystème aquatique (Danielsson et al., 2007; Warrick, 2012). En estuaire de Seine, la baisse générale des régimes de précipitation liée au changement climatique explique aussi en partie la réduction de la quantité de vases mobiles qui alimentent le bouchon vaseux. Ainsi en trois décennies, la surface des vasières intertidales a été réduite par trois (Dauvin et al., 2017). De plus, la création d'infrastructures portuaires et de chenaux de navigation ont également impacté la surface de vasières intertidales de cet écosystème estuarien.

## 2.3. Le biofilm

Sous influence d'un rythme circadien (Falkowski, 1984), les diatomées microphytobenthiques se distinguent de par leur capacité de mobilité. En effet, lors de la période d'exondation, ces micro-algues migrent à la surface du sédiment (voir Figure 2. b.) afin de capter la lumière pour réaliser la photosynthèse (Serôdio et al., 1997). Cette mobilité des diatomées est accomplie via l'excrétion de substances polymériques extracellulaires (Extracellular polymeric substances : EPS) de leur système de raphé (Edgar, 1983; Edgar and Pickett-Heaps, 1983). Le système de raphé consiste en une fente longitudinale observée chez les diatomées pennées. Cette migration puis adhésion de ces espèces pionnières à la surface du sédiment va être la première étape de formation d'un biofilm (Figure 2. a.) de quelques centaines de micromètres d'épaisseur (Herlory et al., 2004). Ces espèces pionnières秘rètent des molécules extra-cellulaires représentant une ressource nutritive pour certains micro-organismes qui coloniseront cette même surface sédimentaire augmentant ainsi la diversité microbienne du biofilm ainsi que sa consolidation. Après cette étape de consolidation, le biofilm va coloniser en 3 dimension la surface du sédiment jusqu'à atteindre un stade mature. A terme, le biofilm sera remis en suspension en fonction de l'érosion tidale, de la composition du sédiment, de l'état physiologique et de l'âge du biofilm (Ubertini, 2015; Joensuu et al., 2018) ainsi que de la bioturbation par la faune benthique (Orvain et al., 2004). Même si, lors du flot, les diatomées migrent en profondeur dans le sédiment afin d'éviter d'être érodées et mises en suspension dans la colonne d'eau (De Jonge and Van Beuselom, 1992; Demers et al., 1987) une partie du MPB sera toutefois érodée et mise en suspension dans la colonne d'eau.

## 2.4. Le microphytobenthos

Le microphytobenthos (MPB) fait partie des producteurs primaires (organismes capables de réaliser la photosynthèse). Ce processus de photosynthèse consiste en la conversion de l'énergie lumineuse en énergie de liaison chimique stockée sous la forme de composés organiques carbonés (Falkowski and Raven, 2013). Globalement, plus de 40 % de la photosynthèse annuelle est réalisée en milieu aqueux (Falkowski, 1994). Dans les zones estuariennes, la majorité de la production primaire est assurée par les plantes halophiles (*e.g.* salicorne, spartine), les macroalgues, le phytoplancton et le MPB. Leur répartition spatiale résultera en partie des caractéristiques locales de la zone estuarienne : type de substrat (rocheux, sableux, vaseux...), dynamique fluviale (débit, turbidité), l'accessibilité à la lumière et la dynamique marine (érosion). Le MPB est un composant clé des écosystèmes estuariens (Cahoon, 2014).

En effet, dans les zones estuariennes sablo-vaseuses, le MPB est souvent considéré comme le principal producteur primaire (Blanchard et al., 1998a) car dans certains cas la production primaire du MPB dépasse celle du phytoplancton (Struski and Bacher, 2006; Underwood and Kromkamp, 1999). Le MPB est principalement constitué de diatomées benthiques (Figure 2. a.; Admiraal, 1984; Méléder et al., 2007; Underwood, 1994). Selon le type de sédiment, différentes catégories de diatomées microphytobenthiques sont observées. Les diatomées sont dites « épipsamiques » lorsqu'elles sont associées à des sédiments sableux (Round, 1971) et sont appelées « épipélique » lorsqu'elles sont associées à des sédiments fins et cohésifs (*i.e.* vaseux).

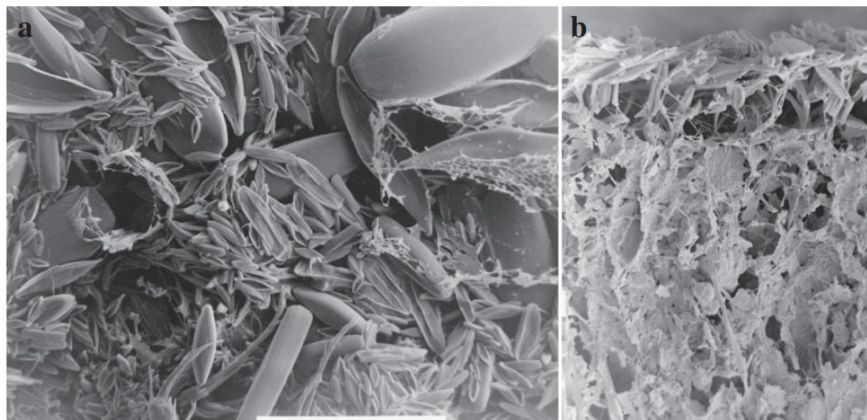


Figure 2 : . Images en microscopie électronique à balayage à basse température d'un biofilm microphytobenthique sur un sédiment, montrant les liens entre les particules de sédiment par le biais des EPS. a. Vue en surface du biofilm. Barre blanche (en bas) : 100  $\mu\text{m}$ . b. Coupe verticale ; la surface des sédiments est en haut. Barre blanche: 10  $\mu\text{m}$ . Adapté de Passarelli et al. (2014).

#### *2.4.1. Les facteurs régulant le développement du MPB*

La production primaire est le résultat d'une multitude de facteurs environnementaux exerçant des pressions physiologiques sur les MPB affectant sa photosynthèse et donc son développement. Parmi ces facteurs, les principaux sont la lumière, la température et les apports en nutriments.

##### *La lumière*

La lumière est un facteur essentiel pour les producteurs primaires (Barranguet et al., 1998). En effet, lorsque les températures sont élevées et les concentrations de nutriments sont abondantes, les performances photosynthétiques du MPB sont directement liées à l'intensité lumineuse (Behrenfeld et al., 2004; Cole and Cloern, 1987). Néanmoins l'habitat du MPB peut jouer un rôle limitant sur l'intensité lumineuse. En effet, l'irradiante solaire arrivant à la surface du sédiment est atténuée avec la profondeur (Kühl et al., 1994; Morelle et al., 2018; Ploug et al., 1993). La distance de pénétration de la lumière dans le sédiment dépend particulièrement du

type de particules sédimentaires (Tester and Morris, 1987). Ainsi, des particules sédimentaires fines seront plus denses et laisseront moins pénétrer la lumière alors que des particules plus grossières la laisseront pénétrer plus en profondeur. Pour un sédiment de type sablo-vaseux, la zone photique du sédiment est donc restreinte à quelques millimètres (MacIntyre et al., 1996; Paterson et al., 1998). Bien qu'elle puisse être limitante du fait de sa faible intensité, la lumière peut à l'inverse être nocive lorsqu'elle est en excès (Cartaxana et al., 2013; Savelli et al., 2018) car le MPB n'est plus capable de réaliser la photosynthèse efficacement. En effet, lorsque l'intensité lumineuse est trop élevée pour le MPB, plusieurs mécanismes de photoprotection vont pouvoir être mis en œuvre. Le plus efficace de ces mécanismes consiste en une migration en profondeur dans le sédiment (Serôdio et al., 2008; Perkins et al., 2010). Ce mécanisme est avantageux pour le MPB car il présente un coût énergétique faible mais son efficacité dépend de la granulométrie du sédiment (Cartaxana et al., 2011). Si cette stratégie n'est pas suffisante, le MPB peut avoir recours au cycle des xanthophylles mais cela se traduit par un coût énergétique important diminuant ses performances photosynthétiques (Lavaud et al., 2007; Cartaxana et al., 2013; Blanchard et al., 1997). De plus, certaines espèces phytoplanctoniques et microphytobenthiques (Perkins et al., 2010) possèdent d'autres mécanismes de photoacclimatation tels que (i) la modification de la concentration pigmentaire (Falkowski, 1984), (ii) la modification de la composition pigmentaire, (iii) la modification de la taille des antennes collectrices (*ie.* l'ensemble de pigments et protéines associées à la chl *a*) des photosystèmes et (iv) la modification du nombre de photosystèmes.

### *La turbidité*

Pour le développement du MPB, la turbidité agit à marée haute de manière indirecte car elle limite la pénétration de la lumière dans la colonne d'eau (Smith and Mobley, 2008). Même si la turbidité joue un rôle bénéfique au fonctionnement des écosystèmes estuariens, elle peut à l'inverse limiter le développement du phytoplancton (Kromkamp et al., 1995). Ainsi du fait de la turbidité importante des estuaires, le MPB remis en suspension contribue grandement à la productivité apparente de la colonne d'eau (De Jonge and Van Beuselom, 1992; de Jong and de Jonge, 1995; Shaffer and Sullivan, 1988). À marée haute, à cause des niveaux de turbidité élevés des vasières la production primaire est considérée comme nulle. Dans des écosystèmes plus sableux (avec une colonne d'eau moins turbide), la production primaire microphytobenthique peut être réalisée mais reste faible et méconnue. L'exemple de la rade de Brest montre que la production primaire microphytobenthique est significative dans des zones jamais exondées (Chatterjee et al. 2013).

### *La température*

Difficilement dissociable de la lumière, la température joue également un rôle prépondérant sur le développement du MPB (Barranguet et al., 1998; MacIntyre et al., 1996). Plusieurs études montrent que le facteur thermique est le principal à déterminer le taux de production primaire (Guarini et al., 1998; Savelli et al., 2018). Ce paramètre joue de manière différente sur le MPB en fonction des espèces. En effet chaque espèce microalgale possède un optimum thermique de croissance. Lorsqu'elle est trop faible, la température peut engendrer une diminution de l'activité enzymatique liée à la photosynthèse limitant de ce fait la production primaire (Falkowski et al., 1992; Gallucci and Netto, 2004; Morgan-Kiss et al., 2006). De même, lorsque la température est trop élevée par rapport à l'optimum thermique du MPB elle peut devenir délétère à son développement. A titre d'exemple, l'espèce *Odontella litigiosa*, diatomée benthique de l'Antarctique, présente généralement une croissance maximale à 0°C et une inhibition complète de sa division cellulaire entre 7 et 9°C (Longhi et al., 2003). Dans les écosystèmes estuariens tempérés du nord de la France, l'optimum thermique a longtemps été estimé à 25°C (Guarini et al., 2000), mais il a été réévalué et est désormais estimé à 18°C (Rakotomalala et al., 2019; Savelli et al., 2018).

### *Les nutriments*

Les nutriments constituent un besoin essentiel aux performances photosynthétiques et au développement du MPB. Parmi les principaux nutriments figurent les ions nitrates ( $\text{NO}_3^-$ ), nitrites ( $\text{NO}_2^-$ ), ammonium ( $\text{NH}_4^+$ ), phosphates ( $\text{PO}_4^{2-}$ ) et silicates ( $\text{SiO}_4^{4-}$ ). Les silicates sont particulièrement importants pour les diatomées (Egge and Aksnes, 1992) car ils sont constitutifs de la paroi externe protectrice des diatomées : le frustule. Lorsque les nutriments sont en quantité limitante les performances photosynthétiques du MPB sont négativement impactées. Cette baisse de performances serait le résultat d'une altération de l'appareil photosynthétique inhibant les capacités de photoacclimatation du MPB (Raven and Geider, 2003). Dans les zones estuariennes souvent eutrophisées et donc riches en nutriments, le MPB bénéficie d'un apport de ressources suffisant pour optimiser son efficacité et sa capacité photosynthétique. Ainsi, en zone néritique estuarienne (zone qui s'étend du niveau de la marée basse jusqu'au bord du plateau continental) les nutriments ne limiteraient pas la biomasse et les taux de croissance du MPB (Underwood and Kromkamp, 1999). Néanmoins, sur l'estran, le type de sédiment joue sur la disponibilité des nutriments. En effet, un sédiment vaseux est associé à de fortes quantités de nutriments alors que le sédiment plus grossier (sableux) est associé à des concentrations en nutriments bien plus faibles (Admiraal, 1984; Underwood and Kromkamp, 1999). Les activités

bioturbatrices de certaines espèces de macrofaune benthique en surface peuvent faciliter la remontée des éléments nutritifs de la subsurface vers l'interface eau-sédiment, les sédiments à quelques centimètres de profondeur étant plus concentrés à la base des galeries ou des terriers de ces invertébrés (Kristensen et al., 2012). La colonisation des biofilms peut donc être stimulée par la présence de faune, même si les espèces dépositoires consomment directement ces biofilms (Chennu et al., 2015; Morelle et al., submitted). A très forte biomasse benthique, le rôle du broutage finit par faire baisser la quantité de biomasse chlorophyllienne microphytobenthique (Orvain et al., 2018).

#### *2.4.2. Rôle biostabilisateur des diatomées*

En plus de la cohésion purement physique des sédiments fins, un autre facteur agit sur la stabilisation du sédiment, il s'agit de la présence de diatomées microphytobenthiques. Cette influence biostabilisatrice est le résultat de l'excrétion d'EPS. Ces EPS créent une matrice 3D cohésive (Stal and de Brouwer, 2003; Tolhurst et al., 2002; Yallop et al., 1994) en lien avec le rythme migratoire des diatomées (Bellinger et al., 2005; Smith and Underwood, 1998). Les EPS sont essentiellement constituées de protéines mais aussi de polysaccharides (Decho, 2000), de protéoglycans et de lipides (Chiovitti et al., 2004; Underwood et al., 2004; Pierre et al., 2010). Ces substances polymériques remplissent diverses fonctions et participent à de multiples processus biologiques présentés dans le Tableau 1. La sécrétion de cette matrice d'EPS, qui représente 90 % du poids sec (Flemming and Wingender, 2010) va notamment jouer un rôle protecteur pour les microorganismes vis-à-vis des pressions environnementales extrêmes des vasières intertidales (comme par exemple la dessication, la sursalure et la présence de polluants).

Tableau 1 : Fonctions des EPS selon leur structure. Traduit de (Xiao and Zheng, 2016), adapté de (Flemming and Wingender, 2010).

Fonctions	Types d'EPS
Adhésion, cohésion du biofilm et agrégation cellulaire	Polysaccharides, protéines et ADN
Rétention d'eau	Polysaccharides et protéines
Sorption de composés organiques et d'ions inorganiques	Polysaccharides chargés et protéines
Source de nutriments	Tout type d'EPS
Source énergétique	Polysaccharides (dégradés par des enzymes)
Activité enzymatique	Protéines
Production d'enzymes	Polysaccharides et enzymes
Anti-virus, anti-oxydant, anti-tumoral et anti-inflammatoire	Polysaccharides
Surfactant, emulsifiant	Substituants (polysaccharides liés à des groupements méthyle et acétyle) et lipides

---

Exportation de composants cellulaires

Acide nucléique, enzymes, lipopolysaccharides et  
phospholipides

---

D'un point de vue structurel, en proximité directe de la cellule se trouvent des EPS formant un réseau compact entre la cellule et son cytosquelette, ce sont les EPS liées. Ces EPS sont jointes par des liaisons avec des cations bivalents et constituent un réseau dense appelé capsule autour de chaque diatomée. Plus en périphérie de la cellule, les EPS forment un réseau plus lâche, ce sont les EPS colloïdales qui sont facilement excrétés dans le milieu. Ces réseaux ne sont pas homogènes et peuvent favoriser la circulation de l'eau et des sédiments (Gibson et al., 2004). Les EPS liées et colloïdales sont composées en deux catégories : celles de bas poids moléculaire (LMW, <1 kDa) et celles de haut poids moléculaire (HMW, >1 kDa) (Amon and Benner, 1996). Ainsi, les EPS jouent une multitude de rôle dont celui biostabilisateur stabilisant la surface du sédiment et limitant ainsi sa remise en suspension.

#### *2.4.3. Remise en suspension du biofilm*

La remise en suspension du biofilm dépend de plusieurs facteurs dont l'âge et l'état physiologique des microorganismes le constituant ainsi que la composition du sédiment (Uberini, 2015; Joensuu et al., 2018). Cette remise en suspension est fortement liée à l'érosion tidale (Blanchard et al., 1997). Afin de limiter les effets de l'érosion, de grandes quantités d'EPS sont produites à la fin de la période d'émersion ce qui semble limiter le niveau de perturbation physique par érosion (van Duyl et al., 1999). L'érosion joue ainsi un rôle d'épuration et de sélection des diatomées en mauvais état physiologique et/ou en fin de vie. Cette élimination des diatomées moribondes aura également un rôle bénéfique au développement du biofilm à la prochaine exondation diurne. En effet, une partie du milieu sera à nouveau disponible pour l'établissement du biofilm se traduisant par un développement et une multiplication des diatomées benthiques. Un autre facteur de remise en suspension est l'activité de bioturbation faite par le macrozoobenthos. En effet, en plus de perturber le développement du biofilm, la bioturbation produite par la macrofaune peut conduire à la remise en suspension de particules (Orvain et al., 2004; Rakotomalala et al., 2015; Cozzoli et al., 2018). Ainsi, en fonction de leur type d'alimentation et de leur motilité, certaines espèces macrozoobenthiques pourraient remanier la surface des sédiments, entraînant ainsi la remise en suspension de particules sédimentaires mais aussi des microalgues associées à une fine couche bioturbée (Orvain et al., 2004).

## 2.5. Le viriobenthos

Les virus, dans le compartiment benthique des écosystèmes côtiers, sont considérés comme une boîte noire. Leur rôle écologique en tant que régulateurs biogéochimiques, de contrôle des populations bactériennes ou en tant qu'agents pathogènes des organismes marins doit être approfondi pour mieux anticiper la vulnérabilité des écosystèmes estuariens aux risques environnementaux et sanitaires (Filippini and Middelboe, 2007). Dans les écosystèmes marins, les virus sont les organismes les plus abondants avec des valeurs couvrant une gamme de  $10^7$  à  $10^{10}$  L $^{-1}$  et sont encore plus abondants dans le compartiment benthique avec des valeurs allant de  $10^7$  à  $10^{10}$  g $^{-1}$  de sédiments marins (Fuhrmann and Suttle, 1993; Weinbauer, 2004). Ces virus du milieu marin peuvent infecter une très large gamme d'hôtes spécifiques tels que les procaryotes (virus bactériophages), les eucaryotes unicellulaires et les métazoaires. Ces infections virales sont très fréquemment suivies de la mort de leur hôte avec un relargage massif de particules virales libres dans l'environnement. Ainsi, ces virus jouent un rôle essentiel dans la régulation des cycles biogéochimiques en assurant des fonctions de médiateur de la transformation et du recyclage de la matière organique et de l'énergie dans la boucle microbienne, avec des taux de mortalité des bactéries de l'ordre de 20 à 50 % et qui peuvent même exceptionnellement atteindre 100% (Danovaro et al., 2011; Heldal and Bratbak, 1991; Suttle, 2007; Wommack and Colwell, 2000). Les abondances virales sont extrêmement variables à microéchelle dans les sédiments et sont plus élevées en surface au sein de biofilms microphytobenthiques autotrophes qui sont une source d'oxygène. En effet, tout comme les activités bactériennes benthiques, le viriobenthos est clairement stimulé par le statut trophique de l'environnement et notamment après sédimentation de la matière détritique (Glud and Mathias, 2004; Hewson et al., 2001). L'abondance virale décroît dans les strates inférieures du sédiment où les accepteurs d'électrons varient graduellement. Les communautés microbiennes liées à la disponibilité chimique des accepteurs d'électron dominants et les plus efficaces en termes de métabolisme énergétique varient également avec les strates du sédiment (Glud and Mathias, 2004). Les abondances virales les plus élevées se trouvent dans les eaux estuariennes et plus particulièrement dans les eaux douces (Maier et al., 2011; Weinbauer, 2004). L'addition d'eau marine dans de l'eau douce en système expérimental montre un impact négatif sur la production virale alors qu'à l'inverse, une addition d'eau douce n'a pas d'effet négatif sur la production virale dans le compartiment marin (Hewson et al., 2001). Il existe également un lien direct positif entre la biomasse chlorophyllienne autotrophique et les concentrations virales

marines et ce résultat se retrouve dans les deux compartiments des écosystèmes marins : pélagiques et benthiques (Danovaro et al., 2011).

## 2.6. La macrofaune benthique

Le macrozoobenthos est un bio-indicateur de la qualité environnementale des écosystèmes côtiers (Dauvin, 2007; Dutertre et al., 2013) puisqu'il a été étudié afin de concevoir des plans de gestion (Carstensen et al., 2014; Dutertre et al., 2013; Keeley et al., 2013). Depuis, ces indicateurs benthiques sont régulièrement mesurés pour évaluer la dynamique spatio-temporelle notamment dans le cadre de la directive-cadre pour la stratégie-cadre pour le milieu marin (DCSMM) I (biodiversité). Certaines espèces macrozoobentiques, de par leur herbivorie, se nourrissent par broutage du MPB régulant ainsi son développement (*e.g.* le mollusque gastéropode *Peringia ulvae*). D'autres espèces du macrozoobenthos dites détritivores vont jouer un rôle très important dans la minéralisation de la matière organique en nutriments. La macrofaune benthique favoriserait ainsi grâce à son activité de bioturbation l'accès à la matière organique par les bactéries facilitant ainsi le rendement de leur activité de minéralisation (Papaspyrou et al., 2007; Welsh, 2003). Ces espèces sont associées à une stratégie de reproduction de type r (croissance rapide, forte descendance, forte croissance et forte mortalité...) et présentent souvent un caractère opportuniste reflétant leur dominance dans les zones polluées en matière organique (Lu and Wu, 1998; Whitlatch and Zajac, 1985). Le macrozoobenthos peut donc jouer un rôle épurateur lors de la contamination des sédiments en matière organique d'origines diverses (Bolam et al., 2004; Mermillod-Blondin et al., 2005; Rossi, 2006)

## 2.7. L'huître creuse *Crassostrea gigas* (Thunberg, 1793)

### 2.7.1. Enjeux économiques

Parmi les différents types d'aquaculture effectués, l'ostréiculture intertidale constitue l'une les plus importantes (FAO, 2006, 2018) en termes de production (15,3 millions de tonnes en 2016) et d'enjeux économiques. Parmi toutes les espèces de bivalves à travers le monde, l'huître *Crassostrea gigas* (Bayne et al., 2017) demeure celle la plus cultivée (FAO, 2018). De ce fait, *C. gigas* constitue un enjeu économique capital pour ce secteur en constant accroissement (Troell et al., 2014). Placée au quatrième rang mondial, la France représente le premier producteur ostréicole Européen (*i.e.* 90 % de la production européenne) avec une production moyenne de 130 000 tonnes en 2015 (Comité National de la Conchyliculture). Cette espèce a été importée en masse sur les côtes françaises dans les années 70 (Mineur et al., 2014) succédant

à l’huître portugaise *Crassostrea angulata* elle-même involontairement introduite d’Asie au XVI<sup>e</sup> siècle (Lapegue et al., 2004) pour pallier les mortalités des huîtres locales *Ostrea edulis*. De nos jours, *C. gigas* représente 99 % des espèces d’huîtres produites en France et pour toutes espèces de coquillages confondues, 54 % de la production conchylicole (Comité National de la Conchyliculture, 2015).

### 2.7.2. *Elevage*

#### *Cycle de culture*

Lors de l’épisode de ponte, les gamètes planctoniques sont libérés dans la colonne d’eau par les géniteurs adultes de *C. gigas*. Après fusion de ces gamètes (*ie.* fécondation puis développement larvaire méroplanctonique) les larves vont suivre différents stades (successivement : larve trochophore, larve D, larve véligère et larve pédivéligère) pour se fixer sur un substrat dur et se métamorphoser *in fine* en juvéniles ou naissain. Les ostréiculteurs capturent ces larves planctoniques lors de leur phase d’adhésion au moyen de collecteurs (*ie.* sur le Bassin d’Arcachon ou à Marennes-Oléron). Certaines années le captage naturel n’est pas jugé satisfaisant et les ostréiculteurs ont de plus en plus recours à des éclosseries pour se procurer du naissain et être moins dépendants des aléas du milieu naturel. Après la phase de naissain, les huîtres passent par une phase de pré-grossissement puis de grossissement durant laquelle elles vont croître jusqu’à atteindre un poids commercialisable de 30 - 45 grammes (calibre 5) à 151 – 200 g (calibre 0). Leur taux de croissance est variable en fonction de l’environnement (température, ressource trophique) et des pratiques d’élevage (Brown, 1988; Brown and Hartwick, 1988; Royer et al., 2007). Le cycle d’élevage peut ainsi varier entre 1 an et demi et 4 ans selon le bassin de production.

#### *Méthodes culturales*

A travers le monde, diverses méthodes de culture sont réalisées par les ostréiculteurs en fonction des caractéristiques du bassin d’élevage régional. Les huîtres peuvent être élevées sur (i) des cordes suspendues dans des lagons côtiers (par exemple, la lagune de Thau), (ii) des tables surélevées dans les zones intertidales (> 90 %) et (iii) des structures en eaux profondes (<10 %). De manière générale, dans les régions de l’Atlantique et de la Manche, les huîtres sont surélevées : placées dans des poches sur des tréteaux surélevés (de 50 à 80 cm de hauteur, 1 m de largeur et 3 m de longueur) appelés tables sur la zone de balancement des marées autrement dit, l’estrang. Ces tables sont mises bout à bout formant ainsi des rangées parallèles pouvant aller jusqu’à une centaine de mètres.

### 2.7.3. *Régime alimentaire de C. gigas*

L'huître est un organisme se nourrissant des particules en suspension dans l'eau de mer en la filtrant via ses branchies. Cet organe joue un rôle fondamental dans la respiration en milieu aquatique mais a considérablement été modifié et agrandi afin de jouer un rôle dans la nutrition chez cette espèce. Ensuite, l'huître va, à travers ses palpes labiaux et ses branchies, trier les particules aspirées afin de différencier les particules assimilables (*ie.* organiques) et celles à éliminer (*ie.* inorganiques). La digestion des particules assimilées va aboutir à la production de fèces et le rejet des particules non ingérées va aboutir à la création de pseudofèces. Par cette activité de filtration, *C. gigas* exerce un contrôle de type top-down sur les microorganismes constitutifs du réseau microbien planctonique (Berg and Newell, 1986; Mostajir et al., 2015) tels que le phytoplancton (Newell et al., 2007) et le MPB remis en suspension (Cognie et al., 2001; Lefebvre et al., 2009; Grangeré et al., 2010), les particules non chlorophylliennes (Charpy et al., 2012) et les microorganismes hétérotrophes : ciliés et flagellés (Dupuy et al., 1999).

### 2.7.4. *Des épisodes de mortalités*

Depuis des décennies, l'ostréiculture fait face à des difficultés liées à des épizooties pouvant nuire à sa pérennité. Les épidémies de mortalité chez les huîtres creuse *Crassostrea gigas* associées à des maladies complexes ont augmenté dans le monde depuis les années 2000 (Solomieu et al., 2015). Les coûts économiques et la vulnérabilité de l'élevage d'huîtres associée à une mortalité accrue ont favorisé les études des facteurs de risque de maladie pour améliorer la gestion de l'exploitation. En effet, par le passé certaines espèces d'huîtres cultivées ont été très largement décimées remettant drastiquement en cause leur utilisation en ostréiculture. Ce fut le cas de l'huître indigène des côtes européennes *Ostrea edulis* (huître plate) décimée par le protozoaire *Marteilia refringens* (Alderman, 1979) et *Bonamia ostreae* (Elston et al., 1987; Mialhe et al., 1988; Montes and Melendez, 1987; Pichot et al., 1981). Par la suite l'huître portugaise *Crassostrea angulata* fut décimée par un iridovirus à la fin des années 1970 (Comps et al., 1976). Ces disparitions quasi totales ont abouti à l'introduction de l'huître creuse *Crassostrea gigas*, d'abord dans le bassin de Marennes-Oléron, puis sur l'ensemble du littoral français. Plus spécifiquement, dans les écosystèmes estuariens tempérés, la mortalité des huîtres adultes est associée à l'augmentation temporelle de la température de l'eau de mer pendant la saison chaude, au débit d'eau douce des rivières et à la baisse subséquente de la salinité, ainsi qu'à l'augmentation excessive des concentrations d'éléments nutritifs et de phytoplancton, induisant des troubles métaboliques associés à l'effort de reproduction et au stress (Delaporte et al., 2006; Go et al., 2017; Royer et al., 2007; Soletchnik

et al., 2007). Il est intéressant de noter que les épisodes de mortalité enregistrés le long de la côte atlantique de la France entre 1986 et 2015 se produisaient généralement plusieurs mois après des hivers dominés par l'apparition de régimes de circulation atmosphériques positifs de l'oscillation nord-atlantique (NAO +) (Thomas et al., 2018). La NAO + se caractérise par des anomalies positives de la température de l'air et des précipitations et se traduit localement par une température de surface de la mer plus élevée, un débit de rivière plus élevé, une salinité plus basse et une concentration chlorophyllienne plus élevée en raison de l'intrusion d'eaux fluviales riches en nutriments (Thomas et al., 2018). De récents cas de mortalités d'huîtres adultes ont souvent été associés à *V. aestuarianus* (Goudénège et al., 2015; Parizadeh et al., 2018; Travers et al., 2017). Parmi les menaces biologiques actuelles pesant sur l'ostréiculture, les surmortalités de naissains d'huîtres induites par l'Ostreid Herpès Virus 1 (OsHV-1) figurent parmi les plus importantes. En effet, les taux de mortalité provoqués par cet agent infectieux qui affecte presque exclusivement les huîtres au stade naissain (Dégremont, 2011; Pernet et al., 2010), peuvent atteindre 80 % menaçant ainsi l'activité ostréicole. Des épisodes d'infection virale liés à un herpès virus ont pour la première fois été observés chez l'huître américaine *Crassostrea virginica* dans les années 1970 (Farley et al., 1972). En France, depuis 2008 les jeunes huîtres (âgées de moins d'un an) sont gravement atteintes par un génotype particulier : le microvariant de l'herpès virus 1 (OsHV-1  $\mu$ Var), alors que les adultes étaient confrontés à la réémergence de la bactérie *Vibrio aestuarianus* (Garnier et al., 2008; Azéma et al., 2017). C'est cependant depuis 1991 que les infections virales liées aux herpès virus se sont globalisées à l'échelle mondiale chez *C. gigas* (Hine, 1992; Nicolas et al., 1992; Renault et al., 1994) et c'est une décennie plus tard que pour la première fois OsHV-1 est observé (Arzul et al., 2002). Ce virus appartient à la famille des *Malacoherpesviridae* et plus particulièrement au genre *Ostreavirus* (Davison et al., 2009). Or depuis 2008, des épisodes de mortalités massives des naissains d'huîtres ont eu lieu en période estivale (Renault, 2011a) et sont régies par différents paramètres environnementaux (Rodgers et al., 2018). Par exemple, ces épidémies liées à OsHV-1  $\mu$ Var sont liées à la température de l'eau de mer (Pernet et al., 2012; Petton et al., 2013; Delisle et al., 2018), la salinité (Fuhrmann et al., 2016), le pH (Fuhrmann et al., 2019), les communautés bactériennes (Lemire et al., 2015; Petton et al., 2015a; de Lorges et al., 2018), la proximité des parcs à huîtres (Pernet et al., 2018; Gangnery et al., 2019) et le régime hydrodynamique (Orvain et al. in prep). Pour faire la synthèse des différents facteurs, l'étude de la connectivité avec les eaux estuariennes provenant des apports fluviaux par l'usage de simulations de modèle physique (MARS3D) permet de mieux comprendre les risques de mortalité et leur dispersion dans le milieu en baie des Veys (Gangnery et al., 2019). Les eaux estuariennes très turbides et

saumâtres sont plus propices aux mortalités et des gradients de mortalité dans les milieux de transition entre les eaux estuariennes et les eaux marines du domaine ouvert (Pernet et al., 2018; Gangnery et al., 2019). Ces mortalités récentes seraient accrues et associées au variant d'OsHV-1 ayant subi une mutation génétique (Segarra et al., 2010a). Les épisodes de mortalités de naissains récents, liés à OsHV-1 μVar (Segarra et al., 2010a, 2014), sont qualifiés d'épisodes de surmortalités pour les différencier des épisodes précédents (Renault, 2011a). Il a récemment été démontré que OsHV-1 μVar n'était pas le seul facteur provoquant la surmortalité des naissains d'huîtres. En effet, il semblerait que la réPLICATION virale de OsHV-1 μVar conduit premièrement à un état immunodéprimé des naissains d'huîtres favorisant dans un second temps une bactériémie provoquée par des bactéries de type opportuniste (de Lorgeril et al., 2018; Petton et al., 2015a) souvent du genre *Vibrio* (De Decker et al., 2011; Schikorski et al., 2011). De nos jours, le rôle de l'habitat ostréicole lié à la culture intertidale reste incertain. Ce type de culture engendre une alternance caractéristique entre tables et allées aboutissant à une structuration à petite échelle de l'habitat ce qui pourrait contribuer aux épisodes de mortalités liés à OsHV-1 μVar.

### **3. Impact des techniques ostréicoles sur l'environnement à l'échelle de la table**

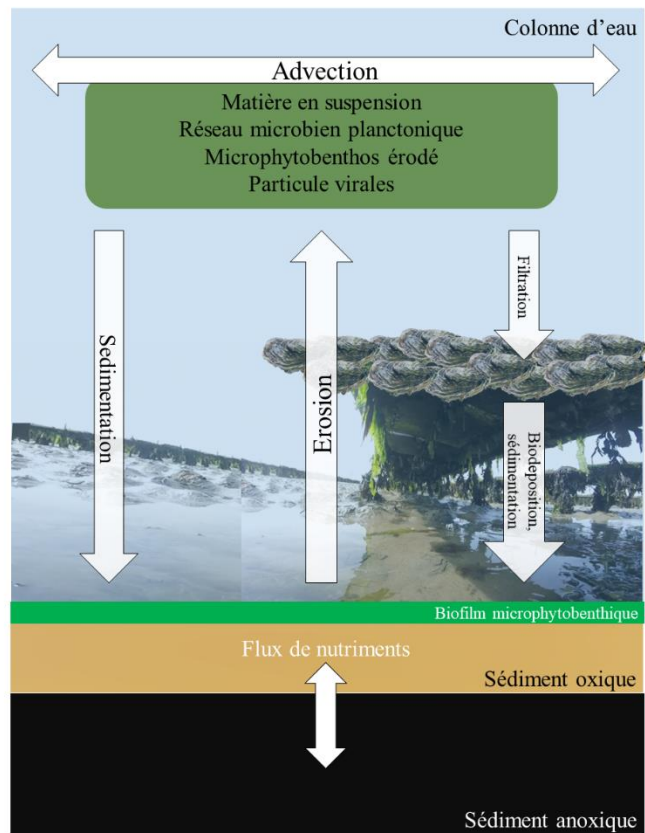
L'ostréiculture est une activité aquacole pouvant impacter le fonctionnement des écosystèmes côtiers (Ubertini et al., 2012; Troell et al., 2014; Echappé et al., 2018). En effet, l'implantation d'une activité de d'élevage s'accompagne de conséquences sur son environnement (Figure 3). Ces perturbations environnementales peuvent être d'autant plus importantes dans le cadre d'une monoculture semi-intensive.

#### **3.1. Influences physiques**

Les structures métalliques disposées sur l'estran pour soutenir les poches à huîtres sont connues pour atténuer la vitesse de friction (Sornin, 1981; Nugues et al., 1996; Kervella et al., 2010). L'étude de Kervella et al., (2010) met en évidence que le développement asymétrique des régimes d'écoulement induit par les tables à huîtres crée un important effet de "flux rasant". Ces tréteaux en acier munis de poches à huîtres peuvent créer des zones locales préférentielles d'envasement et ce processus physique affecte jusqu'à 10 fois la contrainte de cisaillement. Ces auteurs insistent sur le rôle majeur de la direction du flux local dans l'explication de la dynamique potentielle des sédiments, en relation avec l'axe d'alignement de la table. Ainsi le lien écologique entre les huîtres cultivées et l'habitat benthique est très étroit par rapport à

d'autres méthodes de culture car les huîtres sont à proximité immédiate de la surface des sédiments (Orvain et al., 2012; Sornin and Mariojouls, 1987). Les pieds métalliques des tables à huîtres peuvent également représenter un obstacle à l'échouage des macro-algues en haut d'estran afin de constituer la laisse de mer. Ces macroalgues sont ainsi retenues et se dégradent dans les parcs à huîtres. Ainsi, cet apport massif de matière organique peut être considéré comme une forme d'eutrophisation pouvant favoriser une anoxie des sédiments et un stress polluant pour les jeunes huîtres.

- Biodéposition et aggrégation
- Bioturbation : stimulation de la production primaire microphytobenthique
- Envasement local et facilitation d'érosion de surface
- Adhésion virale (biofilm de MPB)



- Effet de la structure physique (frein advectif)
- Biodéposition
- Déplétion en SPM et en biomasse chlorophyllienne
- Excrétion en nutriments
- Changement d'habitat sédimentaire (envasement local) et de biocénose
- Exclusion trophique et enrichissement en matière organique particulaire
- Stimulation de biofilms microphytobenthiques
- Adhésion virale sur les EPS des biofilms

Figure 3 : Schéma des interactions entre bivalves filtreurs, biodéposition, biofilms microphytobenthiques

Les poches à huîtres posées sur les tables vont diminuer la lumière ainsi que la température arrivant à la surface du sédiment créant ainsi un ombrage. Cette altération de la lumière aurait des conséquences sur la croissance, la productivité et la répartition en profondeur du MPB. De plus, les structures sur lesquelles sont cultivées les huîtres fournissent un substrat solide sur lequel peuvent se développer des espèces auparavant absentes sur la zone de culture (Ruesink et al., 2005). Ces espèces peuvent être des invertébrés sessiles et mobiles, ce qui peut attirer des poissons et des oiseaux. Ces structures peuvent aussi faciliter le développement de macroalgues.

### 3.2. Influences biogéochimiques

Lié à son activité de filtration, l'huître *Crassotrea gigas* capte les particules en suspension de la colonne d'eau. Cette activité peut amener dans certains cas à améliorer la qualité de l'eau en limitant les blooms phytoplanctoniques (Porter et al., 2004; Fulford et al., 2007; Cugier et al., 2010) ainsi que la turbidité faisant des huîtres de potentiels bioremédiateurs (Dalrymple and Carmichael, 2015; Mostajir et al., 2015), bien que ce concept reste controversé (Newell et al., 2007). En effet, *C. gigas* n'est pas capable de filtrer efficacement l'ensemble des microorganismes du réseau microbien planctonique et en particulier les picoparticules (Dupuy et al., 2000) et peut favoriser le développement d'organismes hétérotrophes (Lam-Hoai et al., 1997; Souchu et al., 2001). Ainsi ces bivalves peuvent effectuer un forçage sur le réseau microbien planctonique favorisant la mise en place d'un statut hétérotrophe (Dupuy et al., 2000; Mostajir et al., 2015; Richard et al., 2019). Un écosystème hétérotrophe peut tendre vers une hypoxie voire une anoxie et le milieu sera ainsi considéré comme étant en mauvais état écologique. Cette tendance à l'anoxie peut être observée lors d'échouages de macroalgues dans le cas de la Baie des Veys (Normandie, France). De ce fait, l'ostréiculture peut représenter une menace pour l'équilibre transitoire des écosystèmes lorsque cette activité est incorrectement gérée.

En conséquence de son régime alimentaire, *C. gigas* produit des biodépôts (fèces et pseudofèces) issus de la turbidité retenue par les filtres branchiaux et qui s'accumulent dans les sédiments situés sous les structures ostréicoles (Ottmann and Sornin, 1985; Sornin, 1981) ce qui peut considérablement enrichir le sédiment en matière organique (Mitchell, 2006; Newell et al., 2007; Ottmann and Sornin, 1985). Cette matière organique favorise le développement bactérien qui réalise une activité de minéralisation. Dans le cas de la culture intertidale ces effets seraient limités par la marée comparée à la culture sur corde (eg. Lagune de Thau) où le renouvellement en eau est plus limité. Lors de l'écoulement advectif de la masse d'eau, les particules inorganiques en suspension sont captées, triées et éliminées par les huîtres en amont du système digestif via les palpes labiaux. Ainsi, au lieu d'être transportées dans la colonne d'eau, une partie des particules inorganiques est captée et rejetée sous forme de pseudoféces. Cette modification de la dynamique sédimentaire résulte en un flux localisé des particules en suspension vers le compartiment benthique favorisant un envasement de la zone qui peut parfois aboutir à des changements visibles de la topographie (Forrest and Creese, 2006; Ottmann and Sornin, 1982). L'augmentation de la proportion en particules fines dans le sédiment se fait dans

la zone de parc à huîtres ainsi que les zones adjacentes qui reçoivent les eaux riches en biodépôts.

Ces modifications des caractéristiques de l'environnement biogéochimique induites par l'ostréiculture vont impacter les espèces vivant dans l'habitat benthique. Liés aux fèces des huîtres, les apports de MO plus ou moins constants vont façonner l'écosystème ostréicole en profondeur et donc structurer les communautés benthiques associées. En revanche des apports de MO brutaux peuvent survenir dans ces écosystèmes lors d'événements tels que des échouages de macroalgues ou des mortalités massives d'huîtres. Ce largage de MO peut être considéré comme une pollution et certaines espèces ne pourront pas résister à ces conditions environnementales stressantes aboutissant à l'élimination totale de la macrofaune benthique à cause de l'anoxie impactant les sédiments sous-jacents. Certaines espèces peuvent faire face à de fortes quantités de MO telles que certaines qualifiées d'opportunistes (eg. *Tubificoides benedii*, *Capitella capitata*), qui peuvent recoloniser des zones fortement polluées. Ainsi l'ostréiculture est connue pour impacter son environnement à grande échelle et notamment la macrofaune benthique (Coen et al., 2007; Forrest et al., 2009a; Ubertini et al., 2012). Les autres bivalves comme la coque commune sont également exclus des zones de parcs à huîtres à cause de la compétition trophique entre suspensivores et de l'accumulation de matière organique défavorable à la survie des juvéniles de bivalves endogés sous les tables à huîtres.

### **3.3. Structuration de l'habitat à mésoéchelle**

La culture intertidale d'huîtres crée une alternance caractéristique entre table et allées aboutissant à une structuration à petite échelle de l'habitat. Ainsi, deux habitats se distinguaient (Figure 4).

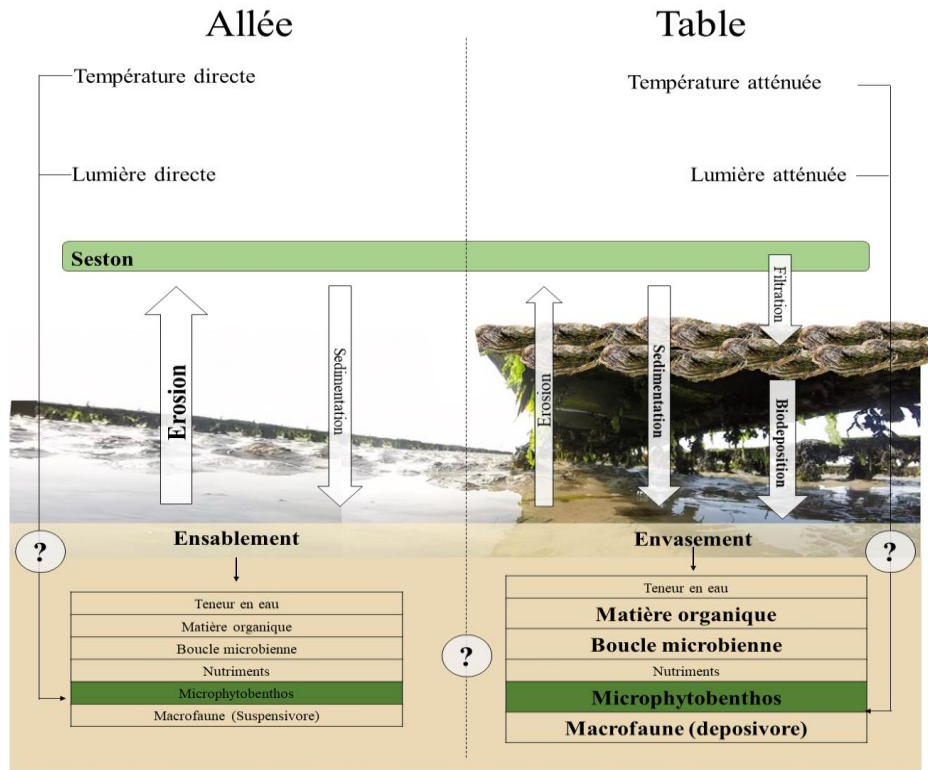


Figure 4 : Caractéristiques théoriques des habitats créés par l’alternance des tables à huître

Le premier, sous les tables à huîtres, présenterait une atténuation de la lumière et donc une quantité moindre de rayonnements UV atteindrait la surface du sédiment. De plus, cette limitation des radiations solaires impactera le développement microphytobenthique avec des zones de croissance préférentielles en fonction de la lumière et de la température. Ainsi ces disparités dans le développement du MPB devraient également induire une sécrétion différente en EPS. Ces substances polymériques favorisent la rétention de l'eau et évite la dessiccation, favorisent la cohésion et agrégation des cellules et offrent globalement une protection contre les stress physicochimiques et la sursalure des eaux interstitielles (Orvain et al., 2014b). En conséquence de cette cohésion des particules la force d'érosion nécessaire à une remise en suspension devra être supérieure. De plus, du fait de l'activité de biodéposition des huîtres une plus forte teneur en MO et en particules sédimentaires fines ( $< 63 \mu\text{m}$ ) sont observées dans les parcs à huîtres (Ubertini et al., 2012) lié à l'envasement retenant ainsi plus durablement l'eau en surface. Ces quantités importantes de matière organique stimuleraient l'activité de minéralisation des bactéries augmentant ainsi la disponibilité des nutriments. A l'inverse, dans les allées, aucune atténuation de la lumière et de la température ne sont provoquées en l'absence de table à huîtres. Ainsi la lumière et la température pourront être des facteurs d'inhibition (photoinhibition et thermoinhibition). De ce fait la photobiologie du MPB sera perturbée et les quantités d'EPS altérées. De même, en l'absence d'huîtres au-dessus de la zone et donc de leur

activité de biodéposition, une quantité de particules fines plus faible et donc de particules plutôt sableuses constitueraient le sédiment. De ce fait, l'érosion de l'habitat benthique se trouverait facilitée. De plus, une fraction de matière organique plus faible serait observée dans les allées ne pouvant que légèrement stimuler la boucle microbienne limitant la régénération de MO en nutriments. Dans ce cas, la croissance du microphytobenthos serait limitée et les espèces dépositoires (*ie.* brouteurs de biofilms microphytobenthiques) de la macrofaune seraient par conséquent relativement rares.

## **4. Dynamique environnementale viriobenthique, tables à huîtres et épisodes de mortalités liés à OsHV-1 μVar**

Les suivis sanitaires de la qualité microbiologique des mollusques exploités doivent mieux intégrer la surface des sédiments marins car les risques de survie et de résistance des formes libres de microorganismes pathogènes sont très prononcés (Luna et al., 2010). Ces mesures de qualité microbiologique des eaux marines sont presque exclusivement basées sur le suivi au sein de la colonne d'eau, alors que le réceptacle à long-terme des microorganismes (dont les pathogènes) se trouve à la surface du sédiment pour lequel de plus en plus d'études montrent que ce réservoir permet la survie, voir la sélectivité des formes de résistance. La remise en suspension du sédiment permet de relarguer des quantités de virus et de bactéries qui peuvent être très élevées (Dupuy et al., 2014; Mallet et al., 2014). Les menaces liées aux bivalves ne sont pas simplement limitées aux virus les contaminant, mais aussi à leur rôle de transmission des virus nuisibles à la santé humaine. En effet, les virus contaminant *Homo sapiens* ne se multiplient pas en dehors des cellules hôtes, mais les eaux estuariennes peuvent être parfois chargées en virus entériques susceptibles de contaminer les mollusques bivalves consommés par les populations humaines (Lees, 2000). Les contaminations virales des bivalves apparaissent de manière très fréquente car ces animaux capturent leur nourriture en filtrant de fines particules et tout particulièrement les micro-algues (Lees, 2000), ils sont alors dits suspensivores. Parmi les organismes marins, les bivalves sont ceux les plus sujets à transmettre des sources virales issues de contaminations fécales (Lees, 2000; Umesha et al., 2008) comme celles responsables d'infections gastroentériques (Calicivirus, Astrovirus, Rotavirus, Adénovirus, Entérovirus) et les virus Hépatiques (A et E). Les poliovirus sont également susceptibles d'être transmis via les bivalves (Lees, 2000). Les virus pathogènes de la macrofaune et en particulier de la malacofaune (*c'est-à-dire* les mollusques) sont aussi susceptibles de se trouver en abondance à la surface des sédiments et tout particulièrement des biofilms microphytobenthiques stimulés par l'activité de biodéposition et de bioturbation de

ces animaux filtreurs (Dupuy et al., 2014). Or, une majorité de ces micro-algues qui participent au régime alimentaire des bivalves filtreurs proviennent du compartiment benthique, réceptacle naturel en microorganismes estuariens (Lefebvre et al., 2009). Cependant, la capacité des pathogènes à survivre, résister et se propager dans le milieu de transition fluvio-marin que sont les estuaires sont des processus à approfondir puisque ces milieux sont à proximité de zones (i) d'activité humaines récréatives, (ii) de culture et/ou de pêche d'organismes marins consommés tels que de nombreux mollusques bivalves (huîtres, moules, coques, palourdes...). Ainsi, les risques de contamination épidémiologique des élevages de mollusques destinés à la consommation humaine, doivent être surveillés de façon optimale afin de préserver une gestion durable de ces milieux côtiers.

#### **4.1. Rôle des EPS sur la survie virale**

Les sédiments côtiers marins forment un habitat très favorable à la survie et au développement des microorganismes pathogènes. En effet, les biofilms à la surface des vasières intertidales subissent une multitude de stress et exercent une pression sélective susceptible de stimuler l'émergence de formes de résistances comme cela a été observé pour la bactérie *Escherichia coli*, devenue résistante aux polluants accumulés dans un biofilm (Luna et al., 2010; Vignaroli et al., 2012). La survie de nombreux pathogènes, serait donc liée à leur association aux floculats biologiques très riches en matière organique (eg. EPS) ou aux particules minérales. L'agrégation en flocs accélère le taux de sédimentation et explique ainsi la richesse des sédiments intertidaux en matière organique et en microorganismes de toute sortes. Dans les biofilms microphytobenthiques, les EPS peuvent être considérées comme des éponges absorbant les molécules organiques et les ions à proximité, tout comme potentiellement des virus et bactéries pathogènes. En parallèle, du fait de l'érosion tidale et des vagues, les diatomées benthiques sont régulièrement mises en suspension dans la colonne d'eau où elles peuvent également capter des particules à leur surface avant de sédimenter à nouveau (comportement tychopélagique). Les virus ont ainsi une tendance à se lier avec ces EPS grâce à la propriété adhésive de cette matrice extracellulaire et/ou aux forces électrostatiques ainsi qu'aux processus physico-chimiques qui s'exercent à leur surface. En effet, les EPS peuvent former des complexes ioniques avec les molécules telles les glycoprotéines que l'on peut trouver à la surface des capsides virales. De même, les EPS liés ont une activité antibactérienne (Agogué et al., 2014; Orvain et al., 2014a; Doghri et al., 2017) qui pourraient inhiber la production bactérienne et la libération d'exoenzymes bactériennes au contact direct des diatomées. Ainsi, parmi la diversité des fonctions attribuées aux EPS (voir Tableau 1), il a été

démontré que la matrice d'EPS des biofilms fournit un refuge aux microorganismes pathogènes, en tamponnant les stress potentiels (et notamment une protection contre le stress halin qui est le premier facteur de stress auquel les microorganismes d'eau douce sont soumis, (Defer et al., 2009; Orvain et al., 2014b). La plupart de ces microorganismes sont sensibles à la concentration en sel (choc halin) ce qui entraîne une forte diminution des abondances virales et bactériennes dans le milieu marin, comparé aux habitats des eaux douces (Filippini and Middelboe, 2007). En outre, ces substances polymériques pourraient favoriser la persistance du viriobenthos dans l'habitat sédimentaire car elles diminuent l'érosion benthique.

## 4.2. Rôle de la lumière sur la survie virale

Les rayonnements UV induits par l'irradiation solaire pourraient être néfastes pour l'intégrité structurelle des virus. En effet, le déclin de virulence (abattement) dans l'environnement marin lorsque le virus est libre est accentué par les UV et l'activité des exoenzymes bactériennes. Bien que le mécanisme exact qui influerait sur la résilience des pathogènes fixés au sein des EPS reste incertain (Decho, 2000) les biofilms microphytobenthiques sont connus pour être des zones d'accumulation de ces virus qui pourraient faciliter la résistance des virus puisque l'activité photosynthétique des diatomées et des cyanobactéries est très efficace pour capter la lumière et ainsi réduire les taux d'irradiation UV. En effet, le coefficient d'extinction de la lumière qui est très élevé pour les diatomées (Forster and Kromkamp, 2004; Serôdio, 2004) et les stratégies de migrations verticales mises en jeu par les diatomées (Mitbavkar and Anil, 2004; Orvain et al., 2003) leur permet d'éviter les irradiations très élevées en surface pendant la période estivale et surtout lorsque les périodes de basse-mer coïncident à l'heure de midi (situation observée en mortes-eaux sur les côtes du Calvados). Des tests de traitement UV ont été réalisés par Leal Diego et al. (2013) sur un cortège de virus gastroentériques humains (contamination fécale). Ces auteurs ont observé que les contaminations virales des huîtres *Crassostrea gigas* ont tout de même lieu malgré le traitement UV. Les virus bénéficiaient donc dans l'environnement estuarien de mécanismes de défense anti-UV qui pourraient notamment s'expliquer par une association aux microalgues benthiques constitutives du biofilm.

## 4.3. Interactions avec la macrofaune

Un autre facteur pouvant jouer sur la dynamique environnementale des malacovirus est la macrofaune benthique. Ces organismes peuvent interagir de manière directe ou jouer sur

conditions environnementales benthique et ainsi sur la persistence potentielle des virus mais aussi représenter un vecteur de transmission (Arzul et al., 2001a, 2001b; Rodgers et al., 2018).

### *Virus en suspension*

Dans le cas des bivalves marins, lorsqu'une virose se produit chez son hôte une grande quantité de virus est produite puis relarguée dans l'environnement avant mais surtout lors de la mort des individus (Evans et al., 2015; Paul-Pont et al., 2015; Schikorski et al., 2011). Ainsi, les valves des mollusques s'ouvrent car le muscle adducteur n'est plus fonctionnel et certaines espèces nécrophages pourraient se nourrir de la chair fraîchement disponible. Ces nécrophages capables de venir directement dans les poches à huîtres vont donc être en contact direct avec le virus. Après digestion, il est probable que le virus ait potentiellement été dégradé et inactivé par ces individus de la macrofaune. Une fois relargué dans l'environnement le virus va se retrouver en suspension et, à terme, sédimentier vers le compartiment benthique. Concernant la fraction en suspension dans la colonne d'eau, elle pourra être captée par les organismes filtreurs (*Mytilus edulis*) et potentiellement dégradée. Cette fraction de virus disponible pourra également se propager par advection de la masse d'eau et infecter d'autres hôtes à proximité en fonction des courants côtiers. Après avoir sédimenté, les particules virales qui n'auront pas été captées vont se retrouver à la surface du sédiment et pourront subir différents stress et trouver des conditions environnementales plutôt favorables.

### *Virus en environnement benthique*

L'ensemble des caractéristiques benthiques et des biofilms laissent à penser que les malacovirus pourraient s'y fixer et trouver les conditions environnementales profitables à leur persistance. Les biofilms peuvent ainsi être très riches en herpès-virus et les organismes qui les consomment peuvent donc être directement contaminées. C'est pourquoi certains ont développé des mécanismes de défense antiviraux. A titre d'exemple la coque (*Cerastoderma edule*) dont le régime alimentaire est dominé par les microalgues benthiques remises en suspension (Lefebvre et al., 2009) est le mollusque possédant dans son hémolymphé le plus fort taux de molécules antivirales contre les herpès-virus (Defer et al., 2009).

Certaines espèces de la macrofaune vont perturber la surface du sédiment par leur activité de locomotion et/ou par leur mode de nutrition : on parle alors de bioturbation. En effet, des espèces telles que le mollusque gastéropode *Peringia ulvae* se nourrissent principalement de biofilms de MPB et vont ainsi perturber l'établissement d'un biofilm mature offrant les meilleures conditions à la persistance des virus. Au delà des espèces qui se nourrissent de MPB,

certaines vont induire des perturbations en surface par leur mobilité effectuant une sorte de labourage. Ainsi ces espèces peuvent potentiellement remettre en suspension des particules (Dupuy et al., 2014; Rakotomalala et al., 2015; Cozzoli et al., 2018) mais surtout perturber le développement microphytobenthique. A l'inverse, le projet GECO-GECO (AESN/CRBN/CG14/CG50) a montré que les coques peuvent ainsi favoriser la stabilité sédimentaire en facilitant l'envasement local et donc l'extension des zones sablo-vaseuses et son rôle essentiel en tant qu'ingénieur d'écosystème. Cette tendance induite à l'envasement pourrait limiter l'érosion benthique et favoriserait la stabilité de l'habitat benthique. De plus, cet animal structurant son habitat sédimentaire, son érodabilité mais aussi les transferts trophiques du compartiment benthique vers le compartiment planctonique cela a permis de mettre en évidence un phénomène de « jardinage écologique ». En effet, les coques peuvent (i) stimuler la production primaire microphytobenthique autour de leurs terriers et (ii) faciliter l'érosion des biofilms microphytobenthiques pour alimenter les juvéniles de coques (Rakotomalala et al., 2015). Etant donné les niveaux importants d'interactions trophiques entre les 2 bivalves principaux de la baie des Veys : *C. gigas* et *C. edule* (Ubertini et al., 2012), il est fortement probable que des sauts inter-espèces en termes de transferts de virus ou des rôles de réservoir aient lieu. Une expérience en laboratoire a été menée au cours de cette thèse pour mieux comprendre le rôle des coques comme intermédiaire facilitant ou encourageant la transmission virale OsHV1 aux naissains d'huîtres. Cetté étude en laboratoire n'est pas présentée dans ce manuscrit, car les résultats n'ont pas permis d'identifier les effets d'interaction attendus. Les interactions possibles et nos hypothèses étaient : 1) un rôle positif sur la survie par une activité suspensivore des coques permettant de retenir les particules virales au fond, 2) un échange de microbiome des branchies des 2 virus qui se traduirait par des interactions positivés et 3) un effet positif des coques sur les taux de transmission virale en jouant positivement sur le développement des biofilms microphytobenthiques, favorisant *in fine* l'accumulation virale à proximité immédiate des huîtres.

#### **4.4. Rôle de l'habitat table à huîtres sur le viriobenthos**

Comme indiqué auparavant, l'ostréiculture intertidale crée une structuration à petite échelle de l'habitat alternant entre les tables et les allées. Cette structuration de l'habitat pourrait jouer sur la répartition du virus OsHV-1 μVar. Sous les tables à huîtres l'atténuation de la lumière et de la température pourrait réduire la quantité de rayonnements UV atteignant la surface du sédiment. Cet ombrage atténuerait l'effet néfaste des rayons UV sur l'intégrité structurelle des virus. De plus, cette limitation des radiations solaires impacterait également le développement

microphytobenthique avec des zones de croissance préférentielles. Ainsi ces disparités dans le développement du MPB pourraient induire une sécrétion en EPS différente. En conséquence de cette cohésion des particules la force d'érosion nécessaire à une remise en suspension devra être supérieure. De plus, du fait de l'activité de biodeposition des huîtres une plus forte teneur en MO et en particules sédimentaires fines ( $< 63 \mu\text{m}$ ) sont observées dans les parcs à huîtres (Ubertini et al., 2012) lié à l'envasement. Les communautés de la macrofaune benthique caractéristiques de l'environnement ostréicole pourrait également être impactées à l'échelle de la table à huîtres. Ces espèces de la macrofaune benthique pourraient impacter le viriobenthos par leur type de locomotion et de nutrition en perturbant la surface du sédiment par bioturbation. La bioturbation englobe des effets de remaniement sédimentaire permettant la formation d'une fine couche granulaire en surface, généralement facilement érodable (Orvain et al., 2004), mais aussi des effets de mouvements fins à l'intérieur de galerie jouant surtout sur la bioirrigation des flux aqueux à travers des sédiments perméables (Chennu et al., 2015). Ainsi, il apparaît nécessaire de mieux connaître les biofilms microphytobenthiques, leur érodabilité ainsi que leurs interactions avec la bioturbation par la macrofaune benthique vivant sous les tables à huîtres dans les écosystèmes conchyliques bas-normands et leur rôle potentiel en tant que réservoir et vecteur de transmission épidémiologique des virus mais aussi des bactéries pathogènes.

## 5. Etudes antérieures à cette thèse en baie des Veys

Plusieurs études ont auparavant été réalisées en Baie des Veys et ont abouti à la mise en place de ce projet de recherche. Les mortalités de naissains d'huîtres liées à OsHV-1  $\mu\text{Var}$  se manifestent lorsque la température de l'eau dépasse un seuil thermique avoisinant les  $15,5^\circ\text{C}$  (Pernet et al., 2012; Petton et al., 2013, 2015b). Néanmoins la dynamique environnementale de cet agent infectieux lors d'un épisode de mortalité reste encore mal connue. En effet, lors d'un épisode de mortalités les chairs dégradées des huîtres mortes vont être transportées dans la colonne d'eau mais le devenir du virus reste incertain. La persistance dans l'environnement des agents pathogènes tel que les virus pourrait être impactée par les caractéristiques environnementales créées par l'ostréiculture intertidale en zone estuarienne. Depuis 2008 et comme sur l'ensemble du littoral français, les surmortalités de naissain d'huîtres creuses *Crassostrea gigas*, associées au virus OsHV-1, sont importantes sur les parcs ostréicoles bas-normands. Lors de ces épisodes de mortalités, le transfert d'animaux infectés entre les bassins ostréicoles et la propagation entre parcs avoisinants paraissent être les causes de la propagation du virus entre les parcs ostréicoles. Les animaux semblent être eux-mêmes le réservoir de virus

(Petton et al., 2015b). En effet, lorsque des spécimens sentinelles (vierges de tout virus) sont introduits sur un parc ostréicole à proximité des zones estuariennes, ils sont rapidement infectés (Petton et al., 2015b), sans qu'il soit possible de discerner la source d'infection entre les huîtres déjà présentes et d'autres potentiels « réservoirs » environnementaux. A ce jour, les études scientifiques n'ont jamais permis d'identifier des « réservoirs » à virus environnementaux. Lors du programme VIAPSE (Centre de Référence sur l'Huître réalisé en 2014) des éléments de réponse ont pu être apportés sur les processus de diffusion du virus lié aux facteurs biotiques (comme la mise en réserve et la reproduction) et abiotiques (température, pratiques zootechniques, milieu...). Sur cette base, ce projet de thèse avait pour objectifs d'approfondir les résultats obtenus au cours du programme VIAPSE pour étudier la dynamique environnementale de OsHV-1 μVar lors d'épisodes de mortalités de naissains d'huîtres.

## 5.1. Résultats antérieurs à cette thèse

### 5.1.1. Dynamique environnementale de OsHV-1 μVar

En 2014 lors du programme VIAPSE, des prélèvements de biofilm et de sédiment ont été réalisés à proximité et dans des parcs ostréicoles afin d'étudier leur capacité à représenter des conditions favorables à la persistance du virus OsHV-1 μVar dans l'environnement ostréicole. Les prélèvements ont été réalisés à deux fréquences : tous les 2 mois (hors période à risque) et tous les mois (durant la période estivale à risque) sur 3 points précis (A, B et C) en Baie des Veys (Figure 5).

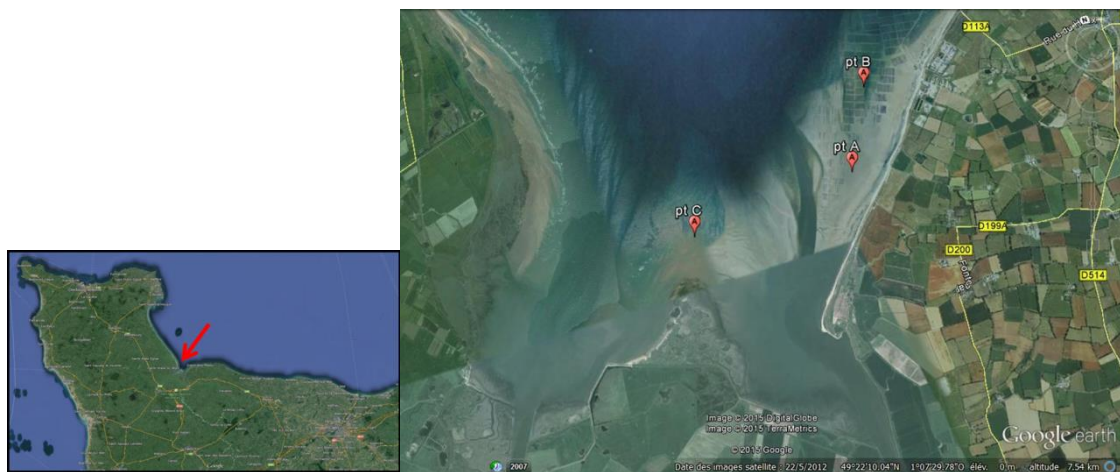


Figure 5 : Cartographie des points de prélèvements réalisés en Baie de Veys lors du projet VIAPSE. Points : A : Sud des parcs de Géfosse, B : Dans les parcs de Géfosse, C : Pointe de Brévands (Sud des parcs).

Le point A (Figure 5) situé au Sud de la zone d'étude reçoit des dépôts sédimentaires issus des parcs ostréicoles de Géfosse-Fontenay représentés par le point B situé au sein des parcs de

Géfosse. Le point C était situé sur la pointe de Brévands, de l'autre côté du chenal et plus éloigné de la zone des parcs (~2 km). A chaque date, des prélèvements de biofilm et de sédiments ont été réalisés (Figure 6) et les charges virales ont été mesurées et rapportées par unité de surface. Ainsi, dans le biofilm, les charges virales retrouvées sur les 3 points étaient toujours supérieures à  $10^6$  Unités Génomiques (UG)/m<sup>2</sup>. Ces charges virales étaient plus faibles en période estivale (Juin à Août) avec  $10^6$  à  $10^7$  UG/m<sup>2</sup> comparées à celles observées en hiver (Février et Octobre – Décembre) avec  $10^7$  à  $10^9$  UG/m<sup>2</sup>. De manière surprenante une très faible charge virale en OsHV-1 μVar était constatée au mois d'Août au Sud des parcs. Une charge plus importante sur la Pointe de Brévands a été observée dans le biofilm en octobre, au point le plus distant des parcs à huître, où les développements de biofilms microphytobenthiques et les populations de coques sont les plus élevés en Baie des Veys (Orvain et al., 2012; Ubertini et al., 2012).

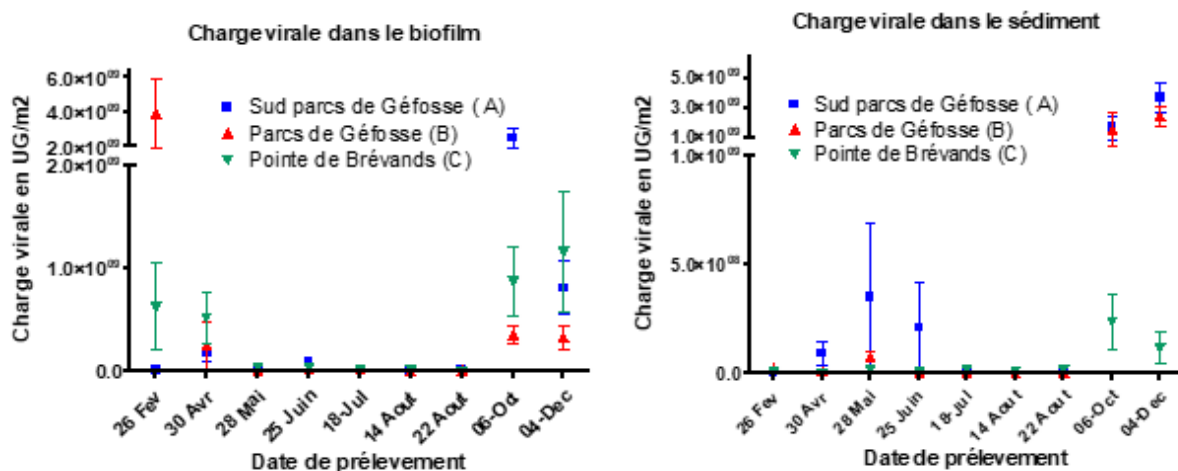


Figure 6 : Charges virales de OsHV-1 μVar quantifiées dans le sédiment et le biofilm dans le Sud des parcs de Géfosse (A), dans les parcs de Géfosse (B) et sur la Pointe de Brévands (C) à 9 dates en 2014.

Concernant les prélèvements de sédiment, les charges virales étaient plus faibles que dans le biofilm durant les 3 premiers mois de l'année 2014 avec des charges virales atteignant  $10^6$  UG/m<sup>2</sup>. Ces charges virales ont ensuite augmenté pour atteindre des valeurs de  $10^6$  à  $10^9$  UG/m<sup>2</sup> (hormis sur la Pointe de Brévands) entre Avril et Juin, correspondant à la période de mortalité survenue fin juin en 2014. Tout comme pour le biofilm, les charges virales étaient quasi nulles en Juillet-Août. En automne, des charges supérieures à  $10^9$  UG/m<sup>2</sup> étaient observées au sud et au sein des parcs mais plus faibles à la pointe de Brévands, contrairement au biofilm. Les charges virales contenues dans le sédiment et le biofilm étaient donc très importantes aux alentours des parcs ostréicoles et ce compartiment pourrait offrir des conditions favorables à la persistance environnementale du virus OsHV-1 μVar. Les charges virales contenues dans le

biofilm et dans le sédiment étaient moins importantes durant la période estivale Ainsi, l'hypothèse émise pour ce phénomène serait que l'action des rayons UV et celle de la température sur l'activité métabolique des consommateurs, plus fortes en été, nuirait à l'intégrité des particules virales présentes à la surface du sédiment. De plus, une augmentation de charges virales juste avant le début des épizooties questionne sur le rôle de l'environnement benthique lors d'épisodes de mortalités liés à OsHV-1 μVar.

### 5.1.2. Remise en suspension de OsHV-1 μVar

Si le lien entre les mortalités et le virus est établi, son mode de diffusion dans l'environnement reste méconnu. Des expériences d'érodimétrie en laboratoire laissent suggérer un rôle majeur des courants et de l'érosion dans le transfert des particules benthiques vers la colonne d'eau (Dupuy et al., 2014; Orvain et al., 2004) et des virus associés (Mallet et al., 2014). Le programme VIAPSE (CRH ; 2014) a pu apporter différents éléments de réponse sur la diffusion de l'OsHV-1 μVar, comme la dynamique du virus dans l'eau de mer et le rôle du sédiment et/ou des microorganismes au sein des biofilms à l'interface eau/sédiment. L'outil d'érodimétrie, couplé aux expérimentations de pathologie s'est révélé être un outil précieux pour cette analyse de diffusion du virus. Les virus libres dans l'eau ont peu de chance de contaminer leurs hôtes bivalves mais l'infection par une voie trophique (phytoplancton, microphytobenthos en suspension) est un vecteur probable de contamination en étant directement avec les palpes labiaux et donc les branchies. Une expérience d'érodimétrie a été réalisée en laboratoire (Figure 7) avec des sédiments prélevés sous une table à huîtres la baie des Veys (Point B, Figure 5).

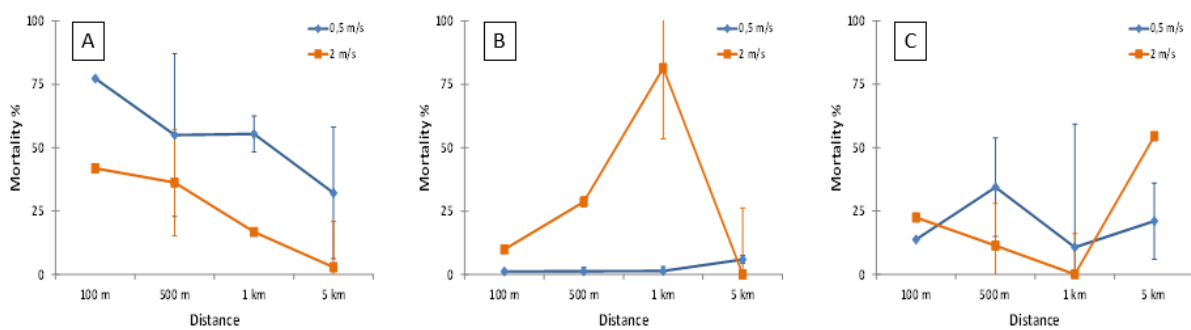


Figure 7 : Taux de mortalité des naissains d'huîtres sentinelles après injection de l'eau de mer contaminée en virus OSHV-1 μvar dans un canal d'érodimétrie. Les taux de mortalité varient en fonction du courant appliqué ( $0.5 \text{ m.s}^{-1}$  en bleu et  $2 \text{ m.s}^{-1}$  en orange) et du temps passé dans le courant du canal (converti en distance équivalente parcouru par le courant, en abscisse) et du traitement du virus : A) directement mis dans l'eau de l'érodimétrie, B) dispersé à la surface d'un échantillon de sédiment pris en baie des Veys et C) à la surface d'un échantillon de sédiment colonisé par un biofilm microphytobenthique.

Une diminution de l'activité du virus en terme de mortalité induite a été observée lors du transport avec le courant dans l'eau de mer (Figure 7 A). Avec une vitesse d'écoulement plus élevée, la diminution de la mortalité induite est alors plus importante et les taux de mortalité

des naissains d'huîtres décroissent. Lorsqu'il est associé à un lit de sédiment, le virus se propagerait par érosion plutôt que par diffusion (Figure 7 B). A une vitesse d'écoulement élevée le virus était libéré brutalement. La mortalité virale induite était la plus élevée après la remise en suspension avec le courant le plus fort ( $2 \text{ m.s}^{-1}$ ). Avec des courants lents et des sédiments, la contamination virale n'a pas été transférée aux huîtres sentinelles. Cela révèle qu'avec une vitesse d'écoulement suffisante, l'érosion des sédiments peut remettre en suspension les infections infectées, ce qui peut contaminer des fermes ostréicoles éloignées lorsque les vitesses du courant sont élevées. La présence d'un biofilm microphytobenthique (Figure 7 C) permet de remettre plus facilement le virus en suspension, mais il n'y a pas eu de baisse significative de la mortalité des huîtres avec écoulement sur une longue distance. Dans ce cas, le virus reste actif même après une longue distance dans le flux du courant. Il semble un effet d'adhérence du biofilm (probablement lié aux EPS microphytobenthiques) maintienne le virus à la surface, en étant facilement remis en suspension. Le biofilm microphytobenthique aurait donc un potentiel effet protecteur pour le virus et cet effet protecteur resterait efficace après une remise en suspension sur de longues distances. Ainsi, la présence d'un biofilm peut être un microhabitat pour la survie du virus et pourrait être impliquée dans le maintien de l'activité du pathogène et dans sa résistance aux effets abrasifs de l'érosion.

## 6. Objectifs

Le rôle du compartiment benthique dans les écosystèmes conchyliques lors des épisodes de mortalités de naissains d'huîtres liées à OsHV-1 μVar reste, de nos jours, méconnu. Il est probable que les caractéristiques de l'habitat table à huîtres fournissent des conditions favorables à la persistance de OsHV-1 μvar dans son environnement. En effet, la structuration et l'alternance de l'habitat benthique table à huître/allée pourrait créer des zones préférentielles de persistance de OsHV-1 μVar ou à l'inverse l'inhiber. De ce fait, nous avons chercher à caractériser l'environnement benthique de cet habitat et son rôle en tant que potentiel « réservoir » du virus OsHV-1 μVar mais aussi des bactéries pathogènes associées aux surmortalités de naissains d'huîtres *C. gigas*.

### 6.1. Expérimentations réalisées lors de ce projet de thèse

Ce travail de thèse visait à tester plusieurs hypothèses concernant la dynamique environnementale de l'agent pathogène OsHV-1 μVar lors d'un épisode de mortalité. La mise à l'épreuve de ces hypothèses s'est donc déroulé en plusieurs étapes décrites ci-dessous.

### *Etudes non présentées dans ce manuscrit*

Certaines hypothèses ont été testées en laboratoire mais ne sont pas présentées dans ce manuscrit.

L'une d'entre elles consistait à évaluer les interactions entre bivalves lors des mortalités de naissains d'huîtres *C. gigas* liées à OsHV-1 μVar car des transferts interespèces peuvent se produire (Arzul et al., 2001a, 2001b). Ainsi le rôle la coque commune *Cerastoderma edule* (autre bivalve le plus abondant en baie des Veys) dans les mortalités de naissains d'huîtres a été étudié. Dans le cadre du projet européen COCKLES des huîtres sentinelles (n'ayant jamais été mis en contact avec le virus) ont été infectées par OsHV-1 μVar et lorsque les premières mortalités induites par OsHV-1 se produisaient, les huîtres étaient retirées et remplacées par des coques pendant 2 jours. Ensuite, de nouvelles huîtres sentinelles étaient ajoutées et le taux de mortalités journalier compté. Le calcul du taux de clairance des huîtres, ainsi que des coques, a été réalisé afin de mettre en évidence l'influence du virus sur la filtration des mollusques.

Une autre étude réalisée en laboratoire visait à étudier la biodéposition du virus OsHV-1 μVar associé aux feces des naissains d'huîtres lors d'un épisode de mortalité. Ainsi des naissains d'huîtres ont été infectés par ce pathogène et nourries avec un mélange de phytoplancton et de particules sédimentaires afin de favoriser la production de feces et de pseudofeces. Certains tests révélaient des mortalités après injection à partir des biodépôts d'autres huîtres, mais une faiblesse des résultats vis-à-vis de certains témoins ne nous permettent pas de conclure de manière parfaitement claire sur la transmission du virus par le relais de biodépôts.

### *Etudes présentées dans ce manuscrit*

La seconde partie présentée dans ce manuscrit correspond à l'étude des caractéristiques du compartiment benthique et du développement microphytobenthique *in situ* afin de mettre en évidence une éventuelle stratification de l'environnement ostréicole (table *versus* allée). En effet, du fait de l'atténuation de la lumière et de la température sous la table à huîtres, le MPB situé dans cet habitat pourrait montrer un meilleur état physiologique et développement comparé à celui dans l'allée qui pourrait subir une thermo et photoinhibition. De plus, des variations environnementales pourraient également être le résultat d'une stratification de l'habitat benthique à l'échelle de la table avec des conditions environnementales plus tamponnées sous la table et des conditions plus hostiles dans les allées. Globalement, la zone d'étude devrait être structurée par les huîtres avec leur activité de biodéposition et les impacts physiques des tables à huîtres.

La troisième partie de ce manuscrit correspond à l'étude de l'impact des mortalités de naissains d'huîtres induites par OsHV-1 sur l'environnement benthique. Cette étude réalisée lors de la même période est basée sur le dénombrement et l'identification de la macrofaune benthique associée aux parcs ostréicoles en s'appuyant sur les caractéristiques environnementales benthiques détaillées dans la partie précédente. A travers l'étude de la macrofaune benthique et le calcul d'indices écologiques tels que l'AMBI (Marine Biotic Index) et le BOPA (Benthic Opportunistic Polychaetes Amphipods) (Borja et al., 2000; Dauvin and Ruellet, 2007) l'état écologique du milieu a pu être évalué vis-à-vis d'un excès de matière organique et l'eutrophisation associée. En parallèle, des individus de la macrofaune benthique ont été prélevés en vue de quantifier leur charge virale en OsHV-1  $\mu$ Var car certains individus pourraient être en contact direct avec le virus (espèces nécrophages) alors que d'autres pourront l'être indirectement (contamination de l'environnement benthique par sédimentation).

La quatrième partie correspond au suivi de la dynamique environnementale du virus OsHV-1  $\mu$ Var dans le biofilm ainsi que dans les naissains d'huîtres à une échelle temporelle journalière. Le suivi des charges virales a été réalisé dans les naissains vivants, moribonds et morts. De plus nous avons cherché à mettre en évidence la dynamique benthique du virus à travers l'étude de la présence du virus à la surface du sédiment au cours de ce même épisode de mortalité de l'été 2017. En parallèle, les communautés bactériennes ont été échantillonnées afin de mettre en évidence d'éventuels phénomènes de co-infection en étudiant les communautés bactériennes des naissains d'huîtres et du biofilm.

La cinquième partie porte sur la reproduction des phénomènes d'érosion estuarienne se produisant sur le compartiment benthique vers la colonne d'eau dans les parcs à huîtres via un circuit clos appelé érodimètre érodimètre grâce auquel un échantillon de sédiment prélevé *in situ* peut être soumis à des phases successives de courant augmentés progressivement toutes les 5 minutes. Le traitement des données permet de tester les variations de l'érodabilité sédimentaire (seuil critiques d'érosion et flux). Par rapport à d'autres instruments de mesure de résistance à l'érosion, cet appareil a l'avantage de pouvoir différencier les caractéristiques d'érodabilité de différents constituant de la matrice sédimentaire : les biofilms microphytobenthiques (chl a), la vase (formant la turbidité dans l'eau après érosion) et le sable se déplaçant par charriage (roulement des particules grossières, appellé « Bed load transport » en anglais). L'étude de ce chapitre visait à mettre en évidence les caractéristiques sédimentaires benthiques et la résistance/vulnérabilité de ce compartiment à l'érosion. L'éventuelle remise en suspension du virus OsHV-1  $\mu$ Var a également été étudiée afin de déterminer son éventuel

mode de transfert vers la colonne d'eau : diffusion ou érosion ? Un objectif supplémentaire était de déterminer à quelles particules le virus pourrait être adsorbé (chlorophylliennes, sédimentaires : sable et/ou vase).

## 6.2. Site d'étude

Les résultats présentés dans ce manuscrit se basent sur une expérience *in situ* réalisée en baie des Veys dans le parc ostréicole de Géfosse-Fontenay du 22 Mai au 01 Juillet 2017. Lors de cette étude, le compartiment benthique a été suivi en dehors et sous les tables à huîtres sur une période couvrant un épisode de mortalité lié à OsHV-1 μVar dans les parcs ostréicoles bas-normands.

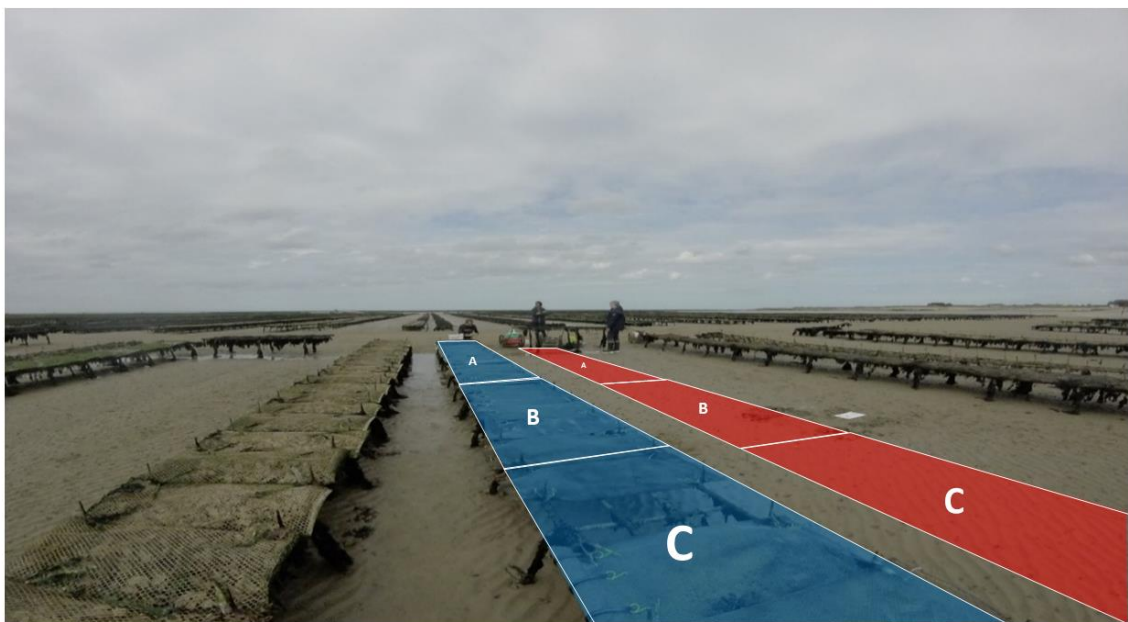


Figure 8 : Design experimental de la table à huîtres étudiée. L'habitat table à huître échantilloné est coloré en bleu (A, B & C) et l'habitat allée en rouge (A, B & C).

Une table à huîtres a été divisée en 3 zones (A, B et C) dans lesquelles 20 poches ont été disposées contenant chacunes 2 pochons remplis de 200 naissains d'huîtres standardisés Ifremer (Figure 8). Ainsi pour le sédiment les variables de chl *a*, la charge virale en OsHV-1 μVar, la teneur en eau, la quantité de matière organique, les communautés bactériennes, les teneurs en EPS et la composition sédimentaire (histogramme de taille des particules sédimentaires, encore appelé granulométrie) ont été échantillonnées. Les sels nutritifs contenus dans les eaux interstitielles ont été quantifiés. Les performances photosynthétiques du MPB ont été étudiées et quantifiées en utilisant un PAM (Pulse-amplitude method). La chl *a* a également été échantillonnée à l'échelle du biofilm, tout comme les charges virales d'OsHV-1 μVar et les

communautés bactériennes. La macrofaune benthique a également été échantillonnée et la couverture algale induite par les échouages a été étudiée. Le taux de mortalité et les charges virale en OsHV-1  $\mu$ Var des naissains d'huîtres a été suivie. De plus des expériences d'érodimétrie ont été menées *in situ* afin de caractériser l'environnement benthique et sa résistance à l'érosion ainsi que la remise en suspension des particules et de l'OsHV-1  $\mu$ Var.





Un prérequis nécessaire à l'étude de la dynamique environnementale de OsHV-1 μVar a été de caractériser l'habitat benthique ostréicole à l'échelle de la table à huîtres. En effet, ce compartiment benthique pourrait fournir des conditions favorables à la protection du virus OsHV-1 μVar dans l'environnement. De ce fait, pour ce projet de thèse une campagne de terrain a été menée en 2017, les caractéristiques de l'habitat benthique ont été étudiées sous une table à huîtres et dans l'allée la bordant. La période d'échantillonnage correspondait à celle de la mortalité des naissains d'huîtres. Ainsi les paramètres physico-chimiques, les performances photosynthétiques et la biomasse microphytobenthique ont été étudiés afin de caractériser l'environnement benthique en vue d'identifier des zones préférentielles de persistence du virus.



**Chapitre 2 : Drivers of the epipelagic  
microphytobenthic photobiology and growth in  
oyster farm**



Charles Vanhuysse, Julien Normand, Lepoittevin Mélanie, Rakotomalala Christiane, Mallet Clarisse, Lelong Christophe, Pernet Fabrice, Francis Orvain

## Drivers of the epipelagic microphytobenthic photobiology and growth in oyster farm

Article soumis à la revue Geosciences

### Abstract

In intertidal areas, oyster farming creates a typical crosshatching pattern between the oyster tables and the aisles. This type of culture creates benthic habitats that differ at mesoscale in oyster biodeposition, on one hand, and on the other hand, by the temperature and light attenuation (shading effect) due to mesh bags full of oysters. The sediments in the aisles are directly exposed to light and temperature while, under the oyster tables, the influence of these factors is reduced. The aim of the present study was to distinguish the complex factors driving microphytobenthos (MPB) photobiology and growth performance among (i) direct effects (light, temperature) and (ii) indirect effects (sediment dynamics). A field survey including a cycle of two spring tides and one neap tide, was conducted to search for the differences in table and aisle habitats along with the short-term MPB dynamics at a small spatial scale. During the survey the biomass of MPB and photobiological parameters related to meteorological, sedimentary and biogeochemical environmental factors were recorded. Among the set of correlations, the most significant one was the positive correlation between active surface chl *a* and ETRmax, the maximum productivity rate expressed as electron transport rate). Our study shows that MPB growth may be subject to bioturbation and grazing pressure by macrofauna while the reconstruction of active biofilm at the sediment surface appears to be a prerequisite for a good diatom growth status. The photosynthetic yield (PY) of MPB decreased with maximum water height and the decrease was more pronounced in the aisle than under the oyster table during neap tides, with minimum values of 0.2 (i.e. poor status) and 0.4 (i.e. medium status), respectively. In both habitats, the PY reached 0.6 (i.e. good status) during spring tides. PY was also negatively correlated with temperature and light in the aisle whereas it was only correlated with temperature under the oyster table. Consequently, thermoinhibition appeared to be the main factor affecting MPB photobiology but light may also be responsible for photosynthetic impairments although to a lesser extent. These two main drivers appeared to mask the role of sediment dynamics in MPB growth, even though some changes in the local accumulation of organic material and NH<sub>4</sub><sup>+</sup> were observed linked to the presence of oyster tables. Oyster tables apparently provide better shelter for MPB in summer conditions.

**List of Abbreviations:**

Ek: Light saturation coefficient

EPS: Exopolysaccharides

ETRmax: maximum electron transport rates

MPB: Microphytobenthos

MWH: Maximum water height

OMF : Organic matter draction

Pemax: Maximum productivity

Pmax: Maximum production

PY : Photosynthetic yield

SLI : Surface light intensity

SST : Surface sediment temperature

## 1. Introduction

Aquaculture is an ancestral activity in the food sector that has had the highest growth rate worldwide (7.8%) in the last three decades (Troell et al., 2014) thereby creating a sustainable alternative to overfishing of marine resources. Among the different types of aquaculture, intertidal oyster cultivation is one of the most important resources (FAO, 2006, 2018). Nevertheless, oyster farming is known to cause several environmental problems (Forrest et al., 2009b) and requires interdisciplinary management for perennial development (Byron et al., 2015). On the French shoreline, oysters are generally grown on elevated tables (50-80 cm in height, 1 m in width, 3 m in length) that are known to attenuate friction velocity (Kervella et al., 2010; Nugues et al., 1996; Sornin, 1981). The ecological link between the cultivated oysters and the benthic habitat is thus tight compared to other methods of cultivation because oysters are in the close vicinity of the sediment surface (Sornin and Mariojouls, 1987; Orvain et al., 2012). A study by Kervella et al. (2010) highlighted the asymmetric development of flow regimes in boundary layers under oyster tables that have a marked "skimming flow" effect. Indeed, the steel trestles holding the oyster bags can create preferential local zones for muddification and this physical process has been shown to clearly affect bed shear stress,

increasing it up to 10 times. These authors underline the major role of the local flow direction in explaining potential sediment dynamics in relation with the alignment axis of the tables.

The bivalve *Crassostrea gigas* (Bayne et al., 2017) filters fine particles through its gills, thereby retaining phytoplankton and reducing water column turbidity. In the pelagic system, bivalve filtration activity also deplete micro-phytoplankton communities by suspension feeders (Berg and Newell, 1986; Mostajir et al., 2015). Labial activity leads to selection of organic particles and rejection of biodeposits mainly comprised of pseudofeces but also of small mounds of fecal pellets. The amount and quality of biodeposits depends on (i) the density of reared animals, (ii) the quantity and quality of suspended particulate matter, and particularly (iii) on the microalgal fraction (Haven and Morales-Alamo, 1966; Porter et al., 2010). Oyster biodeposits make up most of the sediment under the oyster tables (Sornin and Mariojouls, 1987) with significant loadings of fine particles (Mitchell, 2006) that consequently enrich the benthic habitat with organic material (Sornin, 1981; Echappé et al., 2018). Moreover, the settling velocity can reach high values under oyster tables, up to seven times higher than in the aisles (Haven and Morales-Alamo, 1966). Together, the two processes lead to substantial topographic changes in the bed (Ottmann and Sornin, 1982; Forrest and Creese, 2006). There is now strong evidence that the muddification induced by oyster parks locally stimulates microphytobenthic (MPB) growth and that this process continues up to a distance of 1 km beyond the perimeter of oyster beds (Hayakawa, 2001; Orvain et al., 2012; Ubertini et al., 2012). This ecological interaction is indirectly explained by activation of the biogeochemical processes that increase the nutrient fluxes at the water-sediment interface (Van de Koppel, 2001; Hochard et al., 2010; Joensuu et al., 2018) particularly nitrogen dynamics (Newell et al., 2002). Because oysters modify the local environment by enhancing habitat complexity and modifying sediment dynamics, they are therefore considered as ecosystem engineers (Padilla, 2010).

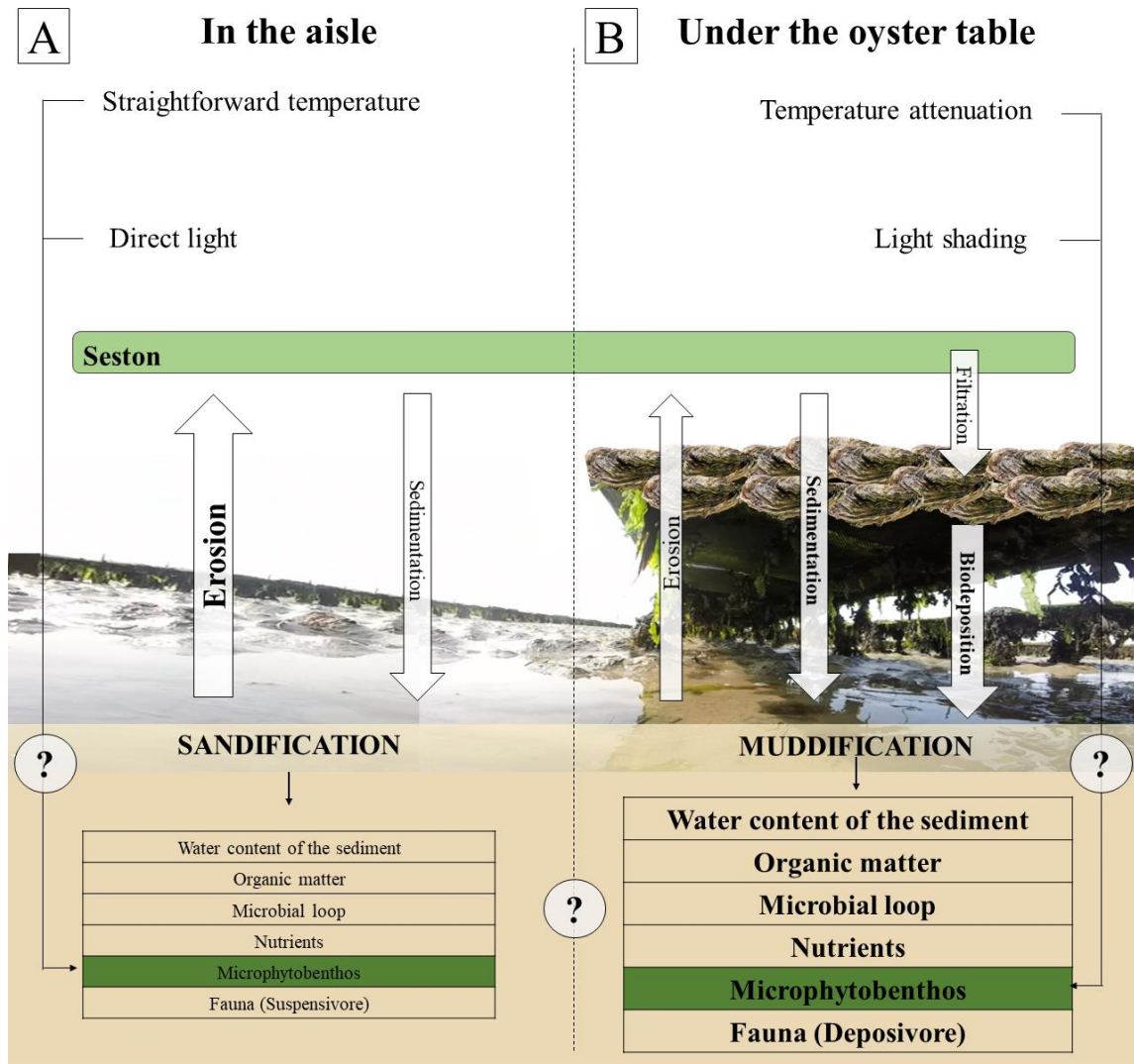


Figure 9 : Conceptual scheme of potential impacts of oyster tables on the benthic habitat. A. Beyond the oyster table, i.e. in the aisle, sediment is exposed to light and high temperatures. The benthic habitat could be mainly sandy, with a low organic matter fraction (OMF) that could slightly stimulate the microbial loop and hence nutrient regeneration. In this case, MPB growth would not be enhanced and macrofauna grazing species would consequently be relatively rare. B. Under the oyster tables, shading reduces exposure to light and temperature. The sediment is muddy, with more OMF due to the oyster biodeposition. The higher OMF promotes the microbial loop and hence nutrient regeneration. MPB growth would consequently be stimulated and macrofauna deposit feeding species would be facilitated rather than suspension feeders.

Oyster tables (Figure 9) also attenuate light intensity (Forrest et al., 2009b; Porter et al., 2004). Temperature and solar irradiance are of paramount importance in benthic primary production (MacIntyre et al., 1996; Barranguet et al., 1998). MPB is known to migrate towards the sediment surface (Pomeroy, 1959; Decho, 2000) during the low tide to capture the light and to migrate downwards to increase nutrient accessibility and/or to cope with excess light (Jenkin, 1937; Ryther, 1956; Cartaxana et al., 2011). The size of sediment particles plays a major role in MPB development (Yallop et al., 1994). A sandy sediment allows deeper light penetration because the grains are larger than in a muddy sediment (Tester and Morris, 1987; Kühl et al., 1994; Bliss and Smith, 2006). The risks of excess light impairing the photosystems are thus

higher in sand than in mud (Jesus et al., 2006; Cartaxana et al., 2011). Conversely, a muddy sediment is associated with a high organic matter fraction (OMF) (Bergamaschi et al., 1997) and a high nutrient remineralization turnover rate due to the microbial loop. The bioavailability of nutrients may limit MPB primary production (Howarth, 1988; Swanberg, 1991; Newell et al., 2002). Thus, a compromise between sandy and muddy particles profits MPB and biofilm growth (Echappé et al., 2018; Morelle et al., submitted).

In intertidal mudflats, primary production is mostly supported by MPB rather than by phytoplankton (Cahoon, 2014; Perissinotto et al., 2002; Struski and Bacher, 2006). MPB is therefore an important resource for suspension feeding species (Cloern et al., 2014) such as oysters (Cognie et al., 2001; Lefebvre et al., 2009; Grangeré et al., 2010) and benthic grazers (Herman et al., 2001; Sahan et al., 2007). Benthic diatom motility causes them to excrete exopolysaccharides (EPS) from their raphe system (Edgar, 1983; Edgar and Pickett-Heaps, 1983), which is linked with the rhythm of their migration (Smith and Underwood, 1998) and plays a major role in local sediment stabilization (Yallop et al., 1994; Tolhurst et al., 2002; Stal and de Brouwer, 2003). Depending on the stability of the sediment, a considerable proportion of MPB production - between 30% and 85% of the total planktonic biomass - may be eroded in the water column (de Jong and de Jonge, 1995). Thus, MPB secretion of EPS could stabilize the sediment and enable the survival of MPB and its biomass under oyster tables.

Although widely studied at the scale of the whole ecosystem, the consequences of oyster farming for its environment have rarely been analyzed at small scale, especially the local impact of the shade provided by the oyster tables and the benthic impacts (Forrest et al., 2009b). Knowing that environmental stressors must be taken into consideration (Van Colen et al., 2014) in field studies, we took the opportunity offered by oyster tables to try and untangle the complex environmental factors including (i) direct effects (light, temperature) and (ii) indirect effects (muddification and biostabilization by EPS) that make up the interaction network depicted in Figure 9. To this end, we conducted an *in situ* study that included a cycle of two spring tide and one neap tide, with a sampling design integrating the day, the table and the moment effect of the tide, and measured and recorded the MPB biomass together with photobiological parameters related to environmental (meteorological, sedimentary and biogeochemical) factors.

## 2. Material & Method

### 2.1. Study site and sampling design

The study was conducted along a row of oysters tables (Figure 10 B) located at Géfosse-Fontenay in the *Baie des Veys* (Normandy, France) on top of the foreshore (from 49°22'53.2" N; 001°05'44.2" W to 49°22'54.6" N; 001°05'43.4" W) from May 22, 2017 to July 1, 2017. The oyster table consisted of three areas (A, B & C) (Figure 10 A) with 20 oyster bags in each zone each containing smaller bags containing two hundred 3-month-old oyster spats. Oysters were produced according to standard hatchery procedures (Petton et al., 2015a).

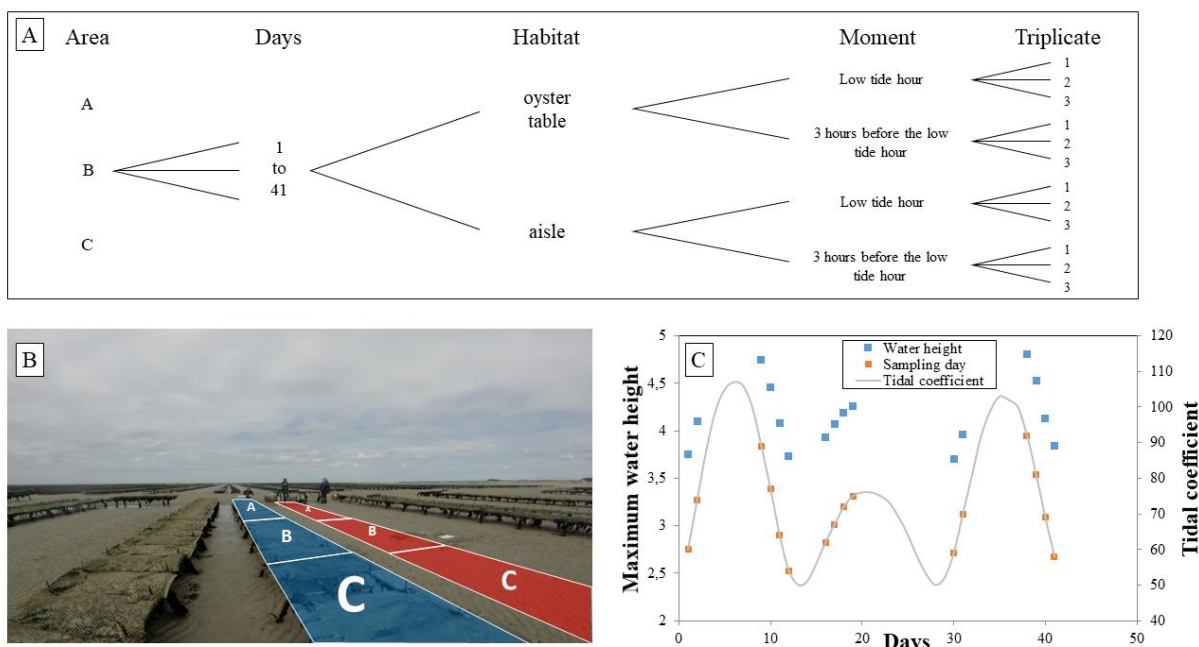


Figure 10 : A. Description of the experimental design. B. Experimental set up in the field, Areas A, B and C were located under oyster tables (blue) or in the aisle (red). Each area included 20 oyster bags. C. Maximum water height (meters) and tidal coefficient during the experiment. Each square represents a sampling occasion.

On each sampling occasion, one bag out of the 20 bags in each area was sampled using a random design that nominating a sampling location. Measurements were made in triplicate at each sampling location (Figure 10 B) in the two habitats studied: (i) under the oyster table and (ii) in the aisle, at two different times: once three hours before low tide and once at low tide. The study lasted 41 days including 16 sampling dates covering a cycle of two spring tides and one neap tide (Figure 10 C).

## 2.2. Abiotic parameters

Variations in water depth (influenced by the tide and the meteorological conditions) were measured continuously over the study period by a probe deployed in the same site by the IFREMER-RESCO survey network (Fleury et al., 2018). From this data set, we computed maximum water height (MWH) as the maximum water height recorded by the probe during the high tide immediately preceding field sampling. Over the same period, the surface light intensity (SLI) and sediment surface temperature (SST) were monitored at 5-minute intervals with Hobo Prosensor probes fixed to the trestles underneath and beside the oyster table studied. In the *Baie des Veys*, low tide is at midday during neap tides, while high tide is at midday during spring tides. Sediment samples were weighed at sampling (fresh weight) and after a drying period of 72 hours at 50 °C (dry weight) in order to obtain the water content of the sediment (fresh weight - dry weight). The dried sediment was then burned at 450 °C for 4 hours and weighed. The difference in weight is a proxy for the organic matter fraction (OMF) of the sediment (%). The particle size of the sediment was measured with a Beckman Coulter LS 13320 (Beckman Coulter). Triplicates of interstitial water samples were pooled and adjusted to 5 mL. Nutrients ( $\text{NO}_3^-$ ,  $\text{NO}_2$ ,  $\text{NH}_4^+$ ,  $\text{PO}_4^{3-}$ ) contained in adjusted interstitial water were analyzed with an automated discrete photometric analyzer Gallery Plus (Thermo Fisher Scientific).

## 2.3. Biotic parameters

### *Chlorophyll a*

The concentration of chl *a* in the sediment is a good proxy for microphytobenthic biomass. MPB was collected using a 49 cm<sup>2</sup> Bluter mesh (100 µm mesh) placed at the surface of the sediment for 30 minutes, thus representing the active surface chl *a*. The meshes were then dipped in 10 mL of filtered (0.2 µm) seawater and a 1 mL aliquot was stored at -20 °C. To extract the pigments, 9 mL were added to the biofilm samples (1 mL), which were then incubated at 4 °C for 24 hours. The first centimeter of sediment sampled using the plate technique was homogenized before being stored at -20 °C. The sediment samples were freeze-dried, crushed and filtered through a 500 µm sieve to remove coarse particles and a sediment mass of between 500 and 1,000 mg was weighed. Ten milliliters of 90% acetone were added to the dried sediment samples, which were then incubated at 4 °C for 24 hours.

Fluorescence was measured with a Trilogy Fluorometer (Turner Designs) in 2 mL glass tubes before and after acidification with 0.3N HCl to quantify pheopigments using the Lorenzen method (Lorenzen, 1967). The concentrations of chlorophyll *a* and pheopigments (µg.gDry

Weight<sup>-1</sup>) in the sediment were calculated using equations 1 and 2 with Kx and (F<sub>0</sub>/Fa)max as calibrated parameters:

$$[\text{Chla}] = \text{Kx} \cdot (\text{Fo/Fa}) \text{ max} \cdot [(\text{Fo} - \text{Fa}) / ((\text{Fo/Fa}) \text{ max} - 1)] \cdot [\text{vext} / \text{gDW}] \quad (\text{Eq. 1})$$

$$[\text{Pheo a}] = \text{Kx} \cdot (\text{Fo/Fa}) \text{ max} \cdot \text{Fa} \cdot [1 - ((\text{Fo/Fa}) - 1) / ((\text{Fo/Fa}) \text{ max} - 1)] \cdot [\text{vext} / \text{gDW}] \quad (\text{Eq. 2})$$

The pheopigment percentage was then calculated (Eq. 3) from the fraction of pheopigments in the total pigments (Cartaxana et al., 2003):

$$\text{Pheo (\%)} = \frac{[\text{Pheopigments}]}{[\text{Pheopigments}] + [\text{chl a}]} \times 100 \quad (\text{Eq. 3})$$

### *Exopolymeric Substances*

EPS were extracted from thawed sediment samples using the protocol of Orvain et al. (2003). First, the sediment sample was freeze-dried and weighed (between 500 mg and 1 g). Then, after vortexing for 10 seconds, 5 mL of distilled water were added. The sample was then placed at 35 °C on a rotary shaker for 1 h and centrifuged (4 °C, 3000 g, 10 min). Next, 2 mL of the supernatant were sampled to which 8 ml of absolute ethanol was added to separate high and low molecular weight EPS and the sample was stored at -20 °C for 18 hours. After centrifugation (4 °C, 3000 g, 30 min), the low molecular weight EPS in the supernatant was separated from the high molecular weight EPS contained in the pellet and then dried at 60 °C in a dry bath under air flow for 6 to 48 hours. The dried samples were then suspended in 1 ml of distilled water. To measure carbohydrate content, 50 µL of 5% phenol and 250 µL of sulfuric acid were added to 50 µL of the extract (Dubois et al., 1956). After one hour of incubation, absorption was read with a FlexStation™ plate reader at 485 nm. A glucose solution was used to determine the sugar moiety. The range of dilution for the glucose solution was 0; 67; 100; 120; 143; 165; 179 and 200 mg/L. The dilution range was performed 10 times (adjusted R<sup>2</sup> = 0.998) to assess EPS concentrations.

### *Photosynthetic performances*

The photobiological performances of the MPB were measured using a PAM-control (Walz). MPB was sampled in cores and acclimated in the dark for 5 minutes to oxydate the quinone A (Q<sub>A</sub>) pool. To assess the minimum fluorescence (F<sub>0</sub>), the samples were exposed to a mild intensity blue light (1 µmol photons.m<sup>-2</sup>.s<sup>-1</sup>, 470 nm, 0.6 kHz frequency). Maximum fluorescence (F<sub>m</sub>) was acquired with the first light irradiance (0.6 s, 1130 µmol photons.m<sup>-2</sup>.s<sup>-1</sup>,

<sup>1</sup>, 470 nm). The maximum PSII quantum yield was calculated according to equation 4 (Genty et al., 1989):

*Maximum PSII quantum yield*

$$= \frac{Fm - F0}{Fm} \quad (\text{Eq. 4})$$

The samples were then exposed to 8 photosynthetically active radiations (PAR) emitted at 15 second intervals with increasing intensity (from 11 to 1130  $\mu\text{mol photons.m}^{-2.\text{s}}^{-1}$ ) to acquire the fluorescence after F and maximum fluorescence during the actinic light flash ( $Fm'$ ). These two parameters made it possible to reach the effective yield according to equation 5:

$$Y(II) = \frac{Fm' - F}{Fm'} \quad (\text{Eq. 5})$$

The photosynthetic yield was estimated from the first light level ( $F0$ ). Electron transfer rates (ETR) correspond to the number of electrons passing through Photosystem II that are efficiently absorbed. Given that the diversity and quantity of MPB was not known, relative ETR (rETR) as calculated using equation 6:

$$rETR = Y(II) * PAR \quad (\text{Eq. 6})$$

To obtain the photosynthetic parameters of this relation, a nonlinear regression model (Eilers and Peeters, 1988) was fitted to the point cloud according to a minimization parameterization method of the least squares criterion of the simplex (Nelder and Mead, 1965). Adjusting the Eilers-Peeters model to observed eETR allowed us to obtain the final parameters (a, b and c) corresponding to the parameters of model equation 7:

$$rETR(E) = \frac{E}{a*E^2 + b*E + c} \quad (\text{Eq. 7})$$

After the model was applied, these 3 constants were extracted using the *fminsearch* function based on the simplex method (Nelder and Mead, 1965). The electron transfer rates were then calculated (Eq. 8):

$$ETR = \frac{PAR}{a*PAR^2 + b*PAR + c} \quad (\text{Eq. 8})$$

$$\text{Next, maximum relative electron transport rate } rETRmax = \frac{1}{b^2 + 2*\sqrt{ac}} \quad (\text{Eq. 9})$$

$$\text{Followed by the saturation light coefficient: } Ek = \frac{Pmax}{\alpha} \quad (\text{Eq. 10})$$

Then photosynthetic efficiency ( $\alpha$ ):  $\alpha = \frac{1}{c}$  (Eq. 11)

Chl *a* biomass was calculated based on the  $F_0$  measured with the same equipment as that used for microphytobenthos: (Eq. 12) Biomass (mgChla.m<sup>-2</sup>) = 0.0613  $F_0$  + 14.3 (Orvain et al., 2014b).

PAM is a very reliable technique to observe the photobiology of microphytobenthic diatoms (Serodio et al. 2012). Even if the instrument does not reproduce primary production rates, the photosynthetic physiology is well described. True primary production rates (carbon incorporation) can be quantified with methods that use isotopic carbon labelling. ETR estimates can be used in a very indirect way by using laws from the literature, if the second method is not applied. This kind of calculation is subject to strong biases and extreme caution should be used when interpreting the results. Anyway, we extrapolated primary production rates from PAM results to obtain a first proxy. To this end, based on rETRmax, the real maximum electron transport rates (ETRmax) were calculated (Eq 13), after which maximum productivity (Pemax) was calculated (Eq. 14) to obtain (Eq. 15) the maximum production (Pmax) with the following set of equations:

$$\text{ETRmax (mmol}(\bar{\epsilon})\text{.mgChla.h}^{-1}\text{)} = \text{rETRmax} * 0.008 * 0.757 * 3.6 \quad (\text{Eq. 13})$$

$$\text{Pemax (mgC.mgChla.h}^{-1}\text{)} = \text{ETRmax} * 0.114 * 12 \quad (\text{Eq. 14})$$

$$\text{Pmax (mgC.m}^2\text{.h}^{-1}\text{)} = \text{Pemax} * \text{Biomass} \quad (\text{Eq. 15})$$

#### *Numerical and statistical analyses*

Data were further explored using “raster”, “sp”, “MASS”, “rmarkdown”, “knitr” and “jtools” R packages (R-project). First, we wanted to look at the variation in the variables to be explained (Tableau 2).

Tableau 2 : Explanatory variables (fixed) and variables to be explained

Explanatory variables:	Maximum water height (MWH), Habitat (Oyster table & aisle), Moment (bLT & LT)
Variables to be explained:	Surface light intensity (SLI), sediment surface temperature (SST), organic matter fraction (OMF), water content of the sediment, granulometry (< 63 µm), nutrients (NO <sub>3</sub> <sup>-</sup> , NO <sub>2</sub> , NH <sub>4</sub> <sup>+</sup> , PO <sub>4</sub> <sup>3-</sup> ), biofilm and sediment Chl <i>a</i> , biofilm and sediment pheopigments percentages, EPS concentrations, photosynthetic yield, light saturation coefficient (Ek), maximum electron transfer rates (ETRmax)

We therefore adjusted the following multivariate regression model (ANCOVA) to the data set, considering as explanatory variables: Moment (2 occasions: bLT & LT), maximum water height (MWH) and habitat (2 locations: oyster table & aisle) :

$$Y = \text{Moment} + \text{Maximum water height} + \text{Habitat} + \text{Moment} * \text{Water height} + \text{Moment} * \text{Habitat} + \text{Habitat} * \text{Water height}.$$

This complete model was then reduced by stepwise selection using the Akaike information criterion (step.AIC function of the “MASS” package), followed by a F-test to evaluate the significance of the effects of the explanatory variables retained after this step. In the Results section, we only present the graphs corresponding to the effects of the explanatory variables qualified as “significant”. If necessary, analyses were performed on the adequate transformation (lambda exponent) of response variables among the Box-Cox family (Box and Cox, 1964). Using the “lmtest” package, the Harrison Mac Cabe test was performed on the reduced model to check the hypothesis of homoscedasticity, and the Durbin-Watson test to check there was no autocorrelation (independence hypothesis). A principal component analysis (PCA) was performed using the “FactoMineR”, “factoextra” and “corrplot” R packages on biofilm chl *a* and pheopigments, ETRmax, Ek, photosynthetic yield, SLI and SST data (variables qualified as “significant”). A quantile regression (“quantreg” package) was also applied on the relationship between the light and temperature factors and its effect on the photosynthetic yield. Correlation matrices were performed on Biofilm chl *a* and pheopigments, ETRmax, Ek, photosynthetic yield, SLI and SST data (variables qualified as “significant”) using the “corrplot” package (corrplot function) and “Hmisc” R packages to investigate correlations between variables under the oyster table and in the aisle.

### **3. Results**

#### **3.1. ANCOVA Analysis**

*Abiotic and biogeochemical variables*

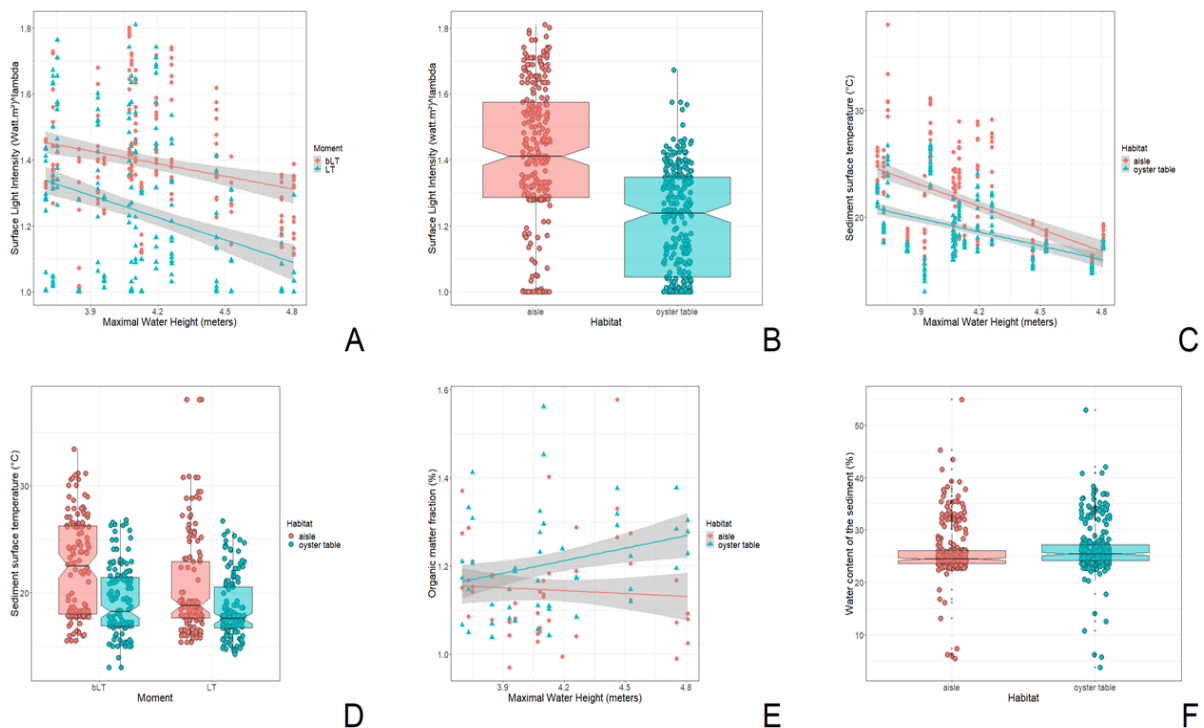


Figure 11 : Linear regression model (ANCOVA) of significant regression statistics (table 2). A. Surface light intensity according to moment and MWH ( $\lambda = 0.10$ ). B. Surface light intensity according to habitat ( $\lambda = 0.10$ ). C. Sediment surface temperature according to habitat and MWH. D. Sediment surface temperature according to habitat and moment. With bLT = before the low tide and LT = Low tide E. Organic matter fraction according to habitat and MWH. F. Sediment water content according to MWH

The detailed kinetics of surface light intensity (SLI) and sediment surface temperature (SST) are given with a full description of short-term dynamics in Appendix 1. For SLI, the significant effects detected by linear models were the interaction between the sampling moment and maximum water height (MWH) and the single effect of the habitat (Tableau 3): under the table or in the aisle (Figure 11 A & B). At the beginning of emersion period (i.e. bLT = abbreviation for the beginning of the low tide), a negative regression was detected between SLI and MWH, according to the following equation:  $SLI = 2.172 - 0.225 * MWH$  ( $R^2 = 0.110$ ;  $p\text{-value} = < 0.0001$ ). The effect of MHW on SLI was even greater at LT, with a lower slope in the following equation:  $SLI = 1.92 - 0.127 * MWH$ ;  $R^2 = 0.060$ ;  $p\text{-value} = < 0.0001$ ). For SST, 2 significant interactions were detected, first, between habitat and MWH (Tableau 3) and second, between moment and habitat (Tableau 3; Figure 11 C & D). Higher tides, coinciding with the higher values of MWH reduced the temperature measured at the surface of the sediment, and the reduction was greater in the aisle ( $SST = 50.580 - 7.042 * MWH$ ;  $R^2 = 0.242$ ;  $p\text{-value} = < 0.0001$ ) than under the oyster table ( $SST = 36.788 - 4.330 * MWH$ ;  $R^2 = 0.216$ ;  $p\text{-value} = < 0.0001$ ; Figure 11 C). Further, the temperature at the surface of the sediment was clearly higher in the aisle than under the table, and this difference was more pronounced at low tide than before low tide

(at low tide the temperature was  $22.33 \pm 4.55$  °C (mean ± standard deviation) in the aisle and  $19.19 \pm 3.25$  °C under the table; before low tide, the temperature was  $20.41 \pm 4.78$  °C in the aisle and  $18.46 \pm 2.92$  °C under the table). The percentage of sediment particles < 63 µm (ranging from 4.11 to 11.9%) was low, average value  $7.38 \pm 1.45\%$ . No significant variation was observed in the set of factors concerning this variable. Water content of the sediment only showed a single effect of moment (Tableau 3). Indeed, the water content of the sediment tended to be slightly higher (2.91%) before low tide ( $26.52 \pm 4.52\%$ ) than 3 hours later at low tide ( $25.74 \pm 5.59\%$ ). Two significant effects were detected for the organic matter fraction (OMF), the first varied with the interaction between MWH and habitat factors (Tableau 3), and the second varied with habitat (single effect). Indeed, the OMF remained relatively stable in the aisle with increasing MWH ( $\text{OMF} = 1.236 - 0.022 * \text{MWH}$ ;  $R^2 = 0.004$ ; p-value=0.553) whereas OMF increased under the oyster table ( $\text{OMF} = 0.813 + 0.095 * \text{MWH}$ ;  $R^2 = 0.074$ ; p-value = 0.007). Low nutrient concentrations were recorded with an average nitrate ( $\text{NO}_3^-$ ) concentration of  $0.01 \pm 0.03 \text{ mg.L}^{-1}$  (from 0 to  $1.43 \text{ mg.L}^{-1}$ ), an average nitrite ( $\text{NO}_2^-$ ) concentration of  $0.84 \pm 3.65 \text{ mg.L}^{-1}$  (from 0 to  $27.68 \text{ mg.L}^{-1}$ ), an average ammonium ( $\text{NH}_4^+$ ) concentration of  $20.00 \pm 27.45 \text{ mg.L}^{-1}$  (from 0 to  $12989.75 \text{ mg.L}^{-1}$ ) and an average phosphate ( $\text{PO}_4^{3-}$ ) concentration of  $0.001 \pm 0.006 \text{ mg.L}^{-1}$  (from 0 to  $1.04 \text{ mg.L}^{-1}$ ). For ammonium ( $\text{NH}_4^+$ ) there was an effect of the single moment, and a significant effect was also detected of the interaction between MWH and habitat (Tableau 3). Indeed, in the aisle,  $\text{NH}_4^+$  concentrations tended to decrease with increasing MWH ( $\text{NH}_4^+ = 1.701 - 0.090 * \text{MWH}$ ; ( $R^2 = 0.026$ ; p-value = 0.018) while the opposite was observed under the oyster table ( $\text{NH}_4^+ = 0.328 + 0.225 * \text{MWH}$ ;  $R^2 = 0.163$ ; p-value = < 0.0001).

Tableau 3 : Summary of linear models (ANCOVA) conducted on abiotic parameters. These results correspond to those that respected the conditions of homoscedasticity. Non-significant effects are not shown. With  $X_1$  = Moment (bLT = 0; LT = 1),  $X_2$  = Maximum water height,  $X_3$  = Habitat (under the table = 0; aisle = 1),  $X_4$  = Moment\*Habitat,  $X_5$  = MWH\*Habitat,  $X_6$  = MWH\*Moment. Significance levels: \* < 0.05, \*\* < 0.01, \*\*\* < 0.0001.

Variable	Formula	lambda	$R^2$	p-value
Surface light intensity (SLI)	$2.17 - 0.24*** \times X_1 - 0.22*** \times X_2 - 0.20*** \times X_3 + 0.1 * X_6$	0.10	0.210	< 0.0001
Sediment surface temperature (SST)	$49.95 + 2.06*** \times X_1 - 7.13*** \times X_2 - 13.42*** \times X_3 - 1.26 * X_4 + 2.77*** \times X_5$	-	0.296	< 0.0001
Water content of the sediment	$26.52 - 0.83 * X_1$	-	0.013	< 0.05
Organic matter fraction (OMF)	$1.23 - 0.02 * X_2 - 0.43** \times X_3 + 0.12 * X_5$	-	0.010	< 0.001
Interstitial water $\text{NH}_4^+$ concentrations	$1.73 - 0.05** \times X_1 - 0.09 * X_2 - 1.38** \times X_3 + 0.32*** \times X_5$	0.10	0.134	< 0.0001

### 3.2. Microphytobenthic variables

For sediment chl *a* concentration, a single effect of the moment (Figure 12 A; Tableau 4) and of the habitat (Figure 12 B; Tableau 4) were detected. Indeed, the concentration of chl *a* in the sediment was higher in the aisle ( $34.05 \pm 16.13 \text{ mg.m}^{-2}$ ) than under the oyster table ( $26.94 \pm 14.25 \text{ mg.m}^{-2}$ ) and was higher at low tide ( $33.17 \pm 15.86 \text{ mg.m}^{-2}$ ) than before low tide ( $30.51 \pm$

14.75 mg.m<sup>-2</sup>). For sediment pheopigments, a single habitat effect was also detected (table 3). Higher percentages were found under the oyster table ( $68.95 \pm 5.15\%$ ) than in the aisle ( $61.75 \pm 6.34\%$ ). The difference between the two habitats was even sharper at low tide than before low tide (Tableau 4). A significant effect of MWH was also detected, with an increase in sediment pheopigments with increasing MWH values (table 3; slope =  $46.08 + 3.99 * \text{MWH}$ ; R<sup>2</sup>= 0.332; p-value = < 0.0001).

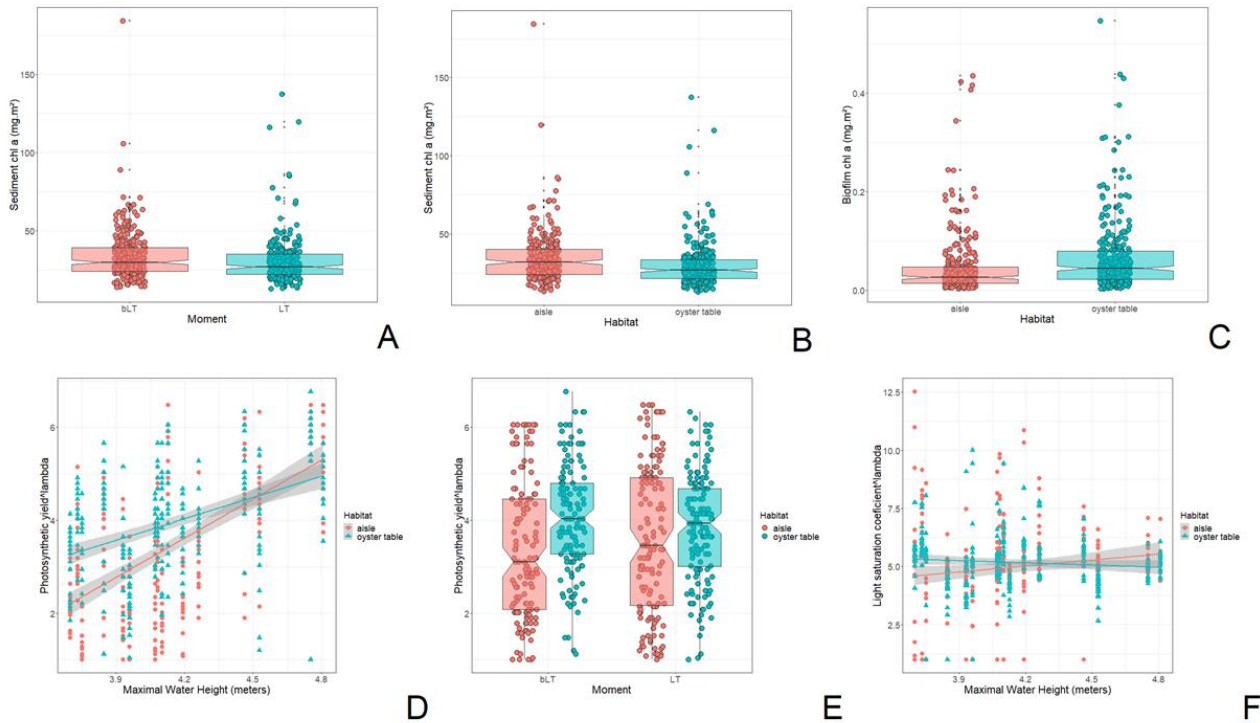


Figure 12 : Significant effects of regression statistics (Tableau 4) for microphytobenthic variables: A. Sediment chl a according to moment; B. Sediment chl a according to habitat; C. Biofilm chl a according to habitat; D. Photosynthetic yield according to habitat and maximum water height ( $\lambda = 3.69$ ); E. Photosynthetic yield according to habitat and moment ( $\lambda = 3.69$ ); F. Light saturation coefficient ( $E_k$ ) according to habitat and maximum water height ( $\lambda = 0.35$ ).

The detailed short-term dynamics of active surface chl a are shown and fully described in Appendix 2. Active surface chl a concentration only showed a significant effect of habitat (Figure 12 C; Tableau 4) with a higher concentration under the oyster table ( $66.54 \pm 14.94$  mg.m<sup>-2</sup>) than in the aisle ( $47.05 \pm 14.15$  mg.m<sup>-2</sup>). However, the variation between before low tide and at low tide was the same in the two habitats with no effects of any interaction with other factors (Tableau 4). Single moment and habitat effects were detected for pheopigments (at the biofilm scale) (Tableau 4). In more detail, concentrations of active surface pheopigments were higher before low tide ( $47.03 \pm 14.01\%$ ) than at low tide ( $43.93 \pm 15.39\%$ ) and were higher (Tableau 4) under the oyster table ( $47.03 \pm 14.62\%$ ) than in the aisle ( $43.94 \pm 14.81\%$ ). No significant effect was found for EPS, with an average value of  $18.43 \pm 19.74$   $\mu\text{g.g}^{-1}$ , range

0 to 239.61  $\mu\text{g.g}^{-1}$ . The detailed kinetics of photosynthetic yield (PY) are also provided with a full description in Appendix 2. Several effects were detected by regression models including MWH, habitat, the interaction between moment and habitat and the interaction between MWH and habitat (Tableau 4). Under the oyster table, a positive correlation was detected between PY and MWH, with a slope of  $-2.399 + 1.531 * \text{MWH}$ ;  $R^2 = 0.186$ ; p-value = < 0.0001) while in the aisle a positive correlation was also detected but with a slope of  $-8.179 + 2.807 * \text{MWH}$ ;  $R^2 = 0.366$ ; p-value = < 0.0001). Furthermore, the PY was clearly lower in the aisle than under the table, and the contrast was more pronounced before low tide than at low tide (respectively, at low tide  $0.36 \pm 0.17$  in the aisle and  $0.45 \pm 0.12$  under the table; at the beginning of low tide, the PY was  $0.39 \pm 0.19$  in the aisle and  $0.43 \pm 0.13$  under the table). Not-transformed data of the PY ranged from 0.04 to 0.65 and increased proportionally with MWH (Figure 12 D) with differences between the two habitats.

Tableau 4 : Summary of liner models (ANCOVA) conducted on biotic parameters. The results presented correspond to those which respected the conditions of homoscedasticity. Non-significant effects are not shown.  $X_1$  = Moment (bLT = 0; LT = 1),  $X_2$  = maximum water height,  $X_3$  = Habitat (under the table = 0; aisle = 1),  $X_4$  = Moment\*Habitat,  $X_5$  = MWH\*Habitat,  $X_6$  = MWH\*Moment. Significance levels: \* < 0.05, \*\* < 0.01, \*\*\* < 0.0001.

Variable	Formula	lambda	$R^2$	P-value
Sediment chl $a$	$32.71 + 2.67 * X_1 - 4.42 ** * X_3$	-	0.029	< 0.01
Sediment pheopigments	$47.3 - 1.8 * X_1 + 3.95 *** * X_2 + 5.63 *** * X_3 + 3.12 ** * X_4$	-	0.332	< 0.0001
Active surface chl $a$	$0.05 + 0.02 ** * X_3$	-	0.044	< 0.0001
Active surface pheopigments	$45.49 - 3.11 ** * X_1 + 3.09 ** * X_3$	-	0.022	< 0.01
Photosynthetic yield	$-8.08 - 0.34 * X_1 + 2.82 *** * X_2 + 5.6 *** * X_3 + 0.56 ** * X_4 - 1.3 *** * X_5$	3.69	0.320	< 0.0001
Light saturation coefficient (Ek)	$1.44 + 0.85 * X_2 + 5.02 * X_3 - 1.15 ** * X_5$	0.35	0.020	< 0.01
ETRmax	$1.41 - 0.17 *** * X_2 - 0.68 ** * X_3 + 0.16 *** * X_5$	-1.11	0.077	< 0.0001
Biomass	$14.48 - 0.58 ** * X_1 + 0.74 * X_2 + 4.27 * X_3 - 1.03 * * X_5$	-	0.032	< 0.01
Pemax	$-0.82 + 0.34 ** * X_2 + 1.55 * X_3 - 0.36 ** * X_5$	-	0.035	< 0.01
Pmax	$-16.46 + 1.3 * * X_1 + 6.28 ** * X_2 + 30.07 * X_3 - 7.04 ** * X_5$	-	0.041	< 0.01

For the light saturation coefficient (Ek), a significant effect of the interaction between the habitat and MWH was detected (Tableau 4). In the aisle, a positive correlation was detected between Ek and MWH (Figure 12 F). with an equation of  $\text{Ek} = 1.676 + 0.867 * \text{MWH}$  ( $R^2 = 0.020$ ; p-value = 0.017) while under the oyster table, the equation was  $\text{Ek} = 6.462 - 0.313 * \text{MWH}$ ;  $R^2 = 0.008$ ; p-value = 0.143). Concerning the ETRmax, the significant effects detected were the interaction between the habitat and MWH and the simple effects of the MWH and the moment (Tableau 4). In the aisle, a negative regression was detected between ETRmax and MWH (Figure 12 G) with an equation of  $\text{ETRmax} = 1.40 - 0.166 * \text{MWH}$  ( $R^2 = 0.098$ , p-value = < 0.0001) while under the oyster table, the equation was  $\text{ETRmax} = 0.726 - 0.010 * \text{MWH}$  ( $R^2 = 0.001$ ; p-value = 0.668). For MPB Biomass, an effect of the interaction

between MWH and habitat was detected but also a simple effect of the moment (Tableau 4). MPB biomass was higher at low tide ( $17.54 \pm 2.09$ ) than before low tide ( $16.96 \pm 1.71$ ). While the MPB biomass was stable under the oyster table (Biomass =  $18.432 - 0.287 \cdot \text{MWH}$ ;  $R^2=0.003$ ; p-value = 0.405) it increased slightly in the aisle (Biomass =  $14.231 + 0.725 \cdot \text{MWH}$ ;  $R^2=0.015$ ; p-value= 0.038).

For maximum productivity (Pemax), a significant effect of the interaction between MWH and habitat was detected, but also a simple effect of the MWH (Tableau 4). While the Pemax was mostly stable under the oyster table (Pemax =  $0.729 - 0.024 \cdot \text{MWH}$ ;  $R^2=0.0003$ ; p-value= 0.741) it increased slightly in the aisle (Pemax =  $-0.824 + 0.337 \cdot \text{MWH}$ ;  $R^2=0.051$ ; p-value= < 0.001). For maximum production (Pmax), a significant effect of the interaction between MWH and habitat was detected, but also a simple effect of the MWH and the moment (Tableau 4). While the Pmax was steady under the oyster table (Pmax =  $14.059 - 0.714 \cdot \text{MWH}$ ;  $R^2=0.001$ ; p-value = 0.593), it increased slightly in the aisle (Pmax =  $-16.091 + 6.341 \cdot \text{MWH}$ ;  $R^2=0.053$ ; p-value=< 0.0001). Furthermore, Pmax tended to be higher at low tide ( $11.36 \pm 8.66 \text{ mgC.m}^{-2} \cdot \text{h}^{-1}$ ) than 3 hours earlier at the beginning of low tide ( $10.00 \pm 7.93 \text{ mgC.m}^{-2} \cdot \text{h}^{-1}$ ).

### 3.3. Multivariate analysis

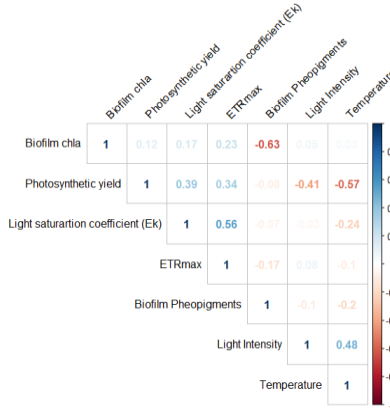


Figure 13 : Pearson correlation coefficients (r) between the variables that showed effects according to linear regression models

Correlation tests were also performed (Figure 13) on variables showing significant relationships according to the ANCOVA tests (Tableau 3 & Tableau 4): active surface chl a, active surface pheopigments, photosynthetic yield, light saturation coefficient, ETRmax, surface light intensity, sediment surface temperature. Active surface Chl a concentration was negatively correlated with percentage pheopigment (Figure 13;  $r = -0.63$ ;  $p < 0.01$ ). The PY was tightly and negatively correlated with temperature ( $r = -0.57$ ;  $p < 0.01$ ) as well as with light ( $r = -0.41$ ;  $p < 0.01$ ). As expected, SST and SLI were correlated together ( $r = 0.48$ ;  $p < 0.01$ ).

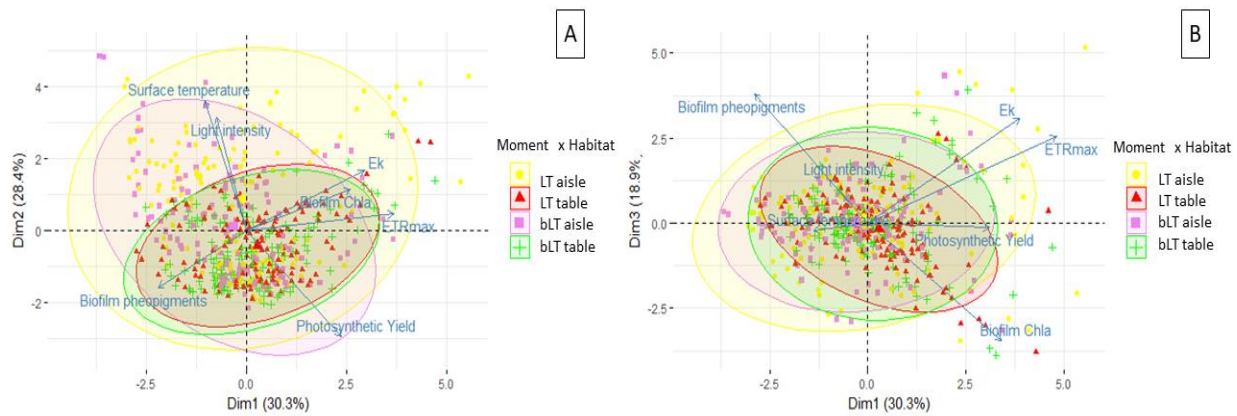


Figure 14 : A. PCA analysis with axes 1 and 2. Axis 1 carries Ek, ETRmax and surface active chl a concentration, axis 2 carries PY, light and temperature. B. PCA analysis with axis 1 and 3. Axis 3 carries surface active chl a concentration and pheopigments.

Finally, a PCA analysis was applied to selected variables to provide an overview of the main trends (Figure 14 A & B). The three first dimensions explained more than 77% of the total inertia. Among the seven variables, dimension 1 carried Ek, ETRmax and nylon web chl a concentration, these four variables contributed more than 1/7 of the total variance. PY, light and temperature were the main variables contributing to dimension 2, and accounted for 28.4% of total variance. Dimension 3 accounted for 18.9% of the total variance and carried Ek, chl a concentration on the nylon mesh and pheopigments. On axis 1, Ek, ETRmax and nylon mesh chl a concentration variables were positively correlated (Figure 14 A) and formed a cluster characterizing the MPB physiological state. A clear negative relationship was observed on axis 2 opposing the PY with temperature and light (Figure 14 A), these two variables accounted for 60% of axis 2. PY appeared to negatively depend on temperature and light. On axis 3 (18.9%), a clear opposing relationship was observed (Figure 14 B) between the chl a concentration on the nylon mesh and pheopigments. Furthermore, centroids under the oyster table ellipses were stacked compared to the ones in the aisle habitat (Figure 14 A).

To disentangle the factors influencing the PY of MPB, a multiple quantile regression was applied to direct factors: SLI and SST (Figure 15). Following a Box-Cox transformation (lambda = 2.97) a very strong effect of SST was observed ( $p\text{-value} < 0.01$ ) and a strong (but lesser) effect of SLI was also observed ( $p\text{-value} < 0.01$ ). The resulting quartile regression was:  $\text{Yield} = -0.023 * [\text{Temperature}] + 1.004$ . A multiple quantile regression was applied to photosynthetic yield and can be described by the following equation:  $\text{Yield} = -0.0196 * [\text{Temperature}] - 0.0003 * [\text{Light}] + 0.9501$ , indicating that both variables (SLI and SST) could

explain variations in PY but with a greater effect of sediment surface temperature followed by surface light intensity.

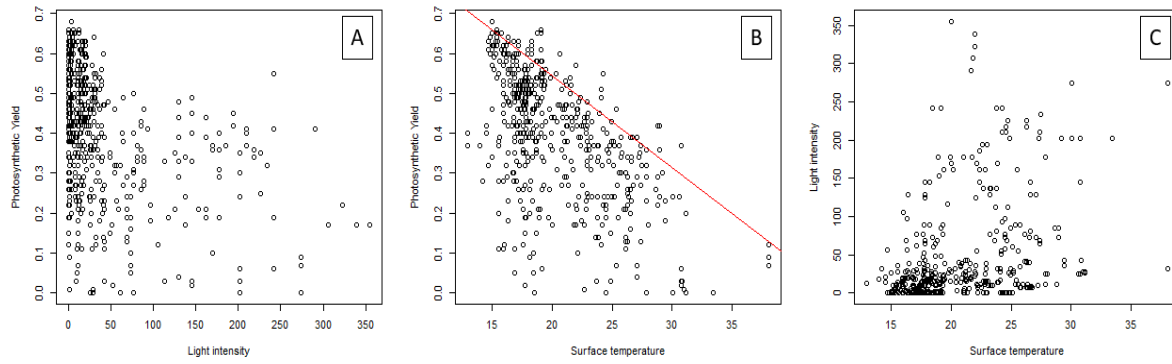


Figure 15 : Relationship between photosynthetic yield of MPB and A. ambient light intensity, and B. Surface temperature during low-tide emersion periods. A quantile regression was adjusted to the second dispersion diagram. C. Relationship between light intensity and surface temperature

Correlation tests were performed to check whether the set of relationships between variables differed between the two habitats. A strong negative correlation was observed between biofilm chl *a* concentration and the percentage of biofilm pheopigments both in the aisle ( $r = -0.7$ ;  $p < 0.01$ ) and under the oyster table ( $r = -0.65$ ;  $p < 0.01$ ). In the aisle, a negative correlation was observed ( $r = -0.32$ ;  $p < 0.01$ ) between Ek and the temperature (Figure 16. A) while under the oyster table, a small positive correlation was observed ( $r = -0.19$ ;  $p < 0.01$ ). In the aisle, a strong negative correlation was observed between PY and SST ( $r = -0.61$ ;  $p < 0.01$ ) (Figure 16 B), whereas the negative correlation was smaller under the oyster table ( $r = -0.39$ ;  $p < 0.01$ ). A strong negative correlation was also observed ( $r = -0.53$ ;  $p < 0.01$ ) in the aisle between PY and light intensity (Figure 16 A) while none was observed under the oyster table (-0.09;  $p = 0.12$ ; Figure 16 B).

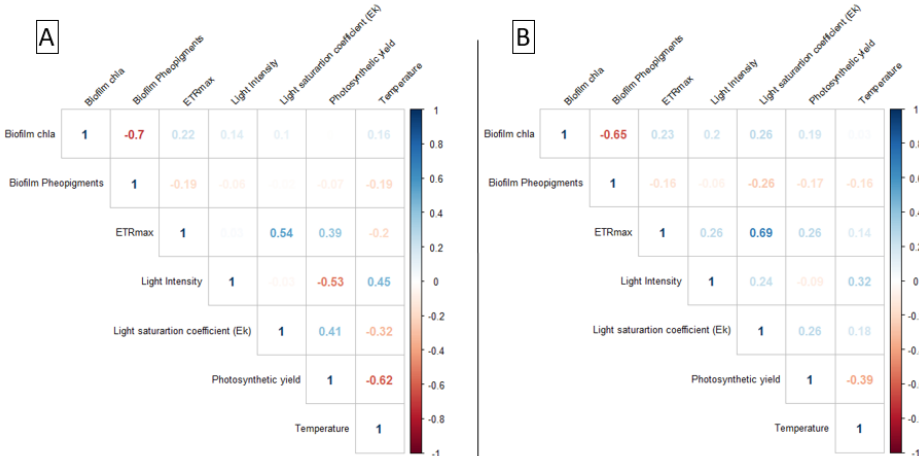


Figure 16 : Correlation matrices A. In the aisle. B. Under the oyster table

## 4. Discussion

### Impact of oyster tables on the benthic habitat

The present study focused on aquaculture-environment interactions at small scale. The impact of oyster cultivation on the quality of the benthic environment is already well documented (Forrest et al., 2009b). Previous observations highlighted potential muddification of the benthic compartment with cascade effects on microphytobenthos growth and macrofaunal community structure of the oyster farm at global scale (Dubois et al., 2007a; Ubertini et al., 2012). But studies on their impacts at small scale (i.e. the oyster table) remain scarce even though small-scale patterns are known to greatly affect ecological processes (Thrush et al., 2013). As Forrest et al., (2009) remarked, the relative importance of shading versus impacts of the seabed were never conclusively established and needed to be investigated in more detail. Following this line of thought, the aim of the present study was to assess the role of oyster farming and the local influence of oyster tables on MPB biofilm dynamics and photobiology.

For surface light intensity (SLI), a significant interaction between moment and maximum water height (MWH) plus a single effect of the habitat were detected. In line with the results obtained by Blanchard et al., (2002), in our study, SLI was clearly affected by tidal synchronization, as revealed by the significant interaction between moment and MWH. In addition, the shading effect was confirmed by the habitat effect we detected: SLI was clearly higher in the aisle than under the oyster table. SLI was also correlated with sediment surface temperature (SST). Light intensity is linked to different parameters such as the tide and the meteorological conditions. For SST, significant interactions were also detected between (i) habitat & MWH and (ii) moment & habitat. Higher tides, coinciding with the higher values of MWH, reduced the SST, and this reduction was even greater in the aisle than under the oyster table. Furthermore, SST was higher in the aisle than under the table, and the difference was more pronounced at low tide than at the beginning of the emersion period. Regarding sediment composition, a small percentage of sediment particles  $< 63 \mu\text{m}$  was observed, with an average value of  $7.38 \pm 1.45\%$  corresponding to a slightly muddy sand (Flemming, 2000). No significant effect of fixed factors (moment, MWH and habitat) was found for granulometry. Due to consolidation processes, the water content of the sediment decreased over time with higher values at the beginning of low tide than at low tide. This observation can be ascribed to a dewatering process and/or to desiccation. The OMF varied significantly depending on the interaction between habitat and MWH. Indeed, while the OMF was mostly stable in the aisle, it tended to increase with MWH

under the oyster table. The difference in OMF between the two habitats was only detected when MWH was high. Therefore, the oyster table was associated with higher levels of OMF. In benthic sediments, the amounts of nutrients depend mainly on the mineralization of organic matter by bacteria. In estuaries, MPB appear to be nutrient-limited due to its ability to migrate towards the deeper layers of sediment where pools of nitrogen (Underwood and Kromkamp, 1999; Orvain et al., 2003) and pools of silicate (Longphuirt et al., 2009; Leynaert et al., 2011) are easily accessible. Among the set of nutrients analyzed here, only ammonium ( $\text{NH}_4^+$ ) varied significantly according to fixed factors. Indeed, in the aisle, concentrations of  $\text{NH}_4^+$  tended to decrease with increasing MWH while the opposite was observed under the oyster table. The increase in  $\text{NH}_4^+$  concentrations was previously reported to increase Chl *a* content (Swanberg, 1991). A difference in sediment composition in benthic habitats at small scale was expected, due to oyster biodeposition (Newell et al. 2002). The absence of observed differences is a little puzzling. Indeed, for decades scientists considered that muddy sediments were the most appropriate to promote MPB colonization and growth, but recent investigations suggest that the sand-mud mixture found in intertidal areas actually provides the best conditions for the growth and fitness of MPB (Ubertini, 2015; Morelle et al., submitted). Indeed, bed muddification promotes cohesiveness and water retention whereas coarser particles allow interstitial water to flow, thereby reducing the water content of the sediment. This decrease in sediment water content was indeed observed between two sampling occasions in our study. The drainage induced by a large granulometry could result in nutrient losses for MPB because sandy sediments can act as a nitrogen sink (Sundbäck et al., 2000). MPB communities can therefore be impacted by nutrients in limiting concentrations (Nilsson et al., 1991), and the limitation would be accentuated in the case of sandy sediments. However, it is recognized that MPB can also reduce nutrient regeneration from the sediments (Sundbäck et al., 2000), so the concentration of nutrients may not be a good proxy to assess the potential influence of nutrient regeneration fluxes within the sediment bed when colonized by MPB. Depending on the habitat, in the present study, variations in parameters such as nutrients (except  $\text{NH}_4^+$ ), water content and sediment composition were not detectable. Thus, the parameters that describe local sediment dynamics did not explain variations in the MPB at a mesoscale in the summer conditions of our study.

The lack of variations among benthic variables could be linked to high dispersion induced by the tide currents and waves. Furthermore, the limited difference in sediment composition between oyster tables and aisles could be explained by oyster biodeposits being transported by

the tide current (Mitchell, 2006). Sediments was clearly fine sand with a samml proportion of mud (6.8% on average). Oyster biodeposits can be dispersed by water currents (Chamberlain, 2001; Hayakawa, 2001) thereby mitigating the small-scale local impact of oyster biodeposition on sediment dynamics, and thereby weakening the crosshatching pattern of oyster parks. Nonetheless, at the scale of the whole oyster park and surrounding habitats, oyster parks are known to entail muddification, as stressed by Orvain et al. (2012) and Ubertini et al. (2012) referring to the same ecosystem. Indeed, at the scale of the oyster park, the sediment composition (e.g. granulometry and OMF) is known to be shaped by oysters and their biodeposition (Haven and Morales-Alamo, 1966; Sornin, 1981). The oysters used in our study were at a low density and were at the spat stage, thus representing a relatively low biomass, likely lessening the potential impact of biodeposition in the context of crosshatching series of sediment habitats. The role of sediment characteristics did not appear to play a major role in explaining short-term dynamics of MPB. Indeed, due to the lack of variations in benthic variables and even though we observed a difference in OMF and  $\text{NH}_4^+$  between the aisle and under the oyster table (especially when MWH was high), the difference was not sufficient to conclude on the influence of the clear crosshatched pattern of the sediment (in the aisle versus under the oyster table) on MPB growth. On the other hand, SLI and SST were clearly attenuated by the oyster table, thus potentially creating a buffered habitat below. Although most sediment characteristics did not really differ much between the two study habitats, SLI and/or SST could play a more important role in MPB photobiology and growth.

## **Response of photobiological variables to habitat characteristics**

As already evidenced by studies of MPB biomass dynamics (e.g. Blanchard et al., 2002), the tide has (i) a short-term effect between the beginning and the end of emersion periods and is the cause of (ii) a bimonthly oscillation related to a combination of meteorological and tidal conditions (Blanchard et al., 2002). When two estuarine systems are compared, the synchronism could occur during different tidal conditions: spring tides (Marennes-Oléron) or during neap tides (*Baie des Veys*). On an intertidal mudflat in the *Baie des Veys*, the best period for MPB to grow corresponds to neap tides (Orvain et al., 2012). The link between light and tide is a really important synchronizer for MPB.

In the aisle, active surface chl *a* concentrations were lower than under the oyster table. This observation is evidence for more microphytobenthic biomass in the habitat under the table. While it is known that physical parameters such as hydrodynamics, temperature, light and

sediment granulometry influence the concentrations of chl *a* (Serôdio and Catarino, 1999; Jesus et al., 2006), we hypothesize that the difference in active surface chl *a* concentrations observed in our study is mainly influenced by the shade created by the oyster table and the tide current. MPB biomass (active surface chl *a*) accumulating at the top of the sediment was positively correlated with ETRmax and Ek with high production capacities, when MPB biofilm can form during low-tide exposure periods. Serôdio et al., (2006) underlined the relevance of migratory patterns and of the hourly variability of biomass productivity (in the sediment photic layer) in interpreting and predicting variability of photo response and primary productivity over time. Our results and particularly the relationship between chl *a* biomass and photosynthetic parameters reinforce observations of links between factors that promote the formation of biofilm and hourly photoresponse (Ek) and primary productivity (ETRmax).

Moreover, a negative relationship was found between active surface chl *a* concentration and associated pheopigment percentages. The same result was also found at the scale of the first centimeter of sediment (sediment chl *a*). The same negative relationship was recently reported by (Kwon et al., 2016) more particularly on intertidal mudflats of the Seine estuary (Morelle et al., submitted). Pheopigments are basically chl *a* deteriorated by photooxidation after cell lysis (Coelho et al., 2011) and mainly increase due to the grazing pressure exerted by macrofauna (Cartaxana et al., 2003; Orvain et al., 2014b; Kwon et al., 2016), such as macrozoobenthic filter feeders or deposit feeders. Previous studies emphasized the important role of this grazing pressure on biofilm in the top-down process that negatively regulates potential MPB growth (Savelli et al. 2018). Our study emphasizes the role of deposit feeders that could exist at high densities in summer conditions particularly under oyster tables, with a high proportion of annelid deposit feeders (Dubois et al., 2007a). This high biomass of deposit feeders directly grazing MPB biofilms could also have a negative top-down control on MPB primary production (Kwon et al., 2016).

In addition to grazing pressure, the locomotor behavior of deposit feeders and resulting surface bioturbation could act like a plow in a grass meadow. Under a “plow effect”, benthic diatoms would need time to renew their photosynthetic capacity after reconstructing their biofilm microhabitat, which is a prerequisite for photosynthesis. Indeed, MPB must actually create a transient biofilm before being able to grow and be photosynthetically active (Serôdio et al., 2006). The “plow effect” of deposit feeders in destroying MPB biofilms must be a strong constraint for benthic diatoms, and must require a lot of energy to recreate the biofilm and continuous migration before again becoming competent for photosynthesis.

Together, grazing pressure and the plow effect appear to negatively regulate MPB development (Figure 14). It might seem odd to observe that chl *a* concentration in the first centimeter of sediment was higher in the aisle than under the oyster table while the opposite was observed for active surface chl *a*. This paradox could be explained by the sensitivity of benthic diatoms to the degree of exposure to extreme levels of light and temperature. In warm sunny conditions (aisle habitat), the first response of MPB is to migrate vertically down into the sediment to avoid these extreme inhibiting conditions. This strategy would not be required by MPB in the shady tempered conditions under the oyster table and instead diatoms would migrate to the photic layer at the top of the sediment resulting in higher active surface chl *a* concentrations and hence MPB biomass. However, high sediment chl *a* values found in the aisle still indicate a global biomass of MPB in this habitat, regardless of its growth health, which is of the prime importance (Barnett et al., 2015).

Unlike MPB, phytoplankton has the ability to activate a xanthophyll cycle to counteract strong irradiance, a process associated with high energy expenditure. MPB appears to be better adapted to their usual extreme light environments during exposure periods at low tide and they can easily cope with photoinhibition process by using a strategy that is exclusive to this group, vertical migration. Avoidance is a very effective and rapid way to avoid excess light using little energy. Thus, in MPB, photoinhibition appears to rarely occur on intertidal mudflats. When vertical migration is not sufficient to cope with strong light irradiance, diatoms can also undertake the xanthophyll cycle process (Lavaud et al., 2007; Cartaxana et al., 2013). This strategy is associated with a reduction in photosynthetic parameters (such as PY) related to physiological photoprotection (Barnett et al., 2015).

Yet, vertical migration generally appears to be less effective in a sandy sediment than in a muddy one (Billerbeck et al., 2007). Knowing that light penetration through sediments decreases with increasing particle size (Tester and Morris, 1987; Kühl et al., 1994; Bliss and Smith, 2006) granulometry appears to be a very important component of MPB strategies to avoid excess light. Sandy sediments generally host epipsammic rather than epipelagic benthic diatoms (Barranguet, 1997; Méléder et al., 2005). Many studies have highlighted the ability of epipelagic diatoms to survive high light intensities in muddy areas through migration, while epipsammic diatoms inhabiting sandy areas are more affected by photo-inhibition impairments (Admiraal, 1984; Cartaxana et al., 2011; Perkins et al., 2001). Epipsammic diatoms cannot migrate due to their reduced motility (and hence reduced EPS production), these diatoms consequently implement physiological strategies such as the xanthophyll cycle induced in

photoinhibition (Cartaxana et al., 2011, 2013) that results in deteriorated photosynthetic parameters (Du et al., 2018) as observed in the aisle.

Benthic diatoms in the aisle habitat showed lower photosynthetic yields (PY) than in the table habitat. Rather than a direct sediment-induced effect, this higher vulnerability of MPB to excess light appears to be related to direct exposure to light in the absence of shading. Thus, benthic diatoms in the aisles were more constrained to use the xanthophyll cycle, resulting in low PY values (0.2), especially when MWH was low (neap tide) in this habitat. Thus, the PY could be qualified as poor during low MWH days in the aisle habitat. The most extreme light conditions occurred during neap tides, when the low tide is at midday. The highest PY observed at the beginning of low tide compared to at low tide in the aisle could reflect a decrease in the physiological state of diatoms during emersion. Indeed, the light intensity observed in the aisle appeared to be in excess, thereby impairing MPB photobiology during the neap tide (Müller et al., 2001; Pomeroy, 1959). As seen above, light intensity and temperature were attenuated under the oyster table, buffering the habitat. In this habitat, the very few times the PY dropped below 0.4 showed that the PY can mostly be qualified as good in this habitat. Between the two moments (beginning and end of the emersion period) the PY remained mostly stable or an increase was even observed in this habitat. In sum, the oyster table habitat appears to provide good conditions for MPB. Thus, in contrast to what happens in the aisle, the photoacclimatation process is not activated under oyster tables and allows benthic diatoms to proliferate, leading to higher active surface chl *a* concentration and a better photobiological status.

## **Summer thermoinhibition versus photoinhibition for MPB**

After comprehensive characterization of the factors influencing MPB productivity and biomass, we studied the mesoscale impact of the oyster table to decipher drivers of the MPB among sediment characteristics, light irradiance and temperature over the sediment bottom, during periods of exposure to low tide. As seen above, sediment characteristics should not be considered as central driving forces of MPB development since we found no difference between the aisles and the oyster tables. Nevertheless, it is recognized that sediment characteristics drive benthic primary production at the scale of whole oyster farms (Orvain et al., 2012; Ubertini et al., 2012) but also alter the macrofaunal assemblages at small scale (Dubois et al., 2007a) likely because of oyster biodeposition.

The lower correlation between light and temperature under the oyster table than in the aisle, supports the hypothesis of abrupt light attenuation and a smoother decrease in the temperature

in the shelter provided by the oyster table. The highest light intensities and temperatures were measured at the surface of the sediment when the low-tide slack time was close to noon in sunny conditions, which also resulted in the highest temperatures recorded during the course of the survey. Thrush et al., (2012) reported that quantile regression provides a better understanding of benthic interactions. This type of regression was done on the relationships between microphytobenthos variables and the meteorological environment that revealed the relationship in SLI and SST and their mutual interaction on the PY. Indeed, since the change in irradiance during a low-tide period can be very sudden due to passing clouds, whereas although temperature may vary in response, this happens very progressively and hence more slowly. Thus, the benthic habitat under the oyster table appears to be more buffered and less subject to sharp variations of these two meteorological factors than the aisle habitat.

The PY of MPB was tightly negatively correlated with SST and at a lower level of significance with SLI. SST and SLI were correlated together, and step-by-step multiple regression revealed temperature to have the main noxious influence on PY. As mentioned previously, MPB is able to cope with intense light (through migration) but is inhibited by high temperature in summer conditions. Thermoinhibition is observed when SST exceeds 25 °C (Blanchard et al., 1998b) but a more recent study updated this thermal threshold to 18 °C (Savelli et al., 2018). The divergence in MPB photoresponses in the two habitats suggests that inhibition would be more harmful for diatom photosynthesis in the aisles than under the oyster tables. Indeed, PY and SLI were not correlated under the oyster table, whereas in the aisle, they were negatively correlated. PY and SST were negatively correlated under the oyster table and even more negatively correlated in the aisle. Thus it appears that under the oyster table, the temperature can inhibit the photosynthetic yield (especially at low MWH) but that MPB is not subject to photoinhibition. In the aisles, thermoinhibition of MPB was even clearer, and one can assume that photoinhibition secondarily affects the MPB. Indeed, MPB would require a lot of energy to survive the high temperatures making it more vulnerable to other inhibiting factors such as light irradiance, and a high fraction of sand. These results also support the results of previous studies on the adaptive nature of photoprotective capacity in diatoms (Serôdio et al., 2012; Cartaxana et al., 2013; Barnett et al., 2015).

Our results show that in oyster parks, of the whole set of factors, temperature is the main factor driving PY in summer conditions and hence MPB productive capacities. Furthermore, if biogeochemistry and nutrient uptakes play a role in MPB productivity in summer conditions, these factors must partly be masked by the two main drivers: temperature and, to a lesser extent,

light. Our results reinforce the previously proposed hypothesis, that in summer conditions, thermo-inhibition and benthic grazing are the main limiting factors of MPB production on mudflats (Cadée and Hegeman, 1974; Sahan et al., 2007; Savelli et al., 2018). Apparently, when MPB is not able to successfully migrate into the sediment and is already inhibited by temperature, light irradiance can also negatively affect MPB fitness.

Surprisingly, once all factors were taken into account (sediment composition, light and temperature) and despite their influence on photosynthetic parameters responding to the very strong contrasts between the two habitats, these variations did not result in any significant differences in terms of primary production proxies. Similarly, there was no difference between the two habitats in terms of EPS contents. EPS secretion is considered as a metabolic route related to photosynthesis (Underwood et al., 2004) so some physiological links probably explain this conclusion. The potential influence of EPS must also be absent to explain some local differences on stabilization. EPS influence could theoretically amplify muddification of the sediment under oyster tables, but this process was apparently not responsible for small-scale sedimentary spatial patterns in our survey. MPB-induced biostabilization must therefore be similar in the two habitats. Higher sediment chl *a* concentrations found in the aisle indicate that, overall, MPB biomass in oyster parks is higher in the aisles than under the tables. Yet, the higher active surface chl *a* associated with higher PY found under the oyster table indicates that MPB photobiological health status is better in the shaded and tempered conditions under oyster tables.

## 5. Conclusion

Even though it is theoretically possible that oyster biodeposition acts as a major driver of MPB growth, muddification did not affect MPB dynamics through any small-scale effects linked to the presence of oyster tables. Indeed, the sediment dynamics appeared to play a secondary role compared to temperature and to a lesser extent, changes in light under the oyster tables. The observed attenuation of light and temperature under the oyster table along with the higher water content of the sediment, revealed the role of the oyster table as a buffer. By contrast, in the aisles, the opposite features could create an environment that harms MPB photobiological performances. On the other hand, the environment created by the oyster tables enriches the sediment in organic matter, leading to potential eutrophication which should also make this habitat more favorable for MPB photosynthetic performances. Our attempt to classify drivers of MPB growth shows that temperature is the major factor, followed to a lesser extent by light and only slightly by sediment composition and related biochemistry (organic fraction and

nitrogen recycling) at this small scale in oyster parks. When extrapolating in the global warming context, an average increase of 2 °C by 2100 (or more according to IPCC), solar irradiation and temperature could become even more deleterious for MPB production, on intertidal areas, in absence of artificial shading.

## Acknowledgements

We are particularly grateful to André-Gilles Taillepied and his team who kindly lent us the oyster table and enough space in their building to store our equipment and to conduct our experiments. Thanks also to C. Roger, B. Adeline and M-P. Dubos for their help with field work. We are grateful to G. Couprit for his work during his internship and to J. Phoenix for his commitment. Thanks to D. Goodfellow for the English review. I acknowledge the *Ministère de l'Enseignement supérieur et de la Recherche* for my PhD grant. We also thank the Normandy Region for the funding the PAM equipment



Globalement, l’envasement créé par les tables à huîtres et l’activité de biodéposition de ces bivalves ne semblaient pas structurer l’environnement benthique à l’échelle de la table même si c’est le cas à l’échelle du parc à huîtres (Ubertini et al., 2012). En effet, les caractéristiques environnementales benthiques correspondent à celles classiquement observées dans l’habitat ostréicole. En revanche, la table à huîtres diminuait la température et la lumière ainsi que leurs fluctuations à la surface du sédiment. Cette atténuation de la lumière et de la température sous la table des huîtres ainsi que la teneur en eau plus élevée des sédiments ont révélé le rôle tampon de la table à huîtres. Ainsi la classification des facteurs régulant la croissance du MPB montre que la température est le facteur principal, suivi dans une moindre mesure par la lumière et plus faiblement par la composition du sédiment et la biochimie connexe (fraction organique et recyclage de l’azote).

Suite à cette caractérisation de l’environnement benthique de l’habitat à l’échelle de la table à huîtres, l’impact de ces mortalités de naissains d’huîtres sur cet environnement a été étudié. Cette épizootie se traduit notamment par l’apport de matière organique à travers les chairs des naissains de *C. gigas* morts. L’étude présentée au chapitre 3 visait à décrire la qualité écologique de l’environnement table à huîtres à mésoéchelle en se basant sur la macrofaune benthique en tant que bioindicateur d’un stress environnement en croisant les résultats avec les données présentées au chapitre 2. La macrofaune benthique est un indicateur biologique bien reconnu de la qualité des écosystèmes côtiers (Dauvin, 2007; Dutertre et al., 2013). Aussi, la réponse du macrozoobenthos en réponse éventuelle à la mortalité des naissains d’huîtres a été étudiée. En effet, ces organismes vont être impactés de manière directe par cette pollution organique et de manière indirecte par des changements des caractéristiques de leur habitat. Lors de cette partie la charge virale en OsHV-1  $\mu$ Var des organismes constitutifs de la macrofaune a également été analysée afin d’identifier d’éventuels vecteurs de ce pathogène.



## **Chapitre 3 : Benthic macrofaunal changes in oyster parks during an OsHV-1 μVar oyster spat mortality outbreak**



# Benthic macrofaunal changes in oyster parks during an OsHV-1 μVar oyster spat mortality outbreak

Vanhuyse Charles, Julien Normand, Lepoittevin Mélanie, Orvain Francis

Article soumis à Marine Pollution Bulletin

## Abstract

In intertidal areas, oyster farming creates a crosshatching pattern between oyster tables and aisles. Tables provide a refuge from the current and solar irradiance (chapter 2) and the oysters facilitate the accumulation of OM, thereby potentially structuring the habitat and the associated macrozoobenthic community. The aim of the present study was to describe the quality of the oyster table environment at mesoscale and the response of the macrozoobenthos to OsHV-1 μvar after and before oyster mortality. The macrozoobenthos was dominated by *Golfingia vulgaris*, *Tubificoides benedii*, *Capitella capitata* and *Scoloplos armiger*. The disturbance of the macrozoobenthic assemblage took place in two phases: 1) after oyster spat mortality and 2) after seaweed stranding resulted in a bad ecological status, as revealed by macrofauna indicators. Large quantities of OsHV-1 DNA were found in some species, including small crabs and amphipods, the week after the mortality crisis. The response of macrozoobenthic ecological indicators revealed above all the strong impact of macroalgae after the episode of mortalities (at the end of the survey, when a massive stranding of dead seaweeds did occur).

## 1. Introduction

Estuaries are a particular type of environment since they are at the interface between the land, a river and the sea. These ecotones are among the most productive biotopes in the world (Whittaker and Likens, 1975). Characterization of the ecological status of estuaries is crucial for integrated coastal management and protection. Benthic macrofauna are a well-recognized biological indicator of the quality of coastal ecosystems (Dauvin, 2007; Dutertre et al., 2013). Indeed, many studies aimed at designing management plans have been based on benthic macrofaunal diversity (Keeley et al., 2013; Dutertre et al., 2013; Carstensen et al., 2014) and benthic indicators are routinely measured to assess spatio-temporal dynamics of coastal benthic assemblages in order to interpret the environmental status of the ecosystem and water quality. These indicators have been measured within the scope of the Marine Strategy Framework Directive (MSFD) Descriptor I (Biodiversity). As reported by Dauvin et al. (2007), soft-sediment macrozoobenthic organisms are considered to be good indicators because they (i) are relatively sedentary and consequently unable to escape deteriorating water/sediment quality, (ii) have relatively long life spans, (iii) include diverse species with different tolerances to stress, and (iv) play a vital role in biogeochemical and material cycling between the underlying sediment and the overlying water column (i.e. benthos-pelagos coupling). Macrozoobenthic assemblages can vary in response to changes at the water-sediment interface including enrichment in organic matter (OM) related to eutrophication (Borja et al., 2000; Ysebaert and Herman, 2002; Dauvin et al., 2007). Indeed, the water-sediment interface is where fluxes (release versus storage) between the two compartments occur. These fluxes can lead to benthic enrichment in OM and inorganic particles that provide a support not only for dissolved and/or adsorbed molecules such as nutrients, heavy metals and microplastics, as recently underlined by (Claessens et al., 2011; Van Cauwenbergh et al., 2013), but also for microorganisms (Rivera-Utrilla et al., 2001; Yee et al., 2000).

The introduction of a species in an established environment can disturb the surrounding biocenosis (Lévéque, 2006). This unbalance can be observed with oyster farming that mostly takes place in highly productive areas like bay estuaries. As a filter feeder, the Pacific oyster *Crassostrea gigas* (Bayne et al., 2017) is known to modify its environment (Padilla, 2010) in several ways. One of the direct effects of *C. gigas* is trophic competition with other suspensivores (e.g. *Cerastoderma edule*). Filter feeding types of oysters cause biodeposition, i.e. produce feces (assimilated i.e. organic particles) and pseudofeces (non-assimilated i.e. inorganic particles) after labial palp sorting.

Oyster farming is known to create particular environmental conditions beneath or adjacent to cultivation areas (Matisson and Lindén, 1983; Ubertini et al., 2012). These disturbances can elevate the topography (Forrest and Creese, 2006) through the accumulation of biodeposits (Haven and Morales-Alamo, 1966; Hily, 1976; Sornin et al., 1983; Mitchell, 2006; Nugues et al., 1996) thereby increasing the OM content of sediment beds (Nugues et al., 1996; Forrest and Creese, 2006; Echappé et al., 2018) which, in turn, creates a more anoxic sediment (Van Duyl et al., 1992; Forrest and Creese, 2006) and triggers bacterial remineralization (Azam et al., 1994; Baines and Pace, 1991; Nagata, 2008). These changes in sedimentary properties lead to the development of microphytobenthic biofilms (Orvain et al., 2012; Engel et al., 2017; Echappé et al., 2018). In addition to the biological impact of the oysters themselves, oyster farming practices also play a role in reshaping the sedimentary environment. Indeed, the elevated tables on which oysters are grown attenuate friction velocity and increase habitat muddification (Kervella et al., 2010; Nugues et al., 1996; Sornin, 1981). The modification of the sediment characteristics directly affects the benthic macrofaunal structure and may lead to the rarefaction of filtering bivalves and a strong colonization by annelids (Sylvand, 1995; Nugues et al., 1996; Dubois et al., 2007b). Indeed, it is recognized that oyster tables determine species assemblages and associated trophic pathways even at the small scale of one oyster table (Dubois et al., 2007a).

Since the first sightings and reports of oyster spat mortality in France in 2008 (Segarra et al., 2010b), noticeable episodes have been observed worldwide (Lynch et al., 2012; Jenkins et al., 2013; Hwang et al., 2013) causing massive losses of stock for oyster farmers. When the water temperature exceeds 16 °C, summer mortalities have mainly been attributed to the Ostreid herpes virus  $\mu$ variant (OsHV-1  $\mu$ Var) (Pernet et al., 2012) which can destroy up to 80% of individuals but with many variations depending on the site, the batch and the year. Recent studies showed that the oysters die of a virus-bacteria co-infection (de Lorgeril et al., 2018; Pathirana et al., 2019). The first step, consisting in the infection of oysters by OsHV-1  $\mu$ Var, is hypothesized to weaken the oysters' immune system thereby favoring the proliferation of opportunistic bacteria and leading to bacteraemia (de Lorgeril et al., 2018). During a mortality outbreak, the flesh of the dead oyster spat is dispersed in the environment by tidal currents. Through this deposition mechanism, the virus associated with dead oyster spat flesh could also move to the benthic compartment. In addition to the flow of OsHV-1 to the sediment, these epizootics can have significant ecological effects (Forrest et al., 2009a) including causing a flux of organic matter toward the sediment. This sudden organic enrichment can have several

impacts on the sediment dynamics and microphytobenthic biofilms and can disturb local benthic communities above and close to the oyster tables. The fate of this pathogen agent and its resilience outside of the host organism, i.e. once the virus is transferred to the bottom sediment, is poorly described to date. Connected to how macrozoobenthic species feed and to their bioturbation activity, some could specifically interact with viral resilience outside the host.

This aim of this *in-situ* study was thus to assess the response of the benthic compartment and particularly the associated macrofauna in the context of summer oyster spat mortality caused by OsHV-1 μVar. The experiment was conducted in the Bay of Veys (Normandy, France), a rearing area where the spat mortality syndrome has been observed every summer since 2008. An oyster farmer gave us access to his rearing facilities which enabled us to work properly. The survey started before the annual spat mortalities began and lasted for 41 days, covering the entire mortality period. Macrofauna were sampled by coring in the aisle and under one oyster table to describe the spatio-temporal dynamics of the soft-sediment macrofauna community. To characterize the benthic environment and the associated benthic macrofauna and their variations, benthic indicators were calculated including BOPA (Dauvin and Ruellet, 2007), AMBI (Borja et al., 2000) and BENTIX (Simboura and Zenetos, 2002). Benthic habitat characteristics including sediment and biofilm chl *a*, sediment water content, sediment organic matter content, NH<sub>4</sub><sup>+</sup> concentrations and sediment grain size were monitored. OsHV-1 μVar DNA was quantified in the most abundant macrofauna species. Multivariate analyses were performed to highlight ecological interactions and ranking between habitats, days and species. The specific objectives of this study were to (i) characterize the benthic environment of oyster farms at the table scale according to benthic indicators, (ii) assess the density and diversity of benthic macrofauna in the aisle and under the oyster tables in response to the viral mortality of oyster spat.

## 2. Material & method

### 2.1. Study site

The Bay of Veys is located in the south-western part of the Seine Bay where 40% of the inputs originate from the River Vire (Jouenne et al., 2007). This bay is an estuarine and shellfish ecosystem that stretches over an intertidal zone of 1.60 km<sup>2</sup>. During spring tide, a tidal range of 8 meters with currents of 3 m.s<sup>-1</sup> can be reached (Orvain et al., 2012). Within this area, oyster farms are mainly located on soft sediment with a natural tendency to slow silting due to tidal currents accentuated by the installation of oyster beds (Kopp et al., 1991). Although growth in

this shellfish basin is the fastest in France, in terms of production, it only comes in second (25 000 tons in 2016; source: *Comité National de la Conchyliculture*).

## 2.2. Experimental design

The study was conducted along a row of oyster tables located at Géfosse-Fontenay in the Bay des Veys (Normandy, France) on the foreshore (from 49°22'53.2" N; 001°05'44.2" W to 49°22'54.6" N; 001°05'43.4" W) from the 22<sup>nd</sup> of May 2017 to the 1<sup>st</sup> of July 2017. One oyster table was divided into three areas (A, B & C) (Figure 17), and in each area, 20 oyster bags each containing smaller bags containing 200 three-month-old oyster spats were placed. Oysters were produced using standard hatchery procedures (Petton et al., 2015a).

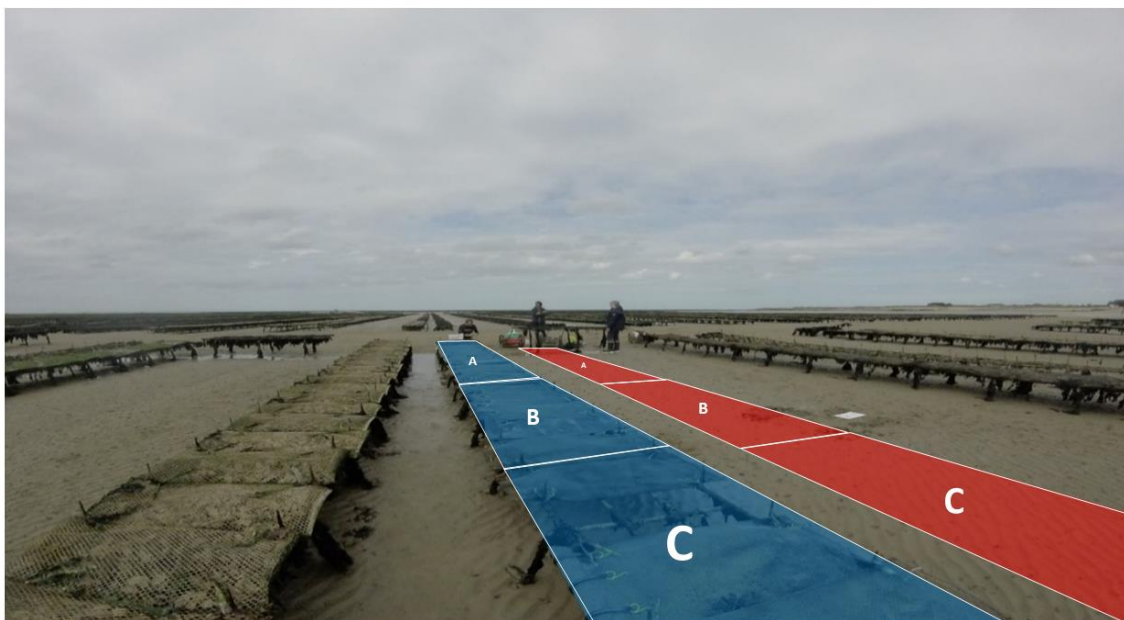


Figure 17 : Experimental field design. The oyster table sample areas are in blue (A, B & C) and the aisle sample areas are in red (A,B & C)

## 2.3. Macrofaunal sampling

Benthic macrofauna were sampled in a 0.2 m diameter PVC core (surface = 0.0314 m<sup>2</sup>) inserted to a maximum depth of 20 cm. Samples were sifted through a 1 mm sieve and fixed in a 4% formol solution before being transferred to ethanol for conservation. The species were then counted and identified using (Lincoln and British Museum, 1979) identification keys for amphipods, (Fauvel, 1923, 1927) identification keys for annelids, and (Hayward and Ryland, 1995) identification keys for decapods and bivalves. On each sampling day, photos were taken of the surface of the sediment to assess the extent of algal coverage.

## 2.4. OsHV-1 sampling

The most abundant and visible macrozoobenthos species on each sampling date were sampled (maximum 5 individuals per species) and conserved at -20 °C for quantification of their OsHV-1 charge. After thawing, sampled organisms were crushed and their DNA was extracted and purified using the NucleoSpin® 96 Blood Kit (Macherey-Nagel). Total extracted DNA was quantified using a Nanodrop 200 (Thermoscientific) for standardization purposes. OsHV-1 DNA in the samples was quantified via real-time qPCR CFX 96™ C1000™ (Biorad).

## 2.5. Data analysis

The habitat diversity was estimated using species richness and the biodiversity index of Shannon & Weaver ( $H'$ ). This index is maximum when all individuals are distributed equally among all species and vice versa. It is expressed by the following equation:

$$H' = - \sum_{n=1}^{n=1} \left( \frac{ni}{N} \right) \times \log(ni/N)$$

where  $H'$  is the diversity index;  $n$  is the number of individuals of taxon  $i$ ; and  $N$  is the total number of individuals. The species evenness was calculated using the index of Piélou ( $J'$ ) which makes it possible to compare the structures of the different environments. This index varies between 0 and 1; it tends to 0 when diversity is low and tends to 1 when all species show the same abundance. This index is calculated as follows:

$$J' = \frac{H'}{H'max}$$

In addition, rank-frequency diagrams were calculated to describe variations in the structure of macrofauna assemblages between table and aisle habitats over time. When the curve is hyperbolic, it reflects very strong disparities between species (dominance relationships, rare species) and potentially highly disturbed ecosystems (Frontier, 1985). On the other hand, when the diversity and abundance of species are strong the curve will be more convex (Frontier et al., 2008)

The Benthic Opportunistic Polychaetes - Amphipods (BOPA) ratio index (Dauvin and Ruellet, 2007) was used to measure the ratio between the frequency of amphipods (the latter being very sensitive to the presence of organic matter) and that of opportunistic polychaete annelids belonging to groups IV and V. This index is determined on a scale from 0 to 0.30103.

$$BOPA = \log \left( \frac{f_p}{f_{A+1}} + 1 \right)$$

The AZTI Marine Biotic Index (AMBI) index (Borja et al., 2000) establishes the ecological quality of a particular site, determined on a scale from 1 to 5 with the calculation of the benthic coefficient (BC) representing the quality of the benthic conditions in ranks. from 0: unpolluted to 7: highly polluted (Hily 1984, Majeed 1987). This index was calculated according to the following formula:

$$AMBI = [(0 * \%GI) + (1,5 * \%GII) + (3 * \%GIII) + (4,5 * \%GIV) + (6 * \%GV)] / 100$$

In continuity with the AMBI, the BENTIX index (Simboura and Zenetos, 2002) was calculated to describe the response of soft substrate benthic communities to different natural and man-made disturbers by reducing the number of ecological groups involved in the formula to limit errors due to the grouping of species. This index is calculated according to the following formula:

$$BENTIX = \{(6 * \%GI) + 2 * (\%GIII + \%GV)\} / 100$$

The ecological groups II and IV of the AMBI index can respectively be associated with ecological groups I and III of the BENTIX index due to their low significance. This index ranges from 2 (poor environmental quality) to 6 (good environmental quality). Characterization of the ecological status according to each index is reported in Tableau 5 :

Tableau 5 : Classification of soft bottom benthic habitats based on BOPA, AMBi and BENTIX indexes

Ecological quality status	BOPA	AMBI	BENTIX
High	0 – 0.04576	0 – 1.2	4.5 – 6.0
Good	0.04576 – 0.13966	1.2 – 3.3	3.5 – 4.5
Moderate	0.13966 – 0.19382	3.3 – 4.3	2.5 – 3.5
Poor	0.19382 – 0.26761	4.3 – 5.5	2.0 – 2.5
Bad	0.26761 – 0.30103	> 5.5	0

Photos were taken of algal coverage during the survey and covering calculated as a percentage of recovered surface using ImageJ software. Data were analyzed using multivariate methods using “vegan”, “MASS”, “ggplot2”, “dplyr”, “tidyR”, “grDevices”, “FactoMineR”, “factoextra”, “corrplot”, “RColorBrewer” and “ade4” packages via the R-studio software. Multivariate analysis (CA, AFC) was performed on the 10 most abundant species with supplementary

variables described in a parallel study (Chapter 2). Rare amphipods and polychaetas were added to the CA as additional variables because of their scarcity.

### 3. Results

#### 3.1. Abundance, diversity and specific richness

A total of 389 individuals belonging to 19 species were identified. The 19 species corresponded to 12 annelids, 5 arthropods, 1 bivalve and 1 sipunculid. The number of taxa was not evenly distributed between the two habitats since 19 species were observed under the table and only 11 in the aisle. Analysis of the faunae showed that the oyster table habitat had a higher faunal density ( $26.88 \text{ ind.m}^{-2}$ ;  $p\text{-value} < 0.0001$ ) than that the aisle habitat ( $7.52 \text{ ind.m}^{-2}$ ). This difference did not apply to biomass ( $p\text{-value} > 0.05$ ) due to a wide standard deviation (oyster table biomass mean =  $49.96 \pm$  standard deviation  $151.93$ ; aisle biomass =  $12.23 \pm 20.35$ ). Abundance increased by 262% between day 179 and day 182 under the oyster table, while it increased by 281% in the aisle.

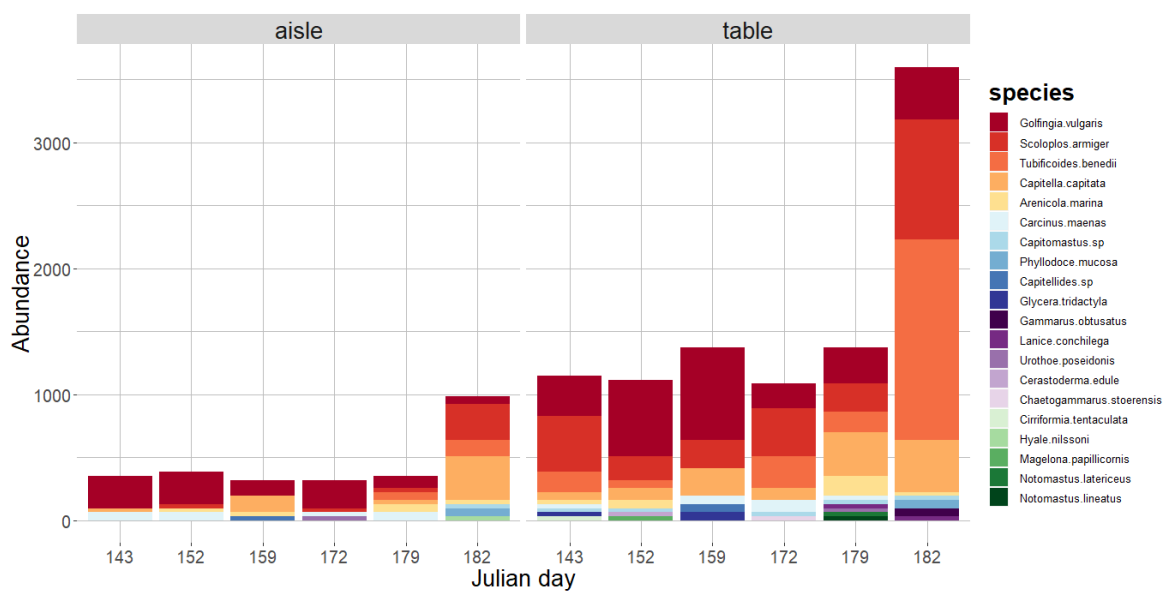


Figure 18: Temporal evolution of species abundance observed according to habitats and days

The most abundant species were *Golfingia vulgaris*, *Scoloplos armiger*, *Tubificoides benedii* and *Capitella capitata* (Figure 18). Species richness remained more or less constant in each habitat (Tableau 6 :) but almost doubled under the table between day 172 and day 179, with values shifting from 7 to 11 species. Consequently the highest values were observed at day 182 in both habitats: respectively,  $3596.9$  and  $986.8 \text{ ind. m}^{-2}$  were found under the oyster table and in the aisle.

Tableau 6 : Shannon index, Species Richness and Pielou index

Julian Day	Habitat	Shannon ( $H'$ )	Species richness	Pielou ( $J'$ )
143	aisle	0,76	3	0,69
143	table	1,66	9	0,75
152	aisle	0,98	4	0,71
152	table	1,48	8	0,71
159	aisle	1,19	4	0,86
159	table	1,35	6	0,76
172	aisle	0,94	4	0,68
172	table	1,65	7	0,85
179	aisle	1,72	6	0,96
179	table	2,00	11	0,83
182	aisle	1,68	8	0,81
182	table	1,48	9	0,67

Species richness ranged from 3 (aisle, day 143) to 11 (table, day 179) and was globally higher under the oyster table (8.33) than in the aisle (4.83). From a temporal view, species richness was always higher under the oyster table, but at the end of the survey, tended to increase in the aisle to almost reach table values. In terms of species diversity, the Shannon index values (Tableau 6 :) ranged from 0.76 (aisle, day 143) to 2.00 (table, day 179). The index was higher under the oyster table ( $H' = 1.60$ ) than in the aisle ( $H' = 1.21$ ). The Pielou index (Tableau 6 :) ranged from 0.67 (Tableau 6 :, day 41) to 0.96 (aisle, day 179). This index averaged 0.762 under the oyster table and 0.78 in the aisle. The Pielou index remained quite stable around 0.75 under the oyster table except on day 172 and 179. More variations were recorded in the aisle specially at the end of the survey.

### 3.2. Frequency rank chart

Rank-frequency distribution was used to characterize species diversity (Figure 19).

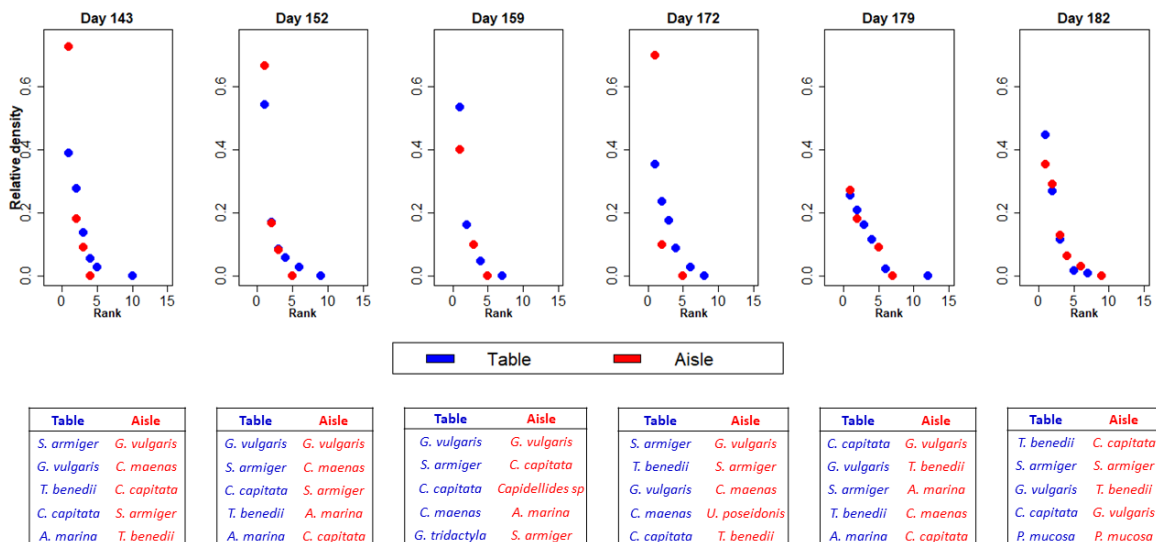


Figure 19: Rank frequency diagrams for sampling days. Blue points correspond to table samples and red points to aisle samples. The table under each diagram corresponds to the five most abundant species for each habitat.

Globally, relative densities under the table tended to be higher than the densities in the aisle except on day 159. There did not seem to be a clear difference in the shape of the curves between the two environments. On the other hand, the aisle habitat was less diversified than under the oyster table. Nevertheless, a three-phase variation in the dominant species was observed over time was observed. During the first phase (days 143, 150 and 159), the species *G. vulgaris* dominated, with a notable presence of *S. armiger*. The second phase, day 172, was a transitional state before the third phase, when *G. vulgaris* and *S. armiger* were still dominant but more *T. benedii* were observed under the table. The third phase (days 179 and 182) was characterized by a decrease in *G. vulgaris* and a massive presence of species such as *T. benedii*, *C. capitata* and *S. armiger*.

### 3.3. Ecological indicators

The BOPA index (Figure 20 A) ranged from 0.56 to 0.09. The mean index under the oyster table was estimated to be 0.39 and 0.28 in the aisle. Except on days 159 and 182, the BOPA index was higher under the oyster tables. There was a gradual increase in the BOPA index over time whatever the habitat.

The AMBI index (Figure 20 B) ranged from 0.6 to 4.35 indicating a contrasted environmental quality ranging from high to poor. The average AMBI index was 2.98 under the table and 2.22 in the aisle. Except on day 159, the calculated AMBI index was higher under the oyster table. The AMBI index tended to increase over time whatever the habitat. The AMBI index reached maximum in the two habitats on day 182. In terms of functional groups, the aisle habitat was mostly composed of group II species (species that are not affected by a slight enrichment in organic matter) and group III (species that tolerate organic matter enrichment) while more group V species (very opportunistic species that characterize disturbed environments) were observed under the oyster table particularly at the end of the survey. Indeed, a gradual dominance of group V species was observed from day 143 to day 182 under the table mainly due to species such as *C. capitata*, *S. armiger*, *T. benedii*.

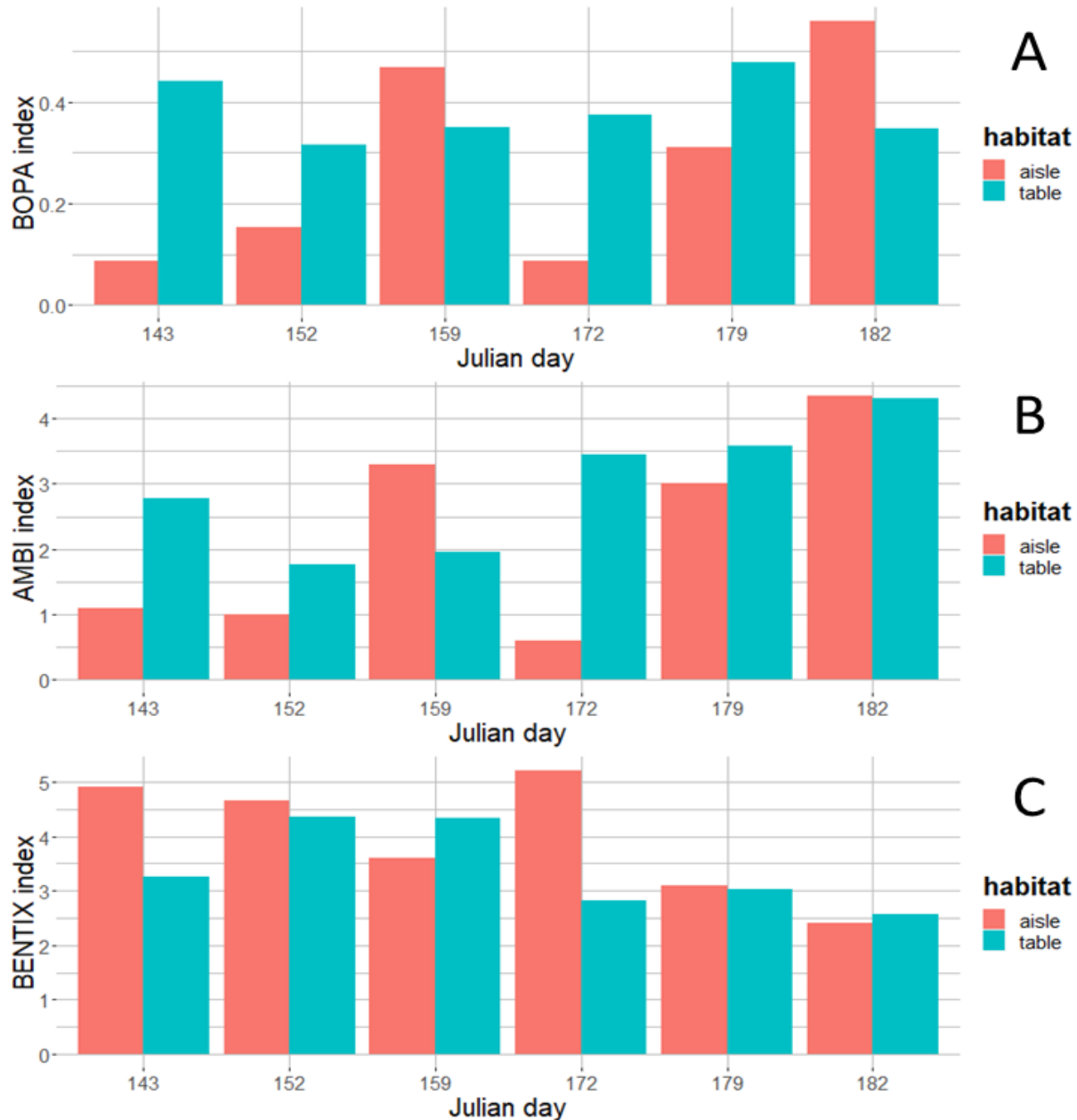


Figure 20 : benthic indexes with A. BOPA index. B. AMBI index. C. BENTIX index

The BENTIX index (Figure 20 C.) ranged from 2.41 to 5.20, with an average of 3.39 under the table and 3.98 in the aisle. Except on day 159, the calculated BENTIX index was higher under the oyster table, but decreased over time in both habitats to reach a minimum value of 2.5 on day 182, confirming the poor quality already detected by the AMBI index.

### 3.4. Multivariate analysis

Axis 1 of the Correspondence Analysis (CA) accounted for more than 49% of total variation, axis 2 accounted for more than 18%, and axis 3 for more than 12% of total variation (Tableau 7 :).

### Chapitre 3. Macrozoobenthos changes after oyster spat mortalities

Tableau 7 : Contribution of species to the first 3 axes of the correspondence analysis

	<b>Dim.1 (49.18%)</b>	<b>Dim.2 (18.87%)</b>	<b>Dim.3</b>
<i>Golfingia.vulgaris (I)</i>	<b>38.84</b>	5.5	1.74
<i>Scoloplos.armiger (III)</i>	6.43	1.33	2.81
<i>Tubificoides.benedii (V)</i>	<b>37.49</b>	10.15	0.02
<i>Capitella.capitata (V)</i>	0.29	<b>50.29</b>	0.11
<i>Arenicola.marina (III)</i>	1.07	9.42	40.33
<i>Carcinus.maenas III</i>	7.65	10.26	18.19
<i>Capitomastus.sp (V)</i>	0.22	0.47	0.5
<i>Phyllocoelum.mucosa (III)</i>	2.76	4.27	0.08
<i>Capitellides.sp (V)</i>	3.55	8.32	19.08
<i>Glycera.tridactyla (II)</i>	1.68	0	17.16

The fluctuations in the abundances of the two species *G. vulgaris* and *T. benedii* were the best represented on Dim. 1 which together accounted for more than 76% of the variation. On the positive part of this axis, *G. vulgaris* was associated with the beginning of the study (Figure 21). On the negative side of the axis 1, *T. benedii* was more associated with the end of the survey (day 182). In the middle of the cloud of individuals, the species *S. armiger*, rare amphipods, rare polychaeta and other polychaeta (e.g. *Capitomastus sp*, *P. mucosa*) were found more on the negative side of the axis 1. *A. marina*, *G. tridactyla* and *C. maenas* were found on the positive side of the cloud of individuals.

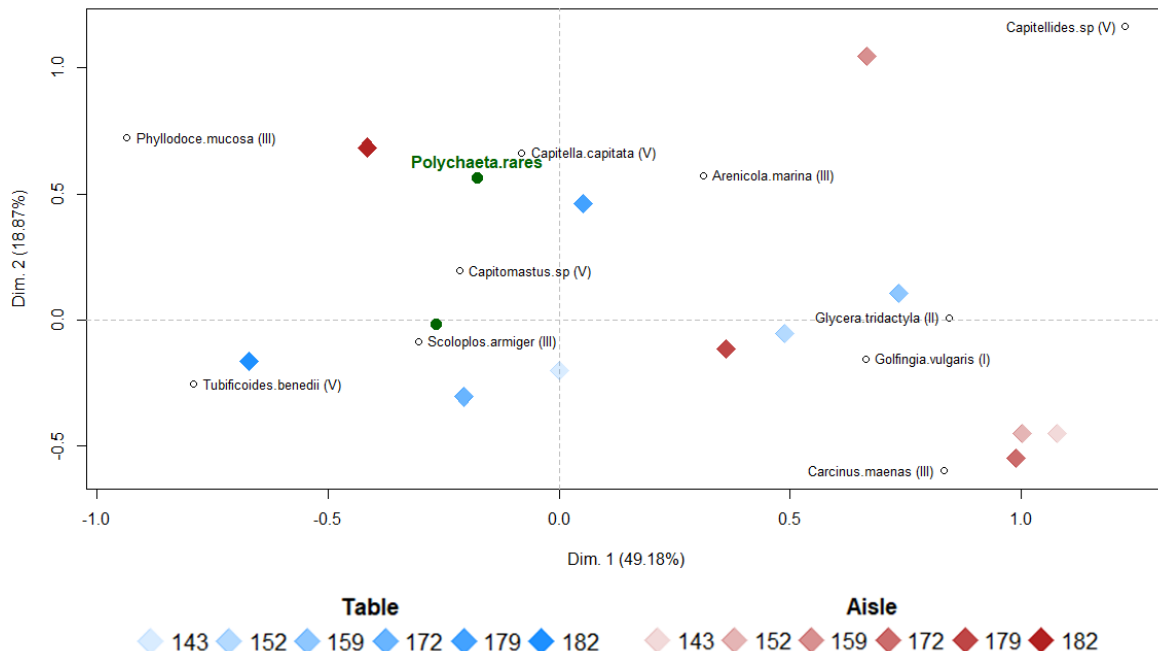


Figure 21: Correspondence analysis. Roman numerals in parentheses after the species name correspond to the AMBI ecological groups.

The fluctuation in the abundance of *C. capitata* was the best represented on Dim. 2 with more than 50% of variation explained by this species. *C. capitata* was associated with positive values on this axis at the end of the study. The species *G. vulgaris* and *C. maenas* were found on the negative part of axis 2. There was no clear difference in habitat (table vs aisle), *T. benedii* was present in table samples on the last day of the survey while *C. capitata* and *G. vulgaris* were found in both habitats.

Following the CA, a principal component analysis (PCA) was performed using sedimentary data and species biomass ordered according to AMBI ecological groups. The algal coverage percentage was included as an additional variable (Figure 22 :).

Tableau 8 : Contribution of variables to the first 4 axes of the principal correspondence analysis

	<b>Dim.1 (27.92%)</b>	<b>Dim.2(26.33%)</b>	<b>Dim.3 (16.1%)</b>	<b>Dim.4 (11.1%)</b>
Water content	<b>25.8</b>	0.62	0.01	12.28
chl a biof	<b>22.19</b>	3.03	3.25	3.34
chl a sed	0.12	<b>24.13</b>	10.47	1.79
NH4	1.64	9.27	3.95	<b>28.13</b>
OM	4.85	3.55	<b>16.48</b>	<b>19.92</b>
Mud content (inf63)	<b>17.15</b>	7.81	10.36	0.37
I	<b>25.96</b>	0.69	0.07	0.92
II	1.67	<b>20.6</b>	<b>12.58</b>	11.6
III	0.13	<b>15.64</b>	<b>32.46</b>	0.63
V	0.48	<b>14.68</b>	10.38	<b>21.03</b>

Axis 1 (27.92% of total inertia) of the PCA contained the biomass of AMBI group I species and three sedimentary variables: mud content (inf63), water content of the sediment and biofilm chl a (Tableau 8 :). More precisely, AMBI group I species biomass, were on the negative part of the axis with biofilm chl a and water content of the sediment opposed to fine sediment particles (Figure 22 :). Axis 2 (26.33% of total variance) of the PCA contained the sediment chl a and group II, III and V AMBI species. These AMBI groups were together on the positive part of the axis in opposition to sediment chl a. Axis 3 (16.1% of total variance) of PCA contained organic matter content (OM) and group II and III AMBI species. These variables were positively correlated together (not shown in Figure 22 :). Axis 4 (11.1% of total variance) of the PCA contained NH<sub>4</sub><sup>+</sup> concentrations, organic matter content (OM) and the group V AMBI species. These species and NH<sub>4</sub><sup>+</sup> concentrations variables were negatively correlated with OM content and therefore opposite on axis 4.

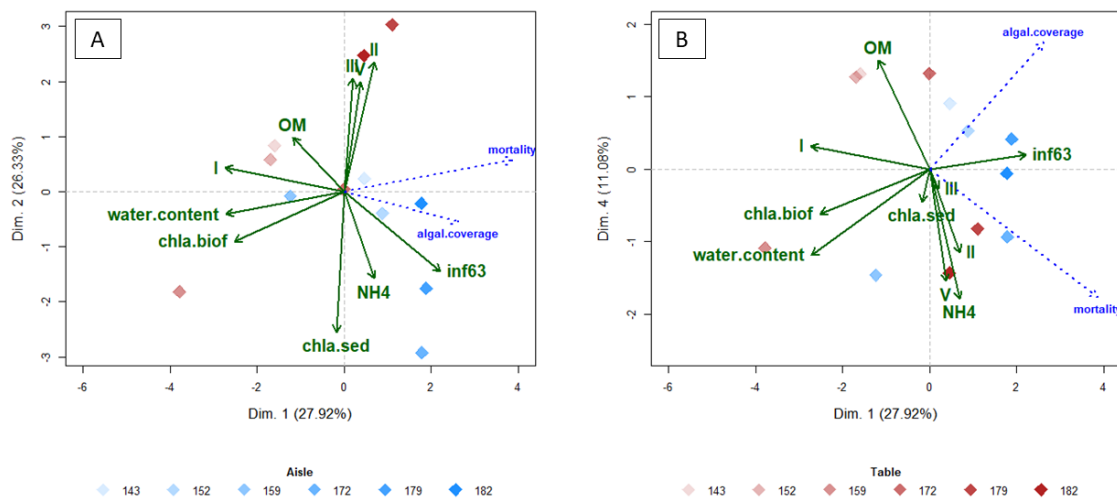


Figure 22 : PCA analysis with A. Dim 1 and 2. Dim 1 carried contained biomass for AMBI II and III species, fine sediment particles (inf63) and organic matter content (OM) variables. Dim 2 contained the sediment water content, the biofilm and sediment chl a and the AMBI I species. B. axis 1 and 4. Dim 4 contained  $\text{NH}_4^+$  concentrations and the species of the AMBI V groups

Algal coverage added as an additional variable, which seemed to be the most associated with mud content (% of sedimentary particles  $< 63 \mu\text{m}$ ) on Dim 1 (Figure 22 : A.), but not to other variables not macrofaunal groups. On the second graph of the PCA (Figure 22 : B.), the algal coverage variable contributed strongly to the variation and was positively associated both with the OM fraction and mud content (Dim. 4) but was clearly opposed to  $\text{NH}_4^+$  concentration. Oyster spat mortality was also included as an additional variable. This variable seemed to behave like algal coverage on Dim 1 and was opposed to water content and chl a concentration within the surface microphytobenthic biofilm (Figure 22 : A). The oyster sat mortality variable (Figure 22 : B) was associated with both  $\text{NH}_4^+$  concentration and with the AMBI groups II and V species (Dim. 4) and opposed to organic matter content (OM).

### 3.5. Oyster mortality episode

After the structure of the macrozoobenthic community was investigated in detail, the link with the context of oyster activity was examined to relocate the oyster spat mortality crisis (OsHV-1  $\mu\text{Var}$ ) in time. The first oyster spat mortalities were recorded on day 157 (Figure 23). Mortalities continued for 20 days until they stabilized at around 40% of survivors on day 177. No obvious correlation was observed between stranding of dead seaweed and oyster spat mortality. However, the dead seaweed stranding happened in the second period (from day 172).

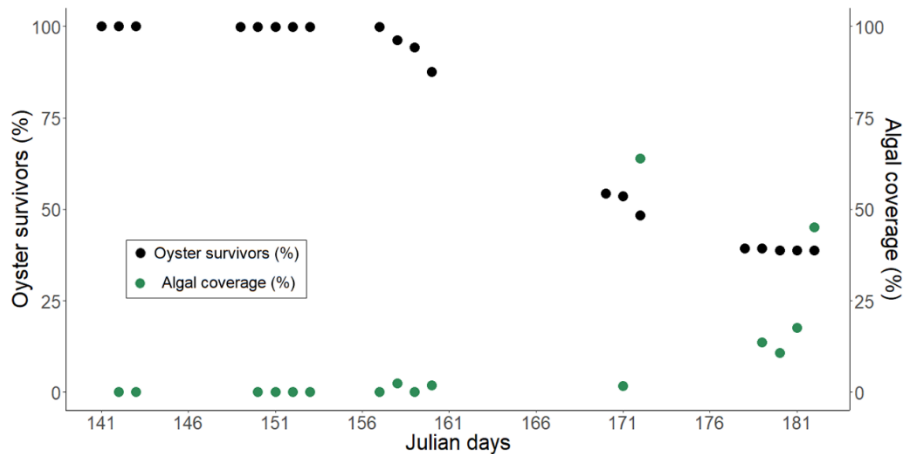


Figure 23: Percentage of survival and algal coverage during the oyster spat mortality in summer 2017

#### *OsHV-1 DNA detection and quantification*

The biggest quantities of viral DNA were found in the tissues of crustaceans (amphipods, barnacles and *C. maenas*) regardless of the day (Figure 24). A trend was observed after oyster spat mortality: the heaviest OsHV-1 DNA copy numbers were found in these organisms after the mortality period, despite the fact that some standard deviations overlapped. A significant increasing gradient of viral detection was observed over time ( $p\text{-value} < 0.001$ ). Significant differences were observed between species on day 159 ( $p\text{-value} < 0.001$ ) and day 179 ( $p\text{-value} < 0.01$ ). On day 159, *Littorina littorea* showed the highest viral contamination (768.54 UG/ng DNA) but with only one individual. In second place came the species *S. armiger* ( $209.44 \pm 319.77$  UG/ng DNA). Conversely, no viral DNA was detected in *M. edulis* on day 159. On day 179, *Balanus sp* had the highest viral load with ( $563.74 \pm 597.64$  UG/ng DNA) followed by *C. edule* ( $393.10 \pm 399.93$  UG/ng DNA). The lowest viral load was associated with *C. maenas* as no OsHV-1  $\mu$ Var was detected in this organism on that day.

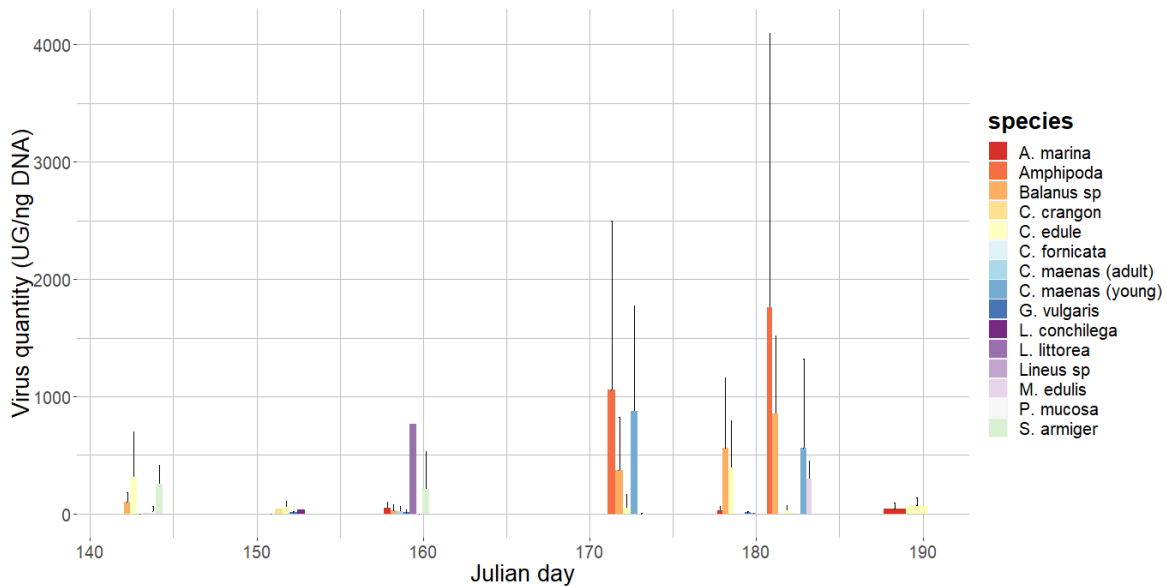


Figure 24: OsHV-1 μVar viral loads in macrozoobenthic fauna during the oyster spat mortality episode of summer 2017

## 4. Discussion

### Macrofaunal community structure of soft sediments in oyster park of Baie des veys

In this study, the most important taxonomic group of soft-sediment macrofaunal community was polychaeta, as usually observed in this estuarine oyster parks (Sylvand, 1995; Ropert and Dauvin, 2000a). This marine worm taxa is considered to be one of the one of the most important in coastal and marine environments, in terms of diversity, abundance and functional role (Fauchald and Jumars, 1979). Their preference for fine or very fine sediment is a common feature in many estuaries (Ysebaert and Herman, 2002). The absence of species such as *Cerastoderma edule* illustrates the trophic competition between filtering organisms induced by the massive presence of *C. gigas*. Indeed *C. edule* has gradually disappeared from this site but was still very abundant and dominant in the rest of the bay in 2012 (Ubertini et al., 2012). Conversely, *L. conchilega*, took advantage of the impact of oyster biodeposition and underwent very strong proliferation in the 1970s and until the beginning of the 2000s (Ropert and Dauvin, 2000) before almost disappearing in 2003, likely before the massive mortality caused by a heat wave that occurred that summer. Amphipods remained scarce and were mainly found at the end of the survey in the form of the genus *Gammarus*. These organisms are mainly detritivorous (Guerra-García et al., 2014) and were found feeding on dead oyster spat flesh. Carnivorous species can be very sensitive to OM inputs (Borja et al., 2000) but they were poorly represented in both habitats, in contrast to the results obtained in another study in the same oyster park

(Dubois et al., 2007). Four species dominated the populations under tables: *Golfingia vulgaris*, *Scoloplos armiger*, *Tubificoides benedii* and *Capitella capitata*.

The species *Golfingia vulgaris* is a Sipunculid deposit-feeder that can be favored by a small increase in organic matter content, which may explain its widespread presence in oyster parks. This species was one of the most abundant species in the present study, and its presence is characteristic of coasts with a soft bottom. *Golfingia vulgaris* was recently observed on the western coast of Cotentin Peninsula (Normandy) in another oyster park (Pezy et al., 2019). When we compared the results of the different studies carried out on the macrozoobenthos in the Bay of Veys (Dubois et al., 2007a; Sylvand, 1995), we were surprised to see the absence of *G. vulgaris* was previously reported. This species may have appeared in this ecosystem in the last decade. This Sipunculid species is also present in Rade de Brest (Afli and Glemarec, 2000) and the appearance of the species of the genus *Golfingia* on the British coasts of the English Channel was already reported by Gibbs (1973).

The species *C. capitata* is known to proliferate in organically polluted sediments and can be observed during early recolonization of azoic areas (Tsutsumi, 1987) due to its tolerance of anaerobic conditions and its high growth potential (R strategy). Like *C. capitata*, the species *T. benedii* can proliferate in anoxic conditions (Giere et al., 1999). These worms can live in dense populations in these stressed habitats which are often characterized by high levels of hydrogen sulfide (Dubilier et al., 1995). These authors also highlighted the fact that *T. benedii* possesses adaptive strategies, making it one of the most successful inhabitants of ecologically stressed, sulfidic benthic environments (Dubilier et al., 1994, 1997; Giere et al., 1988). Thus the massive proliferation of this species on the last date of the study must reflect the occurrence of an episode of pollution that caused environmental conditions favoring the emergence of these two species while penalizing species sensitive to pollution. Indeed, after the disappearance of species that cannot tolerate eutrophic environmental conditions, a recolonization phase by group V pioneer species was observed. These group V species are best equipped to survive in such a degraded ecosystem. In addition, because of their reproductive R strategy, these species have shorter generation times and adaptation to eutrophication. The other species in groups I, II and III have longer generation times and much lower tolerance for eutrophication.

Due to its wide range of tolerance, its high reproductive coefficient (R strategy) and its tolerance to salinity stress, the species *Scoloplos armiger* is one of the most common species in the eastern North Atlantic (Kruse et al., 2004). This species is also known to have hypoxic adaptation

capacities (Schöttler and Grieshaber, 1988) and potential tolerance to the presence of reduced organic matter when it is exposed to diminished oxygen supplies during low tide under detritical seaweed mats (Schöttler, 1980).

These species proliferated particularly at the end of the survey at the beginning of July, during a massive local stranding of dead seaweed. In terms of organic eutrophication dynamics, the oyster spat mortality crisis due to the occurrence of the pathogen agent OsHV-1 μVar occurred first at the beginning of June, while the benthic indicators started to shift to a moderately bad ecological status. In second stage, the massive stranding of dead seaweed occurred on day 172 (*i.e.* the 21<sup>st</sup> of June) was followed by a new shift of the macrozoobenthic community with the emergence and hyper-dominance of *Tubificoides*, indicating a bad ecological status at the end of the survey (end of June and beginning of July). These two events (spat mortality and dead seaweed stranding) represented an important input of OM to the benthic habitat. This OM occurred in two steps and disturbed the macrozoobenthic assemblages.

## Evolution of benthic indexes

Species richness corresponds to the number of species present at each site. The Shannon index makes it possible to estimate the diversity of a habitat from species richness and their relative abundance. In both cases, it appeared that the table habitat hosted more species and higher diversity than the aisle. However, these ecological indicators tended to decline during the last part of the survey because the values of richness and Shannon indicators in the aisle sediments progressively reached those in the table sediments during the second period of the survey. In both cases, this could indicate uniformization of the environmental conditions in the two habitats due to an increase in organic matter content (eutrophication) and a shift from a good to a bad ecological status.

The Pielou index is an equidistribution index, which represents the degree of diversity in relation with the theoretical maximum ( $H'_{\max}$ ). The lower the index (close to 0), the more a species dominates the population, and the higher the index (close to 1), the more equal the abundances of the species present. The Pielou index was mostly higher in the aisle than in the sediments under the oyster table. This suggests that the table habitat is dominated by a few species whereas in the aisle, there is better equidistribution of species. This dominance of a few species (*i.e.* *C. capitata*, *T. benedii*, *S. armiger*) could point to potential eutrophication of the environment due to inputs of OM under the oyster tables at the end of the survey (in July).

The BOPA index (Benthic Opportunistic Polychaetes/Amphipods) is a common indicator that makes it possible to determine the ecological status of an environment (Dauvin and Ruellet, 2007). The presence of Amphipods is a good pollution bioindicator because they are very sensitive to eutrophication (Dauvin and Ruellet, 2007; Gesteira and Dauvin, 2000). A large quantity of OM leads to a reduction in the abundance of amphipods, while, on the contrary some polychaetes are particularly resistant to excessive intake of OM and associated reduced compounds (e.g. sulfides, methane) typical of fine sediments (e.g. *C. capitata*, *T. benedii*). Overall, the BOPA index under the tables reflected a moderate ecological status while the BOPA index in the aisle reflected a good ecological status. More precisely, the BOPA index was globally stable under the oyster table where the environmental quality was qualified as moderate or poor. In contrast, the BOPA index in the aisle appeared to be more subject to variations. At the beginning of the survey, the aisle environment quality was qualified as good, whereas at the end it was qualified as poor or even bad. In terms of changes in the quality of the environment, the classification of the environment according to the AMBI index shows that the two habitats at the beginning of the sampling were globally good and at the end of this survey they were qualified as moderate and almost poor. Overall, according to the AMBI index the environment was in a better health in the aisle than under the oyster table. This change in the ecological status is hypothesized to be the result of the variations of environmental parameters and hence, the faunistic assemblages. Indeed, an important increase in group V species was observed while the abundance of group I species (sensitive to pollution) tended to decrease increasing the AMBI index in both habitats at the end of the survey (in July). The BENTIX index tended to decrease over the survey period. Indeed, the environment ecological status went from good to moderate. Overall, the ecological status was better in the aisle than under the oyster table, but on the last two sampling days, no difference was observed between habitats with minimum values for both. This could mean that the whole environment was polluted.

Calculated benthic indexes show that group I species (sensitive to hypertrophication), were present at the beginning of the survey but decreased over time (particularly after the mortality episode). Under normal conditions, these species are usually dominant in any environment and first disappear during OM enrichment of the environment (Hily, 1984). Conversely, group V species (deposit-feeders) increased over time due the OM input. Moreover, when we focused on the response of the two habitats to a variation in environmental conditions, the oyster habitat seemed to be more impacted by organic stress but more stable over time. Indeed, due to oyster

biodeposition, this habitat would already be somewhat polluted with OM hosting species adapted to these conditions (AMBI group V species). On the other hand, the aisle habitat would be more sensitive to these environmental variations finally resulting in a modification of the macrozoobenthic assemblages in favor of species that are more tolerant to OM. In short, temporal trends appeared to matter more than small-scale effects during this summer survey. Furthermore, while the ecological status of the environment at the beginning of the survey was generally good, it tended to decrease due to progressive eutrophication in June.

## Multivariate analysis

The CA was mainly structured by the most abundant species including *G. vulgaris*, *T. benedii* and *C. capitata*. *G. vulgaris* was mostly observed on the early dates of the survey, whereas *T. benedii* and *C. capitata* species were mainly observed on late dates. This major change in species dominance could be evidence for an environmental shift following a disturbance of environment parameters. Indeed, as can be seen on the PCA, a succession of AMBI groups from group I (e.g. *G. vulgaris*) to group V (e.g. *T. benedii* and *C. capitata*) was observed. This succession of species occurred in three phases of successive dominance, from the initial phase with good ecological status and dominance of *Golfingia* and/or *Scoloplos armiger*) followed by degradation of the benthic habitat in June as a result of the progressive enrichment in organic matter likely due to the oyster spat mortality (from day 156 to 177) and massive dead seaweed stranding on day 172, before the final shift of the benthic habitat to almost poor quality (dominance of AMBI group V).

AMBI group I species include specialist carnivores and some deposit-feeding species, in our case, mostly represented by *G. vulgaris*, a species characteristic of soft-bottom sediment in coastal ecosystems. These species are very sensitive to organic enrichment and are only present in unpolluted conditions. Group I species were correlated with water content of the sediment and biofilm chl *a*. This relationship highlights the trophic link between benthic chl *a* and AMBI group I species such as *G. vulgaris*. This relationship could be evidence for the initial state of the environment in unpolluted conditions with the dominance of species feeding on microphytobenthos.

AMBI group II includes suspension feeders, less selective carnivores and scavenger species, that are mostly not sensitive to increasing OM. We found these species present at low densities with non-significant variations over time. AMBI group III species are surface deposit-feeding species, such as tubicolous spionids and tolerant to excess OM enrichment. These species may

occur under normal conditions, but their populations are stimulated by organic enrichment in sediments. The main species comprising these ecological groups in the present study were *S. armiger* and *A. marina*. These species are typical of sandy mud and are known to be subsurface deposit feeders, so it is not surprising that they are associated with the OM fraction on Dim. 3 and 2 of the PCA. However, on the second axis, group II and III species are associated with group V species and opposed to sediment chl *a*.

AMBI group V species are deposit feeders, which proliferate in reduced sediments including first-order opportunistic species. The presence of these opportunistic species linked to enhanced microphytobenthic production can lead to the rapid removal of pollutants in the sediment and improve remineralization processes (Rossi, 2006). In the present study, this group mainly comprised *T. benedii* and *C. capitata*. These group V species were associated with NH<sub>4</sub><sup>+</sup> concentrations and opposed to OM content (Dim. 4). The increase in the abundance of *C. capitata* and in the concentration of NH<sub>4</sub><sup>+</sup> are two indicators of a hardening of the environment and a reduction in. Indeed, we hypothesize that the increase in OM enhanced NH<sub>4</sub><sup>+</sup> concentrations that would have facilitated the proliferation of opportunistic organisms such as *T. benedii* and Capitellidae species. Indeed, it is known that the accumulation of drifting seaweed can reduce richness and abundance of macrofauna but promote a few small opportunistic species (Thomsen and McGlathery, 2006). The link with algal mat coverage was not straightforward, but we observed a succession of phases: first, patches of dead seaweed were retained by the oyster table at our study site, and these seaweeds were deposited on, or buried in the sediment, with the accumulation of reduced compounds causing major stress for the benthic community, related to eutrophication. In the second step, decomposition and release of algal-derived nutrients influenced the distribution of benthic organisms, responsible for the uptake of ammonium NH<sub>4</sub><sup>+</sup> in sediment porewater. A huge load (more than 30 cm) of seaweed-derived organic matter probably profoundly affected the assimilation and flux pathways. The recycling pathways and the bacterial remineralization rate can be fast after such an event, and the resulting degraded material can be then used by microphytobenthic biofilms (Chapter 2). However, on the PCA, the oyster spat mortality episode was correlated with AMBI group V species and with NH<sub>4</sub><sup>+</sup> concentrations. So, in parallel with the seaweed-related OM input, dead oyster flesh appeared to increase the concentrations of NH<sub>4</sub><sup>+</sup> as well as AMBI group V species biomass.

As revealed by the PCA, OM and fine grain-size sediments were not directly correlated indicating that the origin of the OM was not sediment dynamics but another source (probably

first by the oyster mortality episode, and then by the dead seaweed). As it can be seen on the PCA (Figure 22 : A), the additional variable dead seaweed coverage could explain this input of OM as it is known that it can have wide impacts on sediment dynamics (Anselli et al., 1998; Corzo et al., 2009; Garcia-Robledo and Corzo, 2011). Indeed, in the field, a massive stranding of dead seaweed was clearly visible during the second sampling period. The oyster parks consist of alternating rows of tables and aisles that can succeed for kilometers. These tables consist of trestles whose feet crisscross the foreshore and extend over large areas. These structures therefore represent a considerable obstacle to water flow and can retain dead seaweed carried by the tide. So instead of being stranded at the top of the foreshore on the sea leash, these macroalgae are trapped in the oyster parks where they accumulate. This massive addition of organic matter is mineralized by the microbial loop in  $\text{NH}_4^+$  and also increases the anoxia of the sediment thereby altering community structure (Lyons et al., 2014) and reducing populations of AMBI I, II and III group organisms in favor of group V organisms. The OM observed in this study was thus mainly related to the stranding of dead seaweed, then in background to the production of biodeposits by oysters. The mortality episode may have played a preliminary role in the OM flux to the benthic compartment but it appeared to be negligible compared to the later input of OM from the dead seaweed.

### OsHV-1 $\mu$ Var DNA detection in macrozoobenthos

First it should be noted that the detection of OsHV-1  $\mu$ Var DNA does not imply the presence of infective viruses (enveloped virus particles), but could be due to the persistence of naked (inactivated) viral DNA fragments (Schikorski et al., 2011). Moreover, OsHV-1  $\mu$ Var is known to infect a wide range of host species belonging to the class of bivalve mollusks (Arzul et al., 2017) but it is highly unlikely that it will able to infect organisms from other classes. The detection of OsHV-1 DNA in Annelid or Sipunculid worms and Crustaceans thus indicates that these organisms must - at worst - be considered as healthy passive carriers due to the passive adsorption of virions, or OsHV-1 DNA fragments, or diet-related mechanisms.

The detection of OsHV-1 DNA increased significantly over the course of this study starting on day 159 and peaked on day 179, then dropped in the last days of sampling (early July). Differences in the quantity of OsHV-1 DNA were found depending on species on days 159 and 179. On day 172, viral loads were also high, corresponding to a significant increase in the AMBI index (environmental degradation). Thus, the oyster spat mortality episode probably induced a

first alteration of the environment, but which was less significant than the stranding of dead seaweed, which clearly provoked a strong ecological disturbance (AMBI group V dominance).

Regarding the macrofauna species found in the core samples, some species were missing in the OsHV-1 analysis including the very small worms *T. benedii* and *C. capitata*. This bias was the consequence of the method of sampling used, which was of the species most visible to the naked eye in the field, which were not necessarily the most abundant species observed after sorting the specimens in the bulk sediment in the cores. The high OsHV-1 DNA detections found for these species appear to be related to their diet. Amphipods, whelks and crabs are indeed scavenger species, and *C. maenas* and amphipods (especially those belonging to the *Gammarus* genus) were found in oyster bags feeding on the flesh of dead oysters, in direct contact with viral particles. Filter feeding species (e.g. barnacles) would have also been in contact with OsHV-1  $\mu$ Var but indirectly. Indeed, an additional step in the transfer of OsHV-1  $\mu$ Var to the macrofauna is necessary for these filter feeding organisms. The OsHV-1  $\mu$ Var viruses derived from the flesh of dead oysters would have spread into the environment and adsorbed onto the surrounding particles in suspension in the water column. This OsHV-1  $\mu$ Var-enriched seston would then have been filtered by barnacles thus becoming positive to OsHV-1 detection. Barnacles were the suspensivore species with the highest quantity of OsHV-1  $\mu$ Var for two main reasons. First, these species are found on hard substrates such as oyster tables and are thus in the close vicinity of the reared animals. Second, due to trophic competition with *C. gigas*, other filter organisms such as *C. edule* are strongly excluded, which would mitigate the availability of OsHV-1  $\mu$ Var in the environment. Indeed, our taxonomy results showed suspension feeders to be very uncommon. Among the scavenger species that were not in direct contact with the oysters, *S. armiger* can be seen to carry OsHV-1  $\mu$ Var but in small amounts. This species could be a transmitter of the virus to the benthic habitat because it is a ground deposit feeder (Wolff, 1973). This species was not sampled in the post-mortality period, consequently we cannot conclude on contamination of the benthic compartment even if the increase in the viral loads observed in barnacles suggest that the virus spread in the environment and could also have settled with the adsorbed particles. Despite the small number of data, the viral load present in *L. littorea* ( $728.5 \text{ } \mu\text{g}.\mu\text{l}^{-1}$ ) was high before the mortality episode. This species feeds on macroalgae and diatoms that could have adsorbed the virus on its surface.

## 5. Conclusion

Overall, benthic macrofauna assemblages were more diverse and abundant under the oyster table than in the aisle. However, these assemblages changed in response to a massive input of

organic matter that caused degradation of the benthic habitat. Timewise, this alteration of environmental conditions was first due to the intake of the degraded flesh from dead spats in June. Second, the massive stranding of dead seaweed also stressed the environment at the end of June. The table habitat appeared to be in a bad ecological state throughout the 2-month survey, whereas in the aisle, eutrophication appeared to be due to the massive stranding of dead seaweed (at the end of the survey, in early July). In such a case, this micro-ecosystem ended up being just as destabilized as the one under the oyster tables. Under the tables, massive stranding reinforced the disturbances but the responses of the benthic assemblage were less pronounced over time. Indeed, under the oyster table, benthic macrofauna were already characteristic of a softly eutrophic environment. In this way, the benthic environment under the oyster tables appears to be more resistant to eutrophication mainly because it is already richer in organic matter than the aisle habitat. Benthic macrofauna may have been in contact with OsHV-1  $\mu$ Var for a few days following the oyster mortality episode, but it seems unlikely that macrofauna would be a reservoir that enabled the persistence of the virus in the environment. The local accumulation of dead seaweed trapped by the metal structures of oyster parks may affect local water and sediment quality, thereby reinforcing eutrophication and increasing the risk of oyster mortality.

## Acknowledgements

Special thanks go to André-Gilles Taillepied and his team who kindly lend us the oyster table and plenty of space in their building to store our equipment and conduct our experiments. Thanks to C. Rakotomala, C. Mallet, F. Pernet, C. Lelong, C. Roger, B. Adeline and M-P. Dubos for their help on the field. Thanks to G. Dreux, K. Moerman and L. Derrien for their help during their studies. Thanks to F. Ruffin for his commitment. I am grateful to the *Ministère de l'Enseignement supérieur et de la Recherche* for this PhD grant.





Ainsi, selon cette partie de l'étude, l'environnement benthique sous les tables à huîtres semblerait être plus résistant à l'eutrophisation. Ces résultats renforcent ceux mis en évidence au chapitre 2 avec des conditions environnementales façonnées par les huîtres. Selon les indices de la qualité écologique de l'habitat benthique, sous la table à huîtres le macrozoobenthos serait typique d'un environnement légèrement eutrophisé. Au contraire, dans l'allée l'habitat benthique semblerait plus sensible face aux perturbations environnementales alors que l'habitat table à huîtres lui paraît plus stable car déjà eutrophisé. Suite à l'épisode de mortalité des naissains d'huîtres, la macrofaune benthique a été en contact avec OsHV-1  $\mu$ Var durant quelques jours. Cet épisode de mortalité a donc bien induit un relargage du virus OsHV-1  $\mu$ Var dans l'environnement. La partie suivante s'attarde notamment sur cet aspect avec un suivi de l'ADN viral dans les naissains d'huîtres et à la surface du sédiment: 1<sup>er</sup> centimètre et biofilm microphytobenthique. Ainsi, en lien avec les caractéristiques environnementales présentées aux chapitres 2 et 3, il est probable qu'une différence des quantités d'OsHV-1  $\mu$ Var soit détectée en fonction de l'habitat: table ou allée. En parallèle, les communautés bactériennes ont été échantillonnées afin de mettre en évidence d'éventuels phénomènes de co-infection (de Lorges et al., 2018; Petton et al., 2015a; Rodgers et al., 2018) en étudiant les communautés bactériennes des naissains d'huîtres et du biofilm sous-jacent.



**Chapitre 4 : Environmental dynamics of the Ostreid herpes virus (OsHV-1 μVar) in oyster spats and microphytobenthic biofilms during an *in situ* mortality outbreak**



# **Environmental dynamics of the Ostreid herpes virus (OsHV-1 μVar) in oyster spats and microphytobenthic biofilms during an *in situ* mortality outbreak**

In preparation for a submission to Frontiers in Microbiology

Charles Vanhuyse, Clarisse Mallet, Fabrice Pernet, Lelong Christophe, Mélanie Lepoittevin,  
Francis Orvain

## **Abstract**

Since 2008 large oysters spat mortalities mainly attributed to the Ostreid herpes virus μvariant (OsHV-1 μVar) are happening when the water temperature exceeds 16°C. Yet, environmental parameters favoring the persistence and diffusion of OsHV-1 μVar remains unappreciated. Our results suggests that the environmental conditions prior mortality are important as they could prevent or threaten oysters against OsHV-1. The potential depletion (a decline in post-bloom period growth) could play a role in the mortality crisis weakening young oysters at a time when the requirements needed for somatic growth increase. Microphytobenthic biofilms could represent a vector for OsHV-1 transmission as viral DNA was found in relatively important quantities ( $10^3$  GU.ng DNA $^{-1}$ ) before it was the case in oysters. Nevertheless, biofilms do not appear to be well pre-positioned to promote annual persistence of the virus in the sediment because OsHV-1 DNA quantities gently decreased with time. These biofilms could however help to reduce the rate of post-mortem viral abatement. Concerning oysters, it appears that a letal threshold of OsHV-1 μVar quantities has to be exceed to provoke death ( $10^5$  GU.ng DNA $^{-1}$ ). In case of survival, oysters could be able to partly eliminate OsHV-1 of their tissues although a part can persevere in their tissues.

## 1. Introduction

For decades, massive mortality outbreaks are threatening the Pacific oyster *Crassostrea gigas* (Bayne et al., 2017) faming resulting in an increase of economic costs and vulnerability. Massive mortalities in adults are clearly related to the contamination of *Vibrio* bacteria (Azéma et al., 2016; Samain and McCombie, 2008) with a mortality risk factor associated with freshwater inputs in estuarine ecosystems (Gangnery et al., 2019). These mortalities could also reflect an energetic imbalance between excessive growth rates leading to mass gonadic development and high amounts of gamete release (Royer et al., 2007; Samain and McCombie, 2008). Thus, the energetic costs are maximal (to restore the oyster reserves) whereas the energetic gains are minimal. As a consequence adult bivalves could die massively because summer is a starvation period after rapid spring growth, especially during particular years (NAO<sup>+</sup>), related to the climatic influence (Thomas et al., 2018).

In France, juvenile oysters are affected by annual mass mortalities at the end of spring or the at the beginning of summer (Pernet et al., 2018). Spatial trends exhibit a clear latitudinal gradient along French coasts, with the first mortalities beginning in the southern Mediterranean lagoon ecosystems in April, while they are reported at the end of June or the beginning of July on the northern coast in Normandy (Fleury et al., 2018). The thermal factor is essential and clearly explains this broad scale gradient. Indeed, when the water temperature exceeds approximatively 16 °C (Pernet et al., 2012; Petton et al., 2015) mortality rates can reach up to a value of 80%. Other risk factors also govern the occurrence of mortalities and their severity (Rodgers et al., 2018). These mortalities are generally related to freshwater inputs in estuarine ecosystems (Pernet et al., 2018) and their connectivity to sites associated with spots of oyster juveniles (Gangnery et al., 2019). Recent studies highlighted the importance of bacteria in OsHV-1 μvar mortalities phenomena. However, it seems that the death of oysters would be the product of a virus-bacteria co-infection (Petton et al., 2015; de Lorgeril et al., 2018; Pathirana et al., 2019). Indeed, a first step consisting in the infection of oysters by OsHV-1 μVar would weaken the oysters immune system favoring the proliferation of opportunistic bacteria leading to bacteraemia (de Lorgeril et al., 2018). Yet these outcomes were revealed under controlled parameters and need to be tested *in situ*. Oysters death would be the product of a virus-bacteria co-infection (Petton et al., 2015a; de Lorgeril et al., 2018; Pathirana et al., 2019). This co-infection would occur in two steps, first the infection by OsHV-1 μVar lesening oysters immune system and then a proliferation of opportunistic bacteria leading to fatal bacteraemia (de Lorgeril et al., 2018). In polluted areas, the most frequent bacterial genera detected in living

Pacific oyster *C. gigas* are *Pseudomonas*, *Vibrio*, *Acinetobacter*, and *Aeromonas*. The genera *Vibrio* would be more abundant in oysters than in surrounding waters (Kueh and Chan, 1985; Prieur et al., 1990) and play a major role in oysters death (de Lorgeril et al., 2018). While the *C. gigas* microbiota is globally dominated by the genera *Proteobacteria* (Fernandez-Piquer et al., 2012; Hernández-Zárate and Olmos-Soto, 2006), it appears that the composition changes in response to environmental stresses (Lokmer et al., 2016b, 2016a; Lokmer and Wegner, 2015) and in relation to their filtration mode of nutrition (Le Roux et al., 2016; Lokmer et al., 2016a).

After a mortality outbreak in oyster parks, the flesh of the dead oyster spats spread in the environment and sediment towards the benthic habitat, with an enrichment in organic matter of the sediments (Chapters 2 & 3). Through this sedimentation mechanism, the virus must aggregate to dead oyster flesh that could also contaminate the benthic habitat and communities. Besides the OsHV-1 flux towards the sediment, these epizootics can lead to significant ecological effects (Forrest et al., 2009a) associated with high organic material fluxes towards the seafloor. Sedimentation processes enhanced by oyster activities can reshape the benthic habitat and modify macrofaunal communities (Dubois et al., 2007; Chapter 3). Once the virus is transferred to the bottom sediment, the fate of this pathogen agent and its resilience outside of the host organism remains poorly described. The benthic habitat could offer good circumstances for viral persistence in the environment due to the muddification at the bay scale typical of oyster farms (Newell et al., 2002; Orvain et al., 2012; Echappé et al., 2018). Intertidal oyster farming practices are known to create particular environment characteristics at large scale (Forrest et al., 2009a; Ubertini et al., 2012) as well as at the oyster table scale (Dubois et al., 2007; Forrest et al., 2009, Chapter 2). Indeed, oyster tables create a crosshatching pattern between oyster tables and aisles which structure the benthic habitat but also at shorter scale, related to table organisation in oyster farms. However, this effect of table presence seems to impact more macrozoobenthic community and organic loads (Dubois et al., 2007; Forrest et al., 2009; Chapter 2) than mud proportion. Differences were also clearly detected in terms of microphytobenthic photobiological performances between tables and aisles in between, but not EPS contents. In this study, our main question concerns the potential effects of these differences of sediment properties and benthic factors on OsHV-1 μVar dynamics and persistence and in the benthic habitat (Figure 25). Differences in OsHV-1 dynamics could also be observed according to this spatial pattern.

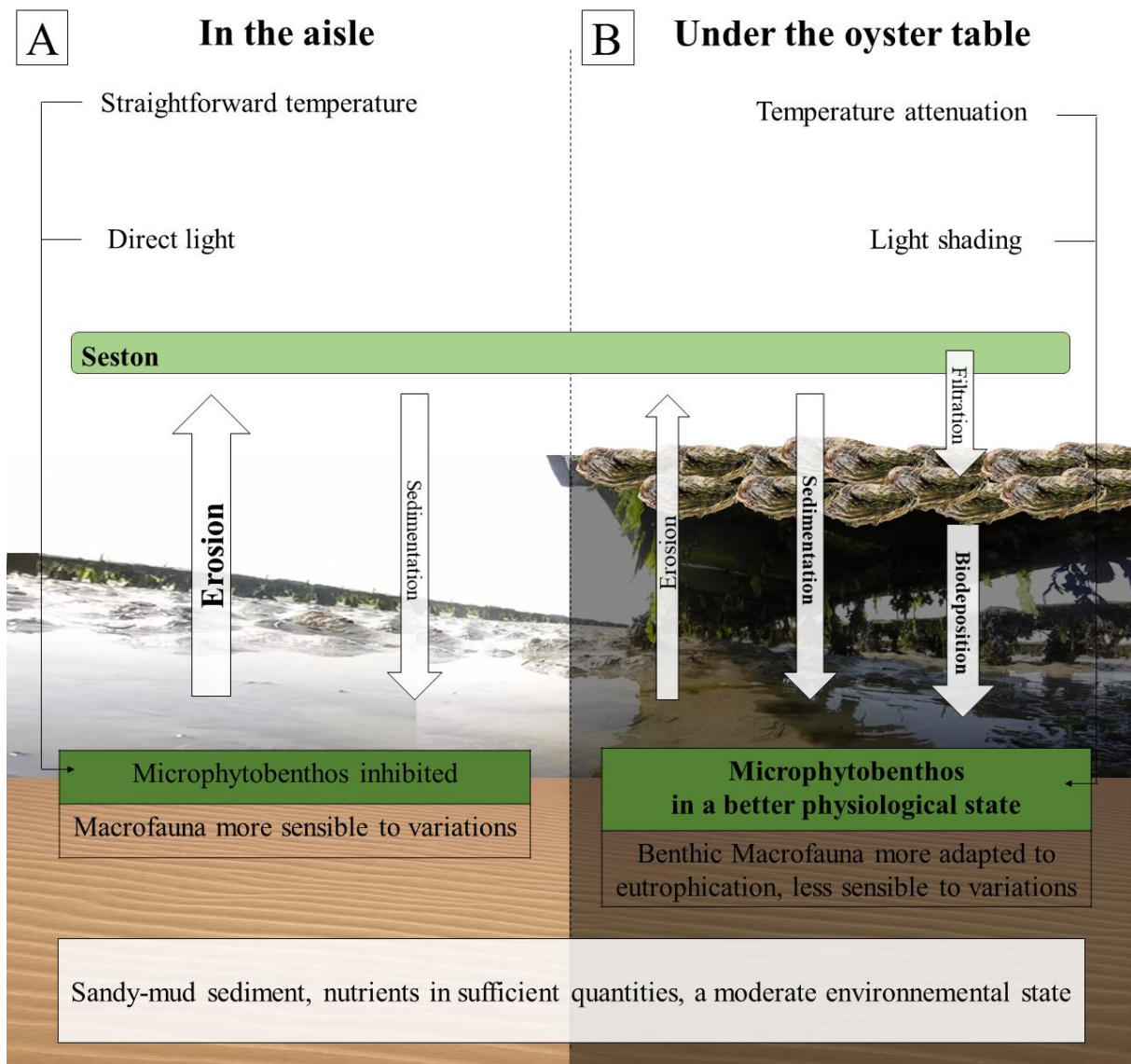


Figure 25 :Conceptual scheme of potential impacts of oyster tables on the benthic habitat. A. in the aisle, sediment is exposed to light and high temperatures. MPB growth is altered due to the thermoinhibition and in a lower extent to photoinhibition. . B. Under the oyster tables, shading reduces exposure to light and temperature. MPB growth is not altered with better photosynthetic performances. In both cases, the benthic habitat appears to be shaped by oysters biodeposition and oyster tables with a muddification of the sediment, regular inputs of organic matter that is remineralized into nutrients by the microbial loop.

The *OsHV-1* μVar virus cannot remain viable more than two days free in artificial seawater but at least more than one week in fresh oyster tissue (Hick et al., 2016). This virus can also be adsorbed by non-covalent attraction forces on suspended particles or even plankton, which can greatly increase viral resilience outside host cells (Paul-Pont et al., 2013). However, the long-term persistence of viral particles and especially from one year to the next one is currently unknown. The hypothesis is that at the end of episodes of mortality, virus particles could sediment and adsorb on the microphytobenthic biofilms (and especially the epipelagic diatoms due to their secretions of EPS) that would guarantee a better protection against factors that can deactivate the virus (such as UV rays). The shading phenomenon caused by oyster tables

would significantly reduce UV exposure between 2 annual mortality episodes. Indeed, the oyster table protects more UV rays and promotes the growth of microphytobenthos (mainly by a nutrient supply in a silted local environment ; see Chapter 2). The benthic diatoms are especially efficient to protect themselves against the excessive light amount observed in the extreme conditions of intertidal flats. These epipelagic diatoms are able of remarkable migratory activities in case of high irradiance in the first millimeters of sediments, but they can also activate the xanthophyll cycles in photosystems (Barnett et al., 2015).

The aim of this study was to determine whether benthic factors (sediment and microphytobenthic biofilms) can affect the amount of OsHV-1 μVar present in the environment and if the benthic habitat could represent a source or a well of OsHV-1 μVar. This is why an *in situ* experiment was conducted on a fixed station of the oyster farms of Grandcamp-Maisy (in the « Baie des Veys » ecosystem) from the end of May to the beginning of July 2017 to study the viral dynamics within biofilms at the water-sediment interface during an OsHV-1 μVar mortality outbreak. During this survey, the different compartments of the ecosystem were sampled as the physico-chemical parameters of the environment (ie temperature, light intensity ; see Chapter 2), the viral load in μvar-OsHV-1 in oyster spat (alive, dead or moribund) and the in microphytobenthic biofilms.

## 2. Material & method

### 2.1. Study site

The Bay of Veys is located in the south-western part of the Seine Bay (Figure 26) where 40% of the inputs originate from the River Vire (Jouenne et al., 2007). This bay is an estuarine and shellfish ecosystem that stretches over an intertidal zone of 16 km<sup>2</sup>. During spring tide, a tidal range of 8 meters with currents of 3 m.s<sup>-1</sup> can be reached (Orvain et al., 2012; Gangnery et al., 2019). Within this area, oyster farms are mainly located on soft sediment with a natural tendency to a small increase in silt content due the installation of oyster beds (Kopp et al., 1991). This modification of the sediment composition is due to biodeposition activities of Pacific oysters and bed friction attenuation due to the presence of the oyster tables. Although growth in this shellfish basin is the fastest in France, in terms of production, it only comes in second out of French basins (25 000 tons in 2016; source: *Comité National de la Conchyliculture*).

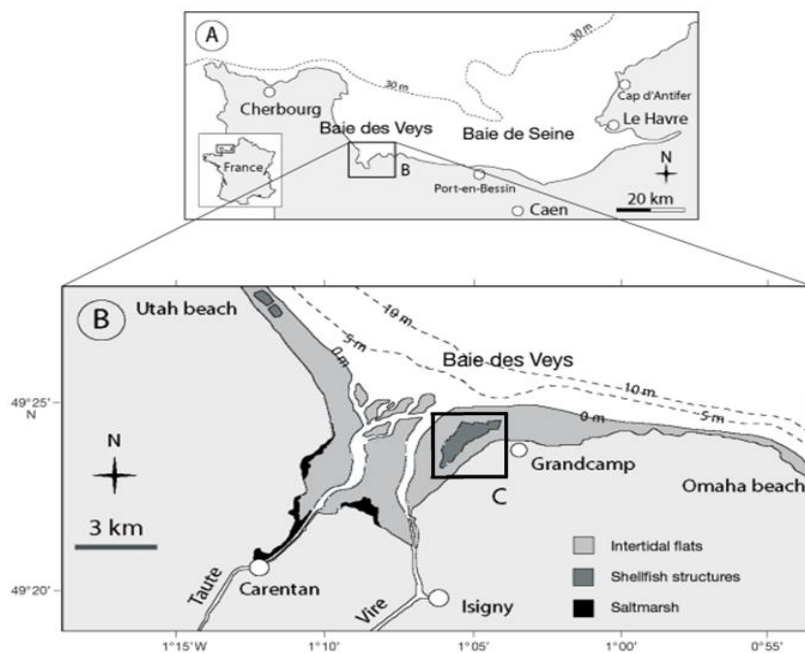


Figure 26 : Location of (A) the Baie des Veys, (B) a closer view of the baie des Veys and (C) the oyster farm in which samples were

## 2.2. Experimental design

The study was conducted along a row of oyster tables located at Géfosse-Fontenay in the Bay des Veys (Normandy, France) on the foreshore (from  $49^{\circ}22'53.2''$  N;  $001^{\circ}05'44.2''$  W to  $49^{\circ}22'54.6''$  N;  $001^{\circ}05'43.4''$  W) from the 22<sup>nd</sup> of May 2017 to the 1<sup>st</sup> of July 2017. One oyster table was divided into three areas (A, B & C) (Figure 27), and in each area, 20 oyster bags each containing smaller bags containing 200 three-month-old oyster spats were placed. Oysters were produced using standard hatchery procedures (Petton et al., 2015). At every sampling date and for the three areas, an oyster bag was randomly selected and samplings were made under the oyster table and in the aisle.

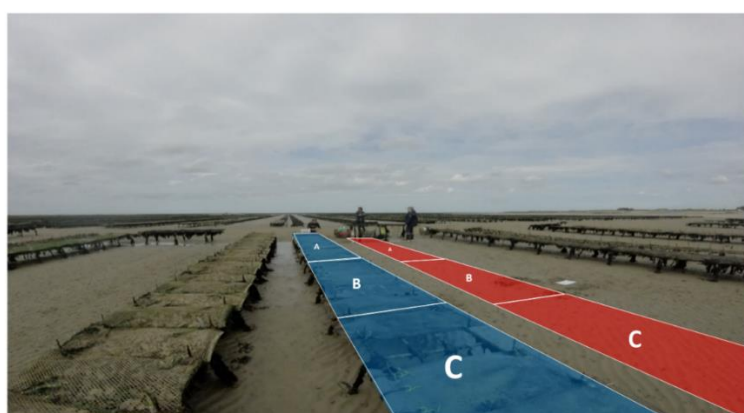


Figure 27 : Experimental field design. The oyster table sample areas are in blue (A, B & C) and the aisle sample areas are in red (A,B & C)

### 2.3. Oyster spat survival

At every sampling date, vital status of oysters was classified into three categories: alive, moribund and dead. In order to determine that status, a little pressure was applied by hand to the shell at the level of the adductor muscle. If oysters were hermetically sealed they were called alive, if they did not close tightly and bubbles were observed they were considered as moribund and the oysters that were open were counted as dead.

### 2.4. OsHV-1 μVar and bacterial sampling in oysters

At every sampling date, 10 alive oysters, up to 10 moribund and 10 dead oysters according to their availability were dissected and conserved at -20 °C for quantification of their OsHV-1 charge. After thawing, sampled organisms were crushed and their DNA was extracted and purified using the NucleoSpin® 96 Blood Kit (Macherey-Nagel). Total extracted DNA was quantified using a Nanodrop 200 (Thermoscientific) for standardization purposes. OsHV-1 DNA in the samples was quantified via real-time qPCR CFX 96™ C1000™ (Biorad). After extraction of the total DNA, an amplification was carried out by PCR, after a first step of Nested PCR. The amplicons were sequenced to assess the bacterial communities. These bacterial community data are not presented in this document so far.

### 2.5. OsHV-1 μVar extraction and bacterial sampling in the biofilm

The concentration of chl *a* is a good proxy for microphytobenthic biomass. MPB was collected using a  $7 \times 7 = 49 \text{ cm}^2$  Bluter mesh (100 µm mesh) placed at the surface of the sediment for 30 minutes, thus representing the active surface chl *a*. The meshes were then dipped in 10 mL of filtered (0.2 µm) seawater and a 1 mL aliquot was stored at -20 °C for quantification of their OsHV-1 charge. After thawing, sampled organisms were crushed and their DNA was extracted and purified using the NucleoSpin® 96 Soil Kit (Macherey-Nagel). Total extracted DNA was quantified using a Nanodrop 2000 (Thermoscientific) for standardization purposes. OsHV-1 DNA in the samples was quantified via real-time qPCR CFX 96™ C1000™ (Biorad). OsHV-1 Genomic Units were calculated to give estimates of concentration per squared centimeter. The equation converts raw data obtained from qPCR by considering the different dilutions and kit volumes as follows :

$$\text{DNA concentration } \left( \frac{\text{UG/ngDNA}}{\text{cm}^2} \right) = \frac{\left[ \frac{\text{PCR result}(2\mu\text{L})}{2} \times V_{\text{elution}} \right]}{S \times n \times \frac{V_{\text{aliquot}}}{V_{\text{total}}} \times \frac{V_{\text{extraction}}}{V_{\text{mix}}}}$$

Where, the PCR result is expressed in GU/ngDNA,  $V_{\text{elution}}$  was of 50  $\mu\text{L}$  (from the kit), S was the biofilm surface ( $7 \times 7 \text{ cm}^2$ ), n was the number of replicated nylon filets which were pooled in the same tube (n=3),  $V_{\text{aliquot}}$  was of 1 ml from the total volume  $V_{\text{total}}$  of 10 mL. The volume of extraction is of 0.3 mL, while the initial volume of the mixture was of 3 mL.

## 2.6. Statistical analyses

Regarding the values of Genomic Units of OsHV-1 in biofilms, the experimental design was established in order to know if the "Period" factor (5 groups of dates were defined by gathering samples from subsequent days), The "Table" factor (under table / Off table) and the "Tidal" factor (with 2 modalities "pre-Low-tide" at the beginning of the tidal discovery on the site and "Low-tide" 3 hours later) were responsible of differences. In order to judge whether the differences between the averages per treatment were significant, a variance analysis test (ANOVA) was first performed, but this parametric test is subject to conditions of residual normality and homogeneity of variances that were not guaranteed even after log transformation. We therefore performed permutation tests (PERMANOVA) not subject to these conditions of application. The analyzes were performed using the R-Studio software and the "vegan" package. To perform a PERMANOVA, 500 permutations were performed and the "euclidean" method was used for each test. For each factor responsible for significant differences, we looked for differences in pairs of groups to rank the modalities and which groups differed significantly. Savage tests were then applied to the data to identify precisely the sources of variation for each factor (function available in the software R corner package). For oysters, the analyses of viral DNA were performed to give the viral dynamics of alive, dead and moribund oysters. One-way PERMANOVA were performed to identify the effect of the period (by comparing the same 5 groups of dates).

### 3. Results

#### 3.1. Oyster mortality episode

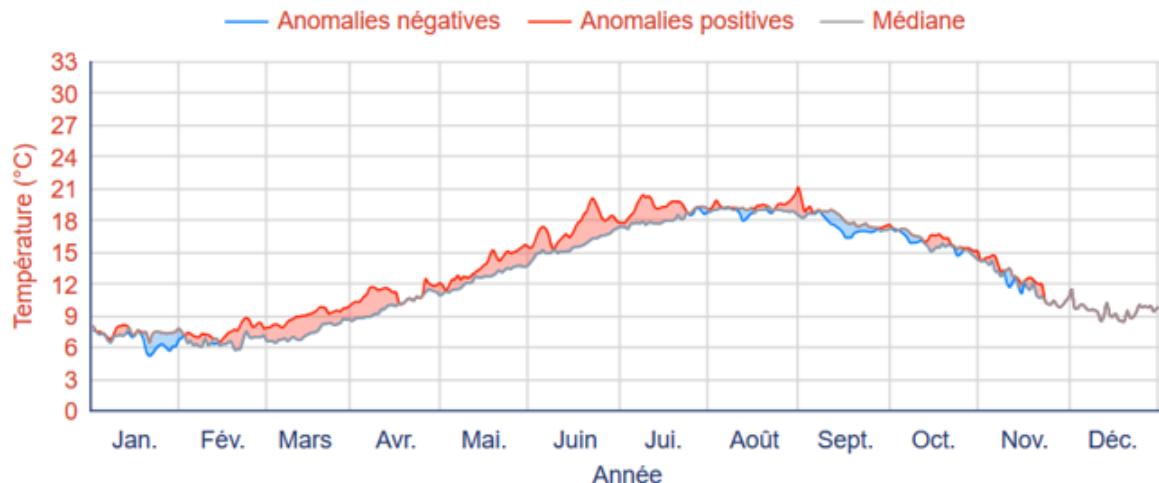


Figure 28 : Water temperatures in the baie des Veys in 2017. [https://www.ifremer.fr/observatoire\\_conchylicole/Resultats-par-annee/Resultats-nationaux-2017/Mortalite-par-site-et-par-classe-d-age](https://www.ifremer.fr/observatoire_conchylicole/Resultats-par-annee/Resultats-nationaux-2017/Mortalite-par-site-et-par-classe-d-age)

Water temperature in the bay des Veys globally increased during spring months to reach 15.7°C on day 148 (May 28<sup>th</sup>), then exceeded 16.6°C on day 152 (Figure 28).

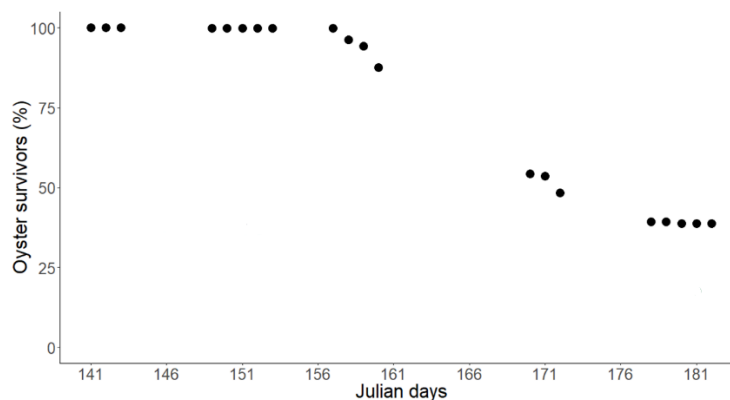


Figure 29 : Percentage of survival during the oyster spat mortality in summer 2017

The first oyster spat mortalities were recorded on day 157 (Figure 29) when the water temperature was 15.5°C. Mortalities continued for 20 days until they stabilized at around 40% of survivors on day 177.

#### 3.2. OsHV-1 μVar in oysters

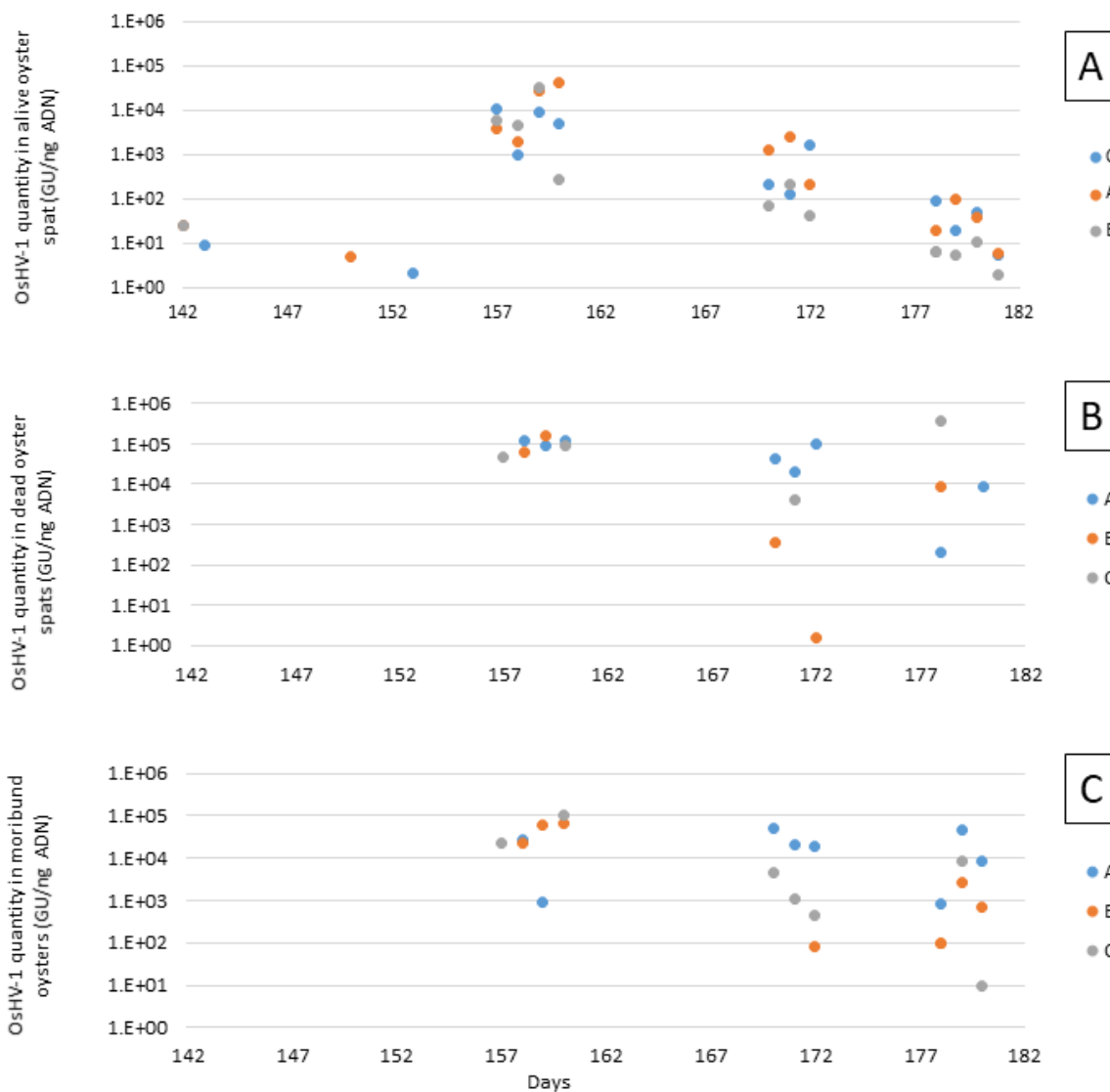


Figure 30 : OsHV-1 μVar viral loads in oyster spats. A. alive oyster spats. B. Moribund oyster spats. C. Dead oyster spats. Each single point represents 10 oyster spats analyzed

Alive oyster spats (Figure 30 A) had only very low Genomic Uniuts (GU) of OsHV-1 DNA at the beginning of the follow up to day 153. The maximal OsHV-1 DNA were observed between days 157 to 160 (p-value < 0.01; PERMANOVA) reaching  $1.24 \times 10^4 \pm 1.42 \times 10^4$  GU.ng DNA $^{-1}$ . A high degree of variability between replicates was observed during this period, with values ranging from  $2.88 \times 10^2$  to  $4.17 \times 10^4$  GU.ng DNA $^{-1}$ . Then, the OsHV-1 DNA quantities in alive oyster spat significantly decreased over time. Concerning viral OsHV-1 DNA detected in moribund oysters (Figure 30 B), the maximal value remained high ( $1 \times 10^5$  GU.ng DNA $^{-1}$ ) during the periods of first mortalities (days 157 to 160). The general trend of the dynamics was similar to the one observed for dead animals, with a higher extent during the 2 subsequent periods and especially, the order of minimum values decreased with time. The level of OsHV-1 DNA then decreased within the range of  $10^1$  to  $4.85 \times 10^4$  GU.ng DNA $^{-1}$  from days 170 to 180.

For dead spats (Figure 30 C), the values of viral DNA were high during the first mortalities (between the day 157 and 160) with a low variability between replicates ( $9.86 \times 10^4 \pm 3.92 \times 10^4$  GU.ng DNA $^{-1}$ ). For the two subsequent periods (days 167-172 and 177-180), there was a higher level of scattering between replicates (respectively  $2.82 \times 10^4 \pm 3.91 \times 10^4$  and  $9.73 \times 10^4 \pm 1.83 \times 10^4$  GU.ng DNA $^{-1}$ ) even if the maximal value did remain at  $1.83 \times 10^5$  GU.ng DNA $^{-1}$ . For this rationale, the PERMANOVA analyses did not reveal significant differences, even though the extent of minimal values decreased with time.

### 3.3. OsHV-1 μVar in the sediment

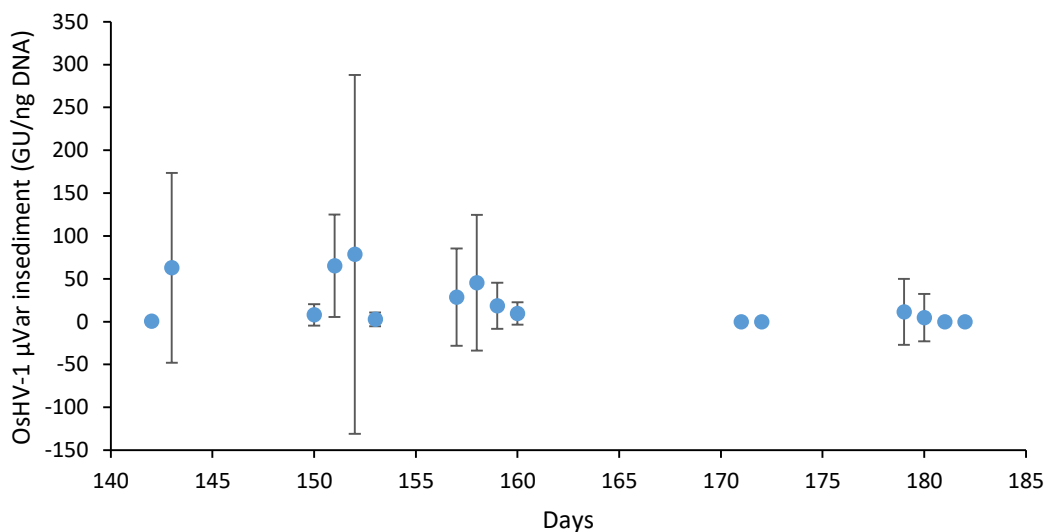


Figure 31 : OsHV-1 μVar DNA quantitites found in the sediment

Data for OsHV-1 viral loads in the sediment remains very low and scattered (Figure 31). The viral DNA was merely detected because the total DNA extracted was also in very small quantities, close to the detection threshold of the PCR. Thus, the extraction protocol should be improved in order to access this information for bulk sediment. Nevertheless, the highest viral loads were found on days 151 and 152, and these results are in line with values recorded in biofilms.

### 3.4. OsHV-1 μVar in the biofilm

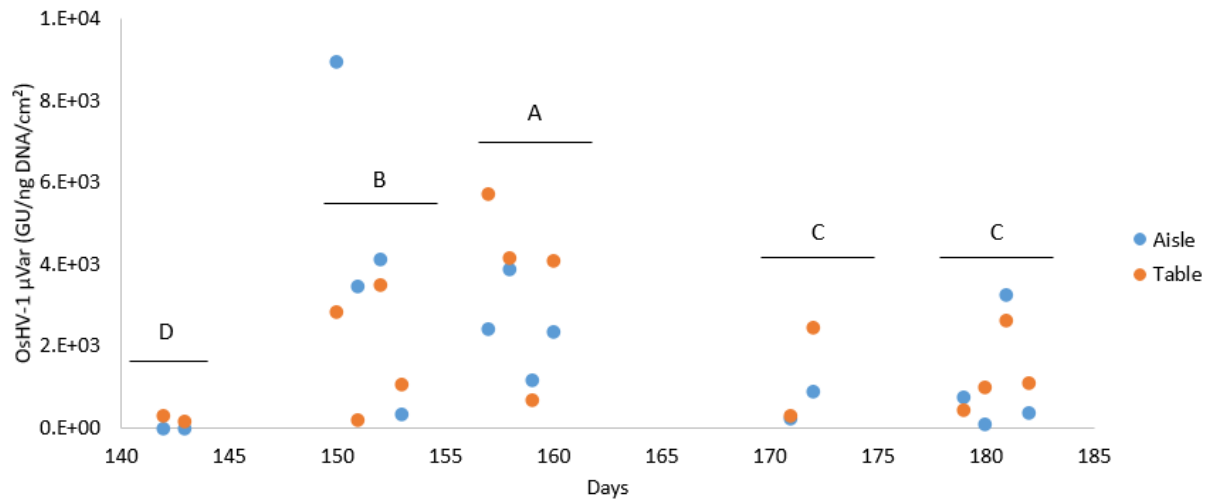


Figure 32 : OsHV-1 μVar DNA found in microphytobenthic biofilms. Each single point represent an average based on 6 samples.

No significant effect of the moment sampled was found (when comparing data 3 hours before the low tide and at the low tide hour). The amount of OsHV-1 DNA in the biofilm was not subjected to the local influence of the table, since there was no difference observed according to the habitat (under the oyster table and off the table). When days were individually analyzed no difference was found in details, but when data are grouped in 5 periods blocks, significant differences can be observed (Figure 32). Thus, for the period from days 142 to 143, almost no OsHV-1 μVar DNA was found. For the second period (from days 150 to 153), an increase was observed ( $3.05 \times 10^3 \pm 2.82 \times 10^3$  GU.ng DNA $^{-1}$ ) to reach its maximum ( $3.06 \times 10^3 \pm 1.70 \times 10^3$  GU.ng DNA $^{-1}$ ) at the 3<sup>rd</sup> period (days 157 to 160), when the first mortalities were reported. Then OsHV-1 μVar DNA quantities significantly decreased in time ( $1.13 \times 10^3 \pm 1.07 \times 10^3$  GU.ng DNA $^{-1}$ ).

## 4. Discussion

### Spat mortality and risk factors

The first mortalities appeared on day 157 (May 31<sup>st</sup>) during the survey. This date fits well with the mortality period generally observed in French oyster farm ecosystems and extending from the beginning of May (in the south of France) until the end of July (in the north of France). In France, the mortalities occur with a clear latitudinal gradient related to the seawater temperature, with the northern sites characterized by the latest mortality outbreaks (Pernet et al., 2018). In bay des Veys, spat mortality crises occur generally between June and July as this

was the case in 2014 (Gangnery et al., 2019). However, it is possible to compare our results with those obtained by Ifremer, who carry out continuous recordings on the same site in 2017. The value of the mortalities accumulated at the beginning of July for the Ifremer survey is worth 34%, which is comparable to the average value obtained by counting the number of dead spat per day in bags randomly drawn (value of 38%).

Among the risk factors involved in OsHV-1 mortality outbreaks, the seawater temperature was identified as the most important one in many studies (Delisle et al., 2018; Pernet et al., 2012). A period of great temperature variations can also be responsible for triggering mortalities, even if the temperature of the water does not exceed the thermal threshold of 16°C (Pernet et al., 2011). The first date on which the water temperature exceeded 16°C was the day 152. Then, this temperature suddenly rose to 17.4 ° C on day 154. This value was the highest temperature recorded during this survey. Thus, first oyster spat mortalities were recorded five days after that the temperature first exceeded the thermal stress threshold of 16°C.

Generally speaking, the onset of mortality is not only related to temperature but also to other extrinsic risk factors, such as salinity (Fuhrmann et al., 2016) and bacterial communities (de Lorgeril et al., 2018). On this site, the salinity was not recorded during the experiment, but the seawater is typically marine with low freshwater inputs in this oyster park (Grangeré et al., 2009; Gangnery et al., 2019). The meteorological context of this survey period did not mention strong rainfall that could induce a salinity decrease below the value of 30 PSU. Concerning the co-infection with bacterial agents, the samples of oyster spats and in biofilms at sediment surface were taken. The DNA extraction and analyses were conducted, but data treatment for bacterial community in each compartment (oysters and biofilms) are still in progress. We cannot take this risk factor in account in the actual analyses of mortality, so that we only focus our attention on OsHV-1 genomic units and their dynamics in spat flesh (alive, dead and moribund) as well as microphytobenthic biofilms.

There are also intrinsic factors that can be detrimental for oyster spats, related to the development of the defense immune system against pathogens. The bivalve age, the breeding site and genetic parameters but also culture practices can be involved as well as the trophic status (well-fed or starved). One of the metabolic parameter that can make spats more vulnerable to OsHV-1 μVar infection is growth and food ingestion. Indeed, during the field survey it appeared that oyster spat tended to grow impressively during the survey with a rapid visible shell-formation. Oysters spats sampled in this study were 5 months old. When oysters

gets older than 22 weeks (for a size of 23.83 mm), a structural change of the gills occurs distinguishing juveniles from adults (Cannuel, 2005). From this point, the gill plication would be increased and the branchial system complete, thus potentially increasing the vulnerability to OsHV-1 μVar. This morphological change could also weaken these bivalves especially as OsHV-1 μVar mainly replicate in fibroblastic-like cells through-out connective tissues like the mantle, labial palps, gills, and digestive gland (Renault, 2011b).

As Rico-Villa et al. (2010) showed, oyster spats might have limited energetic reserves in comparison to adults. Oyster spat energetic resources would be mainly mobilized for growth, in parallel with higher energetic needs. Indeed, sufficient energy reserves in *C. gigas* coincide with a decreased risk of mortality (Pernet et al., 2014) and in particular a good availability in phytoplanktonic chl *a* (Gagnery et al., 2019). Other studies supports the hypothesis that well-fed and growing oysters can succumb to an OsHV-1 infection while scarcely fed oysters do not (Evans et al., 2015; Whittington et al., 2015b). In our case, we can suggest that the experimented oyster spats can be considered unstarved, but in these oyster farms, the risk of depletion have been clearly identified in the southern part of baie des Veys farms in modelling studies (Grangeré et al., 2009; Gagnery et al., 2019). The mortality risk were also identified higher in this area because of a potential depletion in phytoplankton chl *a*. At the beginning of summer, isotopic studies clear showed that the diet of oysters begin to be based on microphytobenthos food items instead of phytoplankton (Lefebvre et al., 2009; Grangeré et al., 2010), and this especially in the southern basin (Marín Leal et al., 2008). The hydrological parameters can be characterized as estuarine in the southern part of the farms compared to the northern marine waters, which are typically enriched in phytoplankton. The less favourable condition for growth combined with a higher proportion of infested microphytobenthos in the diet of oysters must both induce a higher vulnerability. The high viral density observed in microphytobenthic biofilms must thus contribute to expose oyster spats to OsHV1 virus more than marine water can do.

At baseline, low OsHV-1 DNA quantities were detected in alive oyster spat ( $10^1$  GU.ng DNA $^{-1}$ ). The OsHV-1 virus was therefore present in some oysters at the beginning of the field experiment and was clearly detected in the majority of analyzed spats before the first mortalities. However, OsHV-1 concentration were at a too low level to provoke disease and potentially virus replication. Thus it appears that oysters spat were already infected by OsHV-1 3 weeks before the first mortalities, but that the degree of exposure to extrinsic virus should progressively increase during 2 weeks. Oysters could have been contaminated by contact with

*OsHV-1* from the death of other individuals associated with the release of virus particles into the environment, likely from other parts of the basin. An *OsHV-1* peak was then observed on days 157-160. At the moment of the crisis, a good proportion of oysters showed higher concentrations than before, but still below the limit of  $10^5$  GU.ng DNA $^{-1}$  (~30-40% of individuals were above the order of magnitude of  $10^4$ ). For moribund and dead spats, *OsHV-1* DNA quantities was at the order of magnitude of  $10^5$  when the mortality started and these viral concentrations did not show significant temporal variations until the end of the survey, while amounts of virus observed in alive oyster spats gently faded over time. This decrease observed for survivors could reflect a decrease in viral replication after the mortality peak associated with an ability to eliminate the virus from their tissues (Dégremont, 2011). This could also confirm the hypothesis of a genetic basis favoring oyster spats resistance to *OsHV-1* μVar infections (Sauvage et al., 2009; Dégremont, 2011), since a proportion of oyster could have resisted even if they were infected. However, the level of infection seems to be an important intrinsic factor, since the oysters for which a lethal threshold would not have been exceeded ( $10^5$  GU.ng DNA $^{-1}$ ) could have survived after the viral infection. The individual virus level can be eventually more decisive than a genetic trait to determine the potential survival.

### **Role of microphytobenthic biofilmin the transmission of *OsHV-1* μVar**

Microphytobenthic biofilms did not appear to be a reservoir with high viral concentrations at the beginning of the follow-up. On this oyster farm, conditions were clearly unable to allow maintenance of virus particles from one year to another (as seen in Chapter 1; 5.1). In fact, high *OsHV-1* concentrations were observed in winter but on a distant mudflat (~2 km) and not within the area of the oyster farm. The profile of the amount of *OsHV-1* DNA in the biofilm did not differ according to the local “crosshatching” habitat (under the oyster table and in the aisle alternatively). Thus, the oyster table habitat does not seem to provide preferable conditions to *OsHV-1* distribution, compared to aisles between tables. However, there was a significant increase of the amount of *OsHV-1* DNA in biofilms on day 150, seven days before the first mortalities, whatever the habitat (under and off the tables). This period was prior to the observation of the first mortalities and also before the significant increase in the viral load observed in oysters.

In Chapter 2, the quantity of secreted EPS by epipelagic diatoms were relatively high, given the fact the sand proportion was also high (mud content of  $7.38 \pm 1.45\%$  corresponding to a slightly muddy sand). No difference was observed for extracellular polymeric substances according to

the habitat and time ( $18.43 \pm 19.74 \text{ } \mu\text{g.g}^{-1}$  of sediment), but there was a high density of microphytobenthic chl *a* biomass in biofilm under the table compared to the aisle habitat. The photosynthetic yield of benthic diatoms was also higher under the table, probably related to lower temperature and light stresses. Benthic diatoms were clearly less subjected to thermoinhibition and photoinhibition under tables than in the aisles. The table environment can be considered as dampened compared to the sediment exposed to high level of irradiance in the aisle. Our initial hypothesis on the role of biofilms concerned the secretion of these extracellular polymeric substances which could act as a substance favorable to (i) viral accumulation (because diatoms spontaneously form biofilms covering the interface the viral particles must be found) and (ii) the bio-adhesion that would promote fixation of viruses around diatoms (Chapter 2). Extracellular polymeric substances could also help the survival of the virus from the host by providing an optimal microenvironment for potential desiccation and light exposure which is a common occurrence in the intertidal zone at the surface of sediments (McKew et al., 2011). The physiological status of microphytobenthic biofilms can be considered better under tables, but this phenomenon was not directly revealed by the EPS analysis.

So, the positive relationship between EPS secretion and *OsHV-1* μVar quantities cannot be clearly demonstrated from our field survey, since the EPS contents as well as *OsHV-1* did not reveal a local spatial structure related to a “Table” effect, but we must mention that these two variables were both at a high level, in both local conditions (table and aisle habitats). So this armoring effect and protection provided by EPS for *OsHV-1* could have been efficient during the survey, especially when the *OsHV-1* quantities were at the maximal amount, one week before the first mortalities, but this is difficult to be conclusive with this dataset, which cannot allow us to demonstrate an effect of the “Table” factor.

However, biofilm and extracellular polymeric substances can also help viruses to cope with excess light because diatoms (as well as extracellular polymeric substances associated with their frustules) return in sub surface layers (~1 mm) in case of light stress with viruses embedded with them. Chl *a* concentrations and photosynthetic yield were particularly high on days 150-153 (Chapter 2), exactly when the increase of *OsHV-1* was found in the biofilm. It is more likely that this detection of *OsHV-1* in the biofilm at this period is the result of a neighboring spat infection and mortalities that could have released viral particles into the environment and sediment towards the surface of the sediment, before infecting our local oyster spats. The role of biofilm as a “spongy” structure locally accumulating virus though a retention/adsorption mechanism must reinforce the degree of exposure of oyster spats to

extrinsic OsHV-1 prior infection, if this biofilm-related virus can be resuspended in the water column during tidal inundation. We can consider the role of microphytobenthic biofilm as a transmission/amplification relay.

However, the OsHV-1 DNA detected in the biofilm does not guarantee its virulence, since we can only prove the presence of DNA, whatever the pathogenic activity. So it is unclear whether oyster spat could have been contaminated by filtering particles from the biofilm that had been resuspended by tidal erosion.

The OsHV-1 DNA quantities could be considered as low during the pre-mortality period ( $\sim 10^1$  GU.ng DNA $^{-1}$ ), but this could be sufficiently high to infest benthic diatoms which are known to constitute a substantial part of the oysters diet in June, after the phytoplanktonic bloom (Grangeré et al., 2009; Lefebvre et al., 2009). Such an infested food can be accumulated and concentrated in oyster spat flesh, tide after tide. When expressed by cm $^2$ , the order of magnitude of virus particles in biofilms is relatively high ( $\sim 10^4$  GU.ng DNA $^{-1}$ ), and oyster spats can also ingest benthic diatoms from distant areas, after resuspension by the flow tide and advection of water bodies.

The viral loads in microphytobenthic biofilms decreased over time, either by degradation or erosion and diffusion. In addition, UV rays risk was at its peak at this season with very important solar irradiances, especially during neap tide (with midday low-tides). Conditions were likely not gathered to keep a biofilm effective for (i) light protection for the virus after accumulation of OsHV-1 and (ii) for preventing tidal erosion losses by an EPS-mediated sediment biostabilization. The combination of these two processes would lead to the dispersion of OsHV-1 associated to biofilm particles. Nevertheless, the OsHV-1 loads detected were still higher at the end of the survey than those observed before the mortality episode. The rapid decline in OsHV-1 amounts at the sediment surface confirms the results obtained from the monitoring carried out under the VIAPSE project (Centre de référence sur l'huître; 2014). Indeed, during this project, low viral quantities on the surface of biofilms were frequently observed in June or July.

## 5. Conclusion

Through our results it seems that a lethal threshold in OsHV-1 μVar has to be exceeded to provoke death ( $10^5$  GU.ng DNA $^{-1}$ ). In addition, the environmental conditions prior mortality seems important, including a potential role of biofilms as relay of transmission/local accumulation. Indeed, the phytoplankton pass through water advection but the microphytobenthos stays on the

benthic habitat and can have a stronger impact in terms of transmission. Microphytobenthic biofilms do not appear to be well pre-positioned to promote annual persistence of the virus in the sediment, but it could represent a vector for OsHV-1 transmission. These biofilms could also help reduce the rate of post-mortem viral abatement (by association with benthic diatoms particularly endowed for photoprotection by their migratory linked to chronobiological strategies). The trophic status of the ecosystem and the potential depletion (a decline in post-bloom period growth) must play a role in the mortality crisis that could weaken young oysters at a time when their diet is starting to be based on microphytobenthos and the requirements needed for somatic growth increase. Oysters could be able to partly eliminate OsHV-1 of their tissues in case of survival although a part can persevere in their tissues.

## Acknowledgments

Special thanks go to André-Gilles Taillepied and his team who kindly lend us the oyster table and plenty of space in their building to store our equipment and conduct our experiments. Thanks to the Blouin nursery for the oyster spat. Thanks to C. Rakotomalala, C. Roger, B. Adeline and M-P. Dubos for their help on the field. I am grateful to the *Ministère de l'Enseignement supérieur et de la Recherche* for this PhD grant.





Lorsque les huîtres dépassaient le seuil de  $10^5$  unités génomiques de OsHV-1  $\mu$ Var.ng DNA-1 la mort de ces bivalves se produisait induisant un largage de particules virales dans l'environnement. Certaines particules pourraient donc jouer le rôle de vecteur par adsorption et favoriseraient ainsi la sédimentation du virus vers l'habitat benthique. A l'inverse, bien que les biofilms microphytobenthiques ne semblaient pas favoriser la persistance annuelle du virus dans les sédiments ils pourraient néanmoins représenter un vecteur de la transmission de l'OsHV-1, ainsi qu'un amplificateur passif. En effet, les biofilms persistent d'une marée à l'autre avec des teneurs virales augmentant de jour en jour à proximité immédiate des huîtres et cet agent peut encore accentuer les risques que les charges virales atteignent des niveaux léthaux pour les naissains d'huîtres positionnés juste au dessus. Les particules virales accumulées dans les biofilms et dans le sédiment pourraient être remises en suspension et ajouter des particules virales à disposition de l'ingestion par les huîtres, en agissant comme un facteur extrinsèque responsable de bioaccumulation des particules virales pour les jeunes huîtres. Ainsi l'érodabilité de l'habitat sédimentaire a été étudiée en fonction des caractéristiques benthiques ainsi que la remise en suspension de OsHV-1  $\mu$ Var lors d'un épisode de mortalités estivales de naissains d'huîtres.



**Chapitre 5 : *In situ* resuspension of benthic sediments  
and biofilm components during an OsHV-1 μVar  
*Crassostrea gigas* oyster spat mortality episode**



# ***In situ resuspension of benthic sediments and biofilm components during an OsHV-1 μVar *Crassostrea gigas* oyster spat mortality episode***

Vanhuyse Charles, Lepoittevin Mélanie, Guillaume Meynard, Orvain Francis

In preparation for a submission to Journal of Sea Research

## **Abstract**

Since 2008 large oysters spat mortalities are mainly attributed to the Ostreid herpes virus  $\mu$ variant (OsHV-1  $\mu$ Var). Environnemet parameters favoring the persistence and diffusion of OsHV-1  $\mu$ Var could represent a threat and needs to be more studied. In the litterarure it appears that OsHV-1 could be adsorbed to suspended particles. Thus, these particles could represent a horizontal transmission vector. As seen in the previous Chapter, microphytobenthic biofilms and sedimentary particles were carrying OsHV-1  $\mu$ Var. In the present study, the results show that sediments of the oyster beds in the bay des Veys can be resistant to erosion despite a sandy dominance. However, the virus appeared to be released into the water by an erosion process rather than diffusion. The week preceding the first mortalities, OsHV-1 was easily released into the water and detectable in large quantities. Thus, OsHV-1 could preferentially be linked to the biofilm particles because weak currents were sufficient for its resuspension. On the other hand, sediment erosion after the period of mortality (or infection) required higher current velocities, but maximum viral concentrations were obtained for particles preferentially related to sediment.

## 1. Introduction

Since the first disease recordings in 2008 in France (Segarra et al., 2010b) OsHV-1 μVar causes large oysters spat mortalities worldwide (Lynch et al., 2012; Jenkins et al., 2013; Hwang et al., 2013). These summer mortalities are mainly attributed to the Ostreid herpes virus μvariant (OsHV-1 μVar) when the water temperature exceeds 16°C (Pernet et al., 2012) and decimate up to 80% of spat individuals with many variations according to the site. Recent studies showed that the death of oysters would be the result of a virus-bacteria co-infection (de Lorgeril et al., 2018; Pathirana et al., 2019). Indeed, a first step consisting in the infection of oysters by OsHV-1 μVar would weaken the oysters immune system thus favouring the proliferation of opportunistic bacteria leading to bacteraemia (de Lorgeril et al., 2018). Other risk factors can also play a role (Rodgers et al., 2018; Chapter 4). However, before any contamination, the environmental origin and reservoir of OsHV-1 μVar remains poorly described.

A part of the factors must be intrinsic, and the viral proliferation in oyster cells during the initial growth is a processs that is well described (Renault, 2011a). We postulate that there must be also extrinsic viral transmission factors favoring the environmental risks of exposure of the oyster spats to this virus. In general, the first diseases and mortalities start in one special location, before a rapid transmission to neighbors via physical drivers (Evans et al., 2015; Paul-Pont et al., 2013), during the epizootic episode. The first symptoms is the lesion of the gills that are associated to the herpes-like-virus (Vásquez-Yeomans et al., 2010) and the most evident histological alteration is the presence of abnormal nuclei thoughout the connective tissue and hemocyte degeneration (Renault et al., 1994; Friedman et al., 2005). In aquatic systems, the dispersion and the transmission can be very rapid by the movement of water bodies, but there are a lot of hydrodynamics factors that can help or, at contrary, disavantage the transmission probabilities. When animals are sick with gill lesion, high release rates of viral particles must occur, and the virus can be transmitted to the adjacent populations by simple diffusion (Evans et al., 2015; Paul-Pont et al., 2013; Schikorski et al., 2011). Viral particles are also subject to sorption processes and they must rapidly be associated to the turbidity and be integrated in sediment/deposition cycles and transport (Evans et al., 2014, 2015). Sediment surface is always a natural concentration micro-environment because of physical processes (the finest particles being the last to settle). Generally speaking, viruses are the most abundant organisms from marine ecosystems with values ranging from  $10^7$  to  $10^{10}$  L<sup>-1</sup> and are even more abundant in the benthic compartment with values ranging from  $10^7$  to  $10^{10}$  g<sup>-1</sup> of marine sediments (Fuhrmann and Suttle, 1993; Weinbauer, 2004). The resuspension of the sediment makes it possible to

release quantities of viruses and bacteria that can be very high (Dupuy et al., 2014; Mallet et al., 2014).

Advection processes and tidal currents can also play a role by facilitating and enhancing the transmission routes along, and there are also a general role of environmental cues and hydrosedimentary conditions that contribute to explain why some local spots are subjected to high mortality rates, while other ones are more favorable to survival (Pernet et al., 2018; Gangnery et al., 2019). But there are also some evidence (Chapter 1; 5.1) that the transport of the virus with currents is detrimental for its activity along transport, so that a simple dispersion can be eventually more efficient for transmission. In case of high tidal currents ( $\sim 2 \text{ m.s}^{-1}$ ), this decline is even more rapid, and paradoxically, high transport rates can finally limit the transmission efficiency (Chapter 1; 5.1).

During a mortality outbreak, the flesh of dead oysters spread into the environment by tidal currents and may sediment towards the benthic habitat. In addition to simple diffusion, the virus associated to the flesh of dead oyster spats could also massively settle towards the benthic habitat. There are some studies describing numerical models with pathogen transport in different aquatic environment (Sim and Chrysikopoulos, 2000). For instance, modelling approaches are developed to assess the transmission of pathogens between fish farms (Salama and Murray, 2013), but these studies remained theoretical by considering only diffusion and were not applied to OsHV-1. Large-scale surveys are also useful to assess the transmission maps of pathogens at the ecosystem scale and explore the spatio-temporal dynamics (Pernet et al., 2012, 2015; Gangnery et al., 2019). However, small-scale and mechanical analyses of the role of hydrosedimentary factors, turbulence fields and friction stress can be useful to better interpret transmission routes in various ecosystems. This topic remains very scarcely studied and among the objectives of the present paper.

Beside the OsHV-1 flux towards the sediment, such epizootic episodes can lead to significant ecological effects (Forrest et al., 2009a) like a flux of organic matter towards sediment (Chapter 3). Once the virus is transferred to the bottom sediment, the fate of this pathogen agent and its resilience outside of the host organism is poorly described. Yet, it appears that the benthic habitat could establish good circumstances for viral particles persistence in the environment because this virus consists of very small particles that should be among the last to sedimentate, given the particle size of viral capsules. The presence of MPB biofilms endowed of chronobiologic vertical migration in the first millimeters must provide a good refuge for OsHV-

1 particles which could be embedded in a MPB-EPS matrix. Sediment-water interface is the best meeting place for sedimented virus during high-tide phases and epipelagic diatoms during low-tide exposure. The secretions rates of EPS are impressive: ~50% of photoassimilated carbon and offer many biochemical properties related to bioadhesion (Decho, 2000).

During the flow, the rising tide exerts an increasing erosion force at the surface of the sediment. This flow bed friction velocity will provoke a resuspension of particles from the benthos towards the pelagos, therefore increasing the turbidity of the water column. According to the intensity of the tidal shear stress and sediment cohesiveness different particles can be resuspended (Murray, 1977; Le Hir et al., 2011; Joensuu et al., 2018). Regarding biotic components, biofilm microorganisms can be eroded into the water column (Blanchard et al., 1997; Orvain et al., 2004; Dupuy et al., 2014) including the microphytobenthos (MPB) which constitutes a primordial nutritional resource for the oysters (Cognie et al., 2001; Lefebvre et al., 2009; Grangeré et al., 2010). The biofilm is partly responsible for sediment stabilization due to the excretion of biopolymers called Extracellular Polymeric Substances (EPS) in link with the diatoms migratory rythmn (Yallop et al., 2000; Tolhurst et al., 2003). These secreted EPS create a cohesive matrix playing a stabilization role on the sediment (Stal and de Brouwer, 2003; Tolhurst et al., 2002; Yallop et al., 1994). Regarding abiotic components, sediment resuspension depends on grain size, the proportion of sand and mud and consolidation processes (Le Hir et al., 2011; Grasso et al., 2015). Indeed, the shear stress necessary to resuspend sediment particles increase with the proportion of fine particles in the soil sample (Murray, 1977). Thus a sandy sediment is subject to bed load transport a bed disruption must be provoked to transport muddy cohesive sediment, which can be eroded only at high shear stress due to the degree of cohesiveness provided due to fine particles (except for recently deposited fluid layers that easily eroded with typical low critical threshold for erosion). Nevertheless, the coarsest particles will be the first to sediment back to the benthos, in case of dynamic transport. Another factor of resuspension is the bioturbation activity made by macrozoobenthos. Indeed, in addition to disrupting the development of the biofilm, bioturbation made by macrofauna can lead to particles resuspension (Orvain et al., 2004; Rakotomalala et al., 2015; Cozzoli et al., 2018). Thus, according to their feeding type and motility some macrozoobenthic species could bioturbate the sediment surface resulting in a suspension of benthic particles (Orvain et al., 2003). However, other species like the mobile worm *Hediste diversicolor* can create galleries full of mucus, which can induce a biostabilisation in synergy with microphytobenthic biofilms (Passarelli et al., 2012).

Intertidal oyster farming practices are known to create particular environment characteristics on a large (Forrest et al., 2009a; Ubertini et al., 2012) but also at the scale of the oyster table (Dubois et al., 2007; Chapter 2). Indeed, oyster tables create a crosshatching pattern between oyster tables and aisles which structure the benthic habitat at mesoscale. Regarding OsHV-1 μvar, oyster table habitat could be a favorable biotope for its perseverance in the environment. Indeed, oyster tables provide several favorable characteristics to OsHV-1 persistance like the (i) shading achieved by culture structures protecting against UV rays, (ii) biofilm protective properties protecting against physico-chemical stresses (eg. desiccation, acidification, haline stress), (iii) sediment stabilization due to the production of Extracellular Polymeric Substance (EPS) by diatoms, (iv) habitat muddification due to the biodeposition activity of oysters and the friction velocity attenuation caused by elevated structures (Kervella et al., 2010; Nugues et al., 1996; Sornin, 1981). Thus, a habitat difference could be reflected in the spatial distribution of OsHV-1 μvar, in terms of resuspension rates, transmission mode and resistance against erosion.

This *in situ* study was carried out to follow the sequential resuspension of OsHV-1 μvar according to two oyster habitats (table *versus* aisle) during the summer 2017 oyster spat mortality episode. Experiments were performed with a previously described erosion device (Dupuy et al., 2014; Orvain et al., 2014a). The purpose of this study was to answer a series of cascading questions. The first one was to reveal if OsHV-1 μvar could be resuspended from the sediment into the water column (before *versus* after the mortality period). Then, if it is the case, how would this transfer occur : by (i) a simple passive diffusion or (ii) an active erosion due to bed shear stress. Finally, if a transfer to the water column requiring an active erosion force turns out to be true, would OsHV-1 μvar rather be associated with microphytobenthic particles (chl *a*) and/or with inorganic particles (mud *versus* sand) ? In addition, the bioturbation activity exerted by the macrofauna was also studied because it can disturb or stabilize the surface of the sediment and thus increase the resuspension of the benthic habitat. This can be very determining for small particles that are concentrated at the surface like microphytobenthic cells (Dupuy et al., 2014; Savelli et al., accepted), or associated viral particles.

## 2. Material & method

### 2.1. Study site

The Bay of Veys is located in the Southern-Western part of the Bay of Seine with 40% of the inputs originating from the Vire river (Jouenne et al., 2007). This bay is an estuarine and shellfish ecosystem that stretches over an intertidal zone of 1.60 km<sup>2</sup>. During periods of spring

tide, a tidal range of 8 meters with currents of  $3 \text{ m.s}^{-1}$  can be reached (Orvain et al., 2012). On this area, oyster farms are mainly located on soft sediment with a natural tendency to slow silting due to tidal currents and accentuated by the installation of oyster beds (Kopp et al., 1991). Although this shellfish basin is the one for which the growth is the fastest in France, it is in contrast the second one in terms of production (25.000 tons in 2016; Comité National de la Conchyliculture). More details about this ecosystem are given in chapters 1 & 2 and the recent publication by Gangnery et al. (2019).

### 2.2. Experimental design

This study was conducted along a row of oyster tables (Figure 33) located at Géfosse-Fontenay in the Bay des Veys (Normandy, France) on the top of the foreshore (from  $49^{\circ}22'53.2'' \text{ N}$ ;  $001^{\circ}05'44.2'' \text{ W}$  to  $49^{\circ}22'54.6'' \text{ N}$ ;  $001^{\circ}05'43.4'' \text{ W}$ ) from the 22<sup>th</sup> of May 2017 till the 1<sup>st</sup> of July 2017. On this oyster table, 20 oyster bags with in each one two small-bags containing 200 three-months-old oyster spats were followed. Oysters were produced according to standard hatchery procedures (Petton et al., 2015a).



Figure 33 : Experimental field design. Sediment cores were alternately sampled in the aisle (in red) and under the oyster table (in blue)

### 2.3. ALTUS measurements

Water height and bed level variations were recorded using an ALTUS altimeter. This device provided bed variations measurements (elevation/accretion or lowering/erosion) with a sub-millimetric accuracy and a high sampling frequency for the two period of sampling. Multiple environmental variables were recorded as previously described in Chapter 2 in order to compare them to erosion parameters. ALTUS data were analysed to extract the maximal tidal

inundation height. The difference of sediment bed level can be negative (net erosion) or positive (net deposition). The mean bed level was calculated separately for each high-tide period.

#### *OsHV-1 sampling in biofilm before erosion*

Biofilm was collected via Bluter mesh (100 µm mesh) of 49 cm<sup>2</sup> placed at the surface of the sediment during 30 minutes, thus representing the active surface chl *a*. The webs were then dipped in 10 mL of filtered (0.2 µm) seawater and stored at -20 °C. Total DNA was extracted and purified using NucleoSpin® Soil Kit (Macherey-Nagel). The quantification of the total extracted DNA was quantified using a Nanodrop 2000 (Thermoscientific). OsHV-1 μVar genomic units were quantified via real-time qPCR CFX 96™ C1000 ™ (Biorad).

#### *Macrozoobenthos bioturbation*

Because macrofauna bioturbation activity can importantly shape the sediment surface and consequently alter bed shear stress, macrozoobenthos was rigorously sampled. The full description of these results is available in a parallel study (Chapter 3). However, in the present study supplementary macrozoobenthic related data are provided with the calculation of metabolic rates (Cozzoli et al., 2018) to measure the effects of bioturbation on sediment shaping. Thus individual metabolic rates for each species of each sample and was summed in a single community index. The metabolic rates were estimated according to the empirical model of Brey (2010) by using temperature data (Chapter 2) and individual biomass of faunal species (Chapter 3). The overall rate of these processes, the metabolic rate, sets the pace of life. It determines the rates of almost all biological activities and can be very useful to estimate the global bioturbation rate, even though each species must have different bioturbation activities in this site.

### *2.4. Erosion experimentations*

#### *Sampling design*

Each sampling day an alternance of sampling was made between the oyster table and the aisle according to a random draw in the studied area. This way, erodimeter experiments were made on 15 days along the two months survey. A sediment core (9 cm of diameter, 40 cm in height) was withdrawn on the field then the sample was brought to the field laboratory and placed into the erodimeter (Figure 34) to replicate the *in situ* erosion chronology. Only the 4 first centimeters of sediment were cut and placed in the erosion chamber, thanks to a sediment sample transfferer. The erodimeter was then filled with 21 L offiltered (Whatman GF/F filter) and UV-sterilized seawater. In order to simulate erosion a flow discharge was increased on the transferred sediment in the section test of the erodimeter by a step of 0.0792 L.s<sup>-1</sup> from 0.12 to

$2.02 \text{ L.s}^{-1}$  with a succession of 24 steps. The corresponding tested current velocities range from 7.5 to  $125 \text{ cm.s}^{-1}$ . Currents were generated by a pump (KSB, VITACHROOM-65-160/154C2) and were controlled by a frequency converter (HITACHI®)

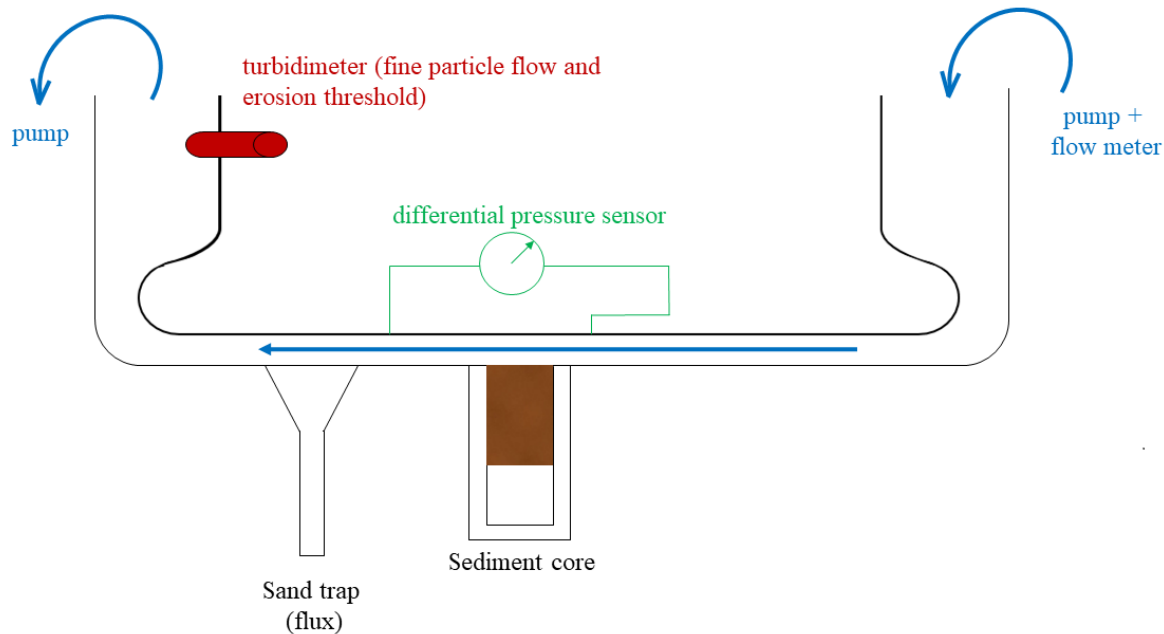


Figure 34 : Experimental erosion device (erodimeter)

Flow discharge and the turbidity were continuously recorded. The concentrations of Suspended Particle Matter were estimated using a nephelometric probe (NTU) that was systematically calibrated by direct comparison to water samples. Turbidity data were calibrated from filtered suspended particle matter (SPM) concentrations ( $\text{g.L}^{-1}$ ), which were converted upon the basis of the most appropriate calibration curve (NTU versus SPM). A linear regression was used to calibrate the turbidity data to provide the best  $R^2 (> 0.92)$ , while a polynomial regression was used for chl *a* ( $R^2=0.99$ ). SPM data were also corrected ( $\text{SPM} = \text{Volt} * 0.00026 ; \% \text{ in g.L}^{-1} ; R^2=0.92$ ) to account for the dilution effect, since 2 L of the sampling was used for filtration at four successive steps all along the erosion experiment, and the same quantity of filtered water was added to maintain the volume constant in the system.

#### *Resuspension of microphytobenthic biofilm*

To calculate the chlorophyll *a* biomass in seawater (chl *a* in  $\mu\text{g L}^{-1}$ ) of the samples, 0.5 L of were filtered on GF/F wheatman filters and photopigments were extracted with acetone. Photopigments were extracted in 10 ml of 90% acetone for 18 h in the dark at  $4^\circ\text{C}$  under continuous mixing by automatic rotation. After centrifugation ( $4^\circ\text{C}$ , 3000 rpm, 10 min), the fluorescence of the supernatant was measured using a Turner Trilogy fluorometer (Turner Designs, Sunnyvale, California, USA) before and after acidification (10  $\mu\text{l}$  of HCl, 0.3 M per 1

ml of sample). The probe calibration (fluorescence) was based on chl *a* and turbidity data from a parallel study with the same experimental setup according to the following equation:

$$\text{Chl } a = \text{Volt}^2 * 0.0128 + 0.7485 * \text{Volt; \% in } \mu\text{L}^{-1} (R^2=0.998)$$

In parallel, at each sampling step, the amount of eroded sand was counted by measuring the height of sand sedimented in the trap (Figure 34) and subsequently converted to an eroded sand depth in dm.m<sup>-2</sup> (surface of the core sample).

#### *OsHV-1 μVar sampling*

For every sampled step, 1 mL of erodimeter seawater was taken and then conserved at -20°C in order to quantify their OsHV-1 charge. Samples were directly lyophilized according to a protocol optimization (Appendix 3) and resuspended into 200 μL of 0.2 μm sterilized seawater. The extraction of DNA was performed on 300 μL using the same protocol as described above.

#### 2.5. Data analysis

The data processing was done using MATLAB®. The analysis took place in 5 steps: (i) conversion of units, (ii) correction of dilution effects (related to water withdrawals), (iii) elimination of outliers (due to bubbles in the system), (iv) data harmonization to have the same number of data in steps and (v) application of a moving average (independently for each level). The probe data was converted into concentrations by calibration parameters based on the 10 SPM (Suspended Particular Matter) and chl *a* measurements on GF/F filters. A conversion of the SPM (g.L<sup>-1</sup>) and chl *a* (μg.L<sup>-1</sup>) data was performed to obtain eroded mass SPM values in g / m<sup>2</sup> (and in μg.m<sup>-2</sup> for the chl *a*), in multiplying the results by the following factor: TSM = Suspended particles × Water volume in the erodimeter (V = 21 L) / Area of the sample (= π × 0.045 m<sup>2</sup>). Then, the critical erosion threshold ( $\tau_{crit}$ ) of the SPM and chl *a* was calculated and corresponded to the minimum stress (frictional tension in Pa) before the onset of erosion. For this, the average frictional tension (Tau or  $\tau$ ) in steps has been calculated for the 24 steps. This made it possible to calculate the average shear rate per stage ( $U^*$  in m.s<sup>-1</sup>), which is equal to  $\sqrt{\tau/\rho}$  (with  $\rho$  the density of the seawater = 1,030 g.L<sup>-1</sup>). Then, the value of critical shear velocity ( $U^{*crit}$  m.s<sup>-1</sup>) was determined by looking for the best regression line (on criterion of  $R^2$ ) between the values of SPM (and chl *a*, average in steps) as a function of Log ( $U^*$ ), and  $U^{*crit} = 10 (-b/a)$ , with "a" corresponding to the slope of the line and "b" corresponding to the ordinate at the origin. Finally, thanks to this value of critical bed shear stress for erosion  $U^{*crit}$ , the value of  $\tau_{crit}$  could be calculated:  $\tau_{crit} = \rho * (U^{*crit})^2$ . This critical threshold value was used to determine the critical step during which SPM or chl *a* erosion begins (Figure 37). From this critical level,

the mean level erosion values of the SPM and chl *a* (in g or  $\mu\text{g} \cdot \text{m}^{-2} \cdot \text{sec}^{-1}$ ) were calculated from the SPM slopes as a function of time for each incremental step. from the moment the critical stress has been exceeded

Fluxes and threshold were confronted to environnemental variables presviously described (Chapter 2) using regression linear models. Regarding virus contenteration in the erodimeter, a Split-plot ANOVA was performed with two main factors, the day (grouped two-by-two) and the presence/absence of table. The effect current velocity was analysed within the “experiment factor, since the water samples were not independent during one erosion experiments.

### 3. Results

#### 3.1. Benthic erosion

##### *Bed level variations*

Concerning the variations of topography provided by the ALTUS data (Figure 35), it is impotant to note that the zero level of the sediment could have varied between the two periods (colored green and red), since the ALTUS instrument was brought back at the laboratory at the end of the first period wad was placed on the field again for second period of the survey. The bed variation between the two periods cannot be analysed and the relative bed variations are more robust than the absolute bed level because of this difference in the starting reference. During the first period (green) daily variations were observed. A decrease in sediment height was observed as the water level increased during spring tides and then appeared to be more stable when the water depth was lower during neap tides. Nevertheless, a clear decrease was observed at the end of the first period, when the water height increased between days 155 and 160. During the second period the topographic level of the sediment tended to decrease when the water height increased (during spring tides), then stabilized when the water level was maximum before increasing again when the water height decreased (during neap tides).

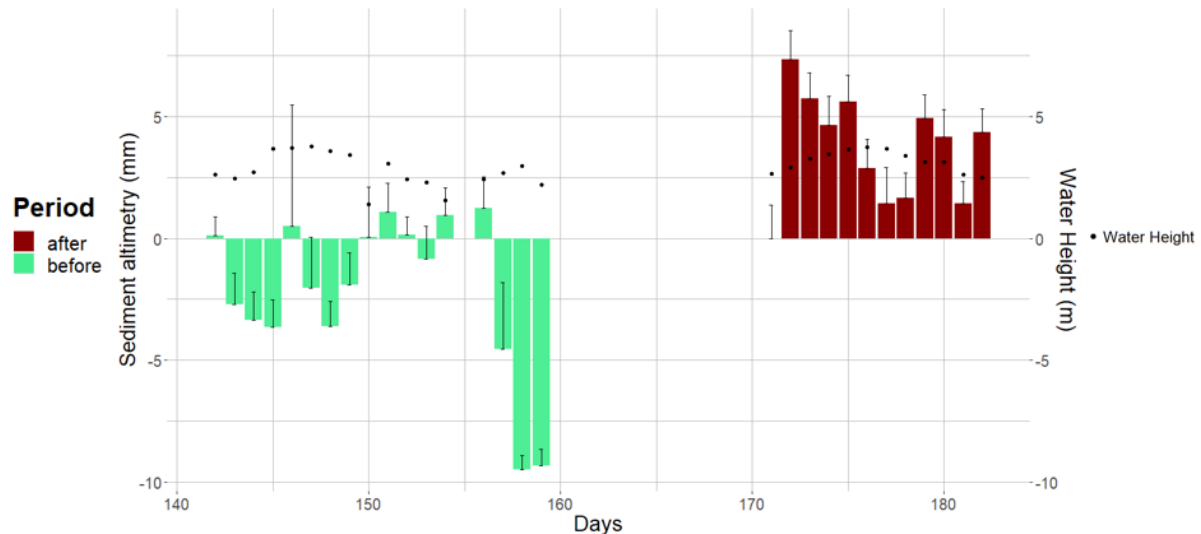


Figure 35 : Topographical bed variations observed during the the samplig periods. The data in green are considered as before the mortality episode and in red after. Points represents the daily maximal water height recorded by the ALTUS device.

From the topography bel level kinetics, we calculated the difference between two subsequent tides to evaluate the net gain or losses of sediment (positive and negative, respectively). Even if there was an apparent effect of the tidal level (in relation with tidal currents) on the sediment losses by erosion during the first period, there was no significant correlation between the water height and the topographical bed variations (Figure 36).

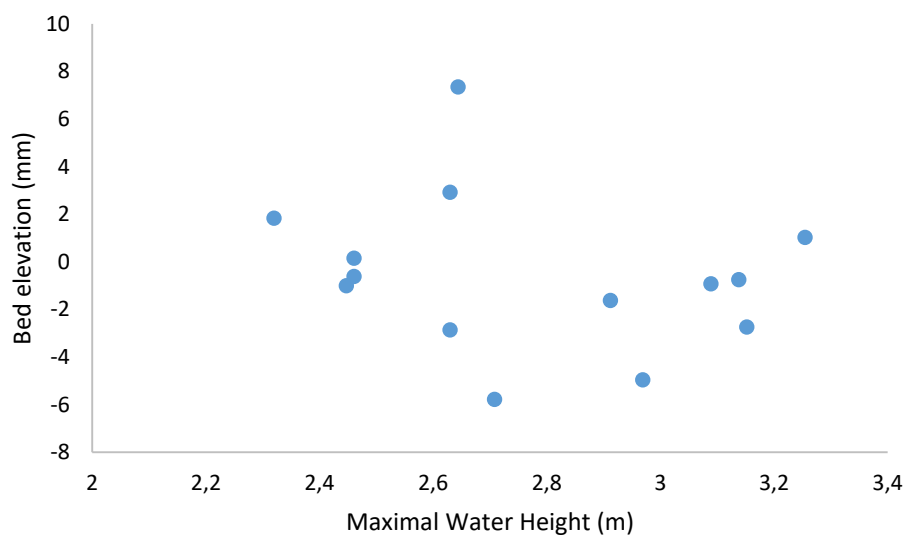


Figure 36 : Correlation between bed topography variation and maximal water height

#### Erosion experiments

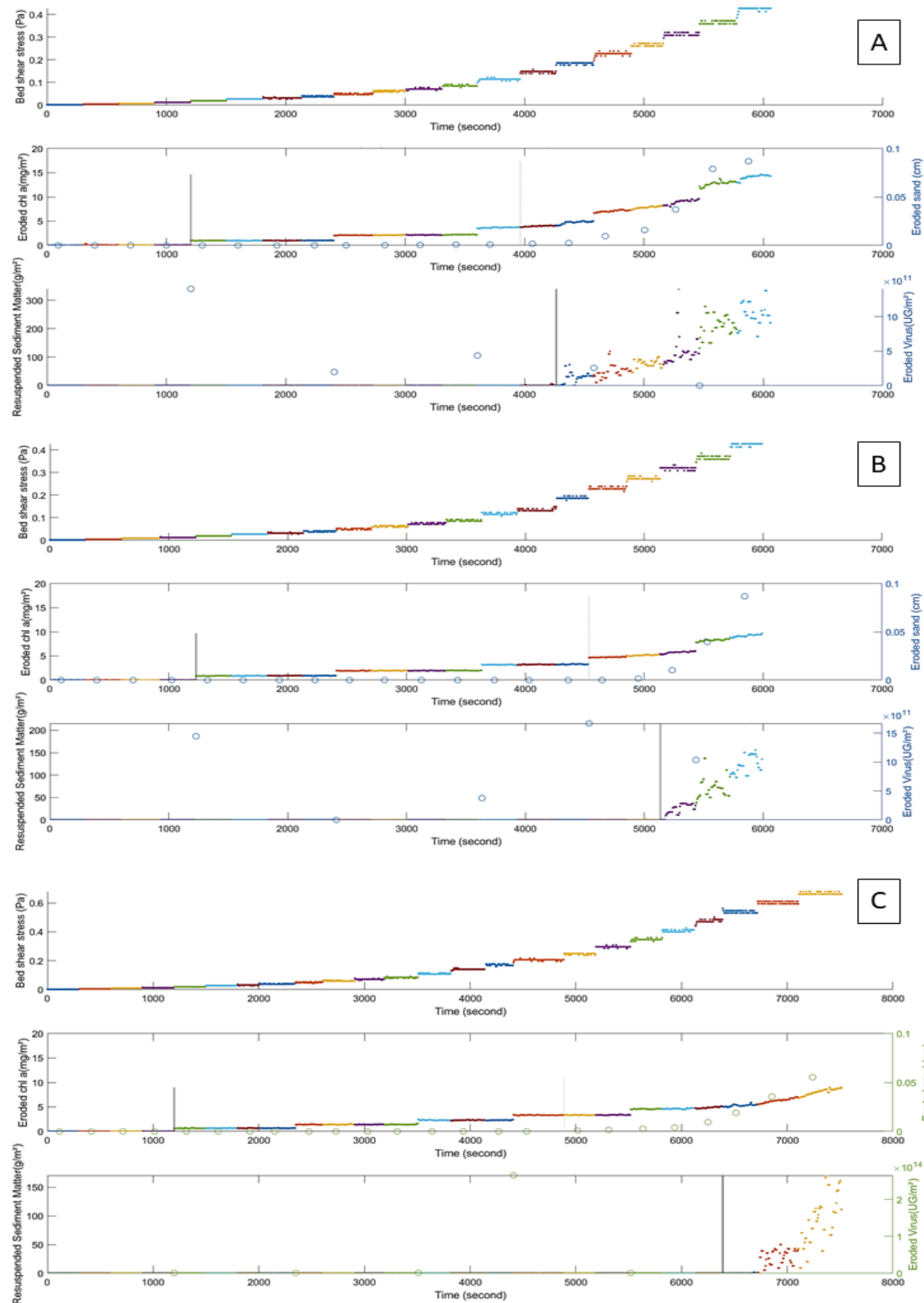


Figure 37 : Each part (A, B & C) presents 3 diagrams with Bed shear stress (Pa), Eroded chl  $a$  ( $\text{mg.m}^{-2}$ ) and resuspended sediment matter ( $\text{g.m}^{-2}$ ) & virus ( $\text{UG.ngDNA}^{-1}$ ) for 3 experiments out of the 15 ones : A. Jour 150 B. Jour153. C. Jour 180. Vertical bars represent the current steps corresponding to the initiation of the erosion (when critical thresholds were overpassed). A. Top graph represents the bed shear stress (Pa) applied in the erodimeter on the sediment core. The middle graph represented the eroded chl  $a$  and sand which on day 150 showed critical threshold for erosion of 0.0094 and 0.12973 Pa respectively. The bottom graph showed the resuspended sediment matter (SPM) with a critical threshold for erosion 0.16477. B. On day 153, eroded chl  $a$  and sand showed critical threshold for erosion of 0.02 and 0.21 Pa respectively. The bottom graph showed the resuspended sediment matter (SPM) with a critical threshold for erosion of 0.30. C. On day 180, eroded chl  $a$  and sand showed critical thresholds of 0.01 and 0.23 Pa respectively. The bottom graph showed the resuspended sediment matter (SPM) with an erosion threshold 0.51.

The jumps visible for chl *a* and sand (Figure 37) were revealed when applying the correction of the dilution induced by the sampling at the targeted steps. In addition to Figure 37, graphs corresponding to other erosion experiments are presented in Appendix 4. The type of particles resuspended always showed the same chronological order with firstly, the chlorophyll particles, then the sand and in at last the most cohesive particles: fine sediment (SPM). Indeed, chl *a* presented lower critical thresholds for erosion compared to sand and even more to mud (Tableau 9).

Tableau 9 : Erosion parameters calculated from erodimeter experiments: Sand, SPM and Chl *a* erosion threshold and fluxes towards the water.

Days	Habitat	Sand erosion threshold (Pa)	SPM erosion threshold (Pa)	Chl <i>a</i> erosion threshold (Pa)	Sand flux (dm/s)	SPM flux (g/m <sup>2</sup> /s)	Chl <i>a</i> flux (μg/m <sup>2</sup> /s)
142	Table	0.2692	0.043502	NA	0.0116	NA	NA
143	Aisle	0.28929	0.10586	NA	0.0895	NA	NA
150	Table	0.12973	0.16477	0.0094	0.031	0.26354	3.6129
151	Aisle	0.15936	0.24884	0.0057	0.0357	0.3124	1.8044
152	Table	0.15845	0.19747	0.0156	0.0113	0.1721	1.7623
153	Aisle	0.20894	0.29627	0.0156	0.4216	0.0742	1.5534
157	Table	0.098654	0.27866	0.0057	0.001288	0	0.5269
158	Aisle	0.12998	0.16592	0.0057	0.0321	0.40543	1.2774
159	Table	0.098228	0.19752	0.0094	0.023	0.04399	2.1226
160	Aisle	0.20414	0.33375	0.0109	0.2484	0.2436	0.77597
171	Table	0.25073	0.29481	0.0068	0.07948	1.6659	1.796
172	Aisle	0.23198	0.45035	0.0156	0.0075	0.4133	0
179	Table	0.16288	0.20021	0.0057	0.0221	0.0341	0.9499
180	Aisle	0.22571	0.50629	0.0109	0.007	0.098	0.3598
181	Table	0.28424	0.28424	0.0109	0.08244	0.0309	0.8978

Erosion fluxes were calculated once the critical thresholds for erosion were overpassed. There was an absence of correlation between erosion fluxes and critical thresholds, whatever the component considered (sand, mud or chl-*a*). Such relationships are generally observed for muddy sediments, for which consolidated sediments have typical high critical thresholds. The sediment was composed of 92.6% of sand in our case and 7.4% (Chapter 2). The limit for which a mixture of sand and mud can be differentiated as cohesive or non-cohesive is of 10% (Grasso et al., 2015). The values of critical threshold for sand erosion were very low (within the range of 0.04 and 0.5 Pa), which is clearly related to an absence of resistance of these sandy beds to erosion. Surprisingly, the muddy part of the sediment matrix showed lower critical thresholds for bed erosion than sand in many cases (Tableau 9). The microphytobenthic chl *a* biomass can be clearly considered an index of epipelagic diatoms colonising the surface since we observed all along the survey the presence of typical brown patches with the brown colour of epipelagic

diatoms. Given the low mud content of these sediment beds, the biofilms of epipellic diatoms were clearly associated to very fine layers of mud (maybe boyster biodeposits), unable to influence bed erodibility. The microphytobenthic chl *a* biofilm apparently offered very low resistance to erosion in these oyster parks, since critical threshold for chl *a* erosion were always below the limit of 0.011 Pa, and they can be considered almost constant (~0.01 Pa), since they were correlated with neither with sedimentary variables, nor macrozoobenthic / microphytobenthic variables.

Linear regression models were explored for each erodability parameters (critical threshold for erosion) and erosion rates, but they only showed significant effects for the critical threshold for mud erosion (SPM) according to the following equation (p-value < 0.05; R<sup>2</sup> = 0.45):

$$\tau_{crit}(SPM) = 0.0103 \times \text{sediment pheopigments (*)} + 0.5037 \times I \text{ Brey (*)} + 0.8867$$

and the sand fluxes according to the following equation (p-value < 0.05; R<sup>2</sup> = 0.39):

$$\text{sand fluxes} = 0.0076 \times \text{sediment chl } a (*) - 0.1595.$$

No significant effects of environmental variables were found for critical thresholds for chl *a*, sand erosion, as well as SPM and chl *a* erosion rates.

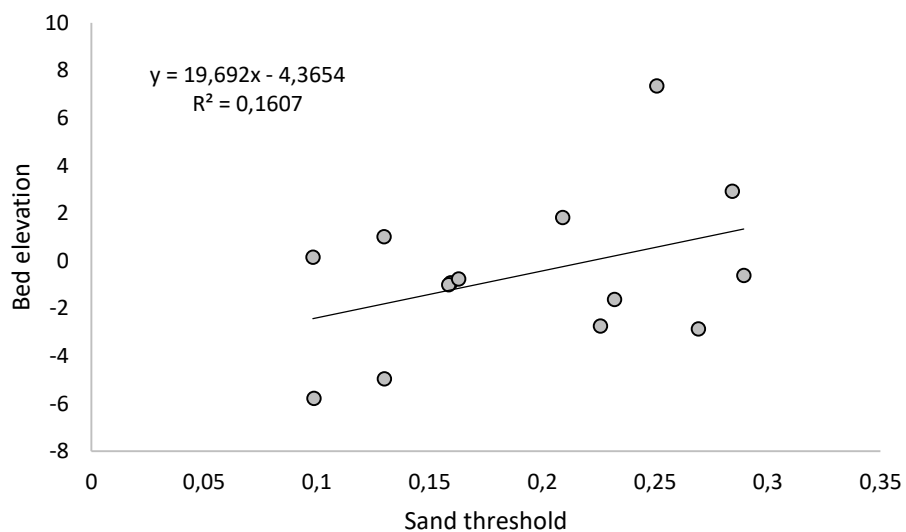


Figure 38 : Bed topography variations (mm) as a function of sand erosion threshold (Pa)

Interestingly, when searching for relationships between the sediment bed variation (ALTUS data) with erodability parameters, the only relationship that can be put in evidence was a low but significant (Pearson correlation coefficient r = 0.4, p-value < 0.05) correlation between the critical threshold for sand erosion and sediment level variation (Figure 38).

### 3.2. OsHV-1 $\mu$ Var erosion

#### *OsHV-1 in biofilm*

The first oyster spat mortalities were recorded on day 157 (Figure 23). Mortalities continued for 20 days until they were stabilized around 40% of survivors on day 180.

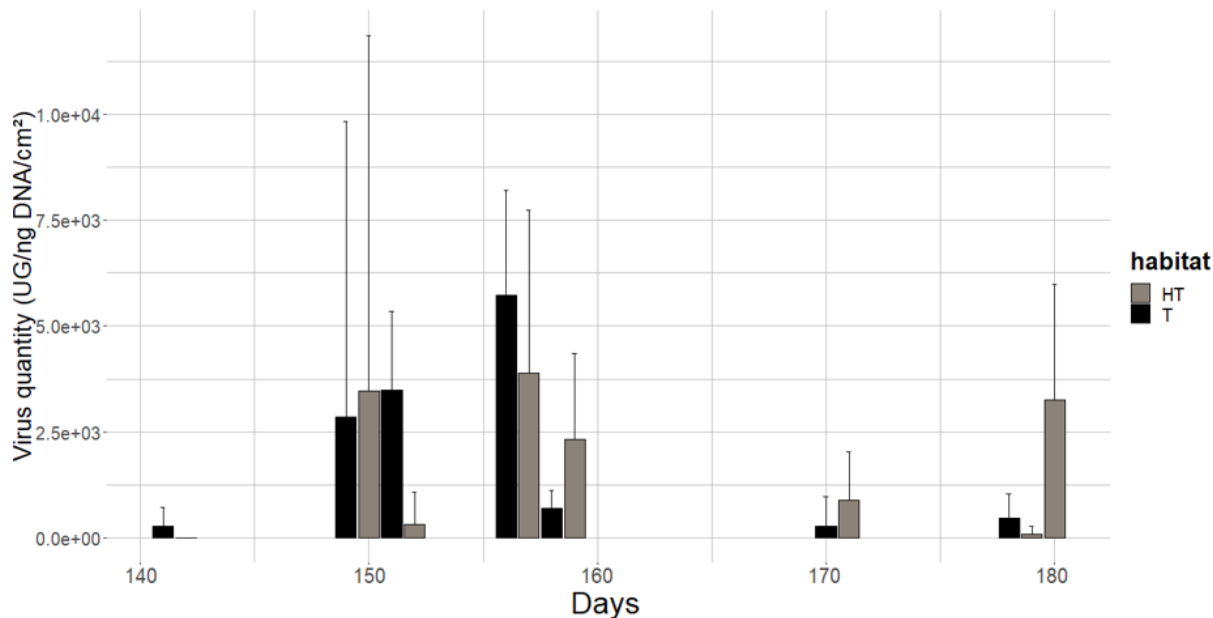


Figure 39 : OsHV-1  $\mu$ Var DNA quantities at the surface of the biofilm. Each day corresponded to an erosion experiment

When focusing on day-by-day variations of viral DNA in biofilms (Chapter 4), no significant difference in biofilm OsHV-1 DNA quantities was detected (Figure 39). On the other hand, when focusing on the period when erosion experiments were performed (groups of days 1 & 2, 9 to 12, 16 to 19, 30 and 31, 38 to 40), a significant effect of days on viral loads was observed ( $p$ -value  $<0.001$ , PERMANOVA). Indeed, an increase in viral concentration in biofilms was observed on days 9 to 12 to reach its maximum on days 16 to 19 and then decrease after the episode of mortality.

The virus concentration in the recirculating seawater were subjected to extreme variability between the 3 replicates (Table 10). This was the case even for the low current steps, when the seawater was very clear (without SPM). This may be related to a very aggregated repartition of virus in seawater that seems not to be homogenously dispersed, but related to aggregates. In fact, there a lot of zeroes in the database, revealing either a total absence of virus or values below the detection limit of the PCR measurements. When comparing the 3 replicates for different treatments, we can also describe “a law of all or nothing”. Interestingly, even for days when the biofilm concentration was low (Figure 40), there was a detected resuspension of virus from the sediment core. This was the case all along the survey.

When analysing statistical analysis on log transformed data (SplitPlot) of the OsHV-1 μVar resuspended quantities during the erodability measurements, no effect of the habitat was found (table or aisle, p-value <0.75). On the other hand, a “current step” effect (p-value <0.01, Table 10) was observed on the quantities of virus as well as an effect of days (p-value <0.01). Thus the quantities of virus were more or less important according to the date but also varied according to the intensity of current velocities. Indeed, on Figure 37 A, a peak in OsHV-1 μVar was found on the first sampled step and then OsHV-1 quantities were less important. When comparing results between erosion experiments, the virus concentration can sometimes be maximal during one the first current step, or sometimes at higher flow velocities.

For instance on day 150 (Figure 37 A, 7 days before the first mortalities), the current velocity corresponding to 5.9 cm.s<sup>-1</sup> (i.e. first step for which virus resuspension was measured) was the one with the maximum concentrations of OsHV-1 DNA and this current step also the first step for which the critical threshold for chl *a* erosion was reached (Figure 37 A). On day 153 (Figure 37 B, just before the first mortalities), 2 peaks of OsHV-1 were observed at current steps 1 and 4 (for a current velocity of 6 and 23 cm.s<sup>-1</sup>). These current steps were respectively the ones just above the critical threshold for chl *a* erosion and the one just before sand erosion. On day 180 (Figure 37C, after mortalities), the maximum of detected virus corresponded to a later step at the hight current velocity (30 cm.s<sup>-1</sup>), just before the erosion of the sand.

The order of magnitude of the maximal viral concentrations that were eroded can be expressed in GU.ng DNA-1.m<sup>-2</sup> of sediment surface (Figure 37). We can try to make a summary analysis even though tendencies are not completely clear by defining the sequence of phases:

- a) 8.10<sup>10</sup> (day 142, current step 5), 5.10<sup>10</sup> (day 143, current step 3).
- b) 1.10<sup>11</sup> (day 150, current step 1), 5.10<sup>10</sup> (day 151, current steps 1 & 5), 1.10<sup>11</sup> (day 152, current step 2), 1.10<sup>11</sup> (day 153, current steps 1 & 4), 0 (day 157), 2.10<sup>12</sup> (day 158, current step 2), 7.10<sup>13</sup> (day 159, current step 1), 7.10<sup>10</sup> (day 160, current step 1), 3.10<sup>12</sup> (day 171, current step 2).
- c) 3.10<sup>16</sup> (day 172 current step 5), 1.10<sup>12</sup> (day 179, current step 4), 3.10<sup>13</sup> (day 180, current step 4), 7.10<sup>11</sup> (day 181, current step 3).

To sum, the values reached the order of magnitude of 10<sup>10</sup> in the erodimeter and these maximums were obtained for high flow velocities for the phase A (at the beginning of the survey). For the phase B (corresponding to the period where viral DNA were maximal in the biofilm), the order of magnitude of viral DNA in erodimeter water were between 10<sup>11</sup> and 10<sup>13</sup>

(except one day with total absence of viral DNA; day 157) and the flow velocities for which this maximal were obtained were always one of the 2 lowest flow velocities (current steps 1 or 2). Finally, for the phase C (3 days after the end of last mortalities), the values were still higher with an order of magnitude between  $10^{11}$  and  $10^{16}$  and these maximum values were obtained for intermediate flow velocities (current steps of 3 or 4).

Tableau 10 : OsHV-1 concentrations at each sampling step with average +/- standard deviation below

OsHV-1 μVar (Genomic Units/L)												
Day	Habitat	Step 1 (5.92 cm. s <sup>-1</sup> )		Step 2 (9.52 cm. s <sup>-1</sup> )		Step 3 (15.51 cm. s <sup>-1</sup> )		Step 4 (22.71 cm. s <sup>-1</sup> )		Step 5 (29.90 cm. s <sup>-1</sup> )		
		Step 1	Step 2	Step 3	Step 4	Step 5	Step 1	Step 2	Step 5	Step 1	Step 2	
142	Table	2.74E+07 9.13 × 10 <sup>6</sup> ± 1.58 × 10 <sup>6</sup>	0.00E+00 0.00E+00	0.00E+00 0.00E+00	0.00E+00 0.00E+00	0.00E+00 1.21E+07	2.51E+07 1.24 × 10 <sup>7</sup> ± 1.26 × 10 <sup>7</sup>	3.65E+07 1.28 × 10 <sup>7</sup> ± 2.08 × 10 <sup>7</sup>	1.55E+06 0.00E+00	1.34E+07 2.32 × 10 <sup>7</sup> ± 2.59 × 10 <sup>7</sup>	0.00E+00 0.00E+00	5.11E+07 1.91E+07
143	Aisle	1.20E+07 9.68 × 10 <sup>6</sup> ± 6.76 × 10 <sup>6</sup>	1.45E+07 0.00E+00	1.95E+06 0.00E+00	2.42E+07 0.00E+00	4.67E+07 0.00E+00	0.00E+00 1.72E+07	1.29E+07 4.10 × 10 <sup>6</sup> ± 7.10 × 10 <sup>6</sup>	0.00E+00 0.00E+00	0.00E+00 0.00E+00	0.00E+00 0.00E+00	
150	Table	3.39E+07 4.25 × 10 <sup>7</sup> ± 4.05 × 10 <sup>7</sup>	2.40E+07 0.00E+00	1.40E+07 0.00E+00	1.75E+07 5.97 × 10 <sup>6</sup> ± 1.03 × 10 <sup>6</sup>	2.75E+07 1.32 × 10 <sup>7</sup> ± 1.38 × 10 <sup>7</sup>	0.00E+00 0.00E+00	0.00E+00 7.77 × 10 <sup>6</sup> ± 1.35 × 10 <sup>7</sup>	2.35E+07 7.77 × 10 <sup>6</sup> ± 1.35 × 10 <sup>7</sup>	0.00E+00 0.00E+00	0.00E+00 0.00E+00	
151	Aisle	0.00E+00 1.54 × 10 <sup>7</sup> ± 1.33 × 10 <sup>7</sup>	2.33E+07 0.00E+00	1.15E+07 5.75 × 10 <sup>6</sup> ± 8.13 × 10 <sup>6</sup>	2.29E+07 2.43E+07	4.02E+06 2.01 × 10 <sup>6</sup> ± 2.84 × 10 <sup>6</sup>	0.00E+00 0.00E+00	0.00E+00 3.60 × 10 <sup>6</sup> ± 6.24 × 10 <sup>6</sup>	1.03E+07 1.63 × 10 <sup>7</sup> ± 1.34 × 10 <sup>7</sup>	5.09E+06 1.63 × 10 <sup>7</sup> ± 1.34 × 10 <sup>7</sup>	1.26E+07 3.11E+07	
152	Table	0.00E+00 4.20 × 10 <sup>6</sup> ± 7.27 × 10 <sup>6</sup>	1.20E+07 0.00E+00	1.56E+07 3.45 × 10 <sup>6</sup> ± 1.91 × 10 <sup>6</sup>	2.27E+07 1.14 × 10 <sup>7</sup> ± 1.05 × 10 <sup>7</sup>	3.03E+07 1.14 × 10 <sup>7</sup> ± 1.05 × 10 <sup>7</sup>	0.00E+00 0.00E+00	0.00E+00 4.30 × 10 <sup>6</sup> ± 7.45 × 10 <sup>6</sup>	1.29E+07 6.80 × 10 <sup>6</sup> ± 7.45 × 10 <sup>6</sup>	2.04E+07 3.14 × 10 <sup>7</sup> ± 5.44 × 10 <sup>7</sup>	0.00E+00 0.00E+00	
153	Aisle	0.00E+00 4.38 × 10 <sup>6</sup> ± 3.80 × 10 <sup>6</sup>	6.32E+07 0.00E+00	0.00E+00 0.00E+00	0.00E+00 0.00E+00	0.00E+00 2.41 × 10 <sup>6</sup> ± 4.09 × 10 <sup>6</sup>	0.00E+00 2.17E+07	0.00E+00 5.03 × 10 <sup>6</sup> ± 8.72 × 10 <sup>6</sup>	0.00E+00 0.00E+00	0.00E+00 0.00E+00	0.00E+00 9.42E+07	
157	Table	0.00E+00 0.00E+00	0.00E+00 0.00E+00	0.00E+00 0.00E+00	0.00E+00 0.00E+00	0.00E+00 0.00E+00	0.00E+00 0.00E+00	0.00E+00 0.00E+00	0.00E+00 0.00E+00	0.00E+00 0.00E+00	0.00E+00 0.00E+00	
158	Aisle	0.00E+00 0.00E+00	0.00E+00 6.32E+07	0.00E+00 6.47E+10	0.00E+00 0.00E+00	0.00E+00 2.21E+09	0.00E+00 0.00E+00	0.00E+00 0.00E+00	0.00E+00 0.00E+00	0.00E+00 0.00E+00	0.00E+00 0.00E+00	
159	Table	0.00E+00 2.16 × 10 <sup>6</sup> ± 3.73 × 10 <sup>6</sup>	6.32E+07 0.00E+00	0.00E+00 0.00E+00	0.00E+00 0.00E+00	0.00E+00 0.00E+00	0.00E+00 4.50E+07	0.00E+00 1.43 × 10 <sup>7</sup> ± 2.48 × 10 <sup>7</sup>	0.00E+00 0.00E+00	0.00E+00 0.00E+00	0.00E+00 0.00E+00	
160	Aisle	6.23E+07 2.09 × 10 <sup>7</sup> ± 3.63 × 10 <sup>7</sup>	0.00E+00 0.00E+00	0.00E+00 0.00E+00	0.00E+00 0.00E+00	0.00E+00 0.00E+00	0.00E+00 0.00E+00	0.00E+00 0.00E+00	2.55E+07 8.53 × 10 <sup>6</sup> ± 1.48 × 10 <sup>7</sup>	0.00E+00 0.00E+00	0.00E+00 0.00E+00	
171	Table	0.00E+00 0.00E+00	0.00E+00 4.29 × 10 <sup>6</sup> ± 3.75 × 10 <sup>6</sup>	5.71E+07 0.00E+00	2.23E+09 7.79 × 10 <sup>6</sup> ± 1.30 × 10 <sup>6</sup>	0.00E+00 0.00E+00	0.00E+00 0.00E+00	0.00E+00 0.00E+00	0.00E+00 0.00E+00	1.97E+07 1.52 × 10 <sup>7</sup> ± 6.43 × 10 <sup>6</sup>	1.06E+07 1.06E+07	
172	Aisle	6.47E+10 3.24 × 10 <sup>10</sup> ± 4.57 × 10 <sup>10</sup>	5.65E+07 4.17E+07	3.53E+07 9.92 × 10 <sup>6</sup> ± 1.09 × 10 <sup>6</sup>	2.25E+08 0.00E+00	1.26E+08 1.57E+08	3.60E+07 9.43 × 10 <sup>7</sup> ± 8.32 × 10 <sup>7</sup>	3.54E+07 2.38 × 10 <sup>7</sup> ± 2.06 × 10 <sup>7</sup>	0.00E+00 0.00E+00	7.23E+07 3.76 × 10 <sup>7</sup> ± 4.91 × 10 <sup>7</sup>	2.69E+13 2.69E+13	
179	Table	6.93E+07 3.67 × 10 <sup>7</sup> ± 3.21 × 10 <sup>7</sup>	0.00E+00 5.00E+00	5.95E+07 4.17E+07	6.14E+07 3.51E+07	9.25E+06 0.00E+00	2.79E+08 9.61 × 10 <sup>7</sup> ± 1.58 × 10 <sup>8</sup>	1.24E+09 4.42 × 10 <sup>8</sup> ± 6.92 × 10 <sup>8</sup>	0.00E+00 0.00E+00	7.41E+07 2.47 × 10 <sup>7</sup> ± 4.28 × 10 <sup>7</sup>	0.00E+00 0.00E+00	
180	Aisle	5.95E+07 3.67 × 10 <sup>7</sup> ± 3.21 × 10 <sup>7</sup>	0.00E+00 5.00E+00	5.00E+07 4.17E+07	5.00E+07 2.96 × 10 <sup>7</sup> ± 2.58 × 10 <sup>7</sup>	3.68 × 10 <sup>7</sup> ± 3.62 × 10 <sup>7</sup>	3.80E+07 3.68 × 10 <sup>7</sup> ± 3.62 × 10 <sup>7</sup>	7.34E+07 2.40E+10	0.00E+00 0.00E+00	6.65E+07 3.44 × 10 <sup>7</sup> ± 3.33 × 10 <sup>7</sup>	3.67E+07 3.44 × 10 <sup>7</sup> ± 3.33 × 10 <sup>7</sup>	

## 4. Discussion

### *Bed levels variations and erosion*

Erosion rates were calculated, once the critical thresholds for erosion were crossed. High levels were observed for erosion fluxes of sand erosion as well the critical thresholds. This feature reveals that the category of sediment transport cannot be really considered as non-cohesive, even if the fine sand proportion is very high. This must be related to the grain size of the sand which were very low (very fine sand) in the present case, and also the presence of mud even if the value were not high (~7.3%). In literature about the mixture of sand and mud (Van Ledden et al., 2004; Le Hir et al., 2011; Ubertini, 2015; Grasso et al., 2015), the limit of 10% of mud content is often given to differentiate cohesive and non-cohesive sediments. Above this limit, the critical threshold increase with mud content. In the present study, despite the high sand proportion, the regime seems cohesive. This could be a feature of sandflats covered by oyster farms, since the sediment matrix seemed relatively compact and softly enriched in muddy biodeposits, but also subject to additional biostabilising mechanisms (see next paragraph of the discussion). In this oyster farms, there is a very high density of tractors circulating between oyster tables every day (even during neap-tide periods). This anthropologic stress must strongly impact and consolidate the sand matrix. The erosive forces required to initiate sand motion were strong and the sand matrix was eroded only at high bed shear stress, corresponding to current velocities of  $\sim 0.3 \text{ m.s}^{-1}$ . So, once the critical thresholds for erosion were overpassed, the erosion rates were also very important, compared to uncompacted sand transport. A correlation was observed between the variations of topographic level (ALTUS) and critical thresholds for sand erosion, whereas there was no relation with tidal water height. The sediment showed a very dominant sand proportion (92.7%), so that variations in sedimentary elevation could be explained rather by the erodibility of sand than by hydrodynamic stress, since no relationship with tidal water height was observed (this variable being considered to reflect the tidal current flow rates). Our results suggest that if the hydrodynamic forcing is limited, the sediment is not resuspended for these sediments. In this oyster park, the tables could have a physical effect by decreasing drag forces on hydrodynamics (Kervella et al., 2010) and the fact of having reduced bed shear stress could explain why there is an absence of influence on sedimentary topography. Indeed, the tables could dampen the incidence of currents and waves favoring a slight siltation as confirmed by the good development of microphytobenthic biofilms (Chapter 2). Erodibility dynamics can thus induce morphosedimentary spatio-temporal variations ( $\tau_{\text{crit}}$ ) more than the bed shear stress ( $\tau$ ).

Surprisingly, the critical threshold for sand erosion were often higher than the ones for mud erosion. Moreover, the values for  $\tau_{\text{crit}}$  for mud erosion seemed not correlated to topography variations. This is very particular since the mud content is generally the factor driving the best erodability dynamics. In fact, the factors explaining the variations of bed erodability of our samples were not the sedimentary parameters.

The linear regression models were obtained from multiple regression tests, to identify the most explanatory variables for each erodability parameters ( $\tau_{\text{crit}}$  and erosion fluxes). This analysis indicated that the critical threshold for mud erosion was related to pheopigment percentage and  $I_{\text{Brey}}$ . This index reflects a general metabolic activity and integrates both the effect of biomass and temperature that affects the total metabolism (respiratory) of the total macrozoobenthic community (Brey, 2010). This observation supports the hypothesis that the contribution of bioturbators to sediment resuspension is directly related to their metabolic and activity rate, rather than to their presence, biovolume or spatial density (Cozzoli et al., 2018). Nevertheless, these authors reported a destabilising effects of the faunal bioturbators on intertidal mudflats. When analysing our data, the conclusion is exactly opposite, since we found a positive effect of the faunal index  $I_{\text{Brey}}$  with the index of bed resistance to erosion. This relationship could reflect an action of surface bioturbation with a positive effect on the critical thresholds as already seen for annelids in laboratory experiments with the gallery-dweller *Hediste diversicolor* (Passarelli et al., 2012, Orvain et al., 2018) and on intertidal sandflats of the Bay of Seine sand flats under the BARBES project (Orvain et al., 2018).

The pheopigment percentages were also positively related to mud erosion threshold. This variable is the direct reflect of grazing intensity by deposit-feeders (Cartaxana et al., 2003; Orvain et al., 2014b, 2018). This observation could be related to the biostabilization process exerted by the fauna of annelids, which are grazers of microphytobenthic biofilms. This result confirms the already described relationship with the macrofaunal total metabolism ( $I_{\text{Brey}}$ ), but this could also be related to the accumulation of oyster bioposits, which must be also especially enriched in pheopigments too. The macrozoobenthic community under these oyster parks are strongly impacted by oyster production, with a proportion of annelid worms at very high densities on a sandflat. The long-term history of macrozoobenthic communities of this site clearly indicated a trend with an increase in the total biomass for 4 decades and a shift in dominance by annelid worms, while this sediment habitat was colonised by high densities of bivalves and amphipods before the installation of oyster parks (Dubois et al., 2007a; Sylvand, 1995).

During this monitoring, the succession of the type of eroded particles was common at each sampling date and comparable to what is conventionally observed (Dupuy et al., 2014; Orvain et al., 2004). In fact, the chlorophyll particles were first eroded, then the sediment. The microphytobenthic chl *a* is resuspended first, in relation to intense surface grazing activities (Orvain et al., 2007, 2014a). There is also a potential resuspension of virus if they are associated to microphytobenthic cells.

#### *Resuspension of OsHV-1 DNA*

There is obviously a problem with virus DNA detection in sediment, biofilms but also in the seawater samples in the erodimeter. The detection of the virus in samples containing sedimentary particles represents a particular difficulty because of the PCR inhibitors contained in the sediments. In the biofilm, there are still a lot of particles that can pose technical problems. The soil kit used in our study improves the yield and limits the impact of PCR inhibitors found on fine particles. But in the water of the erodimeter (initially sterile), we found high levels of virus released from the sediment, sometimes at the 1<sup>st</sup> or 2<sup>nd</sup> flow level. The values were very variable and we can even see in detail that replicates with strong values and others with a total absence of viruses. Beyond the detection problems associated with PCR techniques for samples with sedimentary particles, this undoubtedly shows that the virus is not homogeneously distributed in the water after erosion. Thus it would probably not be a simple diffusion, but rather an association with aggregates of microphytobenthic origin (only particles eroded at this stage). Indeed, there was virtually no GU in the biofilm a few days before its important detection. Thus, a sudden occurrence of purely benthic origin and related to sedimentary dynamics seems less likely than global contamination of the ecosystem. It would be more likely that nearby oyster spats would have suffered mortalities before those observed in this study and could have released virus in the environment. One of the question was: is the virus released in the water column by a simple diffusion? The answer is clearly “No”, because a diffusion mechanism would have led to a constantly increasing value gradient without abrupt peak in the erodimeter. The concentrations would have been high for the first measurements at low flow velocity. Viral DNA seems to be actively resuspended rather than simply diffused and their release of viral DNA requires an initial erosion of surficial sediments. Thus, the distribution and transmission of OsHV-1 in natural seawater might reflect attachment to some form of particulate matter, either abiotic or biotic (Paul-Pont et al., 2013).

The amounts of OsHV-1 μVar DNA in the biofilm were detected at the beginning of this follow-up, but at low concentrations. Higher viral DNA were reported in the biofilm later (days 150-

153), 1 week before the first oyster spat mortalities, which began on day 157. The concentrations of virus DNA then decreased in the biofilm during the second part of the survey.

Thus, two hypotheses may explain this detection of OsHV-1 μVar in the biofilm, ie (i) the biofilm was contaminated by OsHV-1 GU globally present in the oyster environment and/or (ii) the biofilm is an active vector promoting the emergence of OsHV-1 in the environment. In the chapter 4, and basing our analysis on virus concentration in biofilms, we concluded that the second hypothesis seemed less likely (see the conclusion in Chapter 4). However, when regarding the resuspension of viral DNA in the erodimeter water, an amount of associated virus seemed to be associated to the resuspension biofilm (chl *a*) of the biofilm. The microphytobenthic fraction (chl *a*) was always the first one to be resuspended, before sand and mud.

During phase B (from days 150 to 171) which coincided with the period of prior mortality (before day 157) and until the end of the mortality episode (day 170), there was important OsHV-1 μVar quantities (order of magnitude of  $10^{10}$  to  $10^{13}$ ) in the erodimeter and the maximal resuspension of virus was observed at the 1<sup>st</sup> step (flow velocity of  $6 \text{ cm.s}^{-1}$ ) or the 2<sup>nd</sup> one (flow velocity of  $6 \text{ cm.s}^{-1}$ ). Indeed, the virus seems to be eroded during the first stages with chl *a* and thus with the microphytobenthic biofilm. The OsHV-1 virus appeared to be resuspended also later (high flow velocities) and there must be also a viral contamination of the sediment fraction (mud or sand). So, we may suggest that, when the biofilm was well developed and contaminated by virus (or at least viral DNA) on the site, the release of virus in the water occurred at the beginning of erosion experiments, for the 1<sup>st</sup> or 2<sup>nd</sup> flow velocity. So, even if the flow rates were low in the field during the period prior mortality and until the last recorded mortalities, the maximal quantities of virus were easily resuspended in relation with biofilm erosion, since the maximum water concentration of viral DNA were found when the critical threshold for chl *a* erosion was overpassed. Absolutely no sediment was eroded for such flow velocities. The development of a microphytobenthic biofilm seems thus to be a relevant relay accumulating, aggregating and easily resuspending virus and this must be a transmission agent playing a role in the epizooty episode.

During other periods (A & C), when the biofilms were less contaminated by viruses (phase A and C), we can find some resuspended virus in the recirculating water of the erodimeter, but high flow velocities were required to resuspend them, since the maximal values of viral concentrations were found at high bed shear stresses, corresponding to the critical thresholds

for bed erosion (sand or mud). During the last period of the survey (phase C), the highest virus concentrations were found in the erodimeter ( $10^{16}$  on day 172 for instance), and the highest value was observed for the highest current step (5<sup>th</sup>) corresponding to a flow velocity of 30 cm.s<sup>-1</sup>. The critical thresholds for sand and mud erosion were overpassed at such flow velocity. There was a decrease in DNA concentration in the erodimeter at the end of the survey (days 180 & 181) and the maximal viral concentration were obtained for intermediate flow velocities, corresponding to the initiation of sand erosion. The role of a specific macrozoobenthic community that shifted to a dominance of tube dwellers like *Tubificoides benedii* and *Capitellidae* in very high densities (Chapter 4) can be a factor explaining the high viral resuspension rates for the last days of the survey, since they seem to contribute to the increase of bed resistance to erosion.

## 5. Conclusion

Sediments of the oyster beds in the bay des Veys are very rich in sand but are very resistant to erosion, and can be defined as cohesive sediments. This relative resistance can come from various factors, such as compaction caused by a regular pass of tractors, and a fauna 100% dominated by tube-eating annelids consuming microphytobenthic biofilms but acting in synergy with these microalgae in terms of bioadhesion associated with substances of biological origin (Extracellular Polymeric Substances, mucus). The topographic dynamics of elevation observed *in situ* appeared to be more related to variations in erodibility than hydrodynamic stress, which is in any case particularly reduced in oyster beds. The virus appeared to be released into the water by an erosion process rather than diffusion. During the week preceding the first mortalities, the virus released in the water was detectable in large quantities and easily eroded. Thus, OsHV-1 could be linked to the biofilm because its resuspension is not related to the sediment but rather with the biofilm. Such erosion can take place every day because weak currents are sufficient for its resuspension. On the other hand, sediment erosion outside these periods of mortality or infection required higher current velocities, and maximum viral concentrations were obtained in these cases for high current velocities (beyond erosion critical thresholds) related to sediment erosion (sand or mud).

## Acknowledgments

We would like to specially thank André-Gilles Taillepied and his team who kindly lend us the oyster table and a wide space in its building to store our material and do our experiments. Thanks to C. Rakotomala, C. Mallet, F. Pernet, C. Lelong, C. Roger, B. Adeline and M-P.

Dubos for their help on the field. Thanks to G. Sourimant for their help on data treatment and to J. Rocchietta. I am grateful to the Ministère de l'Enseignement supérieur et de la Recherche for this PhD grant.





## **Chapitre 6 : Synthèse générale, discussion et conclusion**



## Caractérisation de l'environnement benthique ostréicole à l'échelle de la table à huître: conséquences sur le microphytobenthos, la macrofaune et l'érodabilité du sédiment

### *Caractéristiques environnementales benthiques*

L'envasement induit par la biodéposition et les tables à huîtres n'a pas affecté la structuration à mésoéchelle de l'habitat benthique. En effet, pour une grande majorité de paramètres environnementaux (granulométrie du sédiment, nutriments) aucune différence n'était observée en fonction de l'habitat observé : table ou allée. Les courants marins peuvent favoriser la dispersion des biodépôts d'huîtres (Chamberlain, 2001; Hayakawa, 2001), atténuant ainsi l'impact local à petite échelle de la biodéposition d'huîtres sur la dynamique des sédiments. Néanmoins, une augmentation de la teneur en matière organique était observée sous les tables à huîtres lorsque la hauteur d'eau augmentait. De plus une teneur en eau du sédiment plus importante était observée sous la table à huître. La granulométrie du sédiment joue sur la rétention d'eau. En effet, des sédiments plus fins, vont limiter la perméabilité du sédiment comparé à un sédiment plus grossier (Murray, 1977), se traduisant ainsi par une teneur en eau supérieure. Aucune différence significative en terme de taille des particules sédimentaires n'était observée en fonction de l'habitat et du temps. Ainsi la teneur en eau supérieure apparente était liée à un autre facteur : la présence directe des poches sur les tables à huîtres ou à leurs effets indirects sur les biofilms microphytobenthique ou la faune benthique. Les poches contenant les huîtres ainsi que les macroalgues se développant sur les tables à huîtres vont retenir l'eau qui va s'écouler petit à petit vers le sédiment lors de la marée basse, représentant ainsi un apport d'eau exclusif limitant la dessication. En plus de ces caractéristiques environnementales, la table à huîtres atténue la lumière et de la température à la surface du sédiment. Ces résultats ont révélé le rôle tampon exercé par la table à huîtres. En revanche, l'habitat allée apparaît comme étant plus vulnérable aux stress environnementaux liés au cycle des marées et aux paramètres météorologiques. Globalement, les caractéristiques sédimentaires et la matière organique ne semblent pas jouer un rôle structurant sur la différence d'habitat entre la table et l'allée.

*Impact des conditions environnementales sur le microphytobenthos et la macrofaune benthique*

La table à huîtres présente des caractéristiques environnementales particulières avec pour conséquences principales une atténuation de la lumière et des températures ainsi que des apports en matière organique réguliers en conséquence de l'activité de biodéposition des bivalves cultivés. Ainsi l'habitat benthique situé sous la table à huître apparaît moins sujets aux variations brutales et donc plus tamponné. Certaines caractéristiques ne différaient pas à l'échelle de table mais reflétaient les caractéristiques du parc à huîtres de la baie des Veys (Orvain et al., 2012; Ubertini et al., 2012).

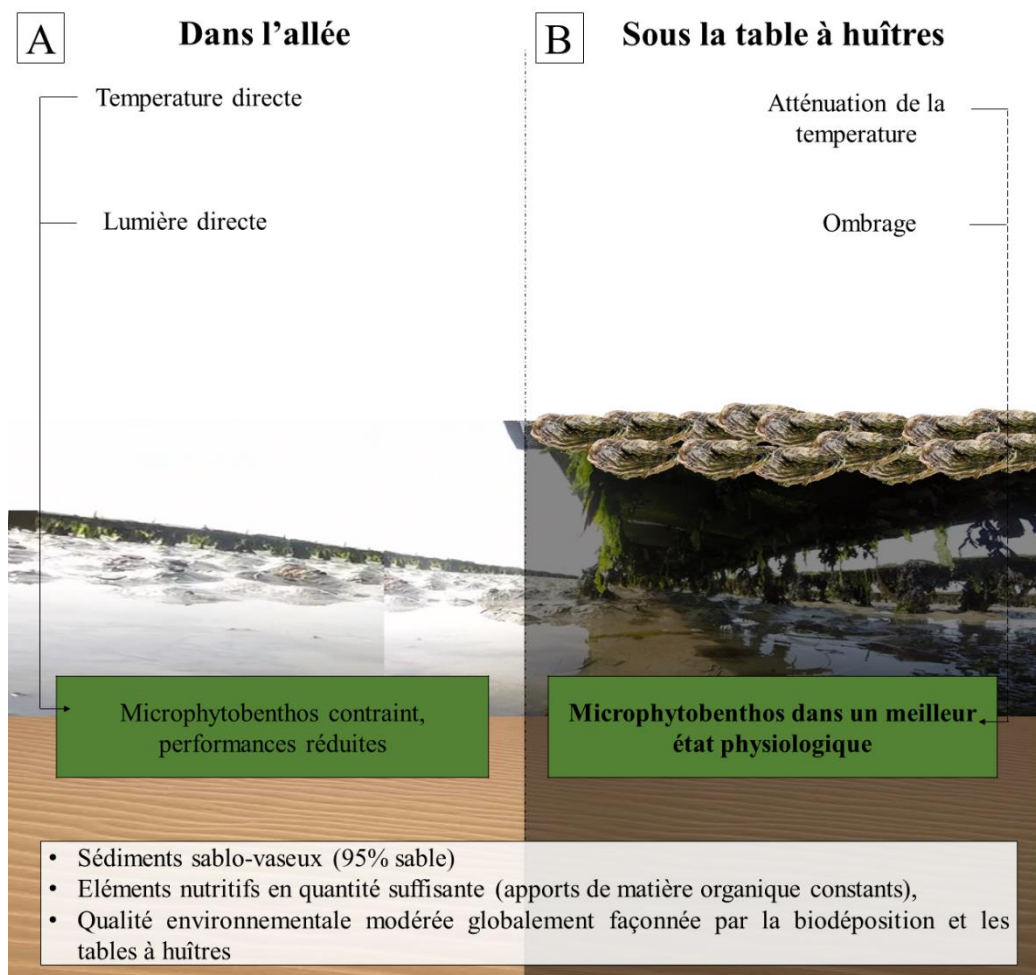


Figure 40 : Synthèse des résultats obtenus au chapitre 2.

La table à huîtres jouait sur la température et la lumière atteignant la surface du sédiment (Figure 40). Ces deux paramètres sont ceux qui limitent le plus la production primaire du microphytobenthos (Barranguet et al., 1998). Ainsi la classification des facteurs régulant la croissance du MPB montre que la température est le facteur principal. Cette observation confirme que la thermoinhibition est le principal facteur régulant le microphytobenthos en été (Pomeroy, 1959; Savelli et al., 2018). Dans une moindre mesure une photoinhibition a

également pu nuire au MPB lors de notre étude, il apparaît que ce facteur peut être inhibiteur du développement microphytobenthique (Cartaxana et al., 2013; Savelli et al., 2018). Les diatomées benthiques possèdent en effet des moyens efficaces pour faire face aux fortes intensités lumineuses (Falkowski, 1984; Lavaud et al., 2007; Serôdio et al., 2008; Perkins et al., 2010; Cartaxana et al., 2013). Associées au sédiment à forte dominance sableuse, les diatomées auront tendance à être de type épipsamiques (Round, 1971). Les diatomées épipsamiques ne peuvent en revanche éviter l'intensité lumineuse par la migration en raison de leur mobilité réduite (et donc de celle de la production d'EPS). Ces microalgues pourront mettre en œuvre des stratégies physiologiques telles que le cycle de la xanthophylle induite par la photoinhibition (Cartaxana et al., 2011, 2013), ce qui entraîne une détérioration des paramètres photosynthétiques (Du et al., 2018) comme observé dans l'allée. Ainsi, l'habitat table à huîtres apparaît comme propice à la prolifération des biofilms microphytobenthiques alors que dans les allées, les fortes intensités lumineuses et températures diminuraient les performances photobiologiques du MPB. Néanmoins dans les deux habitats d'importantes quantités de chl *a* étaient observées traduisant une biomasse microphytobenthique satisfaisante. Cependant, malgré la forte proportion de sable, les biofilms microphytobenthiques sur ces parcs à huîtres sont bien ceux de microalgues épipélique, et cela et certainement lié à des fines couches de vases fines en surface des sables. Le rôle de la biodéposition stimulant les microalgues épipélique dans ce parc à huître de la baie des Veus sont déjà bien décrits (Orvain et al., 2012; Ubertini et al., 2012) ainsi que dans d'autres écosystèmes avec bivalves comme les huîtres (Echappé et al., 2018) ou les moules (Engel et al., 2017).

Dans une moindre mesure, la composition du sédiment et la biochimie connexe (fraction organique et recyclage de l'azote) semblait jouer un rôle moindre sur la production primaire du MPB et son état physiologique avec un sédiment de type sablo-vaseux (93% de sable), des apports en matière organique dans influence locale de la présence des tables à huître. Ainsi l'environnement benthique des parcs à huîtres permet l'établissement de biofilms microphytobenthiques globalement bien présents (apport de chl *a*). Néanmoins ces caractéristiques environnementales benthiques caractéristiques des parcs à huîtres vont structurer les communautés macrozoobenthiques. Bien que la structuration de l'environnement benthique induite par les tables à huîtres et l'activité de biodéposition des huîtres façonnent l'environnement à l'échelle du parc à huîtres (Ubertini et al., 2012), les caractéristiques environnementales benthiques à l'échelle de la table vont également structurer les communautés macrozoobenthiques (Dubois et al., 2007a). La qualité écologique de

l'environnement ostréicole a été étudiée en utilisant des indices basés sur la diversité du macrozoobenthos. La macrofaune benthique est considérée comme un bon indicateur biologique de la qualité des écosystèmes côtiers (Dauvin, 2007; Dutertre et al., 2013). Cette diversité macrozoobenthique est régulièrement mesurée pour évaluer la qualité des écosystèmes marins notamment dans le cadre de la directive-cadre pour la stratégie-cadre pour le milieu marin (DCSMM) I (biodiversité) et de la directive cadre sur l'eau (DCE, Directive 2000/60/CE).

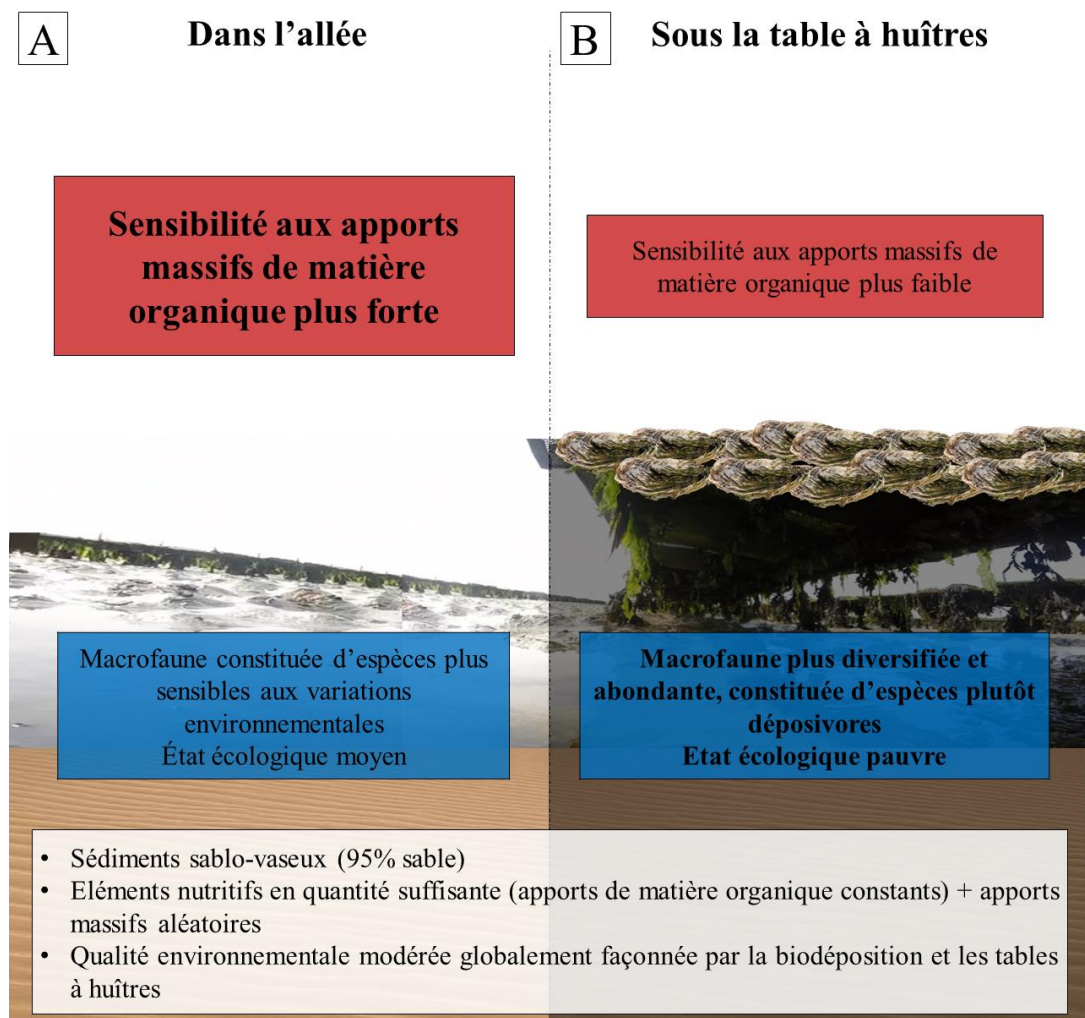


Figure 41 : Facteurs structurants la macrofaune benthique à l'échelle de la table à huîtres

De manière générale, les assemblages de macrofaune benthique observés étaient plus diversifiés et plus abondants sous la table à huîtres que dans l'allée (Figure 41). Ainsi, basé sur l'indice AMBI, une différence des communautés benthiques était observable selon l'habitat. Ainsi l'allée abritait principalement des espèces du groupe fonctionnel II (non affectées par un léger enrichissement en matière organique) et du groupe III (qui tolèrent l'enrichissement en matière organique), tandis que davantage d'espèces du groupe V (espèces très opportunistes caractéristiques des environnements perturbés) étaient observées sous la table à huîtres. L'habitat

table semblait être dans un mauvais état écologique au long du suivi. En effet, sous les tables une dominance des espèces telles que *Capitella capitata* et *Tubificoides benedii* constitutives du groupe V était observée.

#### *Erodabilité du compartiment sédimentaire*

Lors du flot, différents types de particules benthiques peuvent être remises en suspension. Cette remise en suspension peut être facilitée ou limitée en fonction de deux paramètres principaux : (i) l'intensité de la contrainte de cisaillement tidale et (ii) de la cohésion des sédiments (Blanchard et al., 1997; Joensuu et al., 2018; Murray, 1977). La composition sédimentaire sablo-vaseuse (95% sable) observée dans les 2 habitats présente potentiellement une vulnérabilité à l'érosion tidale accrue comparé à un sédiment davantage vaseux qui résistera mieux du fait de la cohésion de ces particules fines (Murray, 1977). Un paramètre supplémentaire jouant sur la cohésion des sédiments est la quantité de substances extracellulaires polymériques (EPS). Ces EPS constituent une matrice cohésive 3D (Stal and de Brouwer, 2003; Tolhurst et al., 2002; Yallop et al., 1994). Aucune différence significative n'était observée concernant ces substances extracellulaires polymériques qui présentaient des concentrations relativement faibles. Ces quantités d'EPS limitées pourraient, au même titre que la dominance sableuse du sédiment, favoriser l'érosion tidale. La macrofaune semble jouer un rôle majeur dans la remise en suspension des particules benthiques. Le calcul de taux d'activité métabolique appliqués à l'ensemble de la communauté macrozoobenthique montrent bien un effet global de la bioturbation sur l'érodabilité. En revanche, les résultats montrent plutôt un effet biostabilisateur et non déstabilisateurs. Certaines espèces macrozoobenthiques秘ètent également un mucus (Storch and Welsch, 1972; Alain et al., 2002) pouvant avoir des propriétés voisines des substances polymériques extracellulaires, favorisant ainsi la cohésion sédimentaire (Passarelli et al., 2012). Ainsi certains facteurs vont faciliter une érosion des particules sédimentaires (sediment sableux, EPS en faibles quantités, activité de bioturbation) alors que d'autres vont plutôt la diminuer (teneur en eau supérieure sous la table, EPS d'origine macrozoobenthique).

Dans le contexte des mortalités de naissains d'huîtres, cette remise en suspension des particules benthiques va pouvoir potentiellement influer sur la dynamique environnementale de OsHV-1 μVar de deux façons: (i) en cas d'une source de OsHV-1 μVar environnementale benthique, cela faciliterait sa filtration par les huîtres, et (ii) après l'épisode de mortalité, le virus sédimenté va pouvoir être érodé et se disperser dans l'environnement. Cette deuxième option ne confirmerait pas l'hypothèse selon laquelle l'habitat table à huîtres favoriserait la perséverence

du virus dans l'environnement ostréicole. De plus, les faibles quantités d'EPS, et le caractère majoritairement sableux du sédiment iraient dans le même sens avec un rôle protecteur limité. En revanche, l'atténuation des rayons UV associés à l'intensité lumineuse sous la table à huîtres pourrait limiter la dégradation des particules virales d'OsHV-1  $\mu$ Var, même si l'ADN viral est toujours détectable. Il est possible que les virus sous les tables restent plus facilement actifs qu'entre les tables.

## Dynamique environnementale de OsHV-1 $\mu$ Var et conséquences des mortalités de naissains d'huîtres

### *Mortalités d'huîtres et ses conséquences*

Les mortalités d'huîtres peuvent indirectement représenter une pollution de par l'apport de matière organique lorsqu'une grande quantité de naissains succombe à OsHV-1  $\mu$ Var à l'échelle du parc ostréicole. Cet apport de matière organique va notamment déséquilibrer le statut trophique de l'écosystème et ainsi changer les caractéristiques environnementales sédimentaires. En conséquence, la macrofaune benthique semblait avoir été altérée par les mortalités d'huîtres mais dans une plus grande mesure par un échouage de macroalgues. Néanmoins, globalement le statut écologique de l'habitat ostréicole se dégrada lors de l'épisode de mortalité et de manière plus intense dans l'habitat allée. En effet, sous la table à huîtres la macrofaune benthique traduit déjà une légère eutrophisation. Ainsi cette tendance globale à l'eutrophisation peut également jouer en défaveur de la survie de *C. gigas* face à OsHV-1  $\mu$ Var. Lors de l'épisode de mortalité, la macrofaune benthique a bien été en contact avec OsHV-1 témoignant de l'épisode de mortalité. En revanche, il semble peu probable que la macrofaune benthique soit un réservoir et/ou une source de virus sur le long terme. Les espèces nécrophages semblent avoir des grandes quantités de virus dans leurs tissus à la fin des périodes de mortalité.

Concernant la relation OsHV-1  $\mu$ Var et naissains d'huîtres, une relation de dose d'OsHV-1 et réponse (mortalité) a déjà été identifiée (Paul-Pont et al., 2015). Dans notre cas, la dose minimale qui semblait provoquer des mortalités était au seuil de  $10^5$  UG.ng ADN. Bien que les unités ne soient pas similaires, à titre comparatif Whittington et al. (2018) constataient que les charges virales de plus de 80% des individus morts dépassaient  $10^4$  copies d'ADN/mg de tissu. Ainsi, lors de notre suivi, les individus n'ayant pas atteint le seuil léthal de  $10^5$  UG.ng ADN<sup>-1</sup> auraient survécu car la dose n'aurait pas été atteinte (Whittington et al., 2018). En cas de survie, les naissains huîtres seraient capables d'éliminer partiellement OsHV-1 de leurs tissus, bien

qu'une partie du pool de virus puisse persévéérer dans les tissus des bivalves expliquant qu'il puisse être encore détecté chez des individus de *C. gigas* adultes (Arzul et al., 2002).

Néanmoins, lors du processus d'infection par OsHV-1 μVar, un largage de particules virales dans l'eau se produit lors de la mort des bivalves (Evans et al., 2015; Paul-Pont et al., 2015; Schikorski et al., 2011) et avant même l'apparition des premières mortalités (Paul-Pont et al., 2015). Ainsi il est probable qu'une transmission horizontale d'OsHV-1 se propage entre individus (Thrusfield, 2007; Webb et al., 2005) par adsorption du virus à des particules (Evans et al., 2015; Whittington et al., 2015a). Ainsi les particules ingérées pour la nutrition de *C. gigas* peuvent représenter un vecteur de transmission de OsHV-1 (Paul-Pont et al., 2013; Evans et al., 2014, 2015; Whittington et al., 2018). En revanche, sous forme libre il semblerait que l'intégrité des particules virales soit atteinte après 48 heures (Evans et al., 2015).

#### *Dynamique environnementale*

Les particules en suspension potentiellement porteuses de OsHV-1 μVar (Evans et al., 2015) pourront à terme sédimenter vers l'habitat benthique. Ainsi cet habitat pourrait représenter un puits à virus et à l'inverse une source. Lors du suivi des quantités d'ADN de OsHV-1 μVar à la surface du sédiment dans les biofilms microphytobentiques, une quantité importante d'ADN viral était observé avant les premières mortalités. Puis, ces quantités d'ADN de OsHV-1 étaient maximales lors des premières mortalités de naissains de *C. gigas*. Le virus est donc bien présent dans l'environnement et les particules représentent un vecteur de OsHV-1 facilitant les fortes concentrations virales à proximité des naissains d'huîtres. En effet lors de nos expérimentations d'érodimétrie des quantités de virus importantes étaient remises en suspension. Ainsi les biofilms microphytobentiques pourraient bien représenter un vecteur de transmissions d'OsHV-1 μVar. Néanmoins, à long terme la persistence du virus viable dans le biofilm pendant longtemps apparaît peu probable. En effet, malgré d'importantes quantités d'EPS, les quantités de virus diminuèrent dans le biofilm au cours du temps dans notre étude malgré d'importantes quantités d'ADN viral retrouvées en hiver (VIAPSE CRH ; 2014). À une échelle journalière, OsHV-1 μVar est détectable dans les biofilm microphytobentiques en été durant une brève période. En dehors de cette période les quantités observées étaient très faibles ce qui explique qu'il soit difficilement détectable à cette période (VIAPSE CRH ; 2014). Néanmoins il est probable que le virus ait été érodé (comme observé en érodimétrie) et transféré par advection des masses d'eau ce qui pourrait potentiellement contaminer d'autres bassins ostréicoles. Toutefois, le processus de transmission du virus dans l'environnement marin dépend en grande partie de la connectivité entre les écosystèmes estuariens (Roughan et al., 2011; Pernet et al.,

2018; Gangnery et al., 2019). Le rôle des facteurs physiques doit encore être exploré afin de mieux mettre en évidence les agents de transmission de ce pathogène. Il faudrait également réussir à prouver la virulence de cet ADN viral observé en grande quantité dans les biofilms et dans l'eau de l'érodimètre.

La réponse du macrozoobenthos à la mortalité des naissains d'huîtres a également été étudiée. En effet, ces organismes vont être impactés de manière directe par la pollution organique et de manière indirecte par des changements des caractéristiques de leur habitat. La charge virale en OsHV-1  $\mu$ Var des organismes constitutifs de la macrofaune analysée a permis d'identifier des vecteurs de ce pathogène à court terme avec surtout les espèces nécrophages, mais la piste d'une source virale macrozoobenthique paraît peu probable (parmi les espèces étudiées). Cependant, les assemblages de macrozoobenthos ont évolué de manière massive à partir de la matière organique (d'abord les mortalités d'huîtres mais surtout un échouage de macroalgues) causée par la dégradation de l'habitat benthique dégradant milieu par eutrophisation.

#### *Naissains d'huîtres, OsHV-1 $\mu$ Var et ressource nutritive*

Chez les naissains d'huîtres, les ressources énergétiques seraient principalement mobilisées pour la croissance, un processus qui requiert d'importants besoins énergétiques. Ces réserves énergétiques pourraient être limitées chez les naissains par rapport aux adultes (Rico-Villa et al., 2010). Une diminution du risque de mortalité est observé chez les naissains présentant des réserves d'énergie suffisantes (Pernet et al., 2014). Ces réserves d'énergie sont en particulier établies à partir de la ressource nutritive de *C. gigas* : les particules chlorophyliennes (phytoplancton et microphytobenthos) dont l'abondance limite les risques de mortalités liés à OsHV-1  $\mu$ Var (Gangnery et al., 2019). *A contrario*, d'autres études soutiennent l'hypothèse que les huîtres bien nourries et en pleine croissance pourraient succomber à une infection à OsHV-1  $\mu$ Var alors que les huîtres non nourries ne le seraient pas (Evans et al., 2015; Whittington et al., 2015b). Ainsi des observations contradictoires semblent apparaître, mais il semblerait qu'un état intermédiaire soit la situation la plus menaçante pour la survie naissains d'huîtres dans un contexte d'infection par OsHV-1  $\mu$ Var.

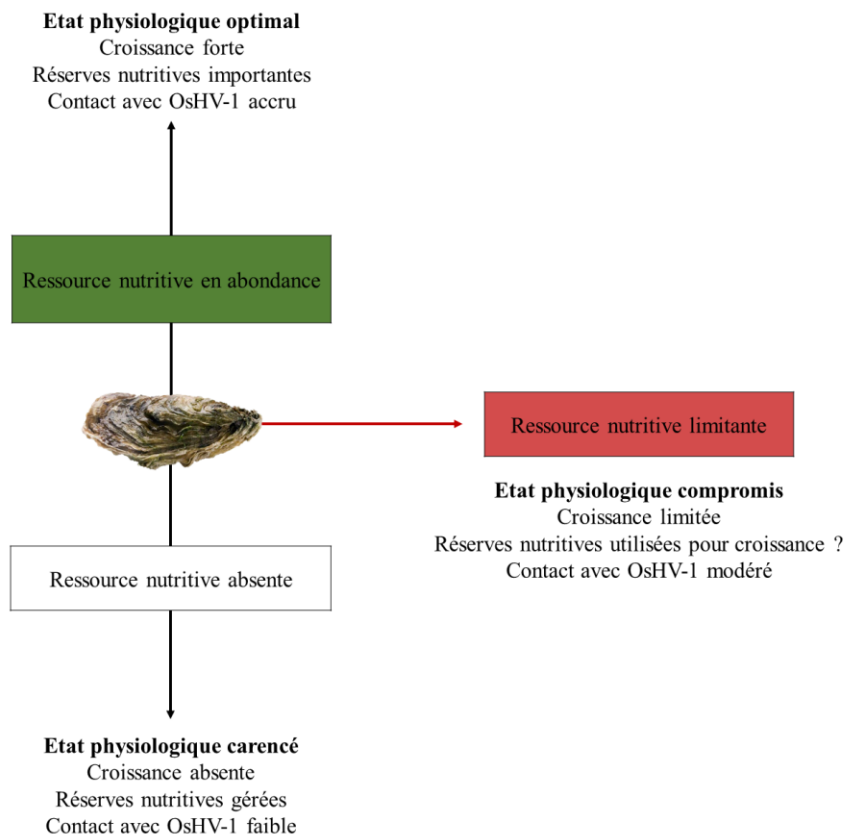


Figure 42 : Hypothèses sur la résistance des huîtres à OsHV-1 μVar en lien avec les caractéristiques environnementales

Dans le cas où la ressource nutritive chlorophylienne (phytoplankton et microphytobenthos) est non limitante (Figure 42), les individus de *C. gigas* juvéniles pourraient théoriquement utiliser cette ressource pour la croissance somatique sans avoir recours à leurs réserves énergétiques. Dans le cas où ces réserves seraient utilisées, les naissains pourraient également capables de rapidement les restaurer. Ainsi dans cette situation, le métabolisme des huîtres serait à son optimum malgré un risque de rencontre (par voie trophique) accru avec OsHV-1 μVar disponible dans l'environnement. En effet, une infection à OsHV-1 peut être contractée à cause l'ingestion de virus adsorbé à des particules en suspension (Evans et al., 2015) et nos résultats suggèrent que les diatomées microphytobenthiques représenteraient un bon candidat en facilitant l'accumulation de virus dans des biofilms et en facilitant son érosion précoce. A l'inverse, lorsque la ressource nutritive est absente et le taux de clairance faible (Figure 42), les huîtres entreraient dans un métabolisme ralenti afin de conserver leur énergie. La croissance de l'organisme se retrouverait alors arrêtée afin de mieux gérer ses réserves nutritives. En l'absence de filtration le risque de contact avec OsHV-1 μVar et sa réPLICATION seraient diminués. Le cas théorique le plus problématique pour la survie des naissains de *C. gigas* face à OsHV-1 μVar serait une situation intermédiaire avec un accès limité à la ressource nutritive (Figure 42) et en particulier une raréfaction les apports alimentaires après une croissance rapide.

En effet, les huîtres se retrouveraient dans un état physiologique compromis avec un apport nutritif compromis réduisant la croissance qui serait la principale dépense d'énergie pour le bivalve juvénile. Ainsi les réserves énergétiques pourraient être utilisées pour la croissance et dans un contexte d'infection virale, les naissains ne disposeraient pas des réserves suffisantes nécessaires à leur survie (Pernet et al., 2014) en privilégiant une allocation d'énergie à la croissance. De plus, du fait de leur activité de filtration les huîtres seraient communément en contact avec OsHV-1 μVar disponible dans l'environnement. En parallèle, l'âge et la taille des naissains d'huître ainsi que le stade de maturation doit également jouer un rôle important dans ce processus (Hick et al., 2018). Une expérience en laboratoire pourrait permettre d'apporter plus de réponses sur ces hypothèses avec des bivalves mis en bassin. Des naissains d'huîtres pourraient être alimentés, puis mis à jeûn et mis en contact avec OsHV-1 μVar pendant la croissance ou après. En parallèle certains individus pourraient subir le même processus sans arrêter l'alimentation et d'autres n'avoir aucune alimentation de tout le suivi mais être mis en contact avec le virus. Les mortalités et les charges virales individuelles pourraient être suivies.

## Conclusion générale

La table à huîtres structurait l'habitat en atténuant principalement la lumière, la température et la dessication du sédiment. Ces caractéristiques favorisaient de bonnes performances photosynthétiques du microphytobenthos sous les tables à huîtres alors que, dans les allées, la photobiologie du MPB semblait être altérée mais tout de même fonctionnelle car d'importantes concentrations de chl *a* étaient observées dans le 1<sup>er</sup> centimètre de sédiment. L'analyse des indicateurs macrozoobenthiques montre une sensibilité du milieu à une eutrophisation (enrichissement en matière organique). L'état écologique des habitats benthiques s'est globalement dégradé, d'abord en réponse à l'épisode de mortalités des naissains d'huîtres (début Juin) puis, suite à un échouage de macroalgues (fin Juin). L'abondance macrozoobenthique a largement augmenté au cours du mois de Juin en montrant un déséquilibre et une dominance d'espèces opportunistes et dépositoires qui tolèrent d'importantes quantités de matière organique. Les premières mortalités de naissains d'huîtres semblaient se produire lorsque le seuil de 10<sup>5</sup> Unités génomiques.ng d'ADN était dépassé dans les chairs d'huîtres. Après l'épisode de mortalités, les huîtres survivantes semblaient capables d'éliminer en grande partie OsHV-1 de leurs tissus. Lors des expérimentations d'érodimétrie, le virus semblait être libéré dans l'eau par un processus d'érosion plutôt que par diffusion. Au cours de la semaine précédant les premières mortalités, le virus dans le biolfilm puis libéré dans l'eau était détectable en grande quantité et s'érodaient facilement avec des courants faibles (entre 5 et 9 cm.s<sup>-1</sup>). Ainsi,

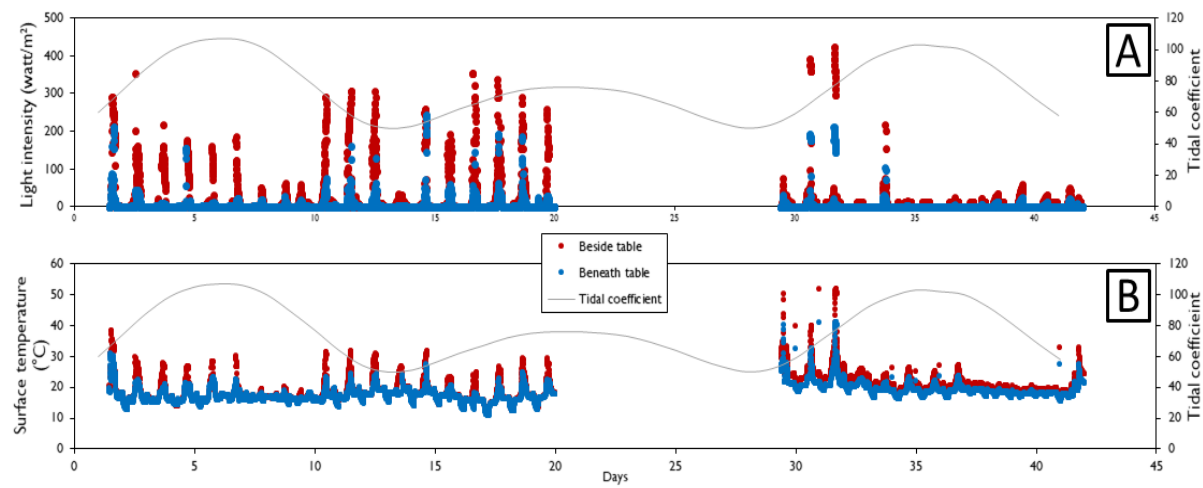
OsHV-1 pourrait être lié au biofilm microphytobenthique dont la remise en suspension était précoce. Selon les jours, ce premier pic de remise en suspension du virus pouvait être suivi ou non d'un second pic lié à une érosion sédimentaire. En dehors de la crise de mortalité, le virus était uniquement remis en suspension avec des courants élevés ( $\sim 30 \text{ cm.s}^{-1}$ ) et en lien avec le sédiment. Le biofilm s'est avéré être porteur de OsHV-1  $\mu$ Var et pourrait ainsi représenter un vecteur potentiel de propagation du virus dans l'environnement.

En extrapolant dans le contexte du réchauffement climatique, avec une augmentation moyenne de  $2^\circ\text{C}$  d'ici 2100 (ou plus selon le GIEC), l'irradiation solaire et la température pourraient devenir encore plus préjudiciables à la production estivale du MPB et donc affecter la dynamique environnementale associée de OsHV-1  $\mu$ Var. Des expérimentations traitant de cet impact climatique pourraient être réalisées en laboratoire. De plus, un enjeu majeur serait de tester la virulence de OsHV-1  $\mu$ Var retrouvé à la surface des biofilms microphytobenthiques. Des tests expérimentaux ont déjà été réalisés mais il s'avère difficile d'isoler le virus d'une matrice sédimentaire et de le concentrer à des doses létales pour les naissains d'huîtres. Une alternative pourrait être d'induire une remise en suspension du virus dans l'eau en érodimétrie à partir de sédiment naturel.



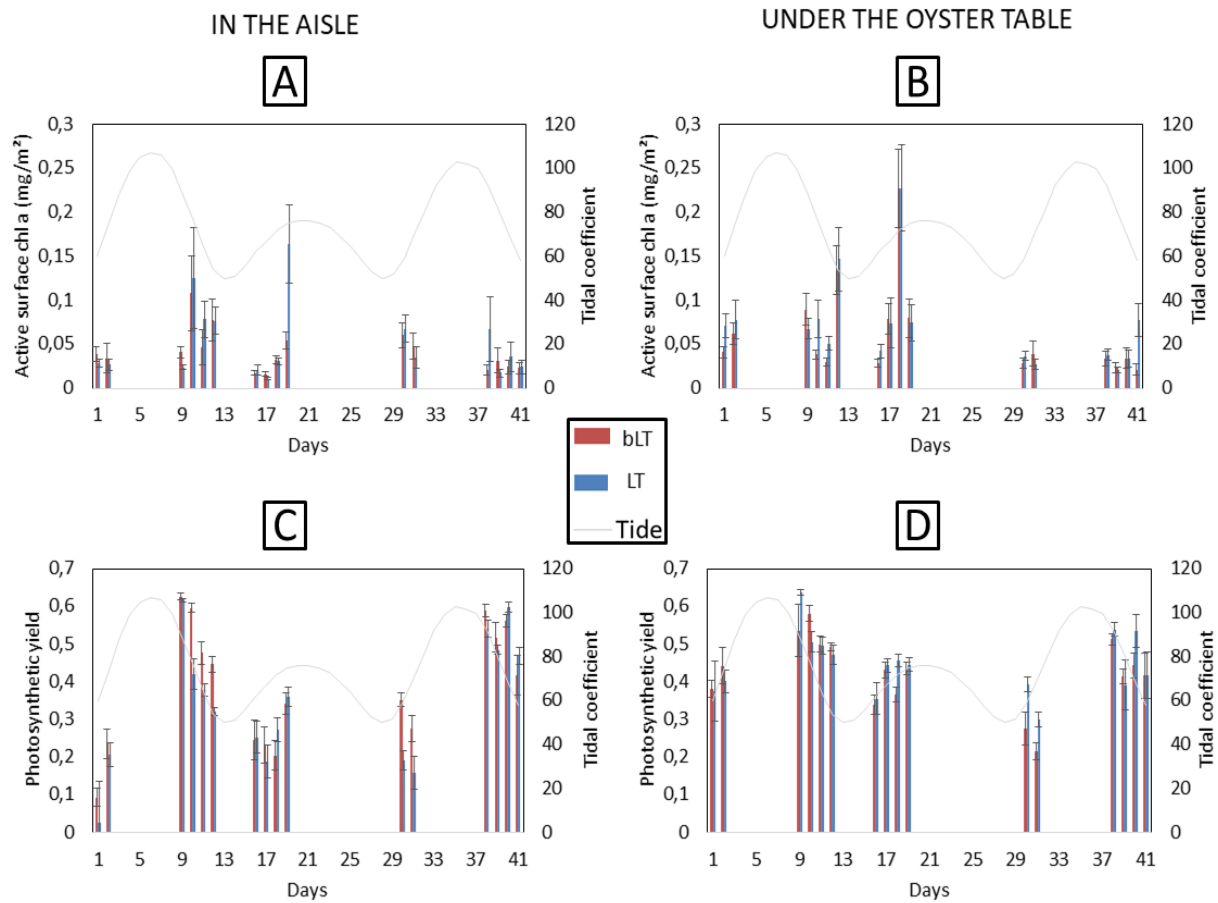
# **Annexes**





Appendix 1: Daily dynamics of surface light intensity (watt.m<sup>2</sup>) (A) and in sediment surface temperature (°C) (B)

Surface light intensity (SLI; appendix 1 A.) and sediment surface temperature (SST; Appendix 1 B.) were lower under the oyster table than in the aisle (next to the table) and the amplitude of daily variations followed the same pattern. Indeed SLI and SST showed a certain correlation together ( $r = 0.37$ ). The attenuation of the SLI caused by the shading effect (e.g. by the oyster table and/or clouds) can be very sudden. This feature could explain the medium correlation ( $r = 0.48$ ) observed between the oyster table and the aisle, in terms of SLI. In contrast, SST showed a higher correlation coefficient ( $r = 0.88$ ) between the oyster table and the aisle. SST may vary in response to shading, but very progressively and hence more slowly. Any attenuation of temperature caused by shading is less sudden than light and appears to be more buffered. The results observed for SLI and SST both highlight the buffering role of the oyster table.



Appendix 2: Daily dynamics of active surface chl a in the aisle (A), of active surface chl a under the oyster table (B). Photosynthetic yield in the aisle (C). Photosynthetic yield under the oyster table (D).

Active surface chl *a* in the aisle (Appendix 2. A.) was on average lower ( $0.048 \pm 14.15 \text{ mg/m}^2$ ) than under the oyster table (Appendix 2. B;  $0.070 \pm 14.94 \text{ mg/m}^2$ ). On the other hand, the variation between the beginning of the emersion period (bLT) and the low tide (LT) was the same in the two habitats with an increase of  $0.010 \pm 0.025 \text{ mg/m}^2$  chl *a*. Thus, in both habitats, the increase could indicate growth of microphytobenthos (MPB). No satisfactory correlation was found between active surface chl *a* and maximum water height (MWH).

A notable correlation ( $r = 0.47$ ) was found between photosynthetic yield (PY) and MWH both under the oyster table and in the aisle. Thus PY seemed to be linked to the tide and MWH. In the aisle (Appendix 2. C.) on days 10, 11, 12, 29, and 30, the photosynthetic yield of MPB observed at low tide (LT) was lower than at the beginning of the emersion period (bLT). So a decrease in photosynthetic yield was observed in this bare habitat. Conversely, under the oyster table (Appendix 2. D.) the PY was stable and sometimes (on days 9, 29 & 30) underwent minor increases. These results may reveal inhibition of PY particularly in the aisle that are less

impaired by light stress under the oyster table. Photosynthetic yield also increased with an increase in the tidal coefficient (period from neap tides to spring tides) under the oyster table.

## Appendix 3 : Lyophylization for improving the quantification of Ostreid herpesvirus-1 in seawater

### Introduction

Since its first description (Segarra et al., 2010a), the detection of OsHV-1 in the environment represents a major challenge in the management of oyster ecosystems. Although detection techniques for this pathogen in oyster spat are now well established, its quantification in the water column remains difficult. Indeed, the majority of available OsHV-1 viral load data are obtained in oyster spat where these concentrations can reach very high values (up to  $10^8$  DNA copy.mg<sup>-1</sup> wet tissue (Pernet et al., 2012)) due to viral replication in the host. Outside of the host, the quantification of OsHV-1 represents a different exercise because these large amounts of virus are diluted. Indeed seawater could act in the horizontal transmission of OsHV-1 (Sauvage et al., 2009) leading to its diffusion into the environment. Nevertheless, very little is known about the fate of OsHV-1 in the environment. Thereby, a method has been proposed by Evans et al. (2014) consisting of a centrifugation of  $1000 \times g$  for 20 minutes. Although this method presents satisfactory results for the detection of OsHV-1 in a qualitative way, a protocol to accurately quantify OsHV-1 in water remains to be defined, especially by separating particles where virus can be adsorbed (seston, phytoplankton) and seawater. This appendix aims to describe a potential protocol in this purpose. Knowing that OsHV-1 has a tendency to adsorb to particles in suspension (Evans et al., 2014; Paul-Pont et al., 2013), we tried to concentrate this pathogen according to different particles : OsHV-1 in seawater with no special particles (except particles  $<0.2 \mu\text{m}$ ), (ii) OsHV-1 with sediment particles and (iii) OsHV-1 with diatoms. Diatoms were studied because they secrete extracellular polymeric substances (EPS) through their mobility process (Edgar, 1983; Edgar and Pickett-Heaps, 1983). These EPS mainly consist of carbohydrates, proteins but also polysaccharides (Decho, 2000), proteoglycans and lipids (Chiovitti et al., 2004; Underwood et al., 2004; Pierre et al., 2010). In addition to their cell surface, the EPS secreted by diatoms could increase the adsorption of exogenous particles. In parallel we tested the concentration of DNA in seawater by a method of lyophilization.

### Material & method

#### *Experiment*

An OsHV-1 suspension was made from previously infected oyster spat. Oyster flesh was crushed and filtered on successive porosity of  $5 \mu\text{m}$ ,  $1.2 \mu\text{m}$ ,  $0.45 \mu\text{m}$  then  $0.2 \mu\text{m}$  in order to

remove macro-debris. The OsHV-1 load of this viral suspension was quantified according to the protocol detailed in the concerned paragraph. For the centrifugation concentration method three conditions of concentration were tested: (i) seawater with an OsHV-1 load of  $1.10^7$  UG/ $\mu$ L, (ii) seawater with an OsHV-1 load of  $1.10^7$  UG/ $\mu$ L containing 50 mg of sediment and (iii) seawater with an OsHV-1 load of  $1.10^7$  UG/ $\mu$ L containing 0.015  $\mu$ g of diatoms (species: *Phaeodactylum sp*). All conditions tested were subject to a 30 min rotation at 40 rpm in the dark and left to settle during another 30 min. Two centrifugation speeds were tested : (i) as Evans et al. (2014)  $1000 \times g$  for 20 min and (ii)  $3000 \times g$  for 20 min both in 15 mL polypropylene tubes (Falcon). For the freeze-dry concentration method, 1.5 mL frozen samples were freeze-dried overnight in Eppendorf tubes and then resuspended in 200  $\mu$ L of sterile seawater (0.2  $\mu$ m filtered) before extracting and purifying DNA.

#### *OsHV-1 quantification*

DNA was extracted and purified via NucleoSpin® 96 Soil Kit (Macherey-Nagel). OsHV-1 was quantified via real-time qPCR CFX 96™ C1000™ (Biorad) according to a routine protocol (Pepin et al., 2008).

#### *Data analysis*

Permanova were performed in order to spot differences between treatments (seawater, sediment, diatoms) and between conditions (pellet or supernatant).

## **Results**

#### *Centrifugation*

No significant difference depending on the speed of centrifugation was observed for all conditions tested (Figure 1). Nevertheless, a higher OsHV-1 load was observed in the pellet than in the supernatant for seawater ( $p$ -value = 0.05 ; PERMANOVA) and sediment ( $p$ -value = 0.001. PERMANOVA) conditions.. Viral loads for the diatom condition did not differ significantly according to the analyzed part or the centrifugation speed ( $8.44.10^5 \pm SD 0.9.10^5$ ). Indeed, about 75% of the initial concentration in the pellet was detected with seawater (and 1000 rpm), about 60% with the sediment (1000 rpm), but which is detected only 20% of the viral load with diatoms, with about half contained in the supernatant this time)

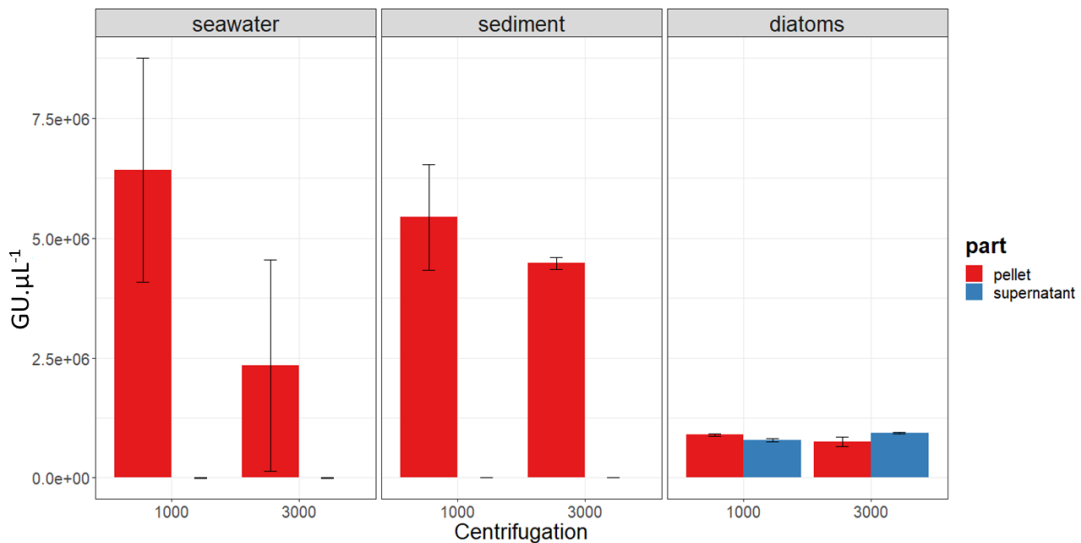


Figure 1: results of centrifugations tested. Genomic Units per  $\mu L$

### *Lyophilization*

OsHV-1 freeze-dried samples showed the same order of magnitude than before lyophilization whatever the initial concentration (**Erreur ! Source du renvoi introuvable.**).

Tableau 1 : Genomic units of OsHV-1 quantified via qPCR after lyophilization

Initial OsHV-1 concentration (GU. $\mu L^{-1}$ )	OsVH-1 genomic units after lyophilization (GU. $\mu L^{-1}$ )
$10^6$	$4.69 \cdot 10^6 \pm SD 0.9 \cdot 10^6$
$10^7$	$3.05 \cdot 10^7 \pm SD 0.1 \cdot 10^7$

### **Discussion**

#### *Centrifugation*

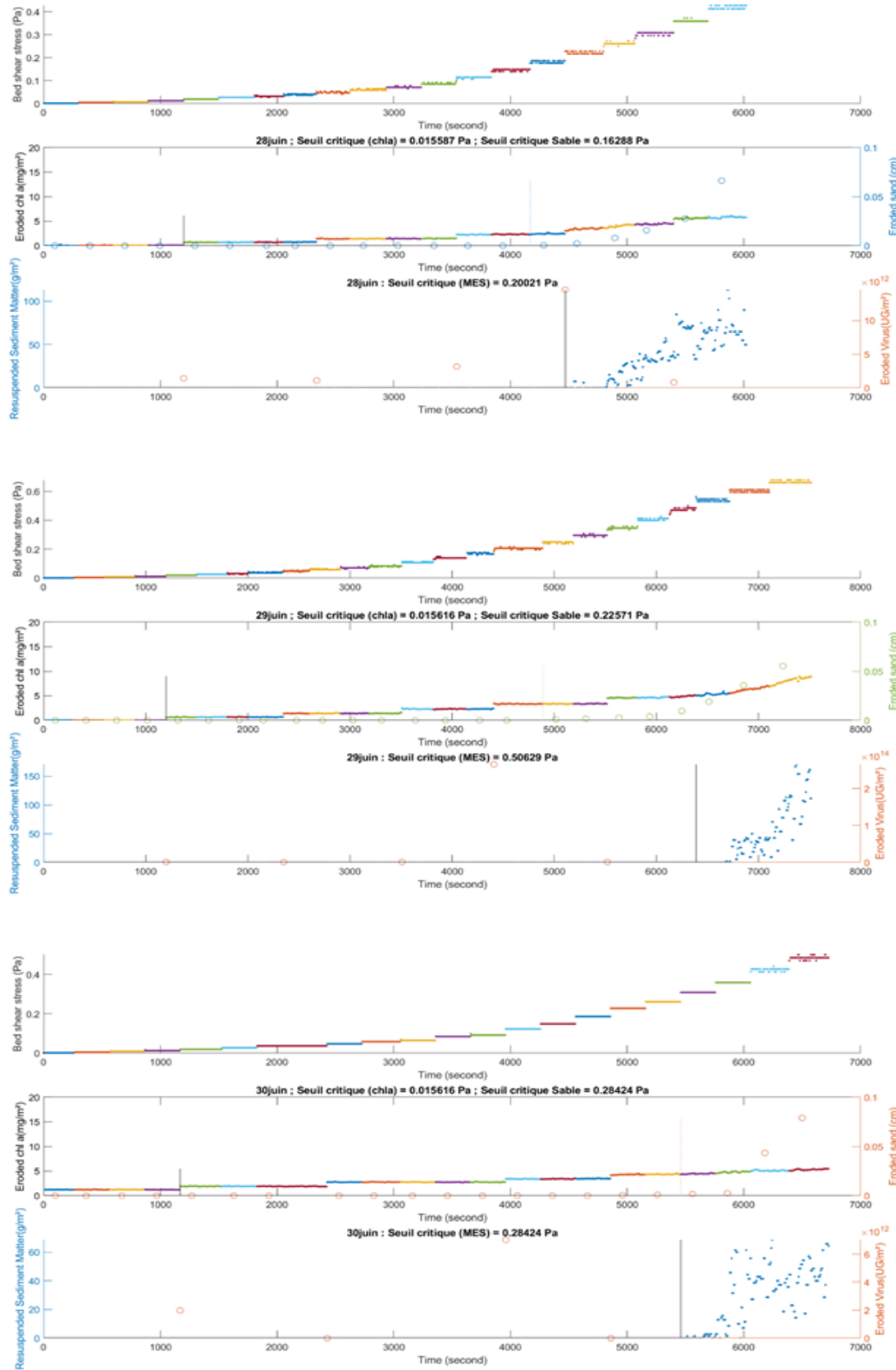
A higher viral load was observed in the pellet compared to the supernatant, regardless of the centrifugation speed. Indeed, the centrifugation speed does not seem to influence the viral load detected in the pellet because no effect was detected according to this factor. The particle size does not seem to increase the detection of the virus in the pellet. In fact, the same amount of virus was observed in the sediment condition (particles  $> 0.2 \mu m$ ) as in the condition (particles  $< 0.2 \mu m$ ). Thus the method proposed by Evans et al. (2014) seems satisfactory in order to increase the detection of OsHV-1 in seawater. Nevertheless, the quantification of OsHV-1 remains unsatisfactory by using a centrifugation method because it lacks precision. Indeed, focusing on the viral load of the pellet (although negligible according to our results) is eclipsed. In addition, it seems difficult to reduce the viral load of the metered pellet against a unit volume.

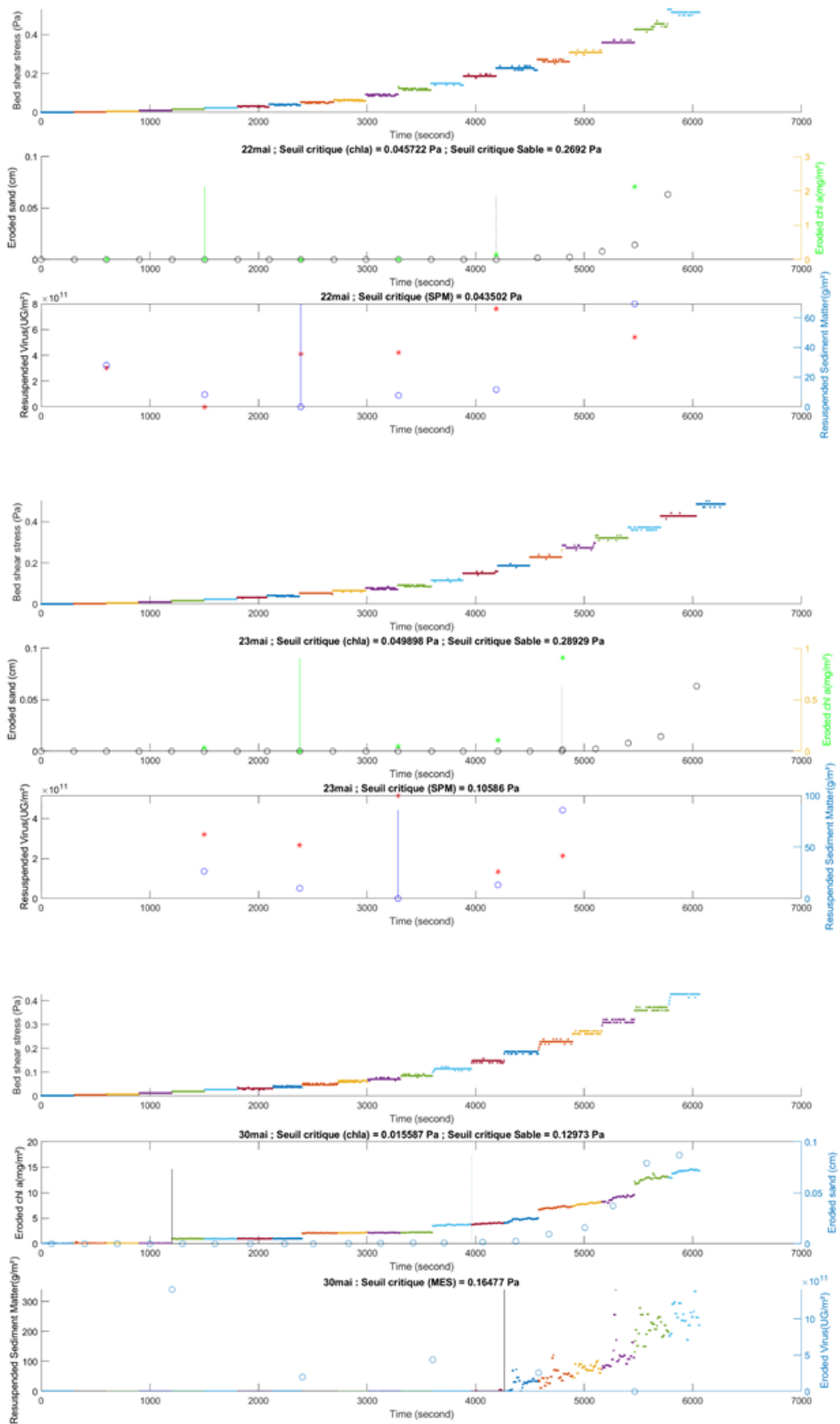
One of the main interests of assaying the amount of OsHV-1 per unit volume would be to relate this data to the filtration rate of oysters. This relationship could be useful for management tools. OsHV-1 loads with the diatoms conditions showed no difference according to the quantified part (pellet *versus* supernatant). The presence of diatoms, completely changes the location of the virus after centrifugation. It is exclusively present with the pellet after centrifugation in seawater with or without sediment, but very present in the supernatant with diatoms. EPS are known to act as a gel with a high adsorptive potential. EPSs consist of different residual, bound and colloidal fractions (Pierre et al., 2012). The colloidal EPS are the loosest and easily excreted in the seawater medium which could explain that a large amount of OsHV-1 is observed in the supernatant because the centrifugation rate is not sufficient to sediment the colloidal EPS loaded with OsHV-1 DNA. This could also be a result of a OsHV-1 degradation due to the adhesive properties of EPS and especially polysaccharides (Flemming and Wingender, 2010; Xiao and Zheng, 2016). Colloidal EPS have been already identified as a gel matrix very efficient to sequester microorganisms (Decho, 2000) and EPS of diatoms seems to act a protective microenvironment where viral DNA is very concentrated. However, it is difficult to know if the extracted DNA relates to infectious virus at this stage.

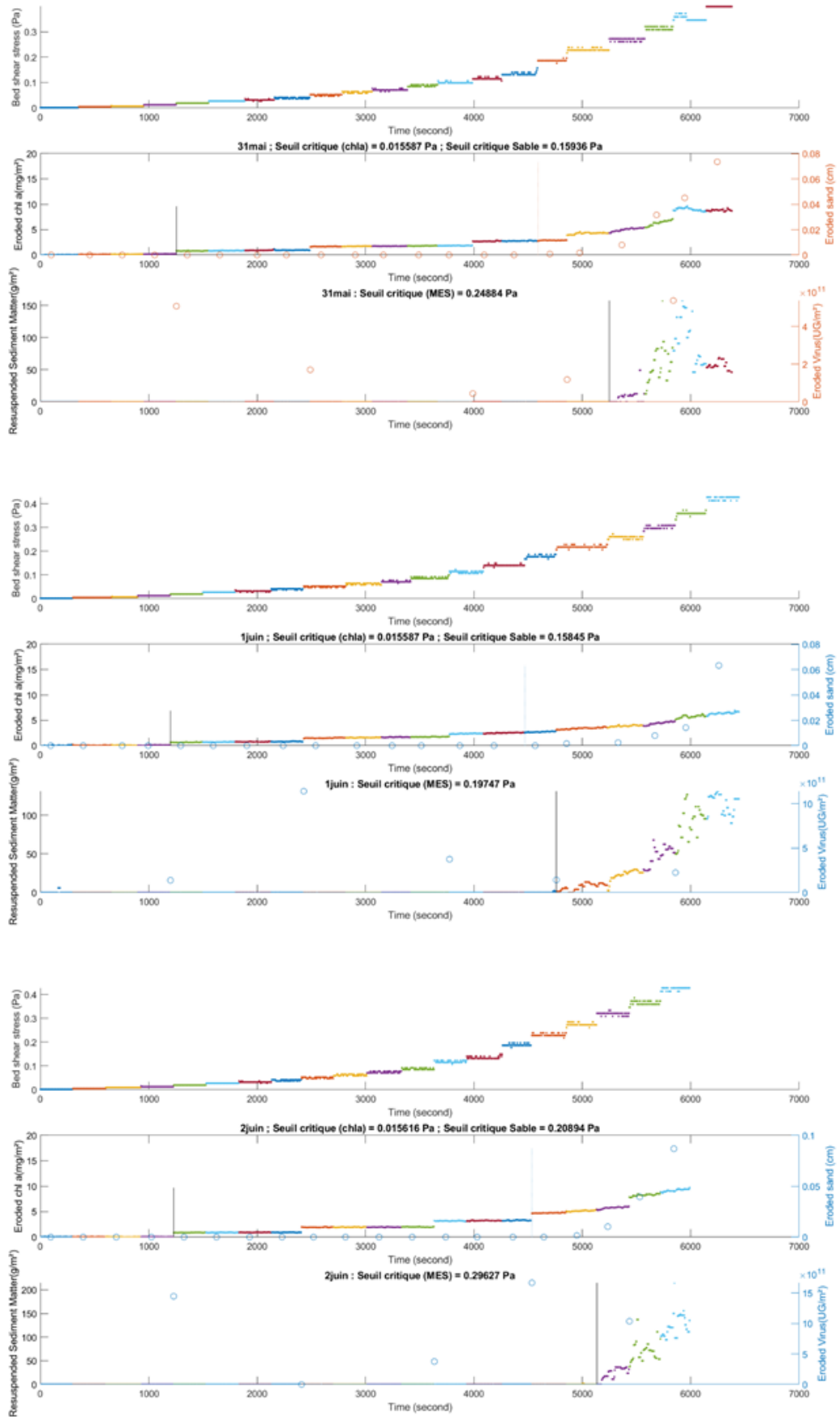
#### *Freeze-drying*

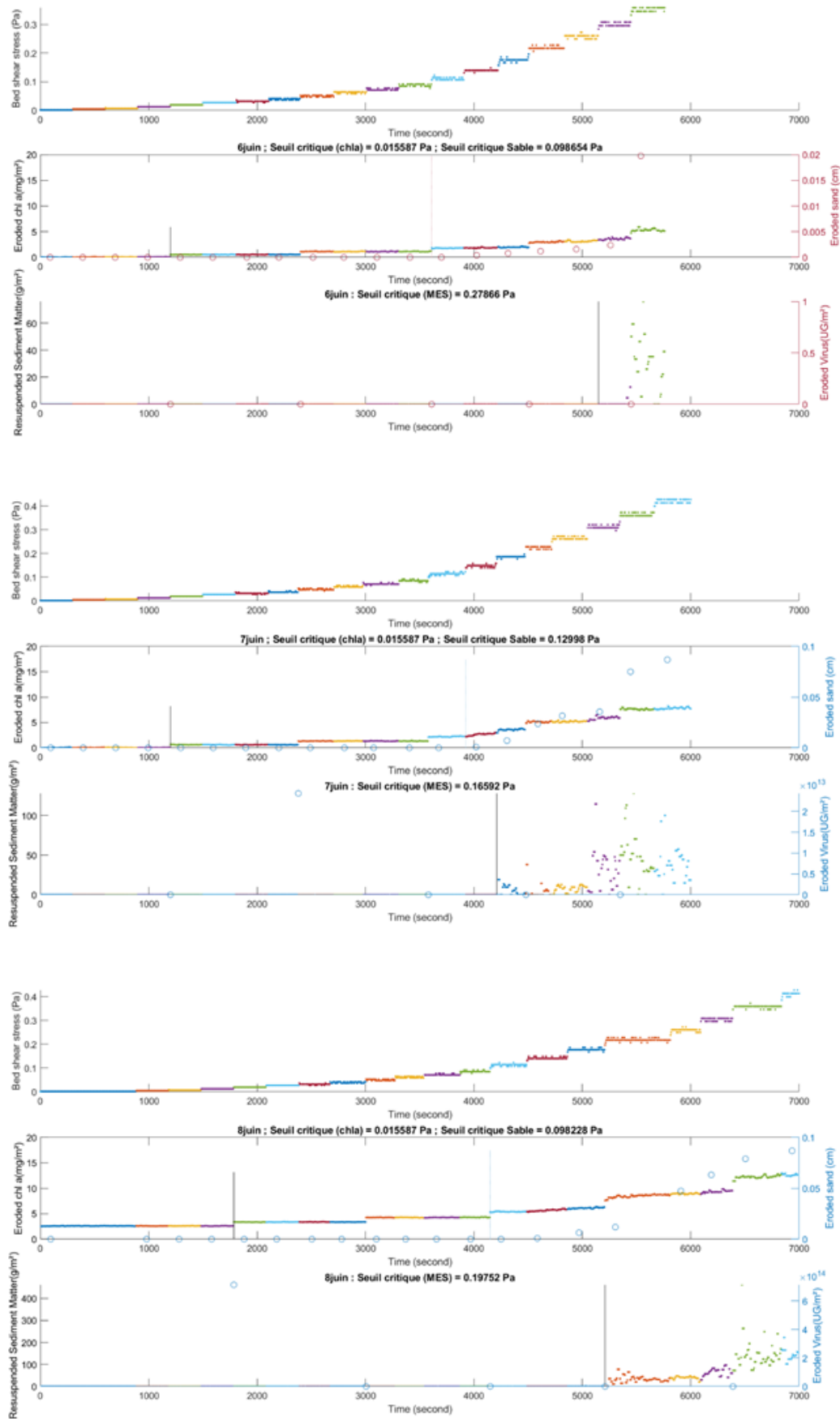
The samples analyzed after freeze-drying had the same viral loads as before. Thus, this assay technique seems satisfactory in order to quantify the viral load in OsHV-1 per unit volume. It would be interesting to perform this type of protocol on larger volumes of water with a suitable lyophilizer. Indeed, better accuracy should be observed with higher volumes.

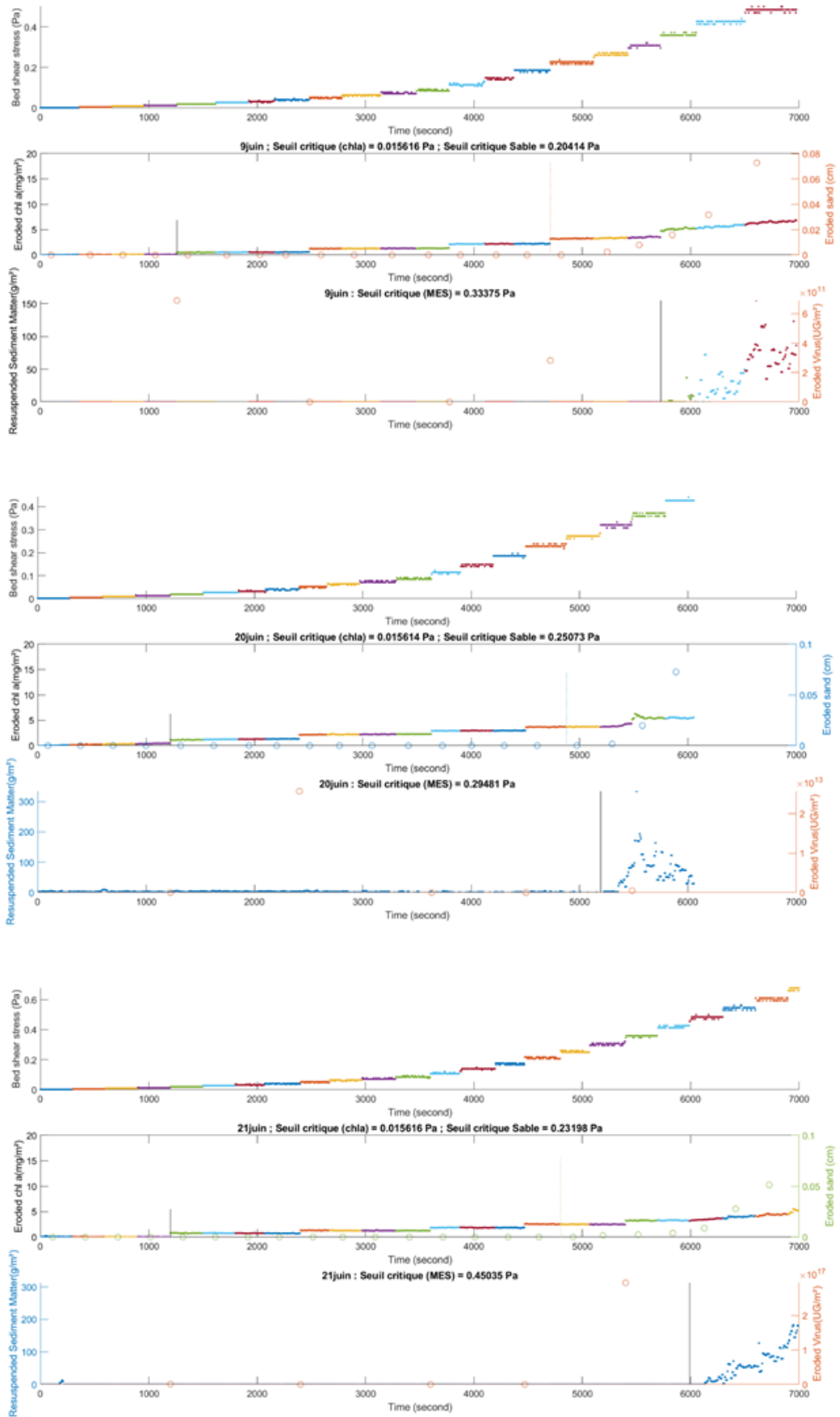
## Appendix 4 : Erosion experiments













## **Références bibliographiques**



Admiraal, W.: The ecology of estuarine sediment-inhabiting diatoms, *Prog. Phycol. Res.*, 3, 269–322, 1984.

Afli, A. and Glemarec, M.: Fluctuation à long terme des peuplements macrobenthiques dans le golfe du Morbihan (Bretagne, France), *Cah. Biol. Mar.*, 41(1), 67–90, 2000.

Agogué, H., Mallet, C., Orvain, F., De Crignis, M., Mornet, F. and Dupuy, C.: Bacterial dynamics in a microphytobenthic biofilm: A tidal mesocosm approach, *J. Sea Res.*, 92, 36–45, doi:10.1016/j.seares.2014.03.003, 2014.

Alain, K., Olagnon, M., Desbruyères, D., Pagé, A., Barbier, G., Juniper, S. K., Quéréllou, J. and Cambon-Bonavita, M.-A.: Phylogenetic characterization of the bacterial assemblage associated with mucous secretions of the hydrothermal vent polychaete *Paralvinella palmiformis*, *FEMS Microbiol. Ecol.*, 42(3), 463–476, 2002.

Alderman, D. J.: Epizootiology of *Marteilia refringens* in Europe, *Mar Fish Rev*, 41(1/2), 67–69, 1979.

Amon, R. M. and Benner, R.: Bacterial utilization of different size classes of dissolved organic matter, *Limnol. Oceanogr.*, 41(1), 41–51, 1996.

Ansell, A., Gibson, R., Barnes, M. and Press, U.: Ecological impact of green macroalgal blooms, *Oceanogr. Mar. Biol. Annu. Rev.*, 36, 97–125, 1998.

Arzul, I., Renault, T., Lipart, C. and Davison, A. J.: Evidence for interspecies transmission of oyster herpesvirus in marine bivalves, *J. Gen. Virol.*, 82(4), 865–870, 2001a.

Arzul, I., Renault, T. and Lipart, C.: Experimental herpes-like viral infections in marine bivalves: demonstration of interspecies transmission, *Dis. Aquat. Organ.*, 46(1), 1–6, 2001b.

Arzul, I., Renault, T., Thébault, A. and Gérard, A.: Detection of oyster herpesvirus DNA and proteins in asymptomatic *Crassostrea gigas* adults, *Virus Res.*, 84(1), 151–160, 2002.

Arzul, I., Corbeil, S., Morga, B. and Renault, T.: Viruses infecting marine molluscs, *J. Invertebr. Pathol.*, 147, 118–135, 2017.

Azam, F., Smith, D. C., Steward, G. F. and Hagström, \AAke: Bacteria-organic matter coupling and its significance for oceanic carbon cycling, *Microb. Ecol.*, 28(2), 167–179, 1994.

Azéma, P., Travers, M.-A., Benabdelmouna, A. and Déremont, L.: Single or dual experimental infections with *Vibrio aestuarianus* and OsHV-1 in diploid and triploid *Crassostrea gigas* at the spat, juvenile and adult stages, *J. Invertebr. Pathol.*, 139, 92–101, doi:10.1016/j.jip.2016.08.002, 2016.

Azéma, P., Lamy, J.-B., Boudry, P., Renault, T., Travers, M.-A. and Déremont, L.: Genetic parameters of resistance to *Vibrio aestuarianus*, and OsHV-1 infections in the Pacific oyster, *Crassostrea gigas*, at three different life stages, *Genet. Sel. Evol.*, 49(1), doi:10.1186/s12711-017-0297-2, 2017.

Baines, S. B. and Pace, M. L.: The production of dissolved organic matter by phytoplankton and its importance to bacteria: patterns across marine and freshwater systems, *Limnol. Oceanogr.*, 36(6), 1078–1090, 1991.

Barnett, A., Méléder, V., Blommaert, L., Lepetit, B., Gaudin, P., Vyverman, W., Sabbe, K., Dupuy, C. and Lavaud, J.: Growth form defines physiological photoprotective capacity in intertidal benthic diatoms, *ISME J.*, 9(1), 32–45, doi:10.1038/ismej.2014.105, 2015.

Barranguet, C.: The role of microphytobenthic primary production in a Mediterranean mussel culture area, *Estuar. Coast. Shelf Sci.*, 44(6), 753–765, 1997.

Barranguet, C., Kromkamp, J. and Peene, J.: Factors controlling primary production and photosynthetic characteristics of intertidal microphytobenthos, *Mar. Ecol. Prog. Ser.*, 173, 117–126, doi:10.3354/meps173117, 1998.

Bayne, B. L., Ahrens, M., Allen, S. K., D'auriac, M. A., Backeljau, T., Beninger, P., Bohn, R., Boudry, P., Davis, J., Green, T., Guo, X., Hedgecock, D., Ibarra, A., Kingsley-Smith, P., Krause, M., Langdon, C., Lapègue, S., Li, C., Manahan, D., Mann, R., Perez-Paralle, L., Powell, E. N., Rawson, P. D., Speiser, D., Sanchez, J.-L., Shumway, S. and Wang, H.: The Proposed Dropping of the Genus *Crassostrea* for All Pacific Cupped Oysters and Its Replacement by a New Genus *Magallana*: A Dissenting View, *J. Shellfish Res.*, 36(3), 545–547, doi:10.2983/035.036.0301, 2017.

Behrenfeld, M. J., Prasil, O., Babin, M. and Bruyant, F.: In search of a physiological basis for covariations in light-limited and light-saturated photosynthesis, *J. Phycol.*, 40(1), 4–25, 2004.

Bellinger, B. J., Abdullahi, A. S., Gretz, M. R. and Underwood, G. J. C.: Biofilm polymers: relationship between carbohydrate biopolymers from estuarine mudflats and unicellular cultures of benthic diatoms, *Aquat. Microb. Ecol.*, 38(2), 169–180, 2005.

Béné, C., Arthur, R., Norbury, H., Allison, E. H., Beveridge, M., Bush, S., Campling, L., Leschen, W., Little, D. and Squires, D.: Contribution of fisheries and aquaculture to food security and poverty reduction: assessing the current evidence, *World Dev.*, 79, 177–196, 2016.

Berg, J. A. and Newell, R. I.: Temporal and spatial variations in the composition of seston available to the suspension feeder *Crassostrea virginica*, *Estuar. Coast. Shelf Sci.*, 23(3), 375–386, 1986.

Bergamaschi, B. A., Tsamakis, E., Keil, R. G., Eglinton, T. I., Montluçon, D. B. and Hedges, J. I.: The effect of grain size and surface area on organic matter, lignin and carbohydrate concentration, and molecular compositions in Peru Margin sediments, *Geochim. Cosmochim. Acta*, 61(6), 1247–1260, doi:10.1016/S0016-7037(96)00394-8, 1997.

Billerbeck, M., Røy, H., Bosselmann, K. and Huettel, M.: Benthic photosynthesis in submerged Wadden Sea intertidal flats, *Estuar. Coast. Shelf Sci.*, 71(3–4), 704–716, doi:10.1016/j.ecss.2006.09.019, 2007.

Blanchard, G., Sauriau, P., Cariou-Le Gall, V., Gouleau, D., Garet, M. and Olivier, F.: Kinetics of tidal resuspension of microbiota: testing the effects of sediment cohesiveness and bioturbation using flume experiments, *Mar. Ecol. Prog. Ser.*, 151, 17–25, doi:10.3354/meps151017, 1997.

Blanchard, G. F., Guarini, J.-M., Bacher, C. and Huet, V.: Contrôle de la dynamique à court terme du microphytobenthos intertidal par le cycle exondation-submersion, *Comptes Rendus Académie Sci.-Ser. III-Sci. Vie*, 321(6), 501–508, 1998a.

Blanchard, G. F., Guarini, J.-M., Gros, P. and Richard, P.: Seasonal effect on the relationship between the photosynthetic capacity of intertidal microphytobenthos and temperature, *Oceanogr. Lit. Rev.*, 3(45), 510, 1998b.

Blanchard, G. F., Simon-Bouhet, B. and Guarini, J.-M.: Properties of the dynamics of intertidal microphytobenthic biomass, *J. Mar. Biol. Assoc. U. K.*, 82(6), 1027–1028, 2002.

Bliss and Smith: Penetration of light into soil and its role in the control of seed germination, *Plant Cell Environ.*, 8(7), 475–483, doi:10.1111/j.1365-3040.1985.tb01683.x, 2006.

Bolam, S. G., Whomersley, P. and Schratzberger, M.: Macrofaunal recolonization on intertidal mudflats: effect of sediment organic and sand content, *J. Exp. Mar. Biol. Ecol.*, 306(2), 157–180, doi:10.1016/j.jembe.2004.01.007, 2004.

Borja, A., Franco, J. and Pérez, V.: A marine biotic index to establish the ecological quality of soft-bottom benthos within European estuarine and coastal environments, *Mar. Pollut. Bull.*, 40(12), 1100–1114, 2000.

Box, G. E. and Cox, D. R.: An analysis of transformations, *J. R. Stat. Soc. Ser. B Methodol.*, 211–252, 1964.

Brey, T.: An empirical model for estimating aquatic invertebrate respiration, *Methods Ecol. Evol.*, 1(1), 92–101, 2010.

Brown, J. R.: Multivariate analyses of the role of environmental factors in seasonal and site-related growth variation in the Pacific oyster *Crassostrea gigas*., *Mar. Ecol. Prog. Ser.* Oldendorf, 45(3), 225–236, 1988.

Brown, J. R. and Hartwick, E. B.: Influences of temperature, salinity and available food upon suspended culture of the Pacific oyster, *Crassostrea gigas*: I. Absolute and allometric growth, *Aquaculture*, 70(3), 231–251, 1988.

Byron, C. J., Jin, D. and Dalton, T. M.: An Integrated ecological-economic modeling framework for the sustainable management of oyster farming, *Aquaculture*, 447, 15–22, doi:10.1016/j.aquaculture.2014.08.030, 2015.

Cadée, G. C. and Hegeman, J.: Primary production of the benthic microflora living on tidal flats in the Dutch Wadden Sea, *Neth. J. Sea Res.*, (2–3), 1974.

Cahoon, L. B.: The role of benthic microalgae in neritic ecosystems, *Oceanogr. Mar. Biol. Annu. Rev.* Vol. 37, doi:10.1201/9781482298550-4, 2014.

Cannuel, R.: Bases biologiques de la production de deux Mollusques d'intérêt économique: reproduction chez *Megathura crenulata*, reproduction et développement chez *Crassostrea gigas*, , 198, 2005.

Carstensen, J., Conley, D. J., Bonsdorff, E., Gustafsson, B. G., Hietanen, S., Janas, U., Jilbert, T., Maximov, A., Norkko, A., Norkko, J., Reed, D. C., Slomp, C. P., Timmermann, K. and Voss, M.: Hypoxia in the Baltic Sea: Biogeochemical Cycles, Benthic Fauna, and Management, *AMBIO*, 43(1), 26–36, doi:10.1007/s13280-013-0474-7, 2014.

Cartaxana, P., Jesus, B. and Brotas, V.: Pheophorbide and pheophytin a-like pigments as useful markers for intertidal microphytobenthos grazing by *Hydrobia ulvae*, *Estuar. Coast. Shelf Sci.*, 58(2), 293–297, 2003.

Cartaxana, P., Ruivo, M., Hubas, C., Davidson, I., Serôdio, J. and Jesus, B.: Physiological versus behavioral photoprotection in intertidal epipelic and epipsammic benthic diatom communities, *J. Exp. Mar. Biol. Ecol.*, 405(1–2), 120–127, doi:10.1016/j.jembe.2011.05.027, 2011.

Cartaxana, P., Domingues, N., Cruz, S., Jesus, B., Laviale, M., Serôdio, J. and Marques da Silva, J.: Photoinhibition in benthic diatom assemblages under light stress, *Aquat. Microb. Ecol.*, 70(1), 87–92, doi:10.3354/ame01648, 2013.

Chamberlain, J.: Impacts of biodeposits from suspended mussel (*Mytilus edulis* L.) culture on the surrounding surficial sediments, *ICES J. Mar. Sci.*, 58(2), 411–416, doi:10.1006/jmsc.2000.1037, 2001.

Charpy, L., Rodier, M., Fournier, J., Langlade, M.-J. and Gaertner-Mazouni, N.: Physical and chemical control of the phytoplankton of Ahe lagoon, French Polynesia, *Mar. Pollut. Bull.*, 65(10–12), 471–477, 2012.

Chennu, A., Volkenborn, N., De Beer, D., Wethey, D. S., Woodin, S. A. and Polerecky, L.: Effects of bioadvection by *Arenicola marina* on microphytobenthos in permeable sediments, *PLoS One*, 10(7), e0134236, 2015.

Chiovitti, A., Molino, P., Crawford, S. A., Teng, R., Spurck, T. and Wetherbee, R.: The glucans extracted with warm water from diatoms are mainly derived from intracellular chrysolaminaran and not extracellular polysaccharides, *Eur. J. Phycol.*, 39(2), 117–128, 2004.

Claessens, M., Meester, S. D., Landuyt, L. V., Clerck, K. D. and Janssen, C. R.: Occurrence and distribution of microplastics in marine sediments along the Belgian coast, *Mar. Pollut. Bull.*, 62(10), 2199–2204, doi:10.1016/j.marpolbul.2011.06.030, 2011.

Cloern, J. E.: Turbidity as a control on phytoplankton biomass and productivity in estuaries, *Cont. Shelf Res.*, 7(11–12), 1367–1381, 1987.

Cloern, J. E., Foster, S. Q. and Kleckner, A. E.: Phytoplankton primary production in the world's estuarine-coastal ecosystems, *Biogeosciences*, 11(9), 2477–2501, doi:10.5194/bg-11-2477-2014, 2014.

Coelho, H., Cartaxana, P., Brotas, V., Queiroga, H. and Serôdio, J.: Pheophorbide a in *Hydrobia ulvae* faecal pellets as a measure of microphytobenthos ingestion: variation over season and period of day, *Aquat. Biol.*, 13(2), 119–126, doi:10.3354/ab00356, 2011.

Coen, L. D., Brumbaugh, R. D., Bushek, D., Grizzle, R., Luckenbach, M. W., Posey, M. H., Powers, S. P. and Tolley, S. G.: Ecosystem services related to oyster restoration, *Mar. Ecol. Prog. Ser.*, 341, 303–307, 2007.

Cognie, B., Barillé, L. and Rincé, Y.: Selective feeding of the oystercrassostrea gigas fed on a natural microphytobenthos assemblage, *Estuaries*, 24(1), 126–134, 2001.

Cole, B. E. and Cloern, J. E.: An empirical model for estimating phytoplankton productivity in estuaries, Mar. Ecol. Prog. Ser., 36(1), 299–305, 1987.

Comps, M., Bonami, J. R. and Vaga, C.: A virus disease of the portuguese oyster [Crassostrea angulata LMK]., Comptes Rendus Hebd. Seances Acad. Sci. Ser. D, 1976.

Corzo, A., Van Bergeijk, S. A. and Garcia-Robledo, E.: Effects of green macroalgal blooms on intertidal sediments: net metabolism and carbon and nitrogen contents, Mar. Ecol. Prog. Ser., 380, 81–93, 2009.

Cozzoli, F., Bouma, T. J., Ottolander, P., Lluch, M. S., Ysebaert, T. and Herman, P. M. J.: The combined influence of body size and density on cohesive sediment resuspension by bioturbators, Sci. Rep., 8(1), 3831, doi:10.1038/s41598-018-22190-3, 2018.

Cugier, P., Struski, C., Blanchard, M., Mazurié, J., Povreau, S., Olivier, F., Trigui, J. R. and Thiébaut, E.: Assessing the role of benthic filter feeders on phytoplankton production in a shellfish farming site: Mont Saint Michel Bay, France, J. Mar. Syst., 82(1), 21–34, doi:10.1016/j.jmarsys.2010.02.013, 2010.

Dagg, M., Benner, R., Lohrenz, S. and Lawrence, D.: Transformation of dissolved and particulate materials on continental shelves influenced by large rivers: plume processes, Cont. Shelf Res., 24(7–8), 833–858, 2004.

Dalrymple, D. J. and Carmichael, R. H.: Effects of age class on N removal capacity of oysters and implications for bioremediation, Mar. Ecol. Prog. Ser., 528, 205–220, 2015.

Danielsson, \AAAsa, Jönsson, A. and Rahm, L.: Resuspension patterns in the Baltic proper, J. Sea Res., 57(4), 257–269, 2007.

Danovaro, R., Corinaldesi, C., Dell'Anno, A., Fuhrman, J. A., Middelburg, J. J., Noble, R. T. and Suttle, C. A.: Marine viruses and global climate change, FEMS Microbiol. Rev., 35(6), 993–1034, doi:10.1111/j.1574-6976.2010.00258.x, 2011.

Dauvin, J.-C.: Paradox of estuarine quality: Benthic indicators and indices, consensus or debate for the future, Mar. Pollut. Bull., 55(1), 271–281, doi:10.1016/j.marpolbul.2006.08.017, 2007.

Dauvin, J.-C. and Ruellet, T.: Polychaete/amphipod ratio revisited, Mar. Pollut. Bull., 55(1–6), 215–224, 2007.

Dauvin, J.-C., Ruellet, T., Desroy, N. and Janson, A.-L.: The ecological quality status of the Bay of Seine and the Seine estuary: Use of biotic indices, Mar. Pollut. Bull., 55(1–6), 241–257, doi:10.1016/j.marpolbul.2006.04.010, 2007.

Dauvin, J.-C., Lucas, S., Navon, M., Lesourd, S., Mear, Y., Poizot, E. and Alizier, S.: Does the hydrodynamic, morphometric and sedimentary environment explain the structure of soft-bottom benthic assemblages in the Eastern Bay of Seine (English Channel)?, Estuar. Coast. Shelf Sci., 189, 156–172, 2017.

Davison, A. J., Eberle, R., Ehlers, B., Hayward, G. S., McGeoch, D. J., Minson, A. C., Pellett, P. E., Roizman, B., Studdert, M. J. and Thiry, E.: The order herpesvirales, Arch. Virol., 154(1), 171–177, 2009.

De Decker, S., Normand, J., Saulnier, D., Pernet, F., Castagnet, S. and Boudry, P.: Responses of diploid and triploid Pacific oysters *Crassostrea gigas* to *Vibrio* infection in relation to their reproductive status, *J. Invertebr. Pathol.*, 106(2), 179–191, 2011.

De Jonge, V. N. and Van Beuselom, J. E. E.: Contribution of resuspended microphytobenthos to total phytoplankton in the Ems estuary and its possible role for grazers, *Neth. J. Sea Res.*, 30, 91–105, 1992.

Decho, A. W.: Microbial biofilms in intertidal systems: an overview, *Cont. Shelf Res.*, 20(10), 1257–1273, doi:10.1016/S0278-4343(00)00022-4, 2000.

Defer, D., Bourgougnon, N. and Fleury, Y.: Screening for antibacterial and antiviral activities in three bivalve and two gastropod marine molluscs, *Aquaculture*, 293(1–2), 1–7, doi:10.1016/j.aquaculture.2009.03.047, 2009.

Dégremont, L.: Evidence of herpesvirus (OsHV-1) resistance in juvenile *Crassostrea gigas* selected for high resistance to the summer mortality phenomenon, *Aquaculture*, 317(1–4), 94–98, doi:10.1016/j.aquaculture.2011.04.029, 2011.

Delaporte, M., Soudant, P., Lambert, C., Moal, J., Pouvreau, S. and Samain, J.-F.: Impact of food availability on energy storage and defense related hemocyte parameters of the Pacific oyster *Crassostrea gigas* during an experimental reproductive cycle, *Aquaculture*, 254(1–4), 571–582, 2006.

Delisle, L., Petton, B., Burguin, J. F., Morga, B., Corporeau, C. and Pernet, F.: Temperature modulate disease susceptibility of the Pacific oyster *Crassostrea gigas* and virulence of the Ostreid herpesvirus type 1, *Fish Shellfish Immunol.*, 80, 71–79, 2018.

Demers, S., Therriault, J.-C., Bourget, E. and Bah, A.: Resuspension in the shallow sublittoral zone of a macrotidal estuarine environment: Wind influence 1, *Limnol. Oceanogr.*, 32(2), 327–339, 1987.

Doghri, I., Lavaud, J., Dufour, A., Bazire, A., Lanneluc, I. and Sablé, S.: Cell-bound exopolysaccharides from an axenic culture of the intertidal mudflat *Navicula phyllepta* diatom affect biofilm formation by benthic bacteria, *J. Appl. Phycol.*, 29(1), 165–177, 2017.

Du, G., Yan, H., Liu, C. and Mao, Y.: Behavioral and physiological photoresponses to light intensity by intertidal microphytobenthos, *J. Oceanol. Limnol.*, 36(2), 293–304, 2018.

Dubilier, N., Giere, O. and Grieshaber, M. K.: Concomitant effects of sulfide and hypoxia on the aerobic metabolism of the marine oligochaete *Tubificoides benedii*, *J. Exp. Zool.*, 269(4), 287–297, 1994.

Dubilier, N., Giere, O. and Grieshaber, M. K.: Morphological and ecophysiological adaptations of the marine oligochaete *Tubificoides benedii* to sulfidic sediments, *Am. Zool.*, 35(2), 163–173, 1995.

Dubilier, N., Windoffer, R., Grieshaber, M. K. and Giere, O.: Ultrastructure and anaerobic metabolism of mitochondria in the marine oligochaete *Tubificoides benedii*: effects of hypoxia and sulfide, *Mar. Biol.*, 127(4), 637–645, 1997.

Dubois, M., Gilles, K. A., Hamilton, J. K., Rebers, P. t and Smith, F.: Colorimetric method for determination of sugars and related substances, *Anal. Chem.*, 28(3), 350–356, 1956.

Dubois, S., Marin-Léal, J. C., Ropert, M. and Lefebvre, S.: Effects of oyster farming on macrofaunal assemblages associated with Lanice conchilega tubeworm populations: A trophic analysis using natural stable isotopes, *Aquaculture*, 271(1–4), 336–349, doi:10.1016/j.aquaculture.2007.03.023, 2007a.

Dubois, S., Jean-Louis, B., Bertrand, B. and Lefebvre, S.: Isotope trophic-step fractionation of suspension-feeding species: Implications for food partitioning in coastal ecosystems, *J. Exp. Mar. Biol. Ecol.*, 351(1), 121–128, doi:10.1016/j.jembe.2007.06.020, 2007b.

Dupuy, C., Le Gall, S., Hartmann, H. J. and Bréret, M.: Retention of ciliates and flagellates by the oyster *Crassostrea gigas* in French Atlantic coastal ponds: protists as a trophic link between bacterioplankton and benthic suspension-feeders, *Mar. Ecol. Prog. Ser.*, 177, 165–175, 1999.

Dupuy, C., Vaquer, A., Lam-Höai, T., Rougier, C., Mazouni, N., Lautier, J., Collos, Y. and Le Gall, S.: Feeding rate of the oyster *Crassostrea gigas* in a natural planktonic community of the Mediterranean Thau Lagoon, *Mar. Ecol. Prog. Ser.*, 205, 171–184, 2000.

Dupuy, C., Mallet, C., Guizien, K., Montanié, H., Bréret, M., Mornet, F., Fontaine, C., Nérot, C. and Orvain, F.: Sequential resuspension of biofilm components (viruses, prokaryotes and protists) as measured by erodimetry experiments in the Brouage mudflat (French Atlantic coast), *J. Sea Res.*, 92, 56–65, doi:10.1016/j.seares.2013.12.002, 2014.

Dutertre, M., Hamon, D., Chevalier, C. and Ehrhold, A.: The use of the relationships between environmental factors and benthic macrofaunal distribution in the establishment of a baseline for coastal management, *ICES J. Mar. Sci.*, 70(2), 294–308, doi:10.1093/icesjms/fss170, 2013.

van Duyl, F. C., de Winder, B., Kop, A. J. and Wollenzien, U.: Tidal coupling between carbohydrate concentrations and bacterial activities in diatom-inhabited intertidal mudflats, *Mar. Ecol. Prog. Ser.*, 191, 19–32, 1999.

Echappé, C., Gernez, P., Méléder, V., Jesus, B., Cognie, B., Decottignies, P., Sabbe, K. and Barillé, L.: Satellite remote sensing reveals a positive impact of living oyster reefs on microalgal biofilm development, *Biogeosciences*, 15(3), 905–918, doi:10.5194/bg-15-905-2018, 2018.

Edgar, L. A.: Mucilage secretions of moving diatoms, *Protoplasma*, 118(1), 44–48, 1983.

Edgar, L. A. and Pickett-Heaps, J. D.: The mechanism of diatom locomotion. I. An ultrastructural study of the motility apparatus, in *Proc. R. Soc. Lond. B*, vol. 218, pp. 331–343, The Royal Society., 1983.

Egge, J. K. and Aksnes, D. L.: Silicate as regulating nutrient in phytoplankton competition., *Mar. Ecol. Prog. Ser.* Oldendorf, 83(2), 281–289, 1992.

Eilers, P. H. C. and Peeters, J. C. H.: A model for the relationship between light intensity and the rate of photosynthesis in phytoplankton, *Ecol. Model.*, 42(3–4), 199–215, 1988.

Elston, R. A., Kent, M. L. and Wilkinson, M. T.: Resistance of *Ostrea edulis* to *Bonamia ostreae* infection, *Aquaculture*, 64(3), 237–242, 1987.

Engel, F. G., Alegria, J., Andriana, R., Donadi, S., Gusmao, J. B., van Leeuwe, M. A., Matthiessen, B. and Eriksson, B. K.: Mussel beds are biological power stations on intertidal flats, *Estuar. Coast. Shelf Sci.*, 191, 21–27, 2017.

Evans, O., Paul-Pont, I., Hick, P. and Whittington, R. J.: A simple centrifugation method for improving the detection of Ostreid herpesvirus-1 (OsHV-1) in natural seawater samples with an assessment of the potential for particulate attachment, *J. Virol. Methods*, 210, 59–66, doi:10.1016/j.jviromet.2014.09.023, 2014.

Evans, O., Hick, P., Dhand, N. and Whittington, R. J.: Transmission of Ostreid herpesvirus-1 in *Crassostrea gigas* by cohabitation: effects of food and number of infected donor oysters, *Aquac. Environ. Interact.*, 7(3), 281–295, 2015.

Falkowski, P. G.: Physiological responses of phytoplankton to natural light regimes, *J. Plankton Res.*, 6(2), 295–307, 1984.

Falkowski, P. G.: The role of phytoplankton photosynthesis in global biogeochemical cycles, *Photosynth. Res.*, 39(3), 235–258, 1994.

Falkowski, P. G. and Raven, J. A.: *Aquatic Photosynthesis*: Second Edition, Princeton University Press., 2013.

Falkowski, P. G., Greene, R. M. and Geider, R. J.: Physiological limitations on phytoplankton productivity in the ocean, *Oceanography*, 5(2), 84–91, 1992.

FAO: State of world aquaculture 2006, [online] Available from: <http://www.fao.org/docrep/009/a0874e/a0874e00.htm> (Accessed 20 December 2018), 2006.

FAO, Ed.: Meeting the sustainable development goals, Rome., 2018.

Farley, C. A., Banfield, W. G., Kasnic, G. and Foster, W. S.: Oyster Herpes-Type Virus, *Science*, 178(4062), 759–760, doi:10.1126/science.178.4062.759, 1972.

Fauchald, K. and Jumars, P.: The diet of worms: a study of polychaete feeding guilds, , 92, 1979.

Fauvel, P.: Faune de France 5, Polychètes errantes, [online] Available from: <http://sci-hub.bz/http://www.sciencedirect.com/science/article/pii/S0044848607002797> (Accessed 24 November 2017), 1923.

Fauvel, P.: Faune de France 16, Polychetes-sententaires, [online] Available from: [http://www.faunedefrance.org/bibliotheque/docs/P.FAUVEL\(FdeFr16\)Polychetes-sententaires.pdf](http://www.faunedefrance.org/bibliotheque/docs/P.FAUVEL(FdeFr16)Polychetes-sententaires.pdf) (Accessed 15 January 2018), 1927.

Fernandez-Piquer, J., Bowman, J. P., Ross, T. and Tamplin, M. L.: Molecular analysis of the bacterial communities in the live Pacific oyster (*Crassostrea gigas*) and the influence of postharvest temperature on its structure, *J. Appl. Microbiol.*, 112(6), 1134–1143, 2012.

Filippini, M. and Middelboe, M.: Viral abundance and genome size distribution in the sediment and water column of marine and freshwater ecosystems: Virus genome size distribution in aquatic systems, *FEMS Microbiol. Ecol.*, 60(3), 397–410, doi:10.1111/j.1574-6941.2007.00298.x, 2007.

Flemming, B. W.: A revised textural classification of gravel-free muddy sediments on the basis of ternary diagrams, *Cont. Shelf Res.*, 20(10–11), 1125–1137, doi:10.1016/S0278-4343(00)00015-7, 2000.

Flemming, H.-C. and Wingender, J.: The biofilm matrix, *Nat. Rev. Microbiol.*, doi:10.1038/nrmicro2415, 2010.

Fleury, E., Normand, J., Lamoureux, A., Bouget, J.-F., Lupo, C., Cochennec-Laureau, N., Petton, S., Petton, B. and Pouvreau, S.: RESCO REMORA Database: National monitoring network of mortality and growth rates of the sentinel oyster *Crassostrea gigas*, SEANOE, 2018.

Forrest, B. M. and Creese, R. G.: Benthic Impacts of Intertidal Oyster Culture, with Consideration of Taxonomic Sufficiency, *Environ. Monit. Assess.*, 112(1–3), 159–176, doi:10.1007/s10661-006-0359-3, 2006.

Forrest, B. M., Keeley, N. B., Hopkins, G. A., Webb, S. C. and Clement, D. M.: Bivalve aquaculture in estuaries: Review and synthesis of oyster cultivation effects, *Aquaculture*, 298(1–2), 1–15, doi:10.1016/j.aquaculture.2009.09.032, 2009a.

Forrest, B. M., Keeley, N. B., Hopkins, G. A., Webb, S. C. and Clement, D. M.: Bivalve aquaculture in estuaries: Review and synthesis of oyster cultivation effects, *Aquaculture*, 298(1–2), 1–15, doi:10.1016/j.aquaculture.2009.09.032, 2009b.

Forster, R. M. and Kromkamp, J. C.: Modelling the effects of chlorophyll fluorescence from subsurface layers on photosynthetic efficiency measurements in microphytobenthic algae, *Mar. Ecol. Prog. Ser.*, 284, 9–22, 2004.

Friedman, C. S., Estes, R. M., Stokes, N. A., Burge, C. A., Hargove, J. S., Barber, B. J., Elston, R. A., Burreson, E. M. and Reece, K. S.: Herpes virus in juvenile Pacific oysters *Crassostrea gigas* from Tomales Bay, California, coincides with summer mortality episodes, *Dis. Aquat. Organ.*, 63(1), 33–41, 2005.

Frontier, S.: Diversity and structure in aquatic ecosystems, *Ocean. Mar Biol.*, 23, 253–312, 1985.

Frontier, S., Pichod-Viale, D., Leprêtre, A., Davoult, D. and Luczak, C.: Ecosystèmes. Structure, fonctionnement, évolution., 2008.

Fuhrmann, J. A. and Suttle, C. A.: Viruses in marine planktonic systems, *Oceanography*, 6(2), 51–63, 1993.

Fuhrmann, M., Petton, B., Quillien, V., Faury, N., Morga, B. and Pernet, F.: Salinity influences disease-induced mortality of the oyster *Crassostrea gigas* and infectivity of the ostreid herpesvirus 1 (OsHV-1), *Aquac. Environ. Interact.*, 8, 543–552, doi:10.3354/aei00197, 2016.

Fuhrmann, M., Richard, G., Quéré, C., Petton, B. and Pernet, F.: Low pH reduced survival of the oyster *Crassostrea gigas* exposed to the Ostreid herpesvirus 1 by altering the metabolic response of the host, *Aquaculture*, 503, 167–174, 2019.

Fulford, R. S., Breitburg, D. L., Newell, R. I., Kemp, W. M. and Luckenbach, M.: Effects of oyster population restoration strategies on phytoplankton biomass in Chesapeake Bay: a flexible modeling approach, *Mar. Ecol. Prog. Ser.*, 336, 43–61, 2007.

Gallucci, F. and Netto, S. A.: Effects of the passage of cold fronts over a coastal site: an ecosystem approach, Mar. Ecol. Prog. Ser., 281, 79–92, 2004.

Gangnery, A., Normand, J., Duval, C., Cugier, P., Grangeré, K., Petton, B., Petton, S., Orvain, F. and Pernet, F.: Connectivities with shellfish farms and channel rivers are associated with mortality risk in oysters, Aquac. Environ. Interact., 11, 493–506, 2019.

Garcia-Robledo, E. and Corzo, A.: Effects of macroalgal blooms on carbon and nitrogen biogeochemical cycling in photoautotrophic sediments: an experimental mesocosm, Mar. Pollut. Bull., 62(7), 1550–1556, 2011.

Garnier, M., Labreuche, Y. and Nicolas, J.-L.: Molecular and phenotypic characterization of *Vibrio aestuarianus* subsp. *francensis* subsp. nov., a pathogen of the oyster *Crassostrea gigas*, Syst. Appl. Microbiol., 31(5), 358–365, 2008.

Genty, B., Briantais, J.-M. and Baker, N. R.: The relationship between the quantum yield of photosynthetic electron transport and quenching of chlorophyll fluorescence, Biochim. Biophys. Acta BBA - Gen. Subj., 990(1), 87–92, doi:10.1016/S0304-4165(89)80016-9, 1989.

Gesteira, J. L. G. and Dauvin, J.-C.: Amphipods are Good Bioindicators of the Impact of Oil Spills on Soft-Bottom Macrofauna Communities, Mar. Pollut. Bull., 40(11), 1017–1027, doi:10.1016/S0025-326X(00)00046-1, 2000.

Gibbs, P. E.: On the genus *Golfingia* (Sipuncula) in the Plymouth area with a description of a new species, J. Mar. Biol. Assoc. U. K., 53(1), 73–86, doi:10.1017/S0025315400056642, 1973.

Giere, O., Rhode, B. and Dubilier, N.: Structural peculiarities of the body wall of *Tubificoides benedii* (Oligochaeta) and possible relations to its life in sulphidic sediments, Zoomorphology, 108(1), 29–39, 1988.

Giere, O., Preusse, J.-H. and Dubilier, N.: *Tubificoides benedii* (Tubificidae, Oligochaeta)—a pioneer in hypoxic and sulfidic environments. An overview of adaptive pathways, in Aquatic Oligochaetes, pp. 235–241, Springer., 1999.

Glud, R. N. and Mathias, M.: Virus and bacteria dynamics of a coastal sediment: implication for benthic carbon cycling, Limnol. Oceanogr., 49(6), 2073–2081, 2004.

Go, J., Deutscher, A., Spiers, Z., Dahle, K., Kirkland, P. and Jenkins, C.: An investigation into mass mortalities of unknown aetiology in Pacific oysters, *Crassostrea gigas*, Port Stephens New South Wales Aust. Aquat Organ, 125, 227–242, 2017.

Goudénège, D., Travers, M. A., Lemire, A., Petton, B., Haffner, P., Labreuche, Y., Tourbiez, D., Mangenot, S., Calteau, A. and Mazel, D.: A single regulatory gene is sufficient to alter *Vibrio aestuarianus* pathogenicity in oysters, Environ. Microbiol., 17(11), 4189–4199, 2015.

Grangeré, K., Ménesguen, A., Lefebvre, S., Bacher, C. and Pouvreau, S.: Modelling the influence of environmental factors on the physiological status of the Pacific oyster *Crassostrea gigas* in an estuarine embayment; The Baie des Veys (France), J. Sea Res., 62(2–3), 147–158, 2009.

Grangeré, K., Lefebvre, S., Bacher, C., Cugier, P. and Ménesguen, A.: Modelling the spatial heterogeneity of ecological processes in an intertidal estuarine bay: dynamic interactions

between bivalves and phytoplankton, Mar. Ecol. Prog. Ser., 415, 141–158, doi:10.3354/meps08659, 2010.

Grasso, F., Le Hir, P. and Bassoullet, P.: Numerical modelling of mixed-sediment consolidation, Ocean Dyn., 65(4), 607–616, 2015.

Guarini, J.-M., Blanchard, G. F., Bacher, C., Gros, P., Riera, P., Richard, P., Gouleau, D., Galois, R., Prou, J. and Sauriau, P.-G.: Dynamics of spatial patterns of microphytobenthic biomass: inferences from a geostatistical analysis of two comprehensive surveys in Marennes-Oléron Bay (France), Mar. Ecol. Prog. Ser., 166, 131–141, 1998.

Guarini, J.-M., Blanchard, G. F., Gros, P., Gouleau, D. and Bacher, C.: Dynamic model of the short-term variability of microphytobenthic biomass on temperate intertidal mudflats, Mar. Ecol. Prog. Ser., 291–303, 2000.

Guerra-García, J. M., Tierno de Figueroa, J. M., Navarro-Barranco, C., Ros, M., Sánchez-Moyano, J. E. and Moreira, J.: Dietary analysis of the marine Amphipoda (Crustacea: Peracarida) from the Iberian Peninsula, J. Sea Res., 85, 508–517, doi:10.1016/j.seares.2013.08.006, 2014.

Guillaud, J.-F.: Les flux de sels nutritifs dans l'estuaire de la Seine (France); rôle et importance du bouchon vaseux au cours du mélange estuarien, Can. J. Fish. Aquat. Sci., 40(S1), s180–s187, 1983.

Haven, D. S. and Morales-Alamo, R.: Aspects of biodeposition by oysters and other invertebrate filter feeders, Limnol. Oceanogr., 11(4), 487–498, 1966.

Hayakawa, Y.: Sedimentation flux from mariculture of oyster (*Crassostrea gigas*) in Ofunato estuary, Japan, ICES J. Mar. Sci., 58(2), 435–444, doi:10.1006/jmsc.2000.1036, 2001.

Hayward, P. J. and Ryland, J. S.: Handbook of the Marine Fauna of North-West Europe, OUP Oxford., 1995.

Hedges, J. I., Keil, R. G. and Benner, R.: What happens to terrestrial organic matter in the ocean?, Org. Geochem., 27(5–6), 195–212, 1997.

Heldal, M. and Bratbak, G.: Production and decay of viruses in aquatic environments, Mar Ecol Prog Ser, 72(3), 205–212, 1991.

Herlory, O., Guarini, J.-M., Richard, P. and Blanchard, G. F.: Microstructure of microphytobenthic biofilm and its spatio-temporal dynamics in an intertidal mudflat (Aiguillon Bay, France), Mar. Ecol. Prog. Ser., 282, 33–44, 2004.

Herman, P. M. J., Middelburg, J. J. and Heip, C. H. R.: Benthic community structure and sediment processes on an intertidal flat: results from the ECOFLAT project, Cont. Shelf Res., 21(18–19), 2055–2071, doi:10.1016/S0278-4343(01)00042-5, 2001.

Hernández-Zárate, G. and Olmos-Soto, J.: Identification of bacterial diversity in the oyster *Crassostrea gigas* by fluorescent in situ hybridization and polymerase chain reaction, J. Appl. Microbiol., 100(4), 664–672, 2006.

Hewson, I., O'Neil, J. M., Fuhrman, J. A. and Dennison, W. C.: Virus-like particle distribution and abundance in sediments and overlying waters along eutrophication gradients in two subtropical estuaries, Limnol. Oceanogr., 46(7), 1734–1746, 2001.

Hick, P., Evans, O., Looi, R., English, C. and Whittington, R. J.: Stability of Ostreid herpesvirus-1 (OsHV-1) and assessment of disinfection of seawater and oyster tissues using a bioassay, Aquaculture, 450, 412–421, doi:10.1016/j.aquaculture.2015.08.025, 2016.

Hick, P. M., Evans, O., Rubio, A., Dhand, N. K. and Whittington, R. J.: Both age and size influence susceptibility of Pacific oysters (*Crassostrea gigas*) to disease caused by Ostreid herpesvirus-1 (OsHV-1) in replicated field and laboratory experiments, Aquaculture, 489, 110–120, 2018.

Hily, C.: Ecologie benthique des pertuis charentais, 1976.

Hily, C.: Variabilité de la macrofaune benthique dans les milieux hyper-trophiques de la rade de Brest, [online] Available from: <http://www.vliz.be/en/imis?refid=13282> (Accessed 10 December 2017), 1984.

Hine, P. M.: Herpesviruses associated with mortalities among hatchery-reared larval Pacific oysters *Crassostrea gigas*, Aquat Org, 12, 135–142, 1992.

Hochard, S., Pinazo, C., Grenz, C., Evans, J. L. B. and Pringault, O.: Impact of microphytobenthos on the sediment biogeochemical cycles: A modeling approach, Ecol. Model., 221(13–14), 1687–1701, doi:10.1016/j.ecolmodel.2010.04.002, 2010.

Howarth, R. W.: Nutrient limitation of net primary production in marine ecosystems, Annu. Rev. Ecol. Syst., 19(1), 89–110, 1988.

Hwang, J. Y., Park, J. J., Yu, H. J., Hur, Y. B., Arzul, I., Couraleau, Y. and Park, M. A.: Ostreid herpesvirus 1 infection in farmed Pacific oyster larvae *Crassostrea gigas* (Thunberg) in Korea, J Fish Dis, 36, 969–972, 2013.

Jenkin, P. M.: Oxygen production by the diatom *Coscinodiscus excentricus* Ehr. in relation to submarine illumination in the English Channel, J. Mar. Biol. Assoc. U. K., 22(1), 301–343, 1937.

Jenkins, C., Hick, P., Gabor, M., Spiers, Z., Fell, S. A., Gu, X., Read, A., Go, J., Dove, M. and Connor, W. O.: Identification and characterisation of an ostreid herpesvirus-1 microvariant (OsHV-1 μ-var) in *Crassostrea gigas* (Pacific oysters) in Australia, Dis. Aquat. Organ., 105(2), 109–126, 2013.

Jesus, B., Mendes, C. R., Brodas, V. and Paterson, D. M.: Effect of sediment type on microphytobenthos vertical distribution: Modelling the productive biomass and improving ground truth measurements, J. Exp. Mar. Biol. Ecol., 332(1), 60–74, doi:10.1016/j.jembe.2005.11.005, 2006.

Joensuu, M., Pilditch, C. A., Harris, R., Hietanen, S., Pettersson, H. and Norkko, A.: Sediment properties, biota, and local habitat structure explain variation in the erodibility of coastal sediments: Variation in the erodibility of coastal sediments, Limnol. Oceanogr., 63(1), 173–186, doi:10.1002/lno.10622, 2018.

de Jong, D. J. and de Jonge, V. N.: Dynamics and distribution of microphytobenthic chlorophyll-a in the Western Scheldt estuary (SW Netherlands), *Hydrobiologia*, 311(1), 21–30, doi:10.1007/BF00008568, 1995.

Jouenne, F., Lefebvre, S., Véron, B. and Lagadeuc, Y.: Phytoplankton community structure and primary production in small intertidal estuarine-bay ecosystem (eastern English Channel, France), *Mar. Biol.*, 151(3), 805–825, 2007.

Keeley, N. B., Forrest, B. M. and Macleod, C. K.: Novel observations of benthic enrichment in contrasting flow regimes with implications for marine farm monitoring and management, *Mar. Pollut. Bull.*, 66(1–2), 105–116, 2013.

Kervella, Y., Germain, G., Gaurier, B., Facq, J.-V., Cayocca, F. and Lesueur, P.: Experimental study of the near-field impact of an oyster table on the flow, *Eur. J. Mech. - BFluids*, 29(1), 32–42, doi:10.1016/j.euromechflu.2009.09.002, 2010.

Kopp, J., Joly, J.-P., Moriceau, J., Legagneur, E. and Jacqueline, F.: La Conchyliculture en Baie des Veys, [online] Available from: <http://archimer.ifremer.fr/doc/00081/19246/> (Accessed 24 November 2017), 1991.

Kristensen, E., Penha-Lopes, G., Delefosse, M., Valdemarsen, T., Quintana, C. O. and Banta, G. T.: What is bioturbation? The need for a precise definition for fauna in aquatic sciences, *Mar. Ecol. Prog. Ser.*, 446, 285–302, 2012.

Kromkamp, J., Peene, J., van Rijswijk, P., Sandee, A. and Goosen, N.: Nutrients, light and primary production by phytoplankton and microphytobenthos in the eutrophic, turbid Westerschelde estuary (The Netherlands), *Hydrobiologia*, 311(1–3), 9–19, 1995.

Kruse, I., Strasser, M. and Thiermann, F.: The role of ecological divergence in speciation between intertidal and subtidal *Scoloplos armiger* (Polychaeta, Orbiniidae), *J. Sea Res.*, 51(1), 53–62, 2004.

Kueh, C. S. and Chan, K.: Bacteria in bivalve shellfish with special reference to the oyster, *J. Appl. Bacteriol.*, 59(1), 41–47, 1985.

Kühl, M., Lassen, C. and Jørgensen, B. B.: Light penetration and light intensity in sandy marine sediments measured with irradiance and scalar irradiance fiber-optic microprobes, *Mar. Ecol. Prog. Ser.*, 139–148, 1994.

Kwon, B.-O., Lee, Y., Park, J., Ryu, J., Hong, S., Son, S., Lee, S. Y., Nam, J., Koh, C.-H. and Khim, J. S.: Temporal dynamics and spatial heterogeneity of microalgal biomass in recently reclaimed intertidal flats of the Saemangeum area, Korea, *J. Sea Res.*, 116, 1–11, 2016.

Lam-Hoai, T., Rougier, C. and Lasserre, G.: Tintinnids and rotifers in a northern Mediterranean coastal lagoon. Structural diversity and function through biomass estimations, *Mar. Ecol. Prog. Ser.*, 152, 13–25, 1997.

Lapegue, S., Batista, F., Heurtebise, S., Yu, Z. and Boudry, P.: Evidence for the presence of the Portuguese oyster, *Crassostrea angulata*, in northern China, *J. Shellfish Res.*, 23(3), 759–763, 2004.

Lavaud, J., Strzepek, R. F. and Kroth, P. G.: Photoprotection capacity differs among diatoms: possible consequences on the spatial distribution of diatoms related to fluctuations in the underwater light climate, *Limnol. Oceanogr.*, 52(3), 1188–1194, 2007.

Le Hir, P., Monbet, Y. and Orvain, F.: Sediment erodability in sediment transport modelling: Can we account for biota effects?, *Cont. Shelf Res.*, 27(8), 1116–1142, doi:10.1016/j.csr.2005.11.016, 2007.

Le Hir, P., Cayocca, F. and Waeles, B.: Dynamics of sand and mud mixtures: a multiprocess-based modelling strategy, *Cont. Shelf Res.*, 31(10), S135–S149, 2011.

Le Roux, F., Wegner, K. M. and Polz, M. F.: Oysters and vibrios as a model for disease dynamics in wild animals, *Trends Microbiol.*, 24(7), 568–580, 2016.

Leal Diego, A. G., Dores Ramos, A. P., Marques Souza, D. S., Durigan, M., Greinert-Goulart, J. A., Moresco, V., Amstutz, R. C., Micoli, A. H., Romeu Cantusio Neto, Célia Regina Monte Barardi and Regina Maura Bueno Franco: Sanitary quality of edible bivalve mollusks in Southeastern Brazil using an UV based depuration system, *Ocean Coast. Manag.*, 72, 93–100, doi:10.1016/j.ocecoaman.2011.07.010, 2013.

Lees, D.: Viruses and bivalve shellfish, *Int. J. Food Microbiol.*, 59(1), 81–116, 2000.

Lefebvre, S., Marín Leal, J. C., Dubois, S., Orvain, F., Blin, J.-L., Bataillé, M.-P., Ourry, A. and Galois, R.: Seasonal dynamics of trophic relationships among co-occurring suspension-feeders in two shellfish culture dominated ecosystems, *Estuar. Coast. Shelf Sci.*, 82(3), 415–425, doi:10.1016/j.ecss.2009.02.002, 2009.

Lemire, A., Goudenege, D., Versigny, T., Petton, B., Calteau, A., Labreuche, Y. and Le Roux, F.: Populations, not clones, are the unit of vibrio pathogenesis in naturally infected oysters, *ISME J.*, 9(7), 1523, 2015.

Leynaert, A., Longphuirt, S. N., An, S., Lim, J.-H., Claquin, P., Grall, J., Kwon, B. O. and Koh, C. H.: Tidal variability in benthic silicic acid fluxes and microphytobenthos uptake in intertidal sediment, *Estuar. Coast. Shelf Sci.*, 95(1), 59–66, 2011.

Lincoln, R. J. and British Museum: British marine amphipoda, gammaridea, London : British Museum (Natural History). [online] Available from: <https://trove.nla.gov.au/version/11914401> (Accessed 4 January 2018), 1979.

Lokmer, A. and Wegner, K. M.: Hemolymph microbiome of Pacific oysters in response to temperature, temperature stress and infection, *ISME J.*, 9(3), 670–682, doi:10.1038/ismej.2014.160, 2015.

Lokmer, A., Goedknecht, M. A., Thieltges, D. W., Fiorentino, D., Kuenzel, S., Baines, J. F. and Wegner, K. M.: Spatial and temporal dynamics of Pacific oyster hemolymph microbiota across multiple scales, *Front. Microbiol.*, 7, 1367, 2016a.

Lokmer, A., Kuenzel, S., Baines, J. F. and Wegner, K. M.: The role of tissue-specific microbiota in initial establishment success of Pacific oysters, *Environ. Microbiol.*, 18(3), 970–987, 2016b.

Longhi, M. L., Schloss, I. R. and Wiencke, C.: Effect of irradiance and temperature on photosynthesis and growth of two Antarctic benthic diatoms, *Gyrosigma subsalinum* and *Odontella litigiosa*, *Bot. Mar.*, 46(3), 276–284, 2003.

Longphuirt, S. N., Lim, J.-H., Leynaert, A., Claquin, P., Choy, E.-J., Kang, C.-K. and An, S.: Dissolved inorganic nitrogen uptake by intertidal microphytobenthos: nutrient concentrations, light availability and migration, *Mar. Ecol. Prog. Ser.*, 379, 33–44, 2009.

Lorenzen, C. J.: Determination of chlorophyll and pheopigments: spectrophotometric equations, *Limnol. Oceanogr.*, 12(2), 343–346, 1967.

de Lorgeril, J., Lucasson, A., Petton, B., Toulza, E., Montagnani, C., Clerissi, C., Vidal-Dupiol, J., Chaparro, C., Galinier, R., Escoubas, J.-M., Haffner, P., Dégremont, L., Charrière, G. M., Lafont, M., Delort, A., Vergnes, A., Chiarello, M., Faury, N., Rubio, T., Leroy, M. A., Pérignon, A., Régler, D., Morga, B., Alunno-Bruscia, M., Boudry, P., Le Roux, F., Destoumieux-Garzón, D., Gueguen, Y. and Mitta, G.: Immune-suppression by OsHV-1 viral infection causes fatal bacteraemia in Pacific oysters, *Nat. Commun.*, 9(1), 4215, doi:10.1038/s41467-018-06659-3, 2018.

Lu, L. and Wu, R. S. S.: Recolonization and succession of marine macrobenthos in organic-enriched sediment deposited from fish farms, *Environ. Pollut.*, 101(2), 241–251, doi:10.1016/S0269-7491(98)00041-4, 1998.

Luna, G. M., Vignaroli, C., Rinaldi, C., Pusceddu, A., Nicoletti, L., Gabellini, M., Danovaro, R. and Biavasco, F.: Extraintestinal *Escherichia coli* carrying virulence genes in coastal marine sediments, *Appl. Environ. Microbiol.*, 76(17), 5659–5668, 2010.

Lynch, S. A., Carlsson, J., Reilly, A. O., Cotter, E. and Culloty, S. C.: A previously undescribed ostreid herpes virus 1 (OsHV-1) genotype detected in the pacific oyster, *Crassostrea gigas*, in Ireland, *Parasitology*, 139(12), 1526–1532, 2012.

Lyons, D. A., Arvanitidis, C., Blight, A. J., Chatzinikolaou, E., Guy-Haim, T., Kotta, J., Orav-Kotta, H., Queirós, A. M., Rilov, G. and Somerfield, P. J.: Macroalgal blooms alter community structure and primary productivity in marine ecosystems, *Glob. Change Biol.*, 20(9), 2712–2724, 2014.

MacIntyre, H. L., Geider, R. J. and Miller, D. C.: Microphytobenthos: the ecological role of the “secret garden” of unvegetated, shallow-water marine habitats. I. Distribution, abundance and primary production, *Estuaries*, 19(2), 186–201, 1996.

Maier, C., de Kluijver, A., Agis, M., Brussaard, C. P. D., van Duyl, F. C. and Weinbauer, M. G.: Dynamics of nutrients, total organic carbon, prokaryotes and viruses in onboard incubations of cold-water corals, *Biogeosciences*, 8(9), 2609–2620, doi:10.5194/bg-8-2609-2011, 2011.

Mallet, C., Agogué, H., Bonnemoy, F., Guizien, K., Orvain, F. and Dupuy, C.: Structures of benthic prokaryotic communities and their hydrolytic enzyme activities resuspended from samples of intertidal mudflats: An experimental approach, *J. Sea Res.*, 92, 158–169, doi:10.1016/j.seares.2014.01.005, 2014.

Marín Leal, J. C., Dubois, S., Orvain, F., Galois, R., Blin, J.-L., Ropert, M., Bataillé, M.-P., Ourry, A. and Lefebvre, S.: Stable isotopes ( $\delta^{13}\text{C}$ ,  $\delta^{15}\text{N}$ ) and modelling as tools to estimate

the trophic ecology of cultivated oysters in two contrasting environments, Mar. Biol., 153(4), 673–688, doi:10.1007/s00227-007-0841-7, 2008.

Matisson, J. and Lindén, O.: Benthic macrofauna succession under mussels, *Mytilus edulis* L. (Bivalvia), cultured on hanging long-lines, Sarsia, 68(2), 97–102, doi:10.1080/00364827.1983.10420561, 1983.

May, C. L., Koseff, J. R., Lucas, L. V., Cloern, J. E. and Schoellhamer, D. H.: Effects of spatial and temporal variability of turbidity on phytoplankton blooms, Mar. Ecol. Prog. Ser., 254, 111–128, 2003.

McKew, B. A., Taylor, J. D., McGinity, T. J. and Underwood, G. J.: Resistance and resilience of benthic biofilm communities from a temperate saltmarsh to desiccation and rewetting, ISME J., 5(1), 30, 2011.

Méléder, V., Barillé, L., Rincé, Y., Morançais, M., Rosa, P. and Gaudin, P.: Spatio-temporal changes in microphytobenthos structure analysed by pigment composition in a macrotidal flat (Bourgneuf Bay, France), Mar. Ecol. Prog. Ser., 297, 83–99, 2005.

Méléder, V., Rincé, Y., Barillé, L., Gaudin, P. and Rosa, P.: Spatiotemporal changes in microphytobenthos assemblages in a macrotidal flat (Bourgneuf Bay, France) 1, J. Phycol., 43(6), 1177–1190, 2007.

Mermillod-Blondin, F., Nogaro, G., Datry, T., Malard, F. and Gibert, J.: Do tubificid worms influence the fate of organic matter and pollutants in stormwater sediments?, Environ. Pollut., 134(1), 57–69, 2005.

Mialhe, E., Bachère, E., Chagot, D. and Grizel, H.: Isolation and purification of the protozoan Bonamia ostreae (Pichot et al. 1980), a parasite affecting the flat oyster *Ostrea edulis* L., Aquaculture, 71(4), 293–299, 1988.

Mineur, F., Le Roux, A., Maggs, C. A. and Verlaque, M.: Positive feedback loop between introductions of non-native marine species and cultivation of oysters in Europe, Conserv. Biol., 28(6), 1667–1676, 2014.

Mitbavkar, S. and Anil, A. C.: Vertical migratory rhythms of benthic diatoms in a tropical intertidal sand flat: influence of irradiance and tides, Mar. Biol., 145(1), doi:10.1007/s00227-004-1300-3, 2004.

Mitchell, I. M.: In situ biodeposition rates of Pacific oysters (*Crassostrea gigas*) on a marine farm in Southern Tasmania (Australia), Aquaculture, 257(1–4), 194–203, doi:10.1016/j.aquaculture.2005.02.061, 2006.

Montes, J. and Melendez, M. I.: Données sur la parasitose de Bonamia ostreae chez l’huître plate de Galice, côte nord-ouest de l’Espagne, Aquaculture, 67(1–2), 195–198, 1987.

Morelle, J., Maire, O., Richard, A., Slimani, A. and Orvain, F.: Contrasted influence of infaunal species (*Hediste diversicolor* and *Scrobicularia plana*) on microphytobenthos performances: study of microscale processes, Front. Microbiol., submitted.

Morelle, J., Orvain, F. and Claquin, P.: Primary production by microphytobenthos on heterogeneous mudflats and heavily anthropogenically influenced in the Seine estuary (France), submitted.

Morelle, J., Orvain, F. and Claquin, P.: A simple, user friendly tool to readjust raw PAM data from field measurements to avoid over- or underestimating of microphytobenthos photosynthetic parameters, *J. Exp. Mar. Biol. Ecol.*, 503, 136–146, 2018.

Morgan-Kiss, R. M., Priscu, J. C., Pocock, T., Gudynaite-Savitch, L. and Huner, N. P.: Adaptation and acclimation of photosynthetic microorganisms to permanently cold environments, *Microbiol Mol Biol Rev*, 70(1), 222–252, 2006.

Mostajir, B., Roques, C., Bouvier, C., Bouvier, T., Foulland, É., Got, P., Le Floc'h, E., Nouguier, J., Mas, S. and Sempéré, R.: Microbial food web structural and functional responses to oyster and fish as top predators, *Mar. Ecol. Prog. Ser.*, 535, 11–27, 2015.

Müller, P., Li, X.-P. and Niyogi, K. K.: Non-Photochemical Quenching. A Response to Excess Light Energy, *Plant Physiol.*, 125(4), 1558–1566, doi:10.1104/pp.125.4.1558, 2001.

Murray, W. A.: Erodibility of coarse sand-clayey silt mixtures, *J. Hydraul. Eng.*, 103(10), 1222–1227, 1977.

Nagata, T.: Organic matter-bacteria interactions in seawater, *Microb. Ecol. Oceans*, 2, 207–241, 2008.

Nash, C.: *The History of Aquaculture*, John Wiley & Sons., 2010.

Nelder, J. A. and Mead, R.: A simplex method for function minimization, *Comput. J.*, 7(4), 308–313, 1965.

Newell, R. I., Kemp, W. M., Hagy III, J. D., Cerco, C. F., Testa, J. M. and Boynton, W. R.: Top-down control of phytoplankton by oysters in Chesapeake Bay, USA: Comment on Pomeroy et al.(2006), *Mar. Ecol. Prog. Ser.*, 341, 293–298, 2007.

Newell, R. I. E., Cornwell, J. C. and Owens, M. S.: Influence of simulated bivalve biodeposition and microphytobenthos on sediment nitrogen dynamics: A laboratory study, *Limnol. Oceanogr.*, 47(5), 1367–1379, doi:10.4319/lo.2002.47.5.1367, 2002.

Nicolas, J. L., Comps, M. and Cochenne, N.: Herpes-like virus infecting Pacific oyster larvae, *Crassostrea gigas*, *Bull Eur Assoc Fish Pathol*, 12(1), 11–13, 1992.

Nilsson, P., Jonsson, B., Swanberg, I. and Sundback, K.: Response of a marine shallow-water sediment system to an increased load of inorganic nutrients, *Mar. Ecol. Prog. Ser.*, 71, 275–290, doi:10.3354/meps071275, 1991.

Nugues, M. M., Kaiser, Spencer and Edwards: Benthic community changes associated with intertidal oyster cultivation, 1996.

Orvain, F., Galois, R., Barnard, C., Sylvestre, A., Blanchard, G. and Sauriau, P.-G.: Carbohydrate Production in Relation to Microphytobenthic Biofilm Development: An Integrated Approach in a Tidal Mesocosm, *Microb. Ecol.*, 45(3), 237–251, doi:10.1007/s00248-002-2027-7, 2003.

Orvain, F., Sauriau, P.-G., Sygut, A., Joassard, L. and Le Hir, P.: Interacting effects of *Hydrobia* ulvae bioturbation and microphytobenthos on the erodibility of mudflat sediments, *Mar. Ecol. Prog. Ser.*, 278, 205–223, 2004.

Orvain, F., Sauriau, P.-G., Le Hir, P., Guillou, G., Cann, P. and Paillard, M.: Spatio-temporal variations in intertidal mudflat erodability: Marennes-Oléron Bay, western France, *Cont. Shelf Res.*, 27(8), 1153–1173, doi:10.1016/j.csr.2006.05.013, 2007.

Orvain, F., Lefebvre, S., Montepini, J., Sébire, M., Gangnery, A. and Sylvand, B.: Spatial and temporal interaction between sediment and microphytobenthos in a temperate estuarine macro-intertidal bay, *Mar. Ecol. Prog. Ser.*, 458, 53–68, doi:10.3354/meps09698, 2012.

Orvain, F., Guizien, K., Lefebvre, S., Bréret, M. and Dupuy, C.: Relevance of macrozoobenthic grazers to understand the dynamic behaviour of sediment erodibility and microphytobenthos resuspension in sunny summer conditions, *J. Sea Res.*, 92, 46–55, doi:10.1016/j.seares.2014.03.004, 2014a.

Orvain, F., De Crignis, M., Guizien, K., Lefebvre, S., Mallet, C., Takahashi, E. and Dupuy, C.: Tidal and seasonal effects on the short-term temporal patterns of bacteria, microphytobenthos and exopolymers in natural intertidal biofilms (Brouage, France), *J. Sea Res.*, 92, 6–18, doi:10.1016/j.seares.2014.02.018, 2014b.

Orvain, F., Le Hir, P., Méléder, V., Lesourd, S., Dancie, C., Israel, S. and Morelle, J.: Associations Biologiques en relation avec le transport sédimentaire : développement d'un modèle de bioturbation par les ingénieurs d'écosystèmes en estuaire de Seine, 2018.

Ottmann, F. and Sornin, J. M.: Relationship between marine bottom elevation and various types of marine culture, *Atlantica*, 5, 88–89, 1982.

Ottmann, F. and Sornin, J. M.: Observations on sediment accumulation as a result of mollusk culture systems in France., 1985.

Padilla, D. K.: Context-dependent Impacts of a Non-native Ecosystem Engineer, the Pacific Oyster *Crassostrea gigas*, *Integr. Comp. Biol.*, 50(2), 213–225, doi:10.1093/icb/icq080, 2010.

Papaspyrou, S., Kristensen, E. and Christensen, B.: *Arenicola marina* (Polychaeta) and organic matter mineralisation in sandy marine sediments: in situ and microcosm comparison, *Estuar. Coast. Shelf Sci.*, 72(1–2), 213–222, 2007.

Parizadeh, L., Tourbiez, D., Garcia, C., Haffner, P., Dégremont, L., Le Roux, F. and Travers, M.-A.: Ecologically realistic model of infection for exploring the host damage caused by *Vibrio aestuarianus*, *Environ. Microbiol.*, 20(12), 4343–4355, 2018.

Passarelli, C., Hubas, C., Segui, A. N., Grange, J. and Meziane, T.: Surface adhesion of microphytobenthic biofilms is enhanced under *Hediste diversicolor* (OF Müller) trophic pressure, *J. Exp. Mar. Biol. Ecol.*, 438, 52–60, 2012.

Passarelli, C., Olivier, F., Paterson, D. M., Meziane, T. and Hubas, C.: Organisms as cooperative ecosystem engineers in intertidal flats, *J. Sea Res.*, 92, 92–101, doi:10.1016/j.seares.2013.07.010, 2014.

Paterson, D. M., Wiltshire, K. H., Miles, A., Blackburn, J., Davidson, I., Yates, M. G., McGrorty, S. and Eastwood, J. A.: Microbiological mediation of spectral reflectance from intertidal cohesive sediments, *Limnol. Oceanogr.*, 43(6), 1207–1221, 1998.

Pathirana, E., Fuhrmann, M., Whittington, R. and Hick, P.: Influence of environment on the pathogenesis of Ostreid herpesvirus-1 (OsHV-1) infections in Pacific oysters (*Crassostrea gigas*) through differential microbiome responses, *Helion*, 5(7), e02101, doi:10.1016/j.heliyon.2019.e02101, 2019.

Paul-Pont, I., Dhand, N. and Whittington, R.: Spatial distribution of mortality in Pacific oysters *Crassostrea gigas*: reflection on mechanisms of OsHV-1 transmission, *Dis. Aquat. Organ.*, 105(2), 127–138, doi:10.3354/dao02615, 2013.

Paul-Pont, I., Evans, O., Dhand, N. and Whittington, R.: Experimental infections of Pacific oyster *Crassostrea gigas* using the Australian ostreid herpesvirus-1 (OsHV-1) μVar strain, *Dis. Aquat. Organ.*, 113(2), 137–147, doi:10.3354/dao02826, 2015.

Pepin, J. F., Riou, A. and Renault, T.: Rapid and sensitive detection of ostreid herpesvirus 1 in oyster samples by real-time PCR, *J. Virol. Methods*, 149(2), 269–276, doi:10.1016/j.jviromet.2008.01.022, 2008.

Perissinotto, R., Nozais, C. and Kibirige, I.: Spatio-temporal Dynamics of Phytoplankton and Microphytobenthos in a South African Temporarily-open Estuary, *Estuar. Coast. Shelf Sci.*, 55(1), 47–58, doi:10.1006/ecss.2001.0885, 2002.

Perkins, R., Lavaud, J., Serôdio, J., Mouget, J., Cartaxana, P., Rosa, P., Barille, L., Brotas, V. and Jesus, B.: Vertical cell movement is a primary response of intertidal benthic biofilms to increasing light dose, *Mar. Ecol. Prog. Ser.*, 416, 93–103, doi:10.3354/meps08787, 2010.

Perkins, R. G., Underwood, G. J. C., Brotas, V., Snow, G. C., Jesus, B. and Ribeiro, L.: Responses of microphytobenthos to light: primary production and carbohydrate allocation over an emersion period, *Mar. Ecol. Prog. Ser.*, 223, 101–112, 2001.

Pernet, F., Barret, J., Marty, C., Moal, J., Gall, P. L. and Boudry, P.: Environmental anomalies, energetic reserves and fatty acid modifications in oysters coincide with an exceptional mortality event, *Mar. Ecol. Prog. Ser.*, 401, 129–146, doi:10.3354/meps08407, 2010.

Pernet, F., Barret, J., Le Gall, P., Lagarde, F., Fiandrino, A., Huvet, A., Corporeau, C., Boudry, P., Quéré, C. and Dégremont, L.: Rapport final du programme de recherche sur les mortalités d'huîtres creuses *Crassostrea gigas* dans l'étang de Thau, 2011.

Pernet, F., Barret, J., Le Gall, P., Corporeau, C., Dégremont, L., Lagarde, F., Pépin, J. and Keck, N.: Mass mortalities of Pacific oysters *Crassostrea gigas* reflect infectious diseases and vary with farming practices in the Mediterranean Thau lagoon, France, *Aquac. Environ. Interact.*, 2(3), 215–237, doi:10.3354/aei00041, 2012.

Pernet, F., Lagarde, F., Le Gall, P. and D'Orbcastel, E. R.: Associations between farming practices and disease mortality of Pacific oyster *Crassostrea gigas* in a Mediterranean lagoon, *Aquac. Environ. Interact.*, 5(2), 99–106, 2014.

Pernet, F., Tamayo, D. and Petton, B.: Influence of low temperatures on the survival of the Pacific oyster (*Crassostrea gigas*) infected with ostreid herpes virus type 1, *Aquaculture*, 445, 57–62, doi:10.1016/j.aquaculture.2015.04.010, 2015.

Pernet, F., Fuhrmann, M., Petton, B., Mazurié, J., Bouget, J.-F., Fleury, E., Daigle, G. and Gernez, P.: Determination of risk factors for herpesvirus outbreak in oysters using a broad-scale spatial epidemiology framework, *Sci. Rep.*, 8(1), 10869, 2018.

Petton, B., Pernet, F., Robert, R. and Boudry, P.: Temperature influence on pathogen transmission and subsequent mortalities in juvenile Pacific oysters *Crassostrea gigas*, *Aquac. Environ. Interact.*, 3(3), 257–273, 2013.

Petton, B., Bruto, M., James, A., Labreuche, Y., Alunno-Bruscia, M. and Le Roux, F.: *Crassostrea gigas* mortality in France: the usual suspect, a herpes virus, may not be the killer in this polymicrobial opportunistic disease, *Front. Microbiol.*, 6, doi:10.3389/fmicb.2015.00686, 2015a.

Petton, B., Boudry, P., Alunno-Bruscia, M. and Pernet, F.: Factors influencing disease-induced mortality of Pacific oysters *Crassostrea gigas*, *Aquac. Environ. Interact.*, 6(3), 205–222, doi:10.3354/aei00125, 2015b.

Pezy, J.-P., Delecrin, C., Baffreau, A., Basuyaux, O. and Dauvin, J.-C.: Anthropogenic impact of oyster farming on macrofauna biodiversity in an eelgrass (*Zostera marina*) ecosystem of the English Channel, *Ecol. Indic.*, 106, 105480, doi:10.1016/j.ecolind.2019.105480, 2019.

Pichot, Y., Comps, M., Tige, G., Grizel, H. and Rabouin, M.-A.: Recherches sur Bonamia ostreae gen. n., sp. n., parasite nouveau de l’huître plate *Ostrea edulis*, *Stud. Bonamia Ostreae Gen N Sp N New Parasite Eur. Flat Oyster Ostrea Edulis Fr Rev Trav Inst Pêch Marit*, 43, 131–40, 1981.

Pierre, G., Graber, M., Orvain, F., Dupuy, C. and Maugard, T.: Biochemical characterization of extracellular polymeric substances extracted from an intertidal mudflat using a cation exchange resin, *Biochem. Syst. Ecol.*, 38(5), 917–923, doi:10.1016/j.bse.2010.09.014, 2010.

Pierre, G., Graber, M., Rafiliposon, B. A., Dupuy, C., Orvain, F., De Crignis, M. and Maugard, T.: Biochemical Composition and Changes of Extracellular Polysaccharides (ECPS) Produced during Microphytobenthic Biofilm Development (Marennes-Oléron, France), *Microb. Ecol.*, 63(1), 157–169, doi:10.1007/s00248-011-9959-8, 2012.

Ploug, H., Lassen, C. and Jørgensen, B. B.: Action spectra of microalgal photosynthesis and depth distribution of spectral scalar irradiance in a coastal marine sediment of Limfjorden, Denmark, *FEMS Microbiol. Ecol.*, 12(2), 69–78, 1993.

Pomeroy, L. R.: Algal Productivity in Salt Marshes of Georgia1, *Limnol. Oceanogr.*, 4(4), 386–397, doi:10.4319/lo.1959.4.4.0386, 1959.

Porter, E., Mason, R. and Sanford, L.: Effect of tidal resuspension on benthic–pelagic coupling in an experimental ecosystem study, *Mar. Ecol. Prog. Ser.*, 413, 33–53, doi:10.3354/meps08709, 2010.

Porter, E. T., Cornwell, J. C., Sanford, L. P. and Newell, R. I. E.: Biofiltration, water quality, and sediment processes, *WATER Qual.*, 9, 2004.

Prieur, D., Nicolas, J. L., Plusquellec, A. and Vigneulle, M.: Interactions between bivalve mollusks and bacteria in the marine-environment, *Ocean. Mar Biol.*, 28, 277–352, 1990.

Rakotomalala, C., Grangeré, K., Ubertini, M., Forêt, M. and Orvain, F.: Modelling the effect of *Cerastoderma edule* bioturbation on microphytobenthos resuspension towards the planktonic food web of estuarine ecosystem, *Ecol. Model.*, 316, 155–167, doi:10.1016/j.ecolmodel.2015.08.010, 2015.

Rakotomalala, C., Guizien, K., Grangeré, K., Lefebvre, S., Dupuy, C. and Orvain, F.: Modelling the functioning of a coupled microphytobenthic-EPS-bacterial system in intertidal mudflats, *Mar. Environ. Res.*, 104754, 2019.

Raven, J. A. and Geider, R. J.: Adaptation, acclimation and regulation in algal photosynthesis, in *Photosynthesis in algae*, pp. 385–412, Springer., 2003.

Renault, T.: Les virus infectant les mollusques marins: un exemple d'actualité, les herpèsvirus, *Bull. Académie Vét. Fr.* 2011 N° 4 Fasc. Thématique Séance Thématique Pathol. Comparée Herpèsviroses-Séance Thématique Pathol. Comparée Herpèsviroses Paris FRA 2011-11-03, 2011a.

Renault, T.: Viruses infecting marine molluscs, *Stud. Viral Ecol. Anim. Host Syst.* Vol. 2, 153–175, 2011b.

Renault, T., Le Deuff, R. M., Cochenne, N. and Maffart, P.: Herpesviruses associated with mortalities among Pacific oyster, *Crassostrea gigas*, in France. Comparative study, *Rev. Médecine Vét.*, 145(10), 735–742, 1994.

Richard, M., Bec, B., Vanhuysse, C., Mas, S., Parin, D., Chantalat, C., Le Gall, P., Fiandrino, A., Lagarde, F. and Mortreux, S.: Changes in planktonic microbial components in interaction with juvenile oysters during a mortality episode in the Thau lagoon (France), *Aquaculture*, 503, 231–241, 2019.

Rico-Villa, B., Bernard, I., Robert, R. and Pouvreau, S.: A Dynamic Energy Budget (DEB) growth model for Pacific oyster larvae, *Crassostrea gigas*, *Aquaculture*, 305(1–4), 84–94, 2010.

Rivera-Utrilla, J., Bautista-Toledo, I., Ferro-García, M. A. and Moreno-Castilla, C.: Activated carbon surface modifications by adsorption of bacteria and their effect on aqueous lead adsorption, *J. Chem. Technol. Biotechnol.*, 76(12), 1209–1215, doi:10.1002/jctb.506, 2001.

Rodgers, C., Arzul, I., Carrasco, N. and Furones Nozal, D.: A literature review as an aid to identify strategies for mitigating ostreid herpesvirus 1 in *Crassostrea gigas* hatchery and nursery systems, *Rev. Aquac.*, doi:10.1111/raq.12246, 2018.

Ropert, M. and Dauvin, J.-C.: Renewal and accumulation of a Lanice conchilega (Pallas) population in the baie des Veys, western Bay of Seine, *Oceanol. Acta*, 23(4), 529–546, 2000a.

Ropert, M. and Dauvin, J.-C.: Renewal and accumulation of a Lanice conchilega (Pallas) population in the baie des Veys, western Bay of Seine, *Oceanol. Acta*, 23(4), 529–546, doi:10.1016/S0399-1784(00)00143-2, 2000b.

Rossi, F.: Small-scale burial of macroalgal detritus in marine sediments: effects of *Ulva* spp. on the spatial distribution of macrofauna assemblages, *J. Exp. Mar. Biol. Ecol.*, 332(1), 84–95, 2006.

Roughan, M., Macdonald, H. S., Baird, M. E. and Glasby, T. M.: Modelling coastal connectivity in a Western Boundary Current: Seasonal and inter-annual variability, *Deep Sea Res. Part II Top. Stud. Oceanogr.*, 58(5), 628–644, 2011.

Round, F.: Benthic marine diatoms, *Ocean. Mar Biol Annu Rev*, 9, 83–139, 1971.

Royer, J., Ropert, M. and Costil, K.: Spatio-temporal changes in mortality, growth and condition of the Pacific oyster, *Crassostrea gigas*, in Normandy (France), *J. Shellfish Res.*, 26(4), 973–985, 2007.

Ruesink, J. L., Lenihan, H. S., Trimble, A. C., Heiman, K. W., Micheli, F., Byers, J. E. and Kay, M. C.: Introduction of non-native oysters: ecosystem effects and restoration implications, *Annu Rev Ecol Evol Syst*, 36, 643–689, 2005.

Ryther, J. H.: Photosynthesis in the ocean as a function of light intensity, *Limnol. Oceanogr.*, 1(1), 61–70, 1956.

Sahan, E., Sabbe, K., Creach, V., Hernandez-Raquet, G., Vyverman, W., Stal, L. J. and Muyzer, G.: Community structure and seasonal dynamics of diatom biofilms and associated grazers in intertidal mudflats, *Aquat. Microb. Ecol.*, 47(3), 253–266, 2007.

Salama, N. K. and Murray, A. G.: A comparison of modelling approaches to assess the transmission of pathogens between Scottish fish farms: the role of hydrodynamics and site biomass, *Prev. Vet. Med.*, 108(4), 285–293, 2013.

Samain, J.-F. and McCombie, H.: Summer mortality of Pacific oyster *Crassostrea gigas*: the Morest Project, Editions Quae., 2008.

Sauvage, C., Pépin, J. F., Lapègue, S., Boudry, P. and Renault, T.: Ostreid herpes virus 1 infection in families of the Pacific oyster, *Crassostrea gigas*, during a summer mortality outbreak: differences in viral DNA detection and quantification using real-time PCR, *Virus Res.*, 142(1), 181–187, 2009.

Savelli, R., Bertin, X., Orvain, F., Gernez, P., Dalle, A., Coulombier, T., Pineau, P., Lachaussée, N., Polsenaere, T., Dupuy, C. and Le Fouest, V.: Impact of chronic and massive resuspension mechanisms on the microphytobenthos dynamics in a temperate intertidal mudflat, accepted, accepted.

Savelli, R., Dupuy, C., Barillé, L., Lerouxel, A., Guizien, K., Philippe, A., Bocher, P., Polsenaere, P. and Le Fouest, V.: On biotic and abiotic drivers of the microphytobenthos seasonal cycle in a temperate intertidal mudflat: a modelling study, *Biogeosciences*, 15(23), 7243–7271, doi:10.5194/bg-15-7243-2018, 2018.

Schikorski, D., Faury, N., Pepin, J. F., Saulnier, D., Tourbiez, D. and Renault, T.: Experimental ostreid herpesvirus 1 infection of the Pacific oyster *Crassostrea gigas*: Kinetics of virus DNA detection by q-PCR in seawater and in oyster samples, *Virus Res.*, 155(1), 28–34, doi:10.1016/j.virusres.2010.07.031, 2011.

Schöttler, U.: Der Energiestoffwechsel bei biotopbedingter Anaerobiose: Untersuchungen an Anneliden, Verh Dtsch Zool Ges, 1980, 228–240, 1980.

Schöttler, U. and Grieshaber, M.: Adaptation of the polychaete worm *Scoloplos armiger* to hypoxic conditions, Mar. Biol., 99(2), 215–222, doi:10.1007/BF00391983, 1988.

Segarra, A., Pépin, J. F., Arzul, I., Morga, B., Faury, N. and Renault, T.: Detection and description of a particular Ostreid herpesvirus 1 genotype associated with massive mortality outbreaks of Pacific oysters, *Crassostrea gigas*, in France in 2008, Virus Res., 153(1), 92–99, doi:10.1016/j.virusres.2010.07.011, 2010a.

Segarra, A., Pépin, J. F., Arzul, I., Morga, B., Faury, N. and Renault, T.: Detection and description of a particular Ostreid herpesvirus 1 genotype associated with massive mortality outbreaks of Pacific oysters, *Crassostrea gigas*, in France in 2008, Virus Res., 153(1), 92–99, doi:10.1016/j.virusres.2010.07.011, 2010b.

Segarra, A., Mauduit, F., Faury, N., Trancart, S., Dégremont, L., Tourbiez, D., Haffner, P., Barbosa-Solomieu, V., Pépin, J.-F. and Travers, M.-A.: Dual transcriptomics of virus-host interactions: comparing two Pacific oyster families presenting contrasted susceptibility to ostreid herpesvirus 1, Bmc Genomics, 15(1), 580, 2014.

Serôdio, J.: Analysis of variable chlorophyll fluorescence in microphytobenthos assemblages: implications of the use of depth-integrated measurements, Aquat. Microb. Ecol., 36(2), 137–152, 2004.

Serôdio, J. and Catarino, F.: Fortnightly light and temperature variability in estuarine intertidal sediments and implications for microphytobenthos primary productivity, Aquat. Ecol., 33(3), 235–241, 1999.

Serôdio, J., Marques da Silva, J. and Catarino, F.: Non destructive tracing of migratory rhythms of intertidal benthic microalgae using *in vivo* chlorophyll a fluorescence, J. Phycol., 33(3), 542–553, 1997.

Serôdio, J., Coelho, H., Vieira, S. and Cruz, S.: Microphytobenthos vertical migratory photoresponse as characterised by light-response curves of surface biomass, Estuar. Coast. Shelf Sci., 68(3–4), 547–556, doi:10.1016/j.ecss.2006.03.005, 2006.

Serôdio, J., Vieira, S. and Cruz, S.: Photosynthetic activity, photoprotection and photoinhibition in intertidal microphytobenthos as studied *in situ* using variable chlorophyll fluorescence, Cont. Shelf Res., 28(10–11), 1363–1375, doi:10.1016/j.csr.2008.03.019, 2008.

Serôdio, J., Ezequiel, J., Barnett, A., Mouget, J., Méléder, V., Laviale, M. and Lavaud, J.: Efficiency of photoprotection in microphytobenthos: role of vertical migration and the xanthophyll cycle against photoinhibition, Aquat. Microb. Ecol., 67(2), 161–175, doi:10.3354/ame01591, 2012.

Shaffer, G. P. and Sullivan, M. J.: Water column productivity attributable to displaced benthic diatoms in well-mixed shallow estuaries, J. Phycol., 24(2), 132–140, 1988.

Sim, Y. and Chrysikopoulos, C. V.: Virus transport in unsaturated porous media, Water Resour. Res., 36(1), 173–179, 2000.

Simboura, N. and Zenetos, A.: Benthic indicators to use in ecological quality classification of Mediterranean soft bottom marine ecosystems, including a new biotic index, *Mediterr. Mar. Sci.*, 3(2), 77–111, 2002.

Smith, D. J. and Underwood, G. J.: Exopolymer production by intertidal epipelagic diatoms, *Limnol. Oceanogr.*, 43(7), 1578–1591, 1998.

Smith, R. C. and Mobley, C. D.: Underwater light, in *Photobiology*, pp. 131–138, Springer., 2008.

Solechnik, P., Lambert, C. and Costiv, K.: Summer mortality of *Crassostrea gigas* (Thunberg) in relation to environmental rearing conditions, , 11, 2007.

Solomieu, V. B., Renault, T. and Travers, M.-A.: Mass mortality in bivalves and the intricate case of the Pacific oyster, *Crassostrea gigas*, *J. Invertebr. Pathol.*, 131, 2–10, 2015.

Sornin, Feuillet, Heral and Deslous-Paoli: Effet des biodépôts de l’huître *Crassostrea gigas* (Thunberg) sur l’accumulation de matières organiques dans les parcs du bassin de Marennes-Oléron, 1983.

Sornin, J.-M.: Processus sédimentaires et biodéposition liés à différents modes de conchyliculture: Baie de Cancale, Anse de l’Aiguillon et Bassin de Marennes-Oléron, PhD Thesis, université de Nantes., 1981.

Sornin, J.-M. and Mariojouls, C.: Surexploitation et détérioration de la qualité des terrains conchyliques : conséquences sur les systèmes d’exploitation ; exemples en France et au Japon, *Norois*, 133(1), 51–61, doi:10.3406/noroi.1987.7402, 1987.

Souchu, P., Vaquer, A., Collos, Y., Landrein, S., Deslous-Paoli, J.-M. and Bibent, B.: Influence of shellfish farming activities on the biogeochemical composition of the water column in Thau lagoon, *Mar. Ecol. Prog. Ser.*, 218, 141–152, 2001.

Stal and de Brouwer: Biofilm formation by benthic diatoms and their influence on the stabilization of intertidal mudflats, 2003.

Storch, V. and Welsch, U.: The ultrastructure of epidermal mucous cells in marine invertebrates (Nemertini, Polychaeta, Prosobranchia, Opisthobranchia), *Mar. Biol.*, 13(2), 167–175, 1972.

Struski, C. and Bacher, C.: Preliminary estimate of primary production by phytoplankton in Marennes-Oléron Bay, France, *Estuar. Coast. Shelf Sci.*, 66(1–2), 323–334, doi:10.1016/j.ecss.2005.09.007, 2006.

Sundbäck, K., Miles, A. and Göransson, E.: Nitrogen fluxes, denitrification and the role of microphytobenthos in microtidal shallow-water sediments:an annual study, *Mar. Ecol. Prog. Ser.*, 200, 59–76, doi:10.3354/meps200059, 2000.

Suttle, C. A.: Marine viruses—major players in the global ecosystem, *Nat. Rev. Microbiol.*, 5(10), 801, 2007.

Swanberg, I.: The influence of the filter-feeding bivalve *Cerastoderma edule* L. on microphytobenthos: a laboratory study, *J. Exp. Mar. Biol. Ecol.*, 151(1), 93–111, doi:10.1016/0022-0981(91)90018-R, 1991.

Sylvand, B.: La baie des Veys (Littoral occidental de la baie de Seine, Manche), 1972-1993: structure et évolution à long terme d'un écosystème benthique intertidal de substrat meuble sous influence estuarienne, PhD Thesis, Caen., 1995.

Tester, M. and Morris, C.: The penetration of light through soil, *Plant Cell Environ.*, 10(4), 281–286, doi:10.1111/j.1365-3040.1987.tb01607.x, 1987.

Thomas, Y., Cassou, C., Gernez, P. and Pouvreau, S.: Oysters as sentinels of climate variability and climate change in coastal ecosystems, *Environ. Res. Lett.*, 13(10), 104009, 2018.

Thomsen, M. S. and McGlathery, K.: Effects of accumulations of sediments and drift algae on recruitment of sessile organisms associated with oyster reefs, *J. Exp. Mar. Biol. Ecol.*, 328(1), 22–34, 2006.

Thrusfield, M. V.: Veterinary epidemiology., 3rd edn.(Blackwell: Oxford), 2007.

Thrush, S. F., Hewitt, J. E. and Lohrer, A. M.: Interaction networks in coastal soft-sediments highlight the potential for change in ecological resilience, *Ecol. Appl.*, 22(4), 1213–1223, doi:10.1890/11-1403.1, 2012.

Thrush, S. F., Hewitt, J. E., Lohrer, A. M. and Chiaroni, L. D.: When small changes matter: the role of cross-scale interactions between habitat and ecological connectivity in recovery, *Ecol. Appl.*, 23(1), 226–238, doi:10.1890/12-0793.1, 2013.

Tolhurst, T. J., Gust, G. and Paterson, D. M.: The influence of an extracellular polymeric substance (EPS) on cohesive sediment stability, in *Proceedings in Marine Science*, vol. 5, pp. 409–425, Elsevier., 2002.

Tolhurst, T. J., Jesus, B., Brotas, V. and Paterson, D. M.: Diatom migration and sediment armouring—an example from the Tagus Estuary, Portugal, in *Migrations and Dispersal of Marine Organisms*, pp. 183–193, Springer., 2003.

Travers, M.-A., Tourbiez, D., Parizadeh, L., Haffner, P., Kozic-Djellouli, A., Aboubaker, M., Koken, M., Dégremont, L. and Lupo, C.: Several strains, one disease: experimental investigation of *Vibrio aestuarianus* infection parameters in the Pacific oyster, *Crassostrea gigas*, *Vet. Res.*, 48(1), 32, 2017.

Troell, M., Naylor, R. L., Metian, M., Beveridge, M., Tyedmers, P. H., Folke, C., Arrow, K. J., Barrett, S., Crépin, A.-S., Ehrlich, P. R., Gren, Å., Kautsky, N., Levin, S. A., Nyborg, K., Österblom, H., Polasky, S., Scheffer, M., Walker, B. H., Xepapadeas, T. and de Zeeuw, A.: Does aquaculture add resilience to the global food system?, *Proc. Natl. Acad. Sci.*, 111(37), 13257–13263, doi:10.1073/pnas.1404067111, 2014.

Tsutsumi, H.: Population dynamics of *Capitella capitata* (Polychaeta; Capitellidae) in an organically polluted cove, *Mar. Ecol. Prog. Ser.*, 36, 139–149, doi:10.3354/meps036139, 1987.

Ubertini, M.: Impact of sediment grain-size and biofilm age on epipelagic microphytobenthos resuspension, *J. Exp. Mar. Biol. Ecol.*, 467, 52–64, doi:10.1016/j.jembe.2015.02.007, 2015.

Ubertini, M., Lefebvre, S., Gangnery, A., Grangeré, K., Le Gendre, R. and Orvain, F.: Spatial Variability of Benthic-Pelagic Coupling in an Estuary Ecosystem: Consequences for

Microphytobenthos Resuspension Phenomenon, edited by S. Thrush, PLoS ONE, 7(8), e44155, doi:10.1371/journal.pone.0044155, 2012.

Umesh, K. R., Bhavani, N. C., Venugopal, M. N., Karunasagar, I., Krohne, G. and Karunasagar, I.: Prevalence of human pathogenic enteric viruses in bivalve molluscan shellfish and cultured shrimp in south west coast of India, *Int. J. Food Microbiol.*, 122(3), 279–286, doi:10.1016/j.ijfoodmicro.2007.12.024, 2008.

Underwood, G. J.: Seasonal and spatial variation in epipelagic diatom assemblages in the Severn estuary, *Diatom Res.*, 9(2), 451–472, 1994.

Underwood, G. J. and Kromkamp, J.: Primary production by phytoplankton and microphytobenthos in estuaries, *Adv. Ecol. Res.*, 29, 93, 1999.

Underwood, G. J. C., Boulcott, M., Raines, C. A. and Waldron, K.: Environmental effects on exopolymer production by marine benthic diatoms: dynamics, changes in composition, and pathways of production: exopolymer production by diatoms, *J. Phycol.*, 40(2), 293–304, doi:10.1111/j.1529-8817.2004.03076.x, 2004.

Van Cauwenberghe, L., Vanreusel, A., Mees, J. and Janssen, C. R.: Microplastic pollution in deep-sea sediments, *Environ. Pollut.*, 182, 495–499, 2013.

Van Colen, C., Underwood, G. J., Serôdio, J. and Paterson, D. M.: Ecology of intertidal microbial biofilms: Mechanisms, patterns and future research needs, *J. Sea Res.*, 92, 2–5, 2014.

Van de Koppel, J.: Do Alternate Stable States Occur in Natural Ecosystems? Evidence from a Tidal Flat, , 82(12), 13, 2001.

Van Duyl, F. C., Kop, A. J., Kok, A. and Sandee, A. J. J.: The impact of organic matter and macrozoobenthos on bacterial and oxygen variables in marine sediment boxcosms, *Neth. J. Sea Res.*, 29(4), 343–355, doi:10.1016/0077-7579(92)90074-O, 1992.

Van Ledden, M., Van Kesteren, W. G. M. and Winterwerp, J. C.: A conceptual framework for the erosion behaviour of sand–mud mixtures, *Cont. Shelf Res.*, 24(1), 1–11, 2004.

Vásquez-Yeomans, R., García-Ortega, M. and Cáceres-Martínez, J.: Gill erosion and herpesvirus in *Crassostrea gigas* cultured in Baja California, Mexico, *Dis. Aquat. Organ.*, 89, 137–144, doi:10.3354/dao02189, 2010.

Vignaroli, C., Luna, G. M., Rinaldi, C., Di Cesare, A., Danovaro, R. and Biavasco, F.: New Sequence Types and Multidrug Resistance among Pathogenic *Escherichia coli* Isolates from Coastal Marine Sediments, *Appl. Environ. Microbiol.*, 78(11), 3916–3922, doi:10.1128/AEM.07820-11, 2012.

Warrick, J. A.: Dispersal of fine sediment in nearshore coastal waters, *J. Coast. Res.*, 29(3), 579–596, 2012.

Webb, P., Bain, C. and Pirozzo, S.: Essential epidemiology, Cambridge, United Kingdom: Cambridge University Press., 2005.

Weinbauer, M. G.: Ecology of prokaryotic viruses, *FEMS Microbiol. Rev.*, 28(2), 127–181, 2004.

Welsh, D. T.: It's a dirty job but someone has to do it: The role of marine benthic macrofauna in organic matter turnover and nutrient recycling to the water column, *Chem. Ecol.*, 19(5), 321–342, doi:10.1080/0275754031000155474, 2003.

Whitlatch, R. B. and Zajac, R. N.: Biotic interactions among estuarine infaunal opportunistic species., *Mar. Ecol. Prog. Ser.* Oldendorf, 21(3), 299–311, 1985.

Whittaker, R. H. and Likens, G. E.: The biosphere and man, in Primary productivity of the biosphere, pp. 305–328, Springer., 1975.

Whittington, R. J., Hick, P., Rubio, A., Dhand, N. and Evans, O.: Aquatic Animal Health Subprogram: Pacific Oyster Mortality Syndrome (POMS)-Risk Mitigation, Epidemiology and OsHV-1 Biology, University of Sydney., 2015a.

Whittington, R. J., Hick, P. M., Evans, O., Rubio, A., Alford, B., Dhand, N. and Paul-Pont, I.: Protection of Pacific oyster (*Crassostrea gigas*) spat from mortality due to ostreid herpesvirus 1 (OsHV-1 μVar) using simple treatments of incoming seawater in land-based upwellers, *Aquaculture*, 437(Supplement C), 10–20, doi:10.1016/j.aquaculture.2014.11.016, 2015b.

Whittington, R. J., Paul-Pont, I., Evans, O., Hick, P. and Dhand, N.: Counting the dead to determine the source and transmission of the marine herpesvirus OsHV-1 in *Crassostrea gigas*, , 21, 2018.

Wofsy, S. C.: A simple model to predict extinction coefficients and phytoplankton biomass in eutrophic waters 1, *Limnol. Oceanogr.*, 28(6), 1144–1155, 1983.

Wolff, W. J.: The estuary as a habitat an analysis of data on the soft-bottom macrofauna of t he estuarine area of the rivers Rhine, Meuse and Scheldt. Communication nr. 106 of the Delta Institute for Hydrobiological Research, , 240, 1973.

Wommack, K. E. and Colwell, R. R.: Virioplankton: viruses in aquatic ecosystems, *Microbiol Mol Biol Rev*, 64(1), 69–114, 2000.

Xiao, R. and Zheng, Y.: Overview of microalgal extracellular polymeric substances (EPS) and their applications, *Biotechnol. Adv.*, 34(7), 1225–1244, 2016.

Yallop, M. L., de Winder, B., Paterson, D. M. and Stal, L. J.: Comparative structure, primary production and biogenic stabilization of cohesive and non-cohesive marine sediments inhabited by microphytobenthos, *Estuar. Coast. Shelf Sci.*, 39(6), 565–582, 1994.

Yallop, M. L., Paterson, D. M. and Wellsbury, P.: Interrelationships between rates of microbial production, exopolymer production, microbial biomass, and sediment stability in biofilms of intertidal sediments, *Microb. Ecol.*, 39(2), 116–127, 2000.

Yee, N., Fein, J. B. and Daughney, C. J.: Experimental study of the pH, ionic strength, and reversibility behavior of bacteria–mineral adsorption, *Geochim. Cosmochim. Acta*, 64(4), 609–617, doi:10.1016/S0016-7037(99)00342-7, 2000.

Ysebaert, T. and Herman, P.: Spatial and temporal variation in benthic macrofauna and relationships with environmental variables in an estuarine, intertidal soft-sediment environment, *Mar. Ecol. Prog. Ser.*, 244, 105–124, doi:10.3354/meps244105, 2002.



# Liste des figures

Figure 1 © RMN-Grand Palais / Martine Beck-Coppola - Louis-Joseph Yperman, La pêche au vivier, peinture murale du Palais des Papes, Avignon, France, 1910 (œuvre originale : 1343-1344).....	3
Figure 2 : . Images en microscopie électronique à balayage à basse température d'un biofilm microphytobenthique sur un sédiment, montrant les liens entre les particules de sédiment par le biais des EPS. a. Vue en surface du biofilm. Barre blanche (en bas) : 100 µm. b. Coupe verticale ; la surface des sédiments est en haut. Barre blanche: 10 µm. Adapté de Passarelli et al. (2014). .....	7
Figure 3 : Schéma des interactions entre bivalves filtreurs, biodéposition, biofilms microphytobenthiques .....	18
Figure 4 : Caractéristiques théoriques des habitats créés par l'alternance des tables à huître .	21
Figure 5 : Cartographie des points de prélèvements réalisés en Baie de Veys lors du projet VIAPSE. Points : A : Sud des parcs de Géfosse, B : Dans les parcs de Géfosse, C : Pointe de Brévands (Sud des parcs). .....	28
Figure 6 : Charges virales de OsHV-1 µVar quantifiées dans le sédiment et le biofilm dans le Sud des parcs de Géfosse (A), dans les parcs de Géfosse (B) et sur la Pointe de Brévands (C) à 9 dates en 2014.....	29
Figure 7 : Taux de mortalité des naissains d'huîtres sentinelles après injection de l'eau de mer contaminée en virus OSHV-1 µvar dans un canal d'érodimétrie. Les taux de mortalité varient en fonction du courant appliqué (0.5 m.s <sup>-1</sup> en bleu et 2 m.s <sup>-1</sup> en orange) et du temps passé dans le courant du canal (converti en distance équivalent parcouru par le courant, en abscisse) et du traitement du virus : A) directement mis dans l'eau de l'érodimétrie, B) dispersé à la surface d'un échantillon de sédiment pris en baie des Veys et C) à la surface d'un échantillon de sédiment colonisé par un biofilm microphytobenthique. ....	30
Figure 8 : Design experimental de la table à huîtres étudiée. L'habitat table à huître échantilloné est coloré en bleu (A, B & C) et l'habitat allée en rouge (A, B & C). .....	34
Figure 9 : Conceptual scheme of potential impacts of oyster tables on the benthic habitat. A. Beyond the oyster table, i.e. in the aisle, sediment is exposed to light and high temperatures. The benthic habitat could be mainly sandy, with a low organic matter fraction (OMF) that could slightly stimulate the microbial loop and hence nutrient regeneration. In this case, MPB growth would not be enhanced and macrofauna grazing species would consequently be relatively rare. B. Under the oyster tables, shading reduces exposure to light and temperature. The sediment is	

muddy, with more OMF due to the oyster biodeposition. The higher OMF promotes the microbial loop and hence nutrient regeneration. MPB growth would consequently be stimulated and macrofauna deposit feeding species would be facilitated rather than suspension feeders.	45
Figure 10 : A. Description of the experimental design. B. Experimental set up in the field, Areas A, B and C were located under oyster tables (blue) or in the aisle (red). Each area included 20 oyster bags. C. Maximum water height (meters) and tidal coefficient during the experiment. Each square represents a sampling occasion.....	47
Figure 11 : Linear regression model (ANCOVA) of significant regression statistics (table 2). A. Surface light intensity according to moment and MWH (lambda = 0.10). B Surface light intensity according to habitat (lambda = 0.10). C. Sediment surface temperature according to habitat and MWH. D. Sediment surface temperature according to habitat and moment. With bLT = before the low tide and LT = Low tide E. Organic matter fraction according to habitat and MWH. F. Sediment water content according to MWH.....	53
Figure 12 : Significant effects of regression statistics (Tableau 4) for microphytobenthic variables: A. Sediment chl a according to moment; B. Sediment chl a according to habitat; C. Biofilm chl a according to habitat; D. Photosynthetic yield according to habitat and maximum water height (lambda = 3.69); E. Photosynthetic yield according to habitat and moment (lambda = 3.69); F. Light saturation coefficient (Ek) according to habitat and maximum water height (lambda = 0.35). .....	55
Figure 13 : Pearson correlation coefficients (r) between the variables that showed effects according to linear regression models .....	57
Figure 14 : A. PCA analysis with axes 1 and 2. Axis 1 carries Ek, ETRmax and surface active chl a concentration, axis 2 carries PY, light and temperature. B. PCA analysis with axis 1 and 3. Axis 3 carries surface active chl a concentration and pheopigments.....	58
Figure 15 : Relationship between photosynthetic yield of MPB and A. ambient light intensity, and B. Surface temperature during low-tide emersion periods. A quantile regression was adjusted to the second dispersion diagram. C. Relationship between light intensity and surface temperature.....	59
Figure 16 : Correlation matrices A. In the aisle. B. Under the oyster table .....	59
Figure 17 : Experimental field design. The oyster table sample areas are in blue (A, B & C) and the aisle sample areas are in red (A,B & C) .....	78
Figure 18: Temporal evolution of species abundance observed according to habitats and days .....	81

Figure 19: Rank frequency diagrams for sampling days. Blue points correspond to table samples and red points to aisle samples. The table under each diagram corresponds to the five most abundant species for each habitat.....	82
Figure 20 : benthic indexes with A. BOPA index. B. AMBI index. C. BENTIX index.....	84
Figure 21: Correspondence analysis. Roman numerals in parentheses after the species name correspond to the AMBI ecological groups. ....	85
Figure 22 : PCA analysis with A. Dim 1 and 2. Dim 1 carries contained biomass for AMBI II and III species, fine sediment particles (inf63) and organic matter content (OM) variables. Dim 2 contained the sediment water content, the biofilm and sediment chl a and the AMBI I species. B. axis 1 and 4. Dim 4 contained NH <sub>4</sub> <sup>+</sup> concentrations and the species of the AMBI V groups .....	87
Figure 23: Percentage of survival and algal coverage during the oyster spat mortality in summer 2017 .....	88
Figure 24: OsHv1 μVar viral loads in macrozoobenthic fauna during the oyster spat mortality episode of summer 2017 .....	89
Figure 25 :Conceptual scheme of potential impacts of oyster tables on the benthic habitat. A. in the aisle, sediment is exposed to light and high temperatures. MPB growth is altered due to the thermoinhibition and in a lower extent to photoinhibition. . B. Under the oyster tables, shading reduces exposure to light and temperature. MPB growth is not altered with better photosynthetic performances. In both cases, the benthic habitat appears to be shaped by oysters biodeposition and oyster tables with a muddification of the sediment, regular inputs of organic matter that is remineralized into nutrients by the microbial loop. ....	107
Figure 26 : Location of (A) the Baie des Veys, (B) a closer view of the baie des Veys and (C) the oyster farm in which samples were .....	109
Figure 27 : Experimental field design. The oyster table sample areas are in blue (A, B & C) and the aisle sample areas are in red (A,B & C) .....	109
Figure 28 : Water temperatures in the baie des Veys in 2017. <a href="https://wwz.ifremer.fr/observatoire_conchylicole/Resultats-par-annee/Resultats-nationaux-2017/Mortalite-par-site-et-par-classe-d-age">https://wwz.ifremer.fr/observatoire_conchylicole/Resultats-par-annee/Resultats-nationaux-2017/Mortalite-par-site-et-par-classe-d-age</a> .....	112
Figure 29 : Percentage of survival during the oyster spat mortality in summer 2017 .....	112
Figure 30 : OsHV-1 μVar viral loads in oyster spats. A. alive oyster spats. B. Moribund oyster spats. C. Dead oyster spats. Each single point represents 10 oyster spats analyzed .....	113
Figure 31 : OsHV-1 μVar DNA quantitites found in the sediment .....	114

Figure 32 : OsHV-1 $\mu$ Var DNA found in microphytobenthic biofilms. Each single point represent an average based on 6 samples.....	115
Figure 33 : Experimental field design. Sediment cores were alternately sampled in the aisle (in red) and under the oyster table (in blue) .....	133
Figure 34 : Experimental erosion device (erodimeter).....	135
Figure 35 : Topographical bed variations observed during the the samplig periods. The data in green are considered as before the mortality episode and in red after. Points represents the daily maximal water height recorded by the ALTUS device.....	138
Figure 36 : Correlation between bed topography variation and maximal water height.....	138
Figure 37 : Each part (A, B & C) presents 3 diagrams with Bed shear stress (Pa), Eroded chl a ( $\text{mg} \cdot \text{m}^{-2}$ ) and resuspended sediment matter ( $\text{g} \cdot \text{m}^{-2}$ ) & virus ( $\text{UG.ngDNA}^{-1}$ ) for 3 experiments out of the 15 ones : A. Jour 150 B. Jour153. C. Jour 180. Vertical bars represent the current steps corresponding to the initiation of the erosion (when critical thresholds were overpassed). A. Top graph represents the bed shear stress (Pa) applied in the erodimeter on the sediment core. The middle graph represented the eroded chl a and sand which on day 150 showed critical threshold for erosion of 0.0094 and 0.12973 Pa respectively. The bottom graph showed the resuspended sediment matter (SPM) with a critical threshold for erosion 0.16477. B. On day 153, eroded chl a and sand showed critical threshold for erosion of 0.02 and 0.21 Pa respectively. The bottom graph showed the resuspended sediment matter (SPM) with a critical threshold for erosion of 0.30. C. On day 180, eroded chl a and sand showed critical thresholds of 0.01 and 0.23 Pa respectively. The bottom graph showed the resuspended sediment matter (SPM) with an erosion threshold 0.51.....	139
Figure 38 : Bed topography variations (mm) as a function of sand erosion threshold (Pa)...	141
Figure 40 : OsHV-1 $\mu$ Var DNA quantities at the surface of the biofilm. Each day corresponded to an erosion experiment .....	142
Figure 41 : Synthèse des résultats obtenus au chapitre 2. ....	157
Figure 42 : Facteurs structurants la macrofaune benthique à l'échelle de la table à huîtres ..	159
Figure 43 : Hypothèses sur la résistance des huîtres à OsHV-1 $\mu$ Var en lien avec les caractéristiques environnementales.....	164

## Liste tableaux

Tableau 1 : Fonctions des EPS selon leur structure. Traduit de (Xiao and Zheng, 2016), adapté de (Flemming and Wingender, 2010) .....	10
Tableau 2 : Explanatory variables (fixed) and variables to be explained .....	51
Tableau 3 : Summary of linear models (ANCOVA) conducted on abiotic parameters. These results correspond to those that respected the conditions of homoscedasticity. Non-significant effects are not shown. With $X_1 = \text{Moment}$ ( $bLT = 0$ ; $LT = 1$ ), $X_2 = \text{Maximum water height}$ , $X_3 = \text{Habitat}$ (under the table = 0; aisle = 1), $X_4 = \text{Moment} * \text{Habitat}$ , $X_5 = \text{MWH} * \text{Habitat}$ , $X_6 = \text{MWH} * \text{Moment}$ . Significance levels: * < 0.05, ** < 0.01, *** < 0.0001.....	54
Tableau 4 : Summary of liner models (ANCOVA) conducted on biotic parameters. The results presented correspond to those which respected the conditions of homoscedasticity. Non-significant effects are not shown. $X_1 = \text{Moment}$ ( $bLT = 0$ ; $LT = 1$ ), $X_2 = \text{maximum water height}$ , $X_3 = \text{Habitat}$ (under the table = 0; aisle = 1), $X_4 = \text{Moment} * \text{Habitat}$ , $X_5 = \text{MWH} * \text{Habitat}$ , $X_6 = \text{MWH} * \text{Moment}$ . Significance levels: * < 0.05, ** < 0.01, *** < 0.0001.....	56
Tableau 5 : Classification of soft bottom benthic habitats based on BOPA, AMBi and BENTIX indexes.....	80
Tableau 6 : Shannon index, Species Richness and Pielou index .....	82
Tableau 7 : Contribution of species to the first 3 axes of the correspondence analysis .....	85
Tableau 8 : Contribution of variables to the first 4 axes of the principal correspondence analysis .....	86
Tableau 9 : Erosion parameters calculated from erodimeter experiments: Sand, SPM and Chl a erosion threshold and fluxes towards the water. ....	140
Tableau 10 : OsHV-1 concentrations at each sampling setp with average +/- standard deviation below .....	145



## **Impacts de l'ostréiculture à mesoéchelle sur le microphytobenthos et ses performances photosynthétiques, la macrofaune benthique et rôle de l'érosion estuarienne dans les mortalités de naissains d'huîtres *Crassostrea gigas* liées à OsHV-1 μVar**

### **Résumé**

Depuis 2008, la mortalité des naissains d'huîtres Pacifique *Crassostrea gigas* est principalement liée au virus de l'ostreid herpesvirus 1 μvariant (OsHV-1 μVar). Les paramètres environnementaux favorisant la persistance et la diffusion du virus pourraient jouer sur sa dynamique de propagation. Les objectifs de cette thèse étaient d'étudier *in situ* les interactions entre les naissains d'huîtres et leur environnement benthique lors d'un épisode de surmortalité. La photobiologie du microphytobenthos sous les tables semblait en meilleur état comparé à celle observée dans les allées pouvant favoriser la résilience virale. Les tables à huîtres atténuaient la lumière, la température et la dessication évitant ainsi une thermo et photoinhibition du microphytobenthos. Les indices de la qualité environnementale de l'habitat benthique basés sur la communauté macrozoobenthique ont traduit une dégradation du milieu suite aux apports de matière organique induits par les mortalités de naissains d'huîtres puis des échouages des macroalgues. Une quantité importante d'OsHV-1 était retrouvée à la surface du biofilm avant les mortalités. Sa remise en suspension était préférentiellement associée aux particules microphytobenthiques avec de faibles courants.

Mots-clés : Microphytobenthos, OsHV-1 μVar virus, *Crassostrea gigas* mortalité, sédiment, érosion, macrozoobenthos

### **Abstract**

Since 2008, the mortality of Pacific oyster spat *Crassostrea gigas* has mainly been linked to the Ostreid herpesvirus 1 μvariant (OsHV-1 μVar). Environmental parameters favoring the persistence and spread of the virus could affect its propagation dynamics. The objectives of this thesis were to study *in situ* the interactions between oyster spat and their benthic environment during an episode of mortality. The photobiology of the microphytobenthos beneath the tables seemed to be in a better state compared to that observed in aisles that could promote viral resilience. The oyster tables attenuated light, temperature and desiccation, thus avoiding thermo and photoinhibition of the microphytobenthos. The benthic habitat environmental quality indices based on the macrozoobenthic community showed a degradation of the environment following the influx of organic matter induced by oyster spat mortalities and strandings of the macroalgae. A significant amount of OsHV-1 was found on the surface of the biofilm before the mortalities. Resuspension was preferentially associated with microphytobenthic particles with small currents.

Keys words : Microphytobenthos, OsHV-1 μVar virus, *Crassostrea gigas* mortality, sediment, erosion, macrozoobenthos